University of Zurich[UZH]

Spatial and Temporal Runoff Generation Processes in a Swiss Pre-alpine Headwater Catchment

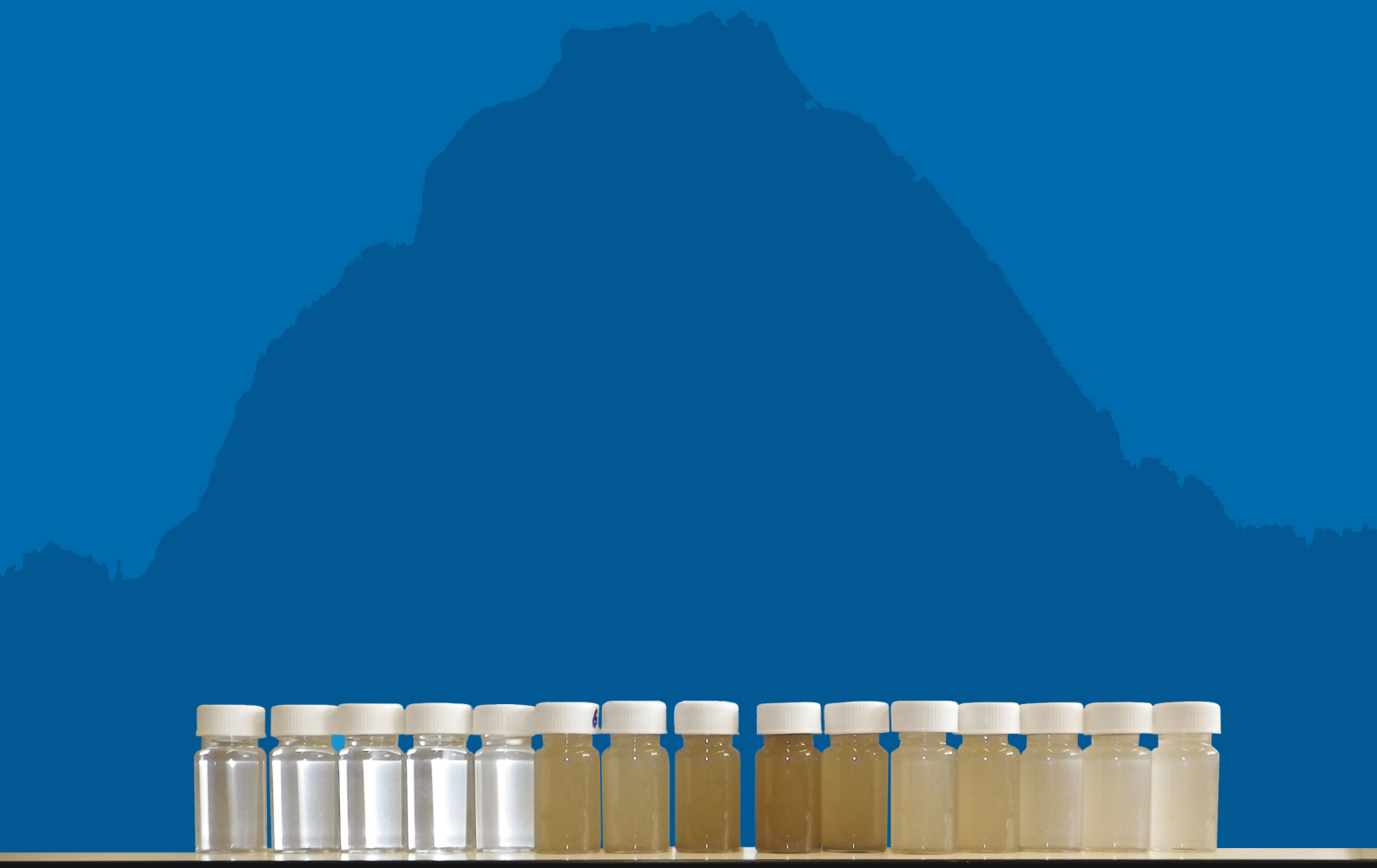

Benjamin Michael Clemens Fischer

Spatial and Temporal Runoff Generation Processes in a Swiss Pre-alpine Headwater Catchment

---

Dissertation

zur

Erlangung der naturwissenschaftlichen Doktorwürde

(Dr. sc. nat.)

vorgelegt der

Mathematisch-naturwissenschaftlichen Fakultät

der Universität Zürich

von

Benjamin Michael Clemens Fischer

aus

Deutschland

Promotionskomitee

Prof. Dr. Jan Seibert (Vorsitz)

Dr. Manfred Stähli

Zürich, 2016

Many of us share a similar childhood memory of the hike in the mountains: The day started with nice and sunny weather. The scenic path went steep up and down. Passed through dark pine forests, and luscious meadows. Jumping over stepping stones across a wetland, along rocky outcrops or soil deposits and finally having a break next to a refreshing mountain stream. One naturally started an unceasing struggle to dam the stream, never wondering about where all the water was coming from. While the sudden rainfall wrecked the perfect playground and turned the way back into a miserably wet and muddy adventure. One was more interested in the squeaking boots than why the stream turned from gentile to dangerously aggressive with much more water or where all the rain water ended up...

...The rain a most particular wet something. 4 x 10^{33} different water molecules trickling down ($P_{tot.}$=30 mm) ... ... creating runoff which could fill 18 Olympic swimming pools. An icebreaker to start a conversation, a nuisance on a weekend stroll and a elixir of life that people perform dances for...

...gauging the ungauged. To study rainfall runoff processes in pre-alpine areas and in the search of a suitable research area the choice fell on the Alptal with long-term good quality data by the WSL, the frequent rainfall and the potential to study spatial and temporal processes. It all started with a new tarmac layer on a long and winding forest road in the Zwäckentobel. Walking weekly up and down to see which streams are ephemeral and which perennial. From the initial 21 streams in the Zwäckentobel 10 streams were gauged with water level recorders and different types of water samples were collected. Having tools to study where the baseflow is coming from and what happens to the rainfall...

... 1 µL of water, less than a raindrop, contains information of hydrological processes!

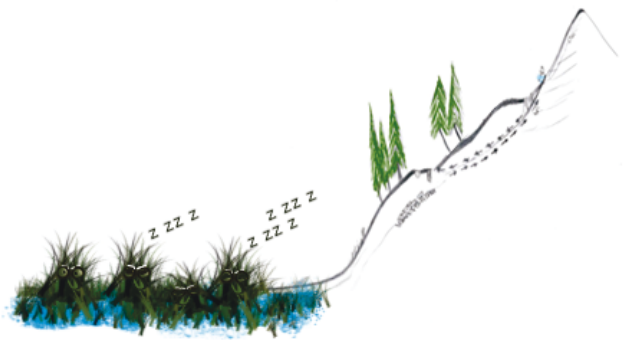

Abstract

In mountainous headwater catchments, with their high variability of hydrological processes and catchment properties together with the limited spatial and long-term data, it remains unclear how the different spatiotemporal controls affect runoff generation during base and stormflow. In this doctoral thesis environmental tracers are used to identify sources contributing to baseflow, observe linkages between different landscape units and discern how rainfall becomes stormflow in a Swiss pre-alpine headwater catchment, the Zwäckentobel (4.25 km^2), with high precipitation amounts (P>2000 mm y^{-1}) and heterogeneous catchment properties. The spatially collected rainfall and its isotopic composition are used to test whether it is reasonable to assume that in small headwater catchments, there is spatially homogenous rainfall and isotopic composition, implying that one sampling location is sufficient. Important tracers in this thesis are the stable isotopes ^{2}H and ^{18}O. The collected water samples were analysed with a laser spectroscope. For this analysis it was tested how many measurements are needed to reduce the memory effect and obtain a desired accuracy. For the Zwäckentobel water samples it was sufficient to measure each sample six times while for highly depleted samples the memory effect was reduced only after seven to eight injections. The water samples collected during three snapshot sampling campaigns were analysed for their isotopic (δ^2H) and hydrochemical components (Ca, DOC, AT, pH, SO_4, Mg and H_4SiO_4) and contained useful information on the different sources and helped to identify the flowpath of the water during baseflow. Although the six subcatchments had different landscape units, the inter- and intra catchment variability of the isotopic and hydrochemical components was generally small and statistically not significant. Streamwater samples at the subcatchment outlets were more similar to springs near the water divide than to groundwater from observation wells and wetlands. The wetlands, with 30-60% of the subcatchment area and large storage capacity, were less connected and acted as passive features with negligible contribution to baseflow runoff. In five subcatchments of the Zwäckentobel headwater catchment, rainfall and streamwater of 13 different rainstorms were sampled to perform a two-component isotope hydrograph separation. Pre-event water contributions based on $\delta^{18}O$ or $\delta^{2}H$ computations were similar. The pre-event water contributions of headwaters depended largely on rainfall (amount and intensity) and varied more between events than between catchments, despite clear differences in land cover between the catchments. With increasing rainfall amount, the proportion of rainfall in runoff increased and changed from pre-event to event water dominated. Antecedent wetness was not found to control the pre-event water contribution. The fact that catchment properties and antecedent conditions were only secondary factors in runoff processes, was mainly due to the dominant and frequent rainfall, which obscured a potential signal indicating differences in catchment properties. At the eight locations sequentially sampled rainfall revealed a spatial variability in total rainfall, rainfall intensity and its isotopic composition. The spatial variability in the isotopic composition varied from event to event. No clear relation between the isotopic composition and rainfall or altitude was observed. The isotope hydrograph separation results varied considerably depending on which temporal weighing technique or rain sampler was used. These results demonstrated that even in small catchments the spatial variability in the isotope composition of event rainwater has to be considered in hydrograph separation studies. When data from only one rain gauge are available, the location of the gauge might largely affect results and this source of uncertainty must be considered. The combination of long-term and spatially short-term hydrometeorological measurements, together with three baseflow sampling campaigns and event water sampling in different neighboring streams and multiple events, complemented each other and helped to overcome individual limitations. The results show the necessity and benefits of this spatially distributed dataset to derive and better understand controlling factors in runoff generation in a headwater catchment with high precipitation amounts and heterogeneous catchment properties.

Zusammenfassung

Voralpine Kopfeinzugsgebiete weisen eine hohe Variabilität an hydrologischen Prozessen und Gebietseigenschaften auf. Zusammen mit der begrenzten Verfügbarkeit räumlich verteilter Daten sowie Langzeitdaten ist es unklar, wie unterschiedliche „Raum-Zeit-Regler“ die Abflussbildung während des Basisabflusses und während Hochwasser beeinflussen. In dieser Doktorarbeit wurden Umwelttracer verwendet, um die Herkunft des Basisabflusses zu identifizieren, Verknüpfungen zwischen unterschiedlichen Landschaftseinheiten zu erkennen, und um die Abflussbildung besser zu verstehen. Dafür wurde ein Schweizerisches voralpines Kopfeinzugsgebiet, der Zwäckentobel, als Untersuchungsgebiet gewählt. Der Zwäckentobel (4,25 km^2) erhält hohe Niederschlagsmengen (P>2000 mm J^{-1}) und weist heterogene Gebietseigenschaften auf. Die Annahme eines räumlich homogenen Regens und dessen Isotopenzusammensetzung wurde überprüft, indem mit einer hohen räumlichen Dichte Regenmenge sowie Isotopenzusammensetzung des Regens gemessen wurde. Damit lässt sich auch feststellen, ob ein einziger Regensammler in kleinen Einzugsgebieten ausreicht um die Variabilität zu erfassen. Wichtige Indikatoren in dieser Arbeit sind die stabilen Isotope ^2H and ^{18}O. Die gesammelten Wasserproben wurden mit einem Laser-Spektroskop analysiert. Vor der Verwendung der Werte in weiteren Analysen wurde geprüft wie viele Messungen nötig sind, um eine gewünschte Genauigkeit zu erhalten und der Einfluss einer Probenverschleppung verringert ist. Für die Wasserproben aus dem Zwäckentobel war es ausreichend, jede Probe sechsmal zu messen. Für Proben mit sehr leichter Wasserisotopie hingegen, war der Einfluss einer Probenverschleppung erst nach sieben bis acht Injektionen reduziert. Die gesammelten Wasserproben von drei Stichtags-Kampagnen wurden auf ihre Isotopen (δ^2H) und hydrochemische Zusammensetzung (Ca, DOC, AT, pH, SO_4, Mg und H_4SiO_4) analysiert und enthielten nützliche Informationen zur Herkunft und zu den Fliesswegen des Basisabflusses. Obwohl die sechs Teileinzugsgebiete unterschiedliche Landschaftseinheiten hatten, war die Variabilität sowohl zwischen den Einzugsgebieten als auch innerhalb eines Einzugsgebietes klein und statistisch nicht signifikant. Die Wasserproben der verschiedenen Teileinzugsgebiete hatten mehr Ähnlichkeit mit den Wasserproben aus den Quellen in der Nähe der Wasserscheide als mit Grundwasserproben und auch Wasserproben aus Feuchtgebieten. Dies deutet darauf hin, dass Feuchtgebiete, trotz ihrer Grösse von 30-60% der Teileinzugsflächen und einer grossen Speicherkapazität, weniger verbunden und vernachlässigbar wenig zum Basisabfluss beitrugen. In fünf Teileinzugsgebieten des Zwäckentobel wurde von 13 verschiedenen Niederschlagsereignissen sowohl Regen als auch Bachwasser verschiedener Wildbäche beprobt, um eine Zweikomponenten Isotopen Ganglinienseparation durchzuführen. Berechnungen des Anteiles des Vorereigniswassers basierend auf $\delta^{18}O$ oder δ^2H waren ähnlich. Der Anteil des Vorereigniswassers von den verschiedenen Kopfeinzugsgebieten hing in grossem Masse vom Niederschlag ab (Menge und Intensität) und variierte mehr zwischen den Ereignissen als zwischen Einzugsgebieten, trotz deutlicher Unterschiede in der Landnutzung zwischen den Einzugsgebieten. Mit steigender Regenmenge stieg auch der Anteil des Ereigniswassers im Abfluss und änderte sich von Vorereigniswasser zu Ereigniswasser signifikant. Vorfeuchte und Einzugsgebietseigenschaften waren nur sekundäre Faktoren bei der Abflussbildung, welche vor allem durch die Dominanz des Regens verursacht wurde dessen Einfluss die Gebietsunterschiede überlagerte. Der an acht Standorten gesammelte Niederschlag zeigte eine räumliche Variabilität von Niederschlagsmenge, Niederschlagsintensität und Isotopenzusammensetzung. Die räumliche Variabilität in der Isotopenzusammensetzung variierte von Ereignis zu Ereignis. Es gab keine klare Beziehung zwischen der Isotopenzusammensetzung und Regenmenge oder Höhe. Die Ergebnisse der Ganglinienseparation variierten erheblich-je nachdem welche zeitliche Bilanzierung der Isotopen oder welcher Regensammler verwendet wurde. Die

Ergebnisse zeigten, dass auch in kleinen Einzugsgebieten die räumliche Variabilität der Isotopenzusammensetzung des Niederschlages bei der Ganglinienseparation in Betracht gezogen werden muss. Wenn nur ein Regensammler verfügbar ist, muss daher berücksichtigt werden, dass der Standort des Regensammlers eine erhebliche Unsicherheit in den Resultaten bewirken kann. Die Kombination von langen, aber räumlich begrenzten und kurzen, aber räumlich höher aufgelösten hydro- meteorologischen Messungen, zusammen mit Stichtags Kampagnen sowie Ereignisbeprobungen in verschiedenen benachbarten Wildbächen ergänzten sich und halfen die individuellen Einschränkungen der Messungen zu überbrücken. Die Ergebnisse zeigen die Notwendigkeit und den Nutzen räumlich verteilter Messungen, um Prozesskenntnisse abzuleiten und die Abflussbildung in Kopfeinzugsgebieten mit hohen Niederschlagsmengen und heterogenen Einzugsgebietseigenschaften besser zu verstehen.

Keywords: headwater catchments, snapshot sampling, spatiotemporal patterns, catchment comparison, scaling, surface & groundwater chemistry, stable isotope hydrology, catchment characteristics, isotope hydrograph separation, runoff generation, precipitation, spatial variability, laser spectroscopes and memory effect between samples

Published by Benjamin Fischer.
Cover: Water samples sorted as collected during an event. Transparent bottles are taken during baseflow, turbid bottles during the highest discharge and changing again slowly to transparent bottles from baseflow. ©B.M.C. Fischer 2016.

University of Zürich, Department of Geography - Hydrology and Climate (H_2K)

drip. drip...

drip. drip...

drip. drip...

drip. drip...

drip. drip...

...rain was fallin and we are soakin wet
hail is beatin down on our heads
the wind is blowin through our hair
faces frozen in the frigid air
... be the rain. (U.N.)

Thesis at a glance

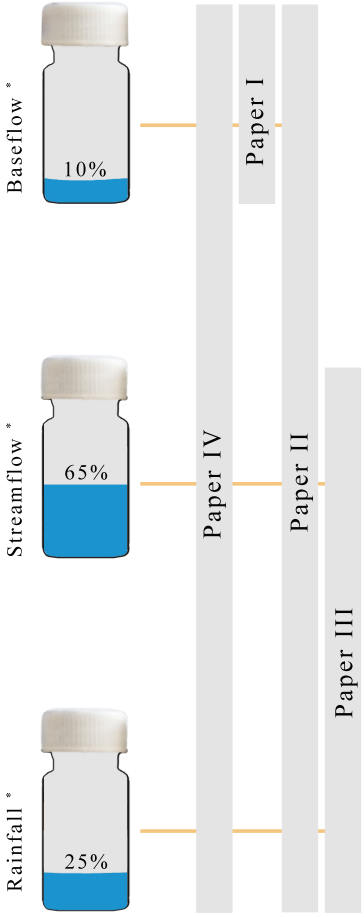

Paper	Aim	Method	Main finding / conclusion
Paper I: Contributing sources to baseflow in pre-alpine headwaters using spatial snapshot sampling	Which sources & landscape units contribute to catchment-scale baseflow in pre-alpine headwater catchments (Implicitly asses spatial δ^2H & $\delta^{18}O$ of pre-event water)	-3x baseflow snapshot sampling campaigns (n>80) -Analyse spatiotemporal differences in baseflow isotope &hydrochemistry to identify catchment-scale runoff contribution	-Inter-& intra catchment variability of isotopic & hydrochemical compositions was small & not significant -Outlets samples had signature of deep groundwater from water divide -Wetlands were less connected&contributed little to baseflow runoff
Paper II: Pre-event water contributions to runoff events of different magnitude in pre-alpine headwaters	How do precipitation and catchment characteristics control runoff processes in steep & wet pre-alpine headwaters with different landscape properties	Rainfall & streamwater of 5 headwaters & 13 different rainstorms were sampled to perform a two-component isotope hydrograph separation	-$\delta^{18}O$ & δ^2H gave similar IHS -The pre-event water contributions depended on rainfall (amount & intensity), and varied between events & not catchments(despite different catchment properties) -Antecedent wetness was not to be found important
Paper III: Effect of small scale variability isotopic composition of precipitation on hydrograph separation results	In which way does the spatiotemporal variability of rainfall & isotopic composition of rainfall affect the isotope hydrograph separation results	Subset of 10 events & 3 headwaters from paper II & all eight sequential rainfall samplers used in isotope hydrograph separation	Spatial variability in the isotope signature of event water in small catchments cannot be assumed to be negligible & has to be accounted for in hydrograph separation studies
Paper IV: Evaluation of between sample memory effects in the analysis of δ^2H & $\delta^{18}O$ of water samples measured by laser spectroscopes	Quantify the memory effect on the measurement precision of different types of laser spectroscopes	Two different types of laser spectroscopes of different generations were used to analyse ten isotopically depleted water samples where each sample was measured 18 times	-In depleted samples isotopic differences stabilised after 7-8 injections -The measurement variability was strongly dependent on the isotopic difference between adjacent vials -To reduce the memory effect operational & post-processing steps are suggested

* Approximately 3000 different water samples were collected which were applied differently and resulted in 4 different papers.

List of papers

The following selected papers, referred to as in order of appearance in the text by their Roman numerals, are included in this thesis.

PAPER I **Contributing sources to baseflow in pre-alpine headwaters using spatial snapshot sampling**
Fischer, B. M. C., Rinderer, M., Schneider, P., Ewen, T. and Seibert, J. *Hydrological Processes*, (2015).
DOI: 10.1002/hyp.10529

PAPER II **Pre-event water contributions to runoff events of different magnitude in pre-alpine headwaters**
Fischer, B. M. C., Stähli, M. and Seibert, J. *Hydrological Research*, (2016).
DOI: 10.2166/nh.2016.176

PAPER III **Effect of small scale variability isotopic composition of precipitation on hydrograph separation results**
Fischer, B. M. C., van Meerveld, H. J. and Seibert, J. *manuscript*, (2016).
DOI: NA

PAPER IV **Technical Note: Evaluation of between-sample memory effects in the analysis of δ^{2}H and δ^{18}O of water samples measured by laser spectroscopes**
Penna, D., Stenni, B., Šanda, M., Wrede, S., Bogaard, T. A., Michelini, M., **Fischer, B. M. C.**, Gobbi, A., Mantese, N., Zuecco, G., Borga, M., Bonazza, M., Sobotková, M., Čejková, B. and Wassenaar, L. I. *Hydrology Earth System Sciences*, **16(10)**, 3925–3933 (2012).
DOI: 10.5194/hess-16-3925-2012

Author's contribution

The aim of this study was to investigate spatiotemporal runoff processes and to compare different headwater catchments. From the initial idea, I developed a field and sampling design. The permits and communication with authorities was done together with Manfred Stähli and Michael Rinderer. To analyse water samples, I set up and supervised a new stable isotope laboratory and performed, for all water samples, the analysis (measurements, data analysis and data quality) .

For the different field and laboratory work I received help and supervised different internship and master students which are stated in the list of acknowledgments. I led, worked on and was responsible for the realization of the papers I-III and contributed as coauthor in paper IV. The different **papers I-IV** are all part of this thesis.

PAPER I

The idea of Paper I was developed together with Philip Schneider and Michael Rinderer. The sampling design and organization of the three snapshot sampling campaigns was done together with Michael Rinderer. The hydrochemical analysis of the water samples was done in the AUA lab of Swiss Federal Institute of Aquatic Science and Technology (EAWAG). The stable isotope samples were analysed by me. All data and GIS analysis and interpretation was done by me. The writing process of **paper I** was a result of all contributing authors. Furthermore I communicated and managed the review and publication processes.

PAPER II& III

For **paper II & III**, I developed and tested the sequential rainfall samplers, ordered all equipment necessary and calibrated instruments. Hereafter the measurement concept was implemented in the field and data collection was started in autumn 2009. All instruments were regularly maintained, data collected and corrected. I organized the event sampling and collection of the water samples before, during and after each sampled event. The collected water samples were prepared for stable isotope analysis. I performed all data analysis & interpretation and led the writing of all papers. The writing of **paper II & III** were a result of all contributing authors as stated on the individual papers. Furthermore I communicated and managed the review and publication processes.

PAPER IV

In **paper IV**, I performed laboratory analysis of one laser spectroscope and contributed as a co-author to the collective writing and revision processes of the paper led by the first author Daniele Penna.

Contents

List of acronyms

$\mathbf{A}_{DS}$ Antecedent dryspell

$\mathbf{A}_{PI7}$ Antecedent precipitation index with seven days prior to an event

$\mathbf{A}_{GL1}$ Antecedent groundwater level

$\mathbf{A}_{Q1}$ Antecedent discharge

BAFU Federal Office for the Environment FOEN

CRDS Cavity ring-down spectroscopy

DEM Digital elevation model

EC Electric conductivity

EAWAG Swiss Federal Institute of Aquatic Science and Technology

$\mathbf{H}_{responds}$ Mean stream responds to rainfall of all headwaters

IAEA International Atomic Energy Agency

IHS Isotope hydrograph separation

IRMS Isotope-ratio mass spectrometers

$\mathbf{M}_{RD}$ Mean Relative Difference

$\mathbf{M}_{TR}$ Mean temporal range in δ^{18}O

NADUF National River Monitoring and Survey program

OA-ICOS Off-axis integrated cavity output spectroscopy

$\mathbf{P}_{length}$ Rainfall duration

$\mathbf{P}_{mean\ tot.}$ Mean event total rainfall of all rain gauges

$\mathbf{P}$ Mean average hourly rainfall intensity of all rain gauges

$\mathbf{P}_{max}$ Maximum hourly rainfall intensity of all rain gauges

$\mathbf{Q}_{peak}$ Maximum specific discharge of WS04

Q/P Runoff coefficient

$\mathbf{S}_R$ Spatial range of weighted mean δ^{18}O

SD Standard deviation

SLAP Standard Light Antarctic Precipitation

$\mathbf{S}_W$ Spatial weighing

TOC Total Organic Carbon

$\mathbf{T}_W$ Temporal weighing

VSMOW Vienna Standard Mean Ocean Water

WSL Swiss Federal Institute for Forest, Snow and Landscape Research

1. Introduction

1.1 Pre-alpine headwaters

Many mountainous headwater catchments are marked by high amounts and frequent precipitation which is especially pronounced in the pre-alpine region, the transition zone between the lowlands and the high alpine ridges (Frei and Schär, 1998). Pre-alpine headwater catchments are characterized by steep gradients, deeply incised streams, shallow soils and a riparian zone is generally missing. The availability of water created an ecosystem with high species richness, economic and recreational value. During the centuries this ecosystem was intensively used and shaped by humans (Bergamini et al., 2009) and resulted in a mosaic of forests, meadows and wetlands in a region which already had a heterogenic landscape. The rainfall not only created an important ecosystem (Bergamini et al., 2009), but also means water is an important resource for the downstream regions. Especially during dry and wet extremes, the upstream region affects the downstream regions (Schmidli and Frei, 2005). The down side of the abundant and recurrent precipitation events is the erosive force of the water which creates a changing dynamic landscape. The rainfall can be very local with considerable local and downstream damage potential (Liechti et al., 2013; Werner and Cranston, 2009). The frequent rainfall can saturate the shallow soils and trigger landslides (Brönnimann et al., 2013; Ruette et al., 2014) but also causes floods and transports sediment to the downstream regions (Turowski et al., 2009). Despite their importance for water resources, headwaters are largely unmeasured (Bishop et al., 2008). This is especially true in mountainous headwaters where hydrological and hydrochemical observations are often difficult. Some catchment scale research sites in mountainous areas with long-term hydrological and hydrochemical data exists (e.g. Hegg et al., 2006; Seneviratne et al., 2012). However these are exceptions and internal spatial hydrological data is limited or neglected. Subsequently, the deficit of spatial and long-term hydrological and hydrochemical data constrain hydrologists in their interpretation of these important wet regions (Viviroli and Weingartner, 2004) and means that the spatiotemporal runoff processes of this region are not yet fully understood.

1.2 Means to trace headwater processes

Only by observing processes, collecting data and exchanging experience between experimentalists and modelers is it possible to understand the organization and thresholds of the complex hydrologic processes and develop and test new hydrological theories (Dooge, 2005; Kirchner, 2006; McDonnell and Beven, 2014; Seibert and McDonnell, 2002). Instead of yet another new experimental catchment it is necessary to compare and investigate differences and similarities (McDonnell, 2003). By using gauged headwaters with long-term data helps to relate and value additional measurements in a wider historic perspective. Together with additional measurements in newly gauged headwaters it helps to evaluate hydrological processes in a wider region. This should be done in a similar way to a medical examination, where stepwise, the headwater properties, water input, internal states and flow sources and pathways of the water are examined (Seibert and McDonnell, 2015). The combined hydrometric and tracer approach has proved

especially useful to study the source and flowpath of the water and discern how rainfall becomes stormflow (McDonnell, 2003; Weiler et al., 2003).
Streamflow integrates water from different sources and tracer approaches are commonly used to study the sources and flowpaths of the water and used in a wide range of different studies (e.g. Barthold et al., 2010; Christophersen and Hooper, 1992; Hrachowitz et al., 2011; Inamdar et al., 2013; Klaus and McDonnell, 2013; Lu, 2014; Penna et al., 2014; Rodgers et al., 2005; Sklash et al., 1976; Soulsby et al., 2007; Tetzlaff and Soulsby, 2008; Vitvar and Balderer, 1997). Non-conservative hydrochemical tracers (i.e., Electric conductivity (EC), Ca or DOC) provide useful information on sources and flowpathways as the concentrations depend on what the water encounters on its way from rain to stream (Inamdar et al., 2013; James and Roulet, 2006; Laudon and Slaymaker, 1997; Likens and Buso, 2006). Instead the stable isotopes ^{18}O and ^{2}H have been found to be useful to identify the flowpath sources of streamflow based on differences in the isotopic composition of geographic and temporal sources since these isotopes are part of the water itself (Klaus and McDonnell, 2013; Sklash et al., 1976). Isotope mass spectrometers were for a long time the only method to analyse the stable isotope composition of water. The recent development and advances of laser spectroscopes revolutionized the field by measuring the composition of both stable isotopes ^{18}O and ^{2}H in a fast and relatively easy manner (Lis et al., 2008; Penna et al., 2010). The price per sample decreased and stimulated the application of stable isotopes in hydrology. Although laser spectroscopes are now widely used, the limits of the technique still needs to be explored as shown by different studies. Only recently has the instrument handling and effect of syringe life time on analysis precision been investigated by Holko (2015) and Lis et al. (2008). Penna et al. (2010) examined the influence of different sampling schemes, accuracy, precision and differences between similar types of spectroscopes. Certain organic compounds from soil extracts or oil containing tree species can cause a isotopologue spectral interference and result in an inaccuracy of the measurement (Brand et al., 2009; Wassenaar et al., 2014; West et al., 2010). The importance of the laboratory workflow on accuracy and precision, i.e., sample preparation, outlier detection, VSMO-SLAP scale normalization to maintenance, is demonstrated by Wassenaar et al. (2014) and interlaboratory comparison to detect potential problems of laboratories by Ahmad et al. (2012). A different aspect that needs to be explored is related to the analysis method. Laser spectroscopy is a relative analysis method, where samples are bracketed between standards and each water sample is measured multiple times to derive the isotopic composition. In this analysis scheme a memory effect, i.e. carryover of traces from the previous sample to the sample being measured, can occur. This memory effect fades away the more measurements of a sample are made. However it is not known how many measurements one must carry out in order to obtain a desired accuracy of the sample to be analysed.

1.3 Snapshot information of the baseflow

Mountainous headwater streamflow processes have been studied by collecting stream water and analysed for their hydrochemical composition. Differences in hydrochemical composition were then postulated to be due to differences in land cover, soil type and geology (Keller, 1970, 1990; Keller et al., 1989). However deriving streamflow processes and contributing areas from hydrochemical composition collected only at the catchment outlet can be misleading. Especially because several studies found evidence of different means of contributing sources. In some headwaters the hydrochemical signal propagated along the longitudinal stream network (Asano et al., 2009). However in other headwaters small active sources from upstream point sources were found to contribute dominantly to streamflow (Zimmer et al., 2012). Instead Tetzlaff and Soulsby (2008) found that glacial valley bottom deposits can sometimes store groundwater from upslope areas and sustain baseflow. Other studies showed that during baseflow conditions the riparian zone (line source) acts as the main input to streamflow generation (Penna et al., 2014; Sidle et al., 2000). Some other studies found a relation with different landscape characteristics (Frisbee et al., 2011; Rodgers et al., 2005). Temnerud et al. (2007) stated that the dampening

of the hydrochemical variability originates not from conservative mixing but from a structured mosaic of landscape units. This demonstrates the necessity to compare and classify different headwaters (Wagener et al., 2007) and make the step beyond the outlet. By doing so, the underlying hydrological processes, linkages of different landscape units and how the different sources of water mix along their flowpaths will be better understood (McDonnell et al., 2007; Temnerud et al., 2007).

A simple and common approach to study spatial variations in runoff contribution to streamflow is to collect different grab samples at various locations throughout a catchment which are then analysed for their isotopic and hydrochemical composition (Fröhlich et al., 2008; Tetzlaff and Soulsby, 2008). Performing snapshot campaigns during baseflow conditions gives insight into the spatial differences of hydrological processes and linkages between different landscape units emerge (Fröhlich et al., 2008). Baseflow sampling campaigns are usually held during one or several days depending on the balance between research focus and logistics, and constrained by dry spells. Different univariate analyses, such as descriptive statistics, have been used to untangle and order the spatial variability of hydrochemical variables and indicate different flowpath or active zones. Buttle et al. (2004) and Kosugi et al. (2006) found soil depth or Asano et al. (2009) and Zimmer et al. (2012) active zones of seeping deep groundwater to be important factors for baseflow generation. A simple informative way to analyse single hydrochemical variables is by representing their concentration as sampled in the spatial plane. Likens and Buso (2006) mapped the hydrochemical patterns of the Hubbard Brook Experimental Forest during two snapshot campaigns and found minor changes between the two seasons, but a large change in hydrochemistry along the stream network. Here, hydrochemical patterns were attributed to differences in vegetation, geologic substrates and wetland areas. Instead Zimmer et al. (2012) could identify the flowpaths through the subsoil and active streamflow contributing zones near the water divide. Representing discharge or hydrochemical variables in relationship to their catchment area, different authors found that small scale variability decreases at areas larger than 0.1-4 km^2 (Asano et al., 2009; Didszun and Uhlenbrook, 2008; Lyon et al., 2012; Shaman et al., 2004; Uchida et al., 2005; Wolock et al., 1997; Wood et al., 1988; Woods et al., 1995). Contrary to this reduction of variability with increasing catchment size, Zimmer et al. (2012) found that the hydrochemical composition is rather scale independent.Temnerud et al. (2007) analysed the mixing of Total Organic Carbon (TOC) along the stream network in a boreal catchment and found that the decrease of variability with scale could not be explained by mixing alone, but was a result of the spatial pattern of landscape units. In addition, the hydrochemical mixing of the different water samples can be assessed by bivariate solute diagrams where hydrochemical boundaries, the end-members, indicate possible sources of the sampled stream water (Hooper et al., 1990).
Different environmental tracers have been found useful to identify sources contributing to streamflow and observe linkages between different landscape units. In mostly homogenous headwaters, different studies could attribute hydrochemical patterns to vegetation, geologic substrates and wetland areas. Furthermore, soil depth or active zones of seeping deep groundwater could be identified as dominant contributing baseflow sources due to their specific hydrochemical composition. Mountainous headwaters however have a large spatial variability of catchment properties and consist of different landscape units (such as forests, meadows and wetlands). In these heterogeneous headwaters it is unclear which landscape units contribute and which sources are contributing to baseflow.

1.4 How rainfall becomes stormflow

The stable isotopes ^{18}O and ^{2}H are not only useful to trace the water of the baseflow, but have proved their value in numerous studies and advanced knowledge on stormflow generation (Klaus and McDonnell, 2013). Using stable isotopes in the two end-member mass balance approach

Table 1.1: List of assumptions used in the IHS studies to separate the hydrograph (based on Buttle (1994) and Klaus and McDonnell (2013))

1. The event and pre-event water are significantly different
2. The event water maintains a constant isotopic signature in space and time, or any variations can be accounted for
3. The isotopic signature of the pre-event water is constant in space and time, or any variations can be accounted for
4. Contributions from the vadose zone must be negligible, or the isotopic signature of the soil water must be similar to that of groundwater
5. Surface storage contributes minimally to the streamflow

(also called two-component isotope hydrograph separation, IHS) makes it possible to study how catchments transform rainfall into runoff. To perform an IHS, it is common to collect different water samples at the catchment outlet. One water sample is taken before the start of a rainfall event which represent the baseflow composition. During an event water samples from the rain and streamflow are taken. These water samples are then analysed for their isotopic composition used in the IHS and allow, provided that different assumptions are satisfied see Table 1.1, to distinguish to which degree rainfall (event water) and water, that has been stored in the catchment before the event (pre-event water), contributes to stormflow in the stormflow hydrograph (Klaus and McDonnell, 2013; Sklash et al., 1976). IHS has been used frequently in single headwaters (e.g. Jordan, 1994; Lyon et al., 2008; McDonnell et al., 1990; Pellerin et al., 2008; Penna et al., 2014; Renshaw et al., 2003; Vitvar and Balderer, 1997). From the multitude of different IHS studies in forested headwaters, the general perception has developed that pre-event water dominates the peak discharge (Buttle, 1994; Klaus and McDonnell, 2013). The repeated outcome of the different IHS studies, that in forested headwaters pre-event water dominated the stormflow, resulted in the fact that the IHS approach was criticized for not providing further insights into hydrological processes (Burns, 2002). Furthermore it is not clear how these few events are related to the magnitude of the events. Consequently it is not clear how representative these few observations are, since they are just a snapshot of frequently occurring processes, which limits the information value of these observations. Few early IHS studies compared different catchments (Rodhe, 1987) and only due to the recent developments of laser spectroscopy is it possible to use the IHS and compare neighboring headwaters (Laudon et al., 2007; Onda et al., 2006) and/or many events (Hrachowitz et al., 2011; James and Roulet, 2009; Lyon et al., 2008; McGlynn et al., 2004; Roa-García and Weiler, 2010; Segura et al., 2012). From these new developments different runoff generation studies observed a more variable event and pre-event water contribution which was contrary to the presumed dominance in pre-event water found in other headwater studies.These differences of pre-event water could be related to temporal controls such as hydrometeorological conditions (e.g. precipitation) and soil moisture. Casper et al. (2003); James and Roulet (2009); Kienzler and Naef (2008); Pellerin et al. (2008) and Penna et al. (2014) explained that the temporal variable contribution of pre-event water was the influence of rainfall processes. These studies relate an increase of event water to rainfall amount, intensities and duration (see also Klaus and McDonnell, 2013). Other temporal controls such as seasonality and the state of the system are controlled by soil moisture and ground water and are assumed to affect the flowpathways of the water (Hinton et al., 1994; Penna et al., 2014). Events with dry antecedent conditions with low connectivity were found to have higher event water contribution compared to events with wet antecedent conditions (Casper et al., 2003; James and

Roulet, 2009; Jordan, 1994) while McGlynn et al. (2004) made opposite observations of higher pre-event water contribution during wet antecedent conditions.
Other studies instead related differences in pre-event water to catchment properties (land-use/cover, soil and geology). In forested headwaters the trees act as a dominant control. Trees affect throughfall, i.e. the timing, amount and the spatial pattern of rainfall that reaches the forest soil (Gerrits et al., 2010). Different studies not only found that trees affect the throughfall but also modify the isotopic composition of the rain water (Allen et al., 2015; Saxena, 1987). Additionally the roots of the trees affect the subsurface connectivity by creating macropores which facilitate water to infiltrate and connect the different soil layers (Weiler et al., 1998). Interception and transpiration of trees together with higher infiltration capacities of the soils can have a delaying effect on stream response resulting in dominant pre-event water during stormflow (Buttle, 1994; Klaus and McDonnell, 2013; Roa-García and Weiler, 2010). In regions with wetlands different results were observed. Roa-García and Weiler (2010) observed high pre-event water fractions while Laudon et al. (2007) and McCartney et al. (1998) observed high event water fractions in wetlands compared to forest and grasslands. Similarly high fractions of event water were observed in catchments with grassland by Bonell et al. (1990). Next to land use and land cover, infiltration capacity, soil type, storage potential of soils (Geris et al., 2015) and macropore distribution (Buttle, 1994) were found to be important controlling factors in runoff generation processes. Headwaters with shallow soils of less than one metre have generally limited water storage in the soil mantel (Pearce et al., 1986) and are therefore considered highly responsive to rainfall. Suecker et al. (2000) used the IHS in a highly responsive headwater and observed higher event water contributions on steep slopes. Relating geology to pre-event water contribution is difficult since subsurface information is generally rare and not homogenous. Although Onda et al. (2006) did not observe a significant relation between soil depth and event water. In headwaters with a "permeable" geology (larger number of cracks and fissures) this study observed a lower event water contribution compared to headwaters with a more impermeable geology. However comparing the different studies from around the world with different types of geology, described in Buttle (1994) or Jordan (1994), it is difficult to observe a general relationship between the fraction of pre-event water and geology. Contradictory observations were also made for catchment size as spatial control on the pre-event water contribution. Brown et al. (1999) and Shanley et al. (2002) observed that event water contribution increases with catchment size, while no relation was found by either James and Roulet (2009) or McGlynn et al. (2004).
Because of the wide application of the IHS, in different headwaters and climate zones, the perception of how headwaters produce runoff has changed. Contrary to the dominant pre-event water, a more variable contribution of pre-event water has been observed and is caused by different temporal and spatial controls. Therefore especially in steep pre-alpine headwaters with high precipitation amounts (P>2000 mm y^{-1}) , which are characterized by a large spatiotemporal variability of precipitation and variation in land cover, topography and geology, it remains to be quantified how the spatial varying catchment properties and temporal controls interact and influence runoff processes.

1.5 Spatial sampling of rainfall isotopes

To separate the hydrograph with the two end-member mass balance approach into its temporal components, event and pre-event water, samples of three different sources are needed. While baseflow (pre-event water) and stormflow samples are collected sometimes by hand (Hrachowitz et al., 2011), the common practice is to use automatic samplers, with a pre-programmed temporal or volume based sampling scheme, which are located at the catchment outlet. In case of a hydrograph separation using non-conservative hydrochemical tracers (e.g. EC, Si or Ca) the precipitation composition is often below the detection limit and therefore set to zero or assumed to be zero and not sampled at all (Laudon and Slaymaker, 1997). In the case of variable tracers such as stable isotopes the composition of rainfall can not be neglected. Therefore it is necessary

to collect water samples of rainfall to be able to perform an IHS. For the collection of rain water samples (event water) a variety of different methods exists. Krupa (2002) and Laquer (1990) listed different ways to collect rain water diverging from sampling by hand (Hrachowitz et al., 2011; Roa-García and Weiler, 2010), integrating volume samplers (James and Roulet, 2009; Lyon et al., 2008; Pellerin et al., 2008; Smith et al., 1979; Vitvar and Balderer, 1997), sequential as volume or in time (Brown et al., 1999; Jordan, 1994; McDonnell et al., 1990; Penna et al., 2014) to high frequency measurements using field deployable laser spectroscope (Berman et al., 2009; Munksgaard et al., 2012). Irrespective of the type of water sample and sampling technique, the challenge is to preserve the signature of the collected water as sampled in the field and prevent fractionation.

From early atmospheric studies it was known that the stable isotope composition of rainfall changes during a rainfall event (Dansgaard, 1953; Gatz et al., 1971). Many early IHS studies (e.g. Sklash et al., 1976) neglected this temporal variability of rainfall and instead used an average stable isotope composition of rainfall to separate the hydrograph. However, Kennedy et al. (1986) stated that it was inappropriate to draw conclusions from IHS studies using the average isotopic compositions of rainfall. McDonnell et al. (1990) incorporated this and used different temporal weighing techniques to account for event water in the IHS, which resulted in different pre-event fractions for the different techniques. This study pointed out the importance of considering the time scales of the precipitation and using the appropriate accounting technique of the isotopic compositions of rainfall. Similar to the temporal variability, early atmospheric studies reported a spatial component in the isotopic composition of rainfall (Dansgaard, 1964). The spatial component of the stable isotope composition of rainfall, are frequently studied for some events but more often on monthly to yearly average time scales. Samples in the spatial plane are usually collected using two samplers (Lyon et al., 2009), multiple samplers (Holko et al., 2012; McGuire et al., 2005), forest throughfall (Allen et al., 2015; James and Roulet, 2009), national monitoring networks (Schürch et al., 2003; Seeger and Weiler, 2014) up to global scales (Araguás-Araguás et al., 2000; Dansgaard, 1964). From these spatial observations, different studies have related the sampled stable isotope composition of rainfall to different factors. Dansgaard (1964) described an "amount" effect where the stable isotope composition of rainfall becomes more depleted with increasing rainfall amount. Contrary to this, no effect between the stable isotope composition of rainfall and rainfall amount was observed by Holko et al. (2012) and Schürch et al. (2003). Different studies observed that the stable isotope composition of rainfall the $\delta^{18}O$ became more depleted ±0.2 ‰ for every 100 m altitude (Holko et al., 2012; Kern et al., 2014; McGuire and McDonnell, 2008). Similar observations were made for air temperature where the stable isotope composition of rainfall became more depleted ±0.5 ‰ for each 1 C° (Dansgaard, 1964; Holko et al., 2012; Schürch et al., 2003).

In many IHS studies, the common practice is to use one or spatial distributed bulk samplers or one sequentially rainfall sampler to separate the hydrograph into its components. This sampling approach agrees beforehand with the the first part of the second assumption *"The isotope signature of stable isotope composition of rainfall is constant in space and time..."* (see 1.1). However, simultaneously the known spatiotemporal variability of rainfall (Goodrich et al., 1995) and its isotopic composition (McDonnell and Beven, 2014) are neglected. Disregarding the important second part of the second assumption *"..., or any variations can be accounted for"*(see 1.1) is neglected by which occurring processes are simplified and uncertainties introduced. Lyon et al. (2009) assessed the influence of the spatiotemporal variability on the pre-event water contribution of one event in a small headwater. Unfortunately, this study used only two sampling locations (two locations as bulk and one location as incremental weighing technique). Since the rainfall and its stable isotope composition can be spatially variable and the temporal accounting of event water can influence the results, the effect of the spatiotemporal variability of stable isotope composition of rainfall on the IHS results is not yet fully understood. Hence, it remains unclear how the different spatiotemporal controls, especially in steep pre-alpine headwaters with high precipitation amounts (P>2000 mm y^{-1}), affect the runoff processes during base and stormflow.

2. Scope of the thesis

2.1 General aim

Previous studies have demonstrated that a combined application of hydrometric and isotopic and hydrochemical observations has helped to advance hydrologic processes knowledge and has revealed a complexity of different temporal and spatial controls (hydrometeorological conditions and catchment properties, respectively) affecting the runoff generation during base and stormflow. Projecting the complexity of different factors to mountainous headwater catchments, with their high variability of hydrological processes and catchment properties together with the limited spatial and long-term data, means that it remains unclear how the different spatiotemporal controls affect runoff generation in this geographic setting. The general aim of this thesis was to better understand the source and flowpath of water during baseflow and discern how rainfall becomes stormflow in a pre-alpine region with high precipitation amounts (P>2000 mm y^{-1}) and heterogeneous catchment properties.

2.2 Specific research questions

The general aim of better understanding the source and flowpath of water during baseflow and stormflow was elaborated in four different articles included in this thesis where each paper had their own specific research questions.

Baseflow

To identify which sources and landscape units contribute to catchment-scale baseflow, three baseflow snapshot sampling campaigns were performed. The collected water samples were analysed for their isotopic and hydrochemical signatures to answer the following specific questions:

1. Is it possible to observe spatial patterns of streamwater composition?
2. Is it possible to relate spatial patterns of streamwater composition to (sub)catchment landscape units?
3. Are the wetlands with large storage capacity and areal extent the dominant contributing landscape unit or do other sources contribute to baseflow?

Runoff events

To better understand how rainfall becomes stormflow in a steep pre-alpine region with high annual precipitation amounts (>2000 mm y^{-1}), five neighboring headwaters with different land cover, topography and geology are investigated. Rainfall and streamwater of 13 different rainstorms were sampled and used to separate the hydrograph into its temporal components from which processes were deduced. This dataset, together with results of **paper I - Baseflow**, were used to

discern how the spatial varying catchment properties and temporal controls interact and influence runoff generation and answer the distinct questions:

1. Is it possible to observe differences in pre-event water contribution between headwaters and different events in steep and wet headwaters with variable catchment properties?

2. Is rainfall or are catchment and antecedent properties the dominant explanatory factors of pre-event water fractions in these headwaters?

Spatial rainfall

The spatial dataset of five neighboring headwaters, consisting of 8 different rainfall sampling locations and stormflow samples of different streams and events were used to assess the effects of spatial variability of stable isotope composition of rainfall on the results of an IHS and answer the specific questions:

1. What is the spatial variability of amount and isotopic composition of rainfall across a small pre-alpine headwater catchment at the event scale?

2. Is the spatial variability in isotopic composition of rainfall related to the total rainfall, rainfall intensity or altitude?

3. Does the choice of the location of the sequential rainfall sampler affect the hydrograph separation results, and if so, does this effect depend on event size.

Spectroscopy

The use of laser spectroscopes has become a popular tool to analyse the stable isotope composition water. In this analysis a memory effect, i.e. carryover of traces from the previous sample to the sample being measured, can occur. This memory effect fades away the more measurements of a sample are made. However it is not known how many measurements one must carry out in order to obtain a desired accuracy and whether there are:

1. Operational solutions to reduce the memory effect.

2. Guidance for post-processing data analysis.

Answering these open questions will increase the understanding of the spatiotemporal variability of runoff processes as a function of precipitation and catchment characteristics for this geographic setting, generalize and conceptualize findings for predicting streamflow quantity and quality of local and downstream regions. Implicitly the thesis will challenge the different assumptions (Table 1.1) which constrain the use of IHS in pre-alpine headwater catchments.

3. Materials and methods

3.1 Study area

The Zwäckentobel headwater catchment (4.25 km^2) is part of the Alptal valley (46.4 km^2) in the northern pre-alps of Switzerland and 40 km south of Zurich (see Figure 3.1). The valley has a longitudinal shape, is confined by a mountain chain of ±1500 m a.s.l. and is draining to the north. The highest mountains are the "Grosser & Kleiner" Mythen (1899 m a.s.l. and 1811 m a.s.l.) and located in the most south-western tip of the valley.

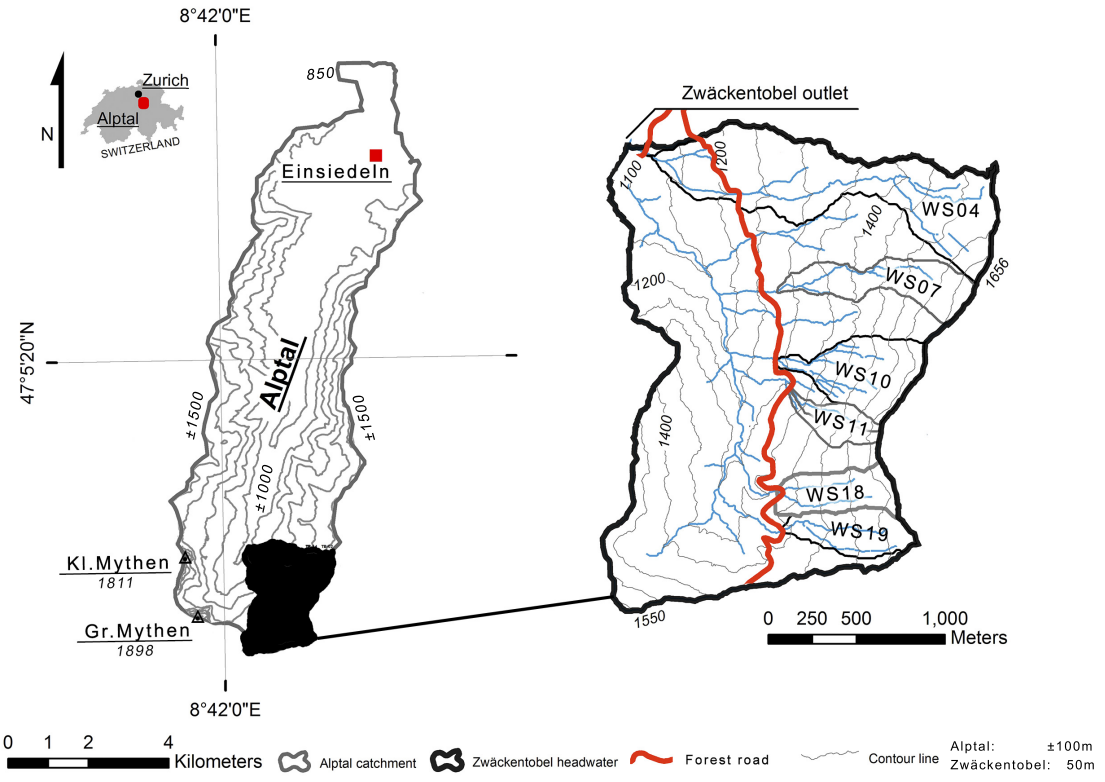

Figure 3.1: The study area - the Alptal valley and the Zwäckentobel with the different subcatchments (WS04-WS19).

The climate is humid-temperate with a mean annual temperature of 6°C (Feyen et al., 1996). The Zwäckentobel lies within a region with high precipitation 1800-3000 mm y^{-1} see Figure 3.2b. The mean annual precipitation is 2300 mm y^{-1} (Standard deviation (SD)= 250 mm y^{-1}) approximately one third of the annual precipitation falls as snow (Stähli and Gustafsson, 2006). During the snow free season (Jun-Oct) the total rainfall is on average 1300 mm with on average every second day rainfall $\geqslant$ 1 mm d^{-1}. The rainfall dominance becomes clear considering the low mean annual actual evaporation of approximately 300 mm y^{-1} (Menzel et al., 2007).

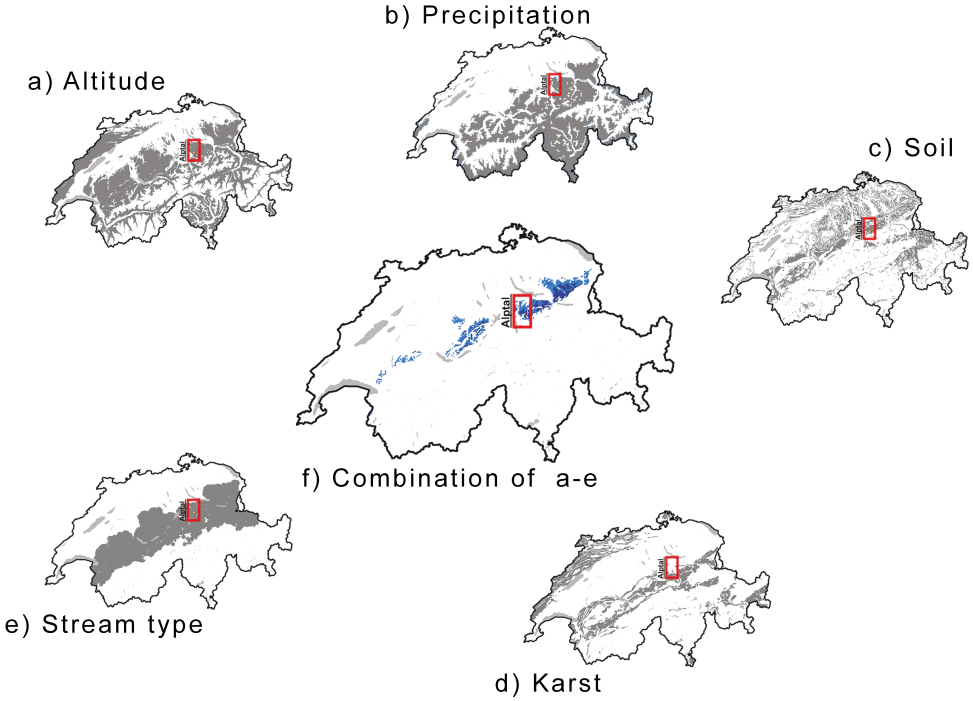

Figure 3.2: Potential similar characteristics as the Alptal (red square) - derived from available data products where the shaded area within Switzerland indicates a) altitude range 800-1900 m a.s.l. (DEM; swissDHM25; Federal Office of Topography Swisstopo, Bern), b) mean annual precipitation 1800-3000 mm y^{-1} (long term precipitation range observed at WG-01 3.4, spatial data from: mean annual corrected precipitation panel 2.2, Hydrological Atlas of Switzerland, BAFU), c) gleyic soil type (LZ 5701318903, BAFU), d) karst (overview of karst areas in Switzerland, Swisskarst-BAFU) e) Small& steep mountain stream in north alps on carbonic geology (type (LZ 5701318903, BAFU) and f) the combination of panel a to e indicating region with similar characteristics as the Alptal.

The Zwäckentobel headwater is a south-north oriented headwater with an altidue range between 1084 and 1656 m a.s.l., with along their main axis steep slopes of more than 20° which are alternated by flatter areas. These flatter areas originating from erosion deposits such as soil creep and landslides. Streams are steep and incised and therefore lacking a riparian zone along the channel network (Hagedorn et al., 2001). The Zwäckentobel headwater catchment consisting of different small mountain streams (WS04-WS19) with a step-pool channel morphology (Keller, 1970; Molnar et al., 2010) (see Figure 3.1 and 3.2e for an overview of small & steep mountain streams in Switzerland). The east facing side of the Zwäckentobel is steep sloped with frequent landslides and has an ephemeral stream network. The perennial streams have a nivo-pluvial préalpin regime (Schaffner et al., 2013) with winter low-flow (Nov-Mar), spring snowmelt (Apr-May) and stormflow during summer (Jun-Oct). During events the streams respond quickly to rainfall and flow increases by several orders of magnitude with high sediment transport rates (Turowski et al., 2009). The streams return to baseflow within approximately one day.

Land use and land cover

Forest is the dominant land cover in the Zwäckentobel and is generally located on the steep slopes. The Norway spruce (Picea abies) is the dominant specie and has a root depth approximately one metre with a plate shaped root network. The non-forested more gentile sloped areas are swampy meadows or wetlands (Rinderer et al., 2012) with some bushes or isolated trees. The subcatchment WS04 to WS07 have a mixed land cover of forest and meadows and one third of the area is covered by wetlands. The central part of the Zwäckentobel is dominant forested with wetlands only in the upper region near the water devide. WS18 and WS19 are covered by meadows with large area of wetlands. The meadows in WS18, WS19 and the upper part of WS04 and WS07 are used as alpine pastures from July until September. The land cover was classified into forest, partly forested and meadow and delineated by Fischer et al. (2015) from an aerial photo (Swiss Federal Office of Topography, 2005) see Figure 3.3a. The wetlands were derived from the available Swiss Cantonal wetland inventory (Swiss Federal Office for Environment, 2007) see Figure 3.3a and Table 3.1.

Geology

The geology of the Zwäckentobel is Tertiary flysch consisting of three sedimentary facies see Figure 3.3b and Table 3.1. Waegitaler flysch is cross layered consisting of sandstone-chalk-marl layers with a dominant north-south orientation. Wild flysch is a thin layered marl-slate with inclusions of external formation such as granite, quartz, dolomite sandstone, conglomerate and brekzien. Schlieren flysch is a regular layered sandstone-marl with a west-east orientation (Hsü and Briegel, 1991; SZNG, 2003). The different flysch classes have different patterns of faults and fissures which can contain groundwater (Brönnimann et al., 2013; Spreafico and Weingartner, 2005). The three different facies of Wild-, Waeggitaler- and Schlieren flysch were digitized from a geological map (Hantke, 1967). Ontop of the flysch parent material are shallow and creeping soils (0.5-2.5 m in depth). The spatial distribution of shallow soils was derived from a geological map with an additional DEM-analysis where slopes <20° were set to a soil depth of 1 metre. This was then spot checked with a hand auger in the field and resulted in an estimate of the shallow soil information (depth <1 m or >1 m) 3.3b. The soils consist of a B_g-horizon with high silt and clay content and the A-horizon of 20-50 cm Muck or Mor humus (Feyen et al., 1996). The clay layer has low matrix permeability but a high drainage capacity in macropores (Feyen et al., 1996). For a more detailed soil description see Feyen et al. (1996) and Figure 3.2c & d for Gleyic soils and Karst in Switzerland respectively.

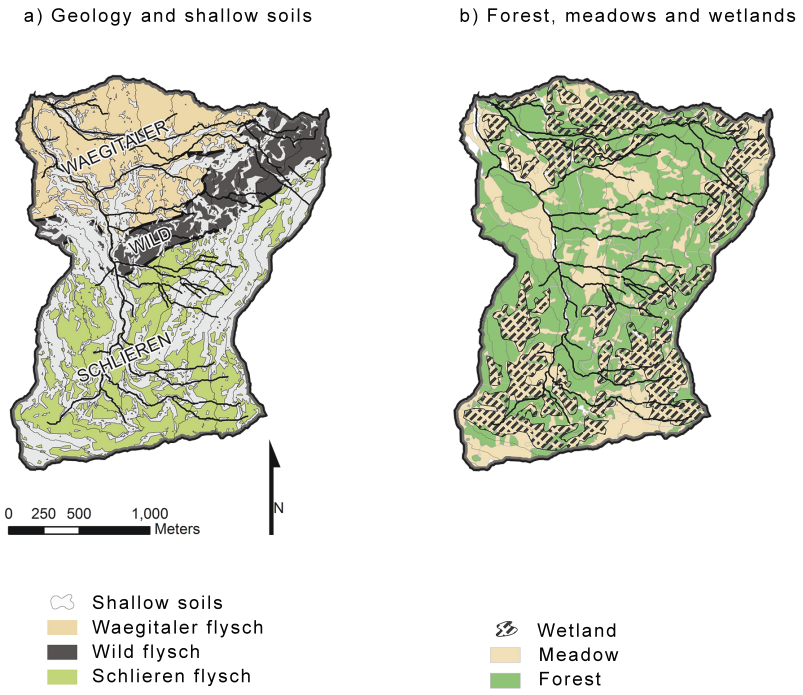

Figure 3.3: The Zwäckentobel - a) land cover: forest and meadows with hatched areas indicating wetlands and b)geology: three different types of flysch and on top the shallow soils ≤ 1 m indicated as hatched areas.Color scheme of Figure 1a and 1b adapted from ColorBrewer. Figure adapted from paper I to III (Fischer et al., 2015, 2016a,b).

3.1.1 Hydrological studies in the Alptal

Catchment scale hydrological studies have a long history in the Alptal (Hegg et al., 2006). The interaction of hydrology and catchment characteristics was studied in the Alpal by comparing hydrochemical components at the outlet of five different headwater catchments (±1 km^2) (Keller, 1970, 1990). Differences in hydrochemical components could be related to differences in land cover, soil type and geology. For a short period between 1971 and 1973, daily water level data were recorded in the Zwäckentobel headwater catchment, minus the Erlenbach (Burch, 1994). A large flood in 1974 destroyed most of the hydrological installations where after only three headwaters catchments were restored with a more permanent character, of which one was the Erlenbach catchment (Hegg et al., 2006). In the 0.7 km^2 Erlenbach headwater catchment (WS04) are since 1964 to present different hydrometeorological and hydrochemical data collected. Furthermore is the Erlenbach part of the National River Monitoring and Survey program (NADUF) program where different water samples are collected to analyse on different hydrochemical variables are collected (Hegg et al., 2006; Schleppi et al., 2006). The data availability forms a good condition and explains the different studies in different fields of research (Hegg et al., 2006). In the Erlenbach catchment, a more detailed bottom up study on runoff processes in three different spatial scales 2x13 m^2 , 3x1500 m^2 and 0.7 km^2 with different tracers (EC, Br and Cl) were performed (Feyen et al., 1996, 1999; Feyen, 1998). Fast flow path in macropores like cracks in fissures were identified. It was found that the runoff dynamics is soil type independent but more related to the type of top soil manifested as saturated areas in the depressions. These wetlands are badly drained and less connected to the deeper soil layers while flow processes are in parallel to the slopes orientated macropores, a fast response with direct contribution of rainfall to runoff and assumed short residence times. The better drained and drier forest soils respond delayed with a larger mixing of soil water and longer residence times. The runoff

Table 3.1: The characteristics of the Zwäckentobel and its subcatchments WS04 to WS19

			ZT	WS04	WS07	WS10	WS11	WS18	WS19
Shape	Size	[km^2]	4.25	0.7	0.21	0.23	0.09	0.15	0.15
	H_{max}		1656	1656	1656	1598	1583	1598	1598
	H_{mean}	[m]	1360	1342	1468	1432	1421	1476	1494
	H_{min}		1084	1109	1262	1276	1292	1351	1384
	Slope max/mean	[°]	56/19	49/17	47/21	53/23	45/24	42/20	43/18
Geology	Wägitaler flysch		29	64	16	0	0	0	0
	Wild flysch	[%]	17	29	42	0	0	0	0
	Schlieren flysch		54	7	42	100	100	100	100
	soils<1m	[%]	29	44	55	73	74	59	49
Landuse	Dense forested		55	53	53	72	81	38	18
	Partly forested	[%]	21	22	27	14	10	10	1
	Meadow		24	25	20	14	9	52	81
	Wetland	[%]	29	33	28	23	21	57	51

processes in the different plots is almost similar where three quarter of the runoff occurred in the gleysol, twenty percent from the A-horizon and only five percent from surface runoff. The spatial distribution of wetlands has an important role in runoff generation processes. At the Erlenbach headwater scale, two dominant runoff processes were identified and composed two parallel flow processes, one dominant at the surface or near-surface runoff from wetland areas (fast process) with dominant event water contribution and smaller second contribution by subsurface flow in the macropores of the subsoil (slow process). At plot scale similar results were found in a neighbouring headwater, the Vogelbach (1.55 km^2), obtained from a sprinkling experiment using bromide with numerical modelling (Weiler et al., 1998). Meadows showed bypass flow in vertical macropores from worms and horizontal from mouse burrows which act in the soil A-horizon) as the major contributing layer to the measured runoff. Forest soils have well developed dense lateral and vertical net of pores and channels forms by plants roots with a bimodal flow system of matrix and mesopores. Additionally a hydrograph separation using bromide from a high intensity sprinkling experiment (60 mm h^{-1}) in a forested site was used to identify process water contribution in stream flow (Weiler et al., 1999). From these experiments it was observed that event water was rapidly delivery by preferential macropores flow and increased with increasing rainfall sums. Rinderer (2015) performed in WS07 (Figure 3.1) a spatial groundwater study and observed that in catchments with steep slopes and shallow soils the topography was a good predictor of groundwater levels and response timing of groundwater levels. Furthermore a new quick and inexpensive field method to classify soil moisture of wet environments was developed by Kollegger (2010) and tested by Rinderer et al. (2012).

3.2 Instrumentation

In addition to WS04 (0.7 km^2, concrete flume with long-term stage/ discharge data), in the year 2009 the Zwäckentobel and its internal perennial streams were gauged. For this, the Zwäckentobel was bi-weekly visited and explored along the road (through the headwater catchment, Figure 3.1) to distinguish between ephemeral and perennial streams. From the approximately 21 streams, the perennial streams WS06, WS07, WS08, WS10, WS11, WS18, WS19, WS20, WS21 were identified. Most of these subcatchments are west facing and oriented parallel to each other. Their shape is either longitudinal or fan like and their size ranges between 0.09-0.21 km^2 (Figure 3.1 and Table 3.1). In the streams of the Zwäckentobel outlet and the subcatchment WS06-WS21, large and stable rocks were used, to install the stream gauges. These gauges consisted by a horizontal steel support arm and vertical stilling well containing the water level loggers. After a destructive flood on 1 August 2010 only six subcatchments (discharge of WS04 and stream flow stage of WS07, WS10, WS11, WS18 and WS19) remained functioning (Figure 3.3a). The

newly gauged streams were equipped with a Keller DCX-22 (Keller AG Switzerland). The different subcatchments were monthly visited for data collection and calibration measurements. Establishing rating curves was tried but appeared to be impossible due to frequently changing stream morphologies. These remaining subcatchments are considered to represent the variability of the different catchment characteristics of the Zwäckentobel. For the Zwäckentobel and its subcatchments different catchment characteristics such as area (km^2), altitude (m a.s.l.) and slope (°) were derived from a digital elevation model (DEM; 2 m resolution; Swisstopo, 2002) using the Whitebox Geospatial Analysis-D8 flow pointer tool (Lindsay, 2009) see Table 3.1.
From 1964 until 2009, two rain gauges situated in the Erlenbach catchment (WS04) measured the precipitation input (WG-01; Ott Pluvio, OTT Hydrometrie AG, Switzerland and TB-14; Joss-Tognini tipping bucket, Lamprecht meteo, Germany Figure 3.4b). To measure the spatial rainfall input of the Zwäckentobel, 13 additional rain gauges were installed (Davis II rain collector-tipping bucket; Davis Instruments Corp., USA with Odyssey data logger; Dataflow Systems, New Zealand see Figure 3.4b). These rain gauges were distributed over the Zwäckentobel to identify potential rainfall gradients and altitude differences. The locations were in the open field at a height of 1.5 m above ground level and measured rainfall during the period 2009-2011. The barometric pressure and air temperature were measured at two sheltered locations near WG-01 and WS19 (Keller DCX-22, Keller AG Switzerland, Figure 3.4b). The in this study used groundwater level data was measured in the vicinity of WG-01. Groundwater level data have been measured since 1992 in a screened groundwater well and an Ott-groundwater data logger (OTT Hydrometrie AG, Switzerland, Figure 3.4b).

3.3 Water sampling

3.3.1 Baseflow

To investigated the spatiotemporal differences in baseflow isotope and hydrochemistry three spatially distributed baseflow snapshot sampling campaigns were performed and used in **paper I - Baseflow** (Fischer et al., 2015). Campaign C-1 was held on 19 November 2010, at the end of the summer season had an early snow cover and was representative of early winter baseflow conditions; C-2 on 7 June 2011, shortly after all snow cover had melted was characterized by short dry spells and higher groundwater levels; and C-3 on 18 October 2011, in autumn with longer dry spells and lower groundwater levels. Due to short dry spells it was important to collect all samples in one day and restricted the sample number to 110. Distributed discharge measurements could not be performed for logistics and practical reasons. Each campaign had 110 predefined sampling points (Figure 3.4a). These sampling locations were selected by following the stream network of the different subcatchment outlets upslope to the water divide. Perennial key locations were chosen at the confluences of different branches (n=65 of which eight samples were taken along an artificial drainage ditch from a wetland (W) within WS04), springs (n=29) and groundwater wells in WS07 (n=16) (Figure 3.4a). Groundwater samples were taken from fully-screened wells with an average depth of about 1 m (for details on the groundwater observation network see (Rinderer et al., 2012). The water samples were collected by five sampling teams which visited each 10-20 sample points which were located with a handheld GPS (Garmin GPSMAP 60CS, field accuracy ±8m). At each sampling location a 20 ml sample for stable isotope analyses (20 ml glass vial with cap and additional Teflon/rubber septum) and a 250 ml sample for hydrochemical analyses (250 ml PE bottle with cap) were taken. A grab sample was taken in stream while in groundwater wells a inertia pump was used to collect the water. In springs with low discharge (10-100 ml s^{-1}) a syringe was used to suck up the water and prevent sample contamination. Depending on the availability of water the number of samples were for C-1 46 samples and for C-2 & C-3 more than 80 (Table 3.2).

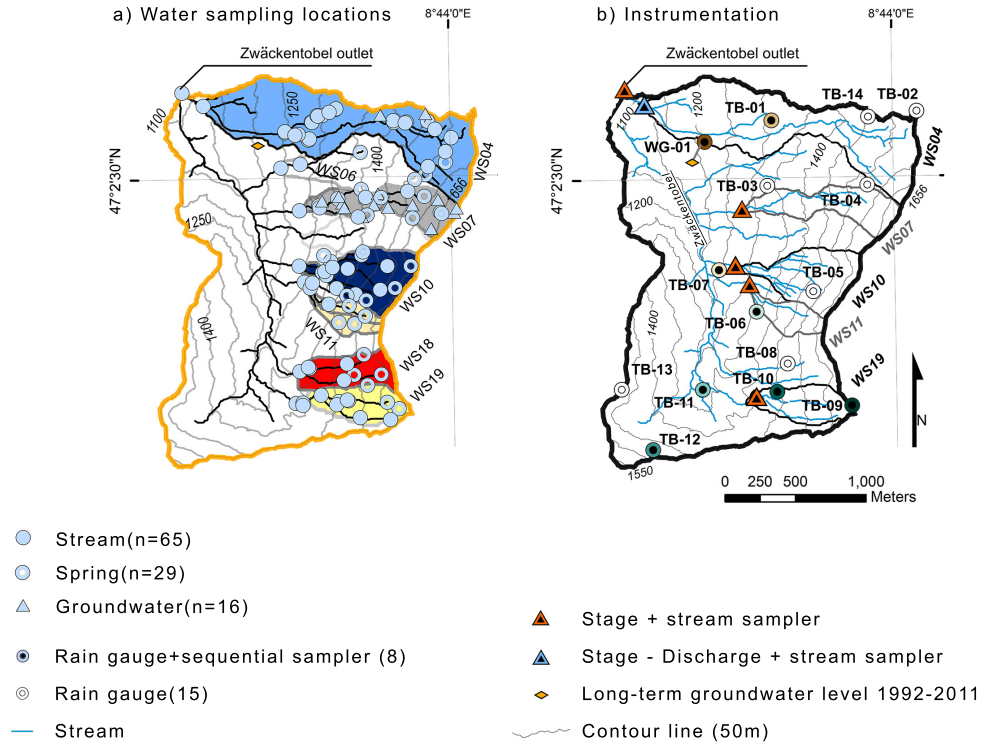

Figure 3.4: Sampling locations of the Zwäckentobel - a) baseflow snapshot sampling campaigns in selected subcatchments WS04, WS07, WS10, WS11, WS18 and WS19 and b) instrumentation and stormflow sampling locations in selected headwaters WS04 to WS19. Adapted Figure 1, **paper I - Baseflow** and **paper II - Runoff events** (Fischer et al., 2015, 2016b).

Table 3.2: Sample number for the three snapshot campaigns of the Zwäckentobel outlet (ZT) and its subcatchments WS04 to WS19

		Tot.	ZT	WS04	WS7	WS10	WS11	WS18	WS19
C-1	(19.11.2010)	46	1	7	14	12	5	0	7
C-2	(07.06.2011)	82	1	16	20	16	8	6	15
C-3	(18.10.2011)	84	1	24	20	14	7	8	10

3.3.2 Event sampling

To assess the differences in pre-event water contribution of different headwaters and different events different rainfall-runoff events were sampled in headwaters WS04, WS07, WS10, WS11 and WS19, during the snow free season of 2010 and 2011 (Table 3.3). These headwaters were selected due to cover all the different catchment properties such as mixed land cover, forest and meadows respectively. A rainfall-runoff event was defined as: precipitation of more than 0.2 mm h^{-1}, dry spell window of less than 24 h and a stream response which is larger compared to baseflow. Before and after every rainfall event a baseflow grab samples was taken from the different headwaters. This water sample represents the pre-event water composition. During events the rainfall and streamflow were sampled with automatic samplers.
Rain water samples for isotope analysis were collected at eight locations with a volume based sequential rainfall samplers (Figure 3.4b). The sequential samplers functioning according to the sampler of Kennedy et al. (1979) but were modified to improve sample handling and logistics. Each sampler contained 12x100 ml honey jars, each representing 5 mm of rain water. The bottles were enclosed in a box as protection and to minimize solar radiation. The rainfall was collected with an adapted tipping bucket. Each tip of the bucket guides water via two funnels and a tube

into the sampler. Inside the sampler after the first bottle is filled the following bottles are filled with cascading principle without mixing of the 5mm increment samples. The sampling design was restricted by logistics because all samples needed to be collected during one day to avoid fractionation; therefore sequential rain sampler were not installed in the upper part of WS04 and WS10 (Figure 3.4b).
Stormflow samples were collected at the catchment outlets of WS04, WS07, WS10, WS11 and WS19 with automatic samplers (ISCO 6712 with 24x1 L-bottles and Liquid Level Actuator, Teledyne Isco, USA, Figure 3.4b). During an event, once the water level of the streams rose more than 1 cm, the different automatic stream samplers were actuated. The sampling program A was programmed that during the rising limb six samples were collected with an interval of 10 min. Hereafter program B was set up that the remaining 18 samples were taken with an hourly interval. This sampling scheme was chosen such that the rising limb was sampled with a high temporal resolution, while taking at least one sample as close as possible to the maximum discharge peak. In large events it was tried to collect all the water samples, the automatic samplers were reprogrammed and restarted (sampling interval 120 or 240 min) to capture the full event. During and or after an event all rainwater and stream samples were bottled in a 20 ml-glass for transport and storage (20 ml-glass with cap and additional Teflon/rubber septum). To prevent future water samples to be contaminated from water samples from a previous event, it was tried to remove all excess water from the sampling equipment (e.g. sampler tubing, bottles and tipping buckets). The high sediment concentration during stormflow or sudden water level rise could (e.g., air bubbles) caused a malfunctioning of the liquid level actuators of the automatic samplers. Additional power failures occurred when temperatures fell below 5°C. These malfunctions resulted that not all events were sampled equally for all streams. The number of water samples for stable isotope analysis per stream and event ranged from 7 samples (short events) up to 54 samples (long events). The number of sampled events varied per stream from 6 to 11 see Table 3.3. With the view on the analysis technique (Cavity Ring-Down Spectroscope) no oil was used to avoid sample contamination (Wassenaar et al., 2014) and facilitated in an improved sample handling. Instead of using oil in rain and stream water sample bottles, rather all samples were directly after a rainfall event collected to minimize fractionation.

3.4 Laboratory methods Paper I - III

All collected baseflow samples for the analysis on hydrochemcial variables were filtered and stored cool prior to analysis with a 0.45 µm filter (⌀47-mm cellulose filter paper, Whatman Germany). The 250-ml water samples were analysed for hydrochemical variables Ca, DOC, (EC, pH, alkalinity (AT), total hardness (TH), Cl, NO_3, SO_4, Na, K, Mg and H_4SiO_4 at the laboratory of the Swiss Federal Institute of Aquatic Science and Technology (EAWAG). The collected baseflow and event water samples were filtered (0.45 µm filter 25 mm PTFE Syringe Filter, Simplepure USA) and pipetted in a vial (1 ml water into a 1.5 ml 32×11.6 mm screw neck vials with cap and PTFE/silicone/PTFE septa) and stored cool prior to analysis. The sampled water was analysed for their stable isotope composition at the stable isotope laboratory of the University of Zurich, Department of Geography. For this a Cavity Ring-Down Spectroscope-Picarro L1102-i Liquid Analyser (1^{st} generation analyser, Picarro Inc., 2008) was used. The analysis scheme of Penna et al. (2010) and **paper IV - spectroscopy** (Penna et al., 2012) were followed where the to be analysed samples were "sandwiched" between two sets of standards (Table 3.4). These laboratory standards consisted of desalinated North sea water (δ^{18}O -0.04(0.3)‰, δ^{2}H 0.3(0.2)‰), filtered Findelen glacier water (δ^{18}O -15.19(0.04)‰, δ^{2}H -111.9(0.1)‰) and Dagmar-tap water as control standard (δ^{18}O -10.78(0.04) ‰, δ^{2}H -77.7(0.1)‰) . Each sample was measured six times. The first three samples were rejected due to potential memory effects while the remaining measurements were averaged in order to obtain the isotopic value of the sample. The precision of the measurement was derived by the standard deviation of the remaining three samples. All measured isotope composition were corrected and reported as δ-values in per mille (‰) relative

Table 3.3: Hydrometeorological characteristics, number of rainfall and number of stream samples of the thirteen sampled events.

event nr.	1	2	3	4	5	6	7	8	9	10	11	12	13
year	2010				2011								
day-month	8 Sep	17 Sep	24 Sep	4 Oct	29 Jun	8 Jul	14 Jul	15 Aug	24 Aug	27 Aug	4 Sep	18 Sep	6 Oct
Event characteristics													
A_{DS} [d]	7	1	5	2	3	5	1	2	3	0	0	1	14
A_{PI7} [mm]	2	50	6	10	24	5	41	23	2	10	9	26	0
A_{GL1} [cm]	-34	-23	-28	-19	-28	-36	-12	-28	-38	-41	-37	-23	-42
A_{Q1} [l s$_{-1}$km$_{-2}$]	7	16	3	7	10	7	11	7	1	4	0	13	1
P_{length} [h]	10	8	70	10	23	11	30	37	2	19	11	11	33
$P_{mean\ tot.}$ [mm]	22 (2.6)	11 (1.4)	109 (16)	10 (1)	84 (19)	25 (1.5)	56 (17)	50 (15)	11.8 (2)	20.4 (1)	51 (11)	25 (2)	31(12)
P[mm h^{-1}]	2.2(0.3)	1.3 (0.2)	1.5 (0.2)	0.9 (0.1)	3.6 (0.9)	2.5 (0.2)	2 (0.6)	1.4 (0.4)	6 (1)	1 (0.1)	1.9 (0.4)	1.6 (0.2)	0.9 (0.4)
P_{max} [mm h^{-1}]	4.5 (0.6)	2.3 (0.3)	7.6 (1.1)	2.4 (0.4)	18 (8.4)	9 (0.9)	6.7 (1.6)	10 (2.7)	10 (3)	7.3 (0.7)	7 (1.4)	6 (1.4)	8.6 (3.5)
$H_{responds}$ [h]	0.6 (1)	1 (0.6)	0.2 (0)	0.3 (0.3)	0.2 (0.1)	0.1 (0.1)	0.3 (0.2)	0.7 (0.3)	0.1 (0.1)	0.4 (0.3)	0.3 (0.2)	0.3 (0.2)	1.3 (0.5)
Q_{peak} [l s^{-1} km^{-2}]	353	106	1010	53	3004	390	1197	1287	86	334	589	504	509
Q/P [-]	0.35	0.36	0.7	0.29	0.6	0.25	0.68	0.55	0.12	0.25	0.52	0.52	0.28
Number of rainfall samples													
WG-01		4	25	2	11	4	4	9	4	5	11	4	3
TB-01	5	3	12*	2		6	12	0					
TB-06	4	3	19	3	10	4	9	7	5	4	12	3	
TB-07	5	3	18	3	6		7	8	4	4	11	5	5
TB-09	5	4	9*	3		4	5	6		3	4*	5	
TB-10	5	3	5*	3	5		11		3	4	12	5	7
TB-11	5	4	13*	3	11	4	12	10	3	3	4*	4	
TB-12	4	3	13*	2		6	12	9	3	4	9		
Number of stream samples													
WS04		23	46		23	15	26	45	10	20	26	29	21
WS07	24		49		34			9				24	20
WS10	24		53	24	35		7	6	8	10	20	23	24
WS11			54				15	15	20		23	18	24
WS19	24	23	54	24	34	13						22	23

Table 3.4: "Sandwich" analysis scheme with deionized water (DW), standard (STD) and sample (S)

DW	STD1	STD2	STD3	S5	S4	S3	S2	S1	STD1	STD2	STD3	S6	S7	S8	S9	S10	STD1	STD2	STD3

to Vienna Standard Mean Ocean Water (VSMOW). Most samples could be measured with a precision for δ^2H of < 0.5‰ and for δ^{18}O of < 0.1‰. Due to some technical issues with the spectroscope, for some samples the accuracy for δ^2H >0.5‰ while for δ^{18}O it remained <0.1‰. The sample accuracy was assessed by reanalyzing, a randomly selected subset of all samples, at the stable isotope laboratory of the University of Freiburg im Breisgau. Most samples deviated <0.1 ‰ for δ^{18}O and <1 ‰ for δ^2H.

3.5 Data analysis

3.5.1 Paper I - Baseflow

The three snapshot campaign datasets, consisting of selected isotopic and hydrochemical variables, were in **paper I - Baseflow** (Fischer et al., 2015) investigated to understand whether spatial patterns of streamwater composition could be observed. The spatial variability of different hydrochemical variables was assessed by representing the streamflow, geology, organic matter (δ^2H, Ca and DOC respectively) as sampled throughout the Zwäckentobel.

The same variables (δ^2H, Ca or DOC) were used to assess the mixing along the stream network, where the variability is expressed for each variable of each sample point as a function of different upslope controlling landscape features such as the catchment area, altitude, slope, topographic wetness index, land cover (forest, meadow and wetland), geological facies and shallow soils. For every sampling point the local and different upslope controlling landscape features were derived such as the area (km^2), altitude (m a.s.l.), slope (°) and, topographic wetness index using a Geographic Information System (GIS) framework. Additionally, for each sampling location the upslope percentage of forest, meadow and wetlands were derived from the land cover map. The percentage of the different types of geology and shallow soils was derived from the geological map and the estimated shallow soil information Figure 3.3b.
Bivariate solute diagrams (Ca, DOC) and a PCA (δ^2H, Ca, DOC, AT, SO_4, Mg and H_4SiO_4) were used to examine the hydrochemical mixing and investigate spatiotemporal patterns of the isotopic and hydrochemical variables. The different diagrams of the different campaigns were compared to give an indication of hydrochemical compositions. Only the two end-members groundwater and springs were available to explain streamflow. This restriction by the sampling design conditioned to use the information as an explorative element explaining the contribution to streamflow. Because of the snow cover and the reduced number of sampling points campaign C-1 was excluded from the presented analyses and the focus was on campgain C-2 and C-3.

3.5.2 Paper II - Runoff events

Isotope hydrograph separation

In **paper II - Runoff events** (Fischer et al., 2016b) the collected baseflow samples and event samples of rainfall and stormflow were used to assess the differences in pre-event water , f_{PE} contribution in storm runoff between the different headwaters and different events. As central method was the, by Sklash and Farvolden (1979) first applied, two end-member mass balance approach (IHS see eq. (3.1) and eq. (3.2)) used to derive the fraction of pre-event water f_{PE} during stormflow.

$$Q_S = Q_E + Q_{PE} \tag{3.1}$$

$$f_{PE} = \frac{C_S - C_E}{C_{PE} - C_E} \tag{3.2}$$

The symbol Q indicate streamflow [l s^{-1}], C describes the stable isotope composition [‰] and the subscripts S, PE and EC represent streamflow, pre-event water (baseflow prior to the event) and event water (rainfall) respectively. The incremental intensity mean (McDonnell et al., 1990) was used to account for the event water eq. (3.3). Here I_i is the rainfall intensity [5 mm T^{-1}] and δi is the stable isotope composition of the accompanying precipitation. Some sequential rainfall samplers malfunctioned during some events. Therefore the nearest sequential rainfall sampler, which sampled the majority of the events, was assigned to each headwater (WG-1 for WS04 and WS07, TB-6 for WS10 and WS11 and TB-10 for WS19) to be used in the IHS with eq. (3.3) and used in eq. (3.2).

$$C_E = \frac{\sum_{i=1}^{n} I_i \delta_i}{\sum_{i=1}^{n} I_i} \tag{3.3}$$

For each of the thirteen events, the uncertainty of the pre-event water contributions was quantified based on eq. (3.4) (Genereux, 1998) with a confidence level of 0.05. The symbols $W_{f_{PE}}$, f_{PE} and f_E represent the uncertainty in the pre-event water, and the fraction of pre-event and event water respectively. W_{C_E} is the uncertainty in event water and estimated using the standard deviation of the collected stable isotope composition of the nearest sequential rainfall sampler. To quantify the uncertainty of pre-event water W_{C_P} the stable isotope information of campaign C-2 and C-2 collected in **paper I - Baseflow** (Fischer et al., 2015) was used. For each headwater catchment the baseflow samples within the catchment were used to calculate the standard deviation of the stable isotope composition. For streamwater the uncertainty, W_{C_S}, was based on the laboratory precision of repeat measurements.

$$W_{f_{PE}} = \left\{ \left[\frac{f_E}{C_E - C_{PE}} W_{C_E} \right]^2 + \left[\frac{f_{PE}}{C_E - C_{PE}} W_{C_{PE}} \right]^2 + \left[\frac{-1}{C_E - C_{PE}} W_{C_S} \right]^2 \right\}^{\frac{1}{2}} \tag{3.4}$$

Data analysis

Next to the derived f_{PE} for each sampled event, three proxies were used to describe the antecedent conditions of the headwaters (Table 3.3). Based on rain gauge WG-01 (1998-2011), the antecedent precipitation index, with seven days prior to an event (A_{PI7}), was calculated. Additionally the antecedent discharge (A_{Q1}; WS04) and groundwater level (A_{GL1}; long term groundwater well near WG-01) were derived, both for one day prior to an event. Using the rain gauge network (14 rain gauges) for each event the mean and standard deviation of different rainfall characteristics were derived. Because only in WS04 discharge data was available, this headwater was used as a reference and proxy indicating the event magnitude (maximum discharge Q_{max}) and runoff coefficient for the adjacent headwaters. For the runoff coefficient baseflow was subtracted from the total stormflow and divided by the event total rainfall, analogous to Burch et al. (1996). As baseflow a straight line from the rise of the hydrograph to the inflection point where the hydrograph in the semi-logarithmic domain flattens was assumed. For every event, the exceedance probabilities of maximum event discharge (WS04, 1998-2011) and event total rainfall (WG-1, 1998-2011) were determined.
For each event the hydrograph, precipitation, air temperature, stable isotope and calculated pre-event water were represented. Additionally the f_{PE} (near the maximum discharge) of the different headwater and events were related to rainfall characteristics, antecedent conditions and

baseflow, one day before an event (WS04). To asses the influence of different processes and antecedent conditions on the f_{PE} different types of linear and multiple linear regression were performed. For each type, the rainfall characteristics, antecedent conditions and baseflow one day before an event (WS04), were added stepwise to relate to the observed minimum f_{PE} to explain differences in pre-event water.

3.5.3 Paper III - Spatial rainfall

Accounting for spatiotemporal variability in the isotopic composition of rainfall in isotope hydrograph separation

In **paper III - Spatial rainfall** (Fischer et al., 2016a) the effects of the spatiotemporal variability in the isotopic composition of rainfall and its effect on the IHS results is examined. As base of this study served the in **paper II - Runoff events** (Fischer et al., 2016b) sampled events. In this study the headwaters with most sampled events were used, i.e., WS04, WS10 and WS19. Instead of using only three sequential rainfall samplers all eight samplers were used to asses the spatiotemporal variability in the isotopic composition of rainfall. With exception of the sequential samplers of WG-1, TB-6 and TB-10 some sequential samplers malfunctioned in event 7, 8 and 13 and were therefore excluded from this analysis (to have as many samplers as possible).The event 3 and 5 had four rain samplers but to illustrate the rainfall pattern of these large events, these event not rejected and included in this analysis.
In order to determine which rain gauge was most representative for the Zwäckentobel catchment, we calculate the Mean Relative Difference $(\mathrm{M}_{RD})_j$ for event total rainfall using the method of Vachaud et al. (1985):

$$M_{RD_j} = \frac{1}{Z} \sum_{t=1}^{Z} \frac{P_{j,t} - \overline{P_t}}{P_t} \tag{3.5}$$

The M_{RD_j} in 3.5 is the M_{RD_j} for rain gauge j, $\mathrm{P}_{(j,t)}$ is the rainfall measured at rain gauge [mm] j for event t, $\overline{P_t}$ is the average rainfall for all rain gauges for event t, and Z is the number of events (Z=10). The M_{RD_j} of the event average isotopic composition of rainfall was calculated similarly. The effect of the spatiotemporal variability of isotopic composition of rainfall of the 10 rainfall events was examined and related to different variables such as total rainfall, intensity or altitude. The effect of the observed spatiotemporal variability of isotopic composition of rainfall on the IHS was assessed separately as 1) temporal and 2) spatial influences. The temporal effect of the spatiotemporal variability of isotopic composition of rainfall was examined by using different temporal weighing techniques used in eq. (3.2) as described by (McDonnell et al., 1990) technique: (I) weighted mean value eq. (3.6), (II) intensity mean eq. (3.7), (III) incremental mean eq. (3.6) and (IV) incremental intensity mean eq. (3.7). Here P_i is the rainfall amount [mm] of sample i to n, I_i is the rainfall intensity [5 mm T^{-1}] and δ_i is the stable isotope composition of the accompanying precipitation of sample i to n.

$$C_E = \frac{\sum_{i=1}^{n} P_i \delta_i}{\sum_{i=1}^{n} P_i} \tag{3.6}$$

$$C_E = \frac{\sum_{i=1}^{n} I_i \delta_i}{\sum_{i=1}^{n} I_i} \tag{3.7}$$

The spatial effect of the spatiotemporal variability of isotopic composition of rainfall on the IHS was examined by using all eight rainfall samplers. In rotation all of the eight rainfall samplers with the temporal weighing technique IV eq. (3.7) were used in eq. (3.2) to calculate different fraction of pre-event water in WS04, WS10 and WS19 for all events.

Table 3.5: The isotopically depleted samples (derived from snow surface samples collected at different locations in Antarctica, provided by the Isotope Geochemistry Laboratory of the University of Trieste) and laboratory standards (in relation to the VSMOW-SLAP scale (IAEA, 2009)). The reported values are measured using a IRMS represent the average and the standard deviation of ten replicates.

ID	δ^2H (SD) [‰]	δ^{18}O (SD) [‰]
1	−231.7 (0.5)	−29.83 (0.02)
2	−258.7 (0.4)	−33.07 (0.01)
3	−277.5 (0.5)	−34.96 (0.02)
4	−303.8 (0.4)	−38.26 (0.03)
5	−312.2 (0.6)	−39.47 (0.02)
6	−334.7 (0.4)	−42.24 (0.02)
7	−338.5 (0.5)	−43.73 (0.02)
8	−373.1 (0.4)	−48.02 (0.02)
9	−390.4 (0.5)	−50.20 (0.02)
10	−421.1 (0.5)	−53.41 (0.02)
STD1	−221.8 (0.5)	−29.06 (0.04)
STD2	−313.8 (0.4)	−40.22 (0.02)
STD3	−422.8 (0.4)	−53.83 (0.02)

3.5.4 Paper IV - Spectroscopy

Laser spectroscopes and mass spectrometer

Ten different depleted water samples (see Table 3.5) were analysed using six laser spectroscopes of different manufacturers and generations (see Table 3.6, three Off-axis integrated cavity output spectroscopy (OA-ICOS): Delft University of Technology, the Netherlands, Czech Technical University in Prague and Czech Geological Survey, Czech Republic; three Cavity ring-down spectroscopy (CRDS) instruments: University of Trieste, Italy, University of Zurich, Switzerland, International Atomic Energy Agency, Vienna, Austria) and one Isotope-ratio mass spectrometers (IRMS) used as reference (University of Trieste). For the analysis in all the used instruments a new syringes was used and the spectroscopes were operated according to the manufacturers recommendations. For each analysis run the injection port septums were replaced and in machines with transfer lines and injection blocks, these components were cleaned. Information regarding the theory of operation of the two laser spectroscopes is reported elsewhere (OA-ICOS: Sayres et al. (2009)and Wang et al. (2009) and CRDS: Brand et al. (2009) and Gkinis et al. (2010)).

Samples and analysis scheme

The preparation of water samples and standards (pipetting of 1 ml water into a 1.5 ml 32×11.6 mm screw neck vials with cap and PTFE/silicone/PTFE septa) was performed in one laboratory to ensure quality of the samples. The analysis of the samples followed the procedure suggested by the Isotope Hydrology Laboratory at the International Atomic Energy Agency (IAEA) IAEA (2009) and Penna et al. (2010). The to be analysed samples were ”sandwiched” between two sets of standards (STD1 & 2 Table 3.4 and 3.5) where each vial was measured 18 times. These standards were used in a linear regression, where the intercept and slope are used to calculate the unknown composition of the ”sandwiched” samples. A third standard was used as a control standard (STD3, Table 3.4 and 3.5). The isotopic composition of the different samples had a wide range where the smallest difference between samples was 2‰ for δ^2H and 1‰ for δ^{18}O while the largest differences between samples was 201‰ for δ^2H and 25‰ for δ^{18}O (3.5). The memory effect was computed as described by Gröning (2011) by assuming a constant decreasing memory effect with increasing amount of measurements. For each pair of adjacent vials (k and j) in the analysis scheme, the isotopic difference (d) between the mean of the last three injections and the their true isotopic difference was calculated where i_{16},i_{17} and i_{18} represent the last three out of

Table 3.6: Different types and generations of laser spectroscopes used in this analysis.

1. OA-ICOS (used in comparison): Liquid Water Isotope Analyser, model DLT-100 with measurement precision <0.6‰ for δ^2H and <0.1‰ for δ^{18}O. Each measurement consisted of 0.75 µ l water. All OA-ICOS were manufactured by Los Gatos Research Inc. (LGR, Mountain View, California, USA) named:
    - LGR-1 908-0008 (1^{st} generation)
    - LGR-2 908-0008-2000 (2^{nd} generation)
    - LGR-3 908-0008-3000 (3^{d} generation)
2. CRDS (used in comparison): Liquid Water Isotope Analyser, model L1102-i liquid analysers (first generation) and one L2130-i (second generation) with measurement precision <0.5‰ for δ^2H and <0.1‰ for δ^{18}O. Each measurement consisted of 2 µ l water. All were manufactured by Picarro (Picarro, Santa Clara, California, USA), named:
    - PIC-1 and PIC-2 (1^{st} generation)
    - PIC-3 (2^{nd} generation)
3. IRMS (used as reference): Thermo Fischer Delta Plus Advantage mass spectrometer (Thermo Fisher Scientific Inc., Massachusetts, USA) connected to a GFL 1086 equilibration device. The measurements were carried out with a classical dual-inlet system using a CO_2 / H_2 water equilibration technique (Epstein and Mayeda, 1953; Horita et al., 1989). The external measurement precision ± 0.7‰ and ± 0.05‰ for δ^2H and δ^{18}O measurements, respectively. (used to

18 measured isotopic compositions see eq. (3.8). Instead of using the 18^{th} or last measurement as purposed by Gröning (2011), the mean of the last three measurements was calculated to avoid possible influences of random fluctuations or the occurrence of "bad injections" (Penna et al., 2010).

$$d = (\overline{i_{16}, i_{17}, i_{18}})_k - (\overline{i_{16}, i_{17}, i_{18}})_j \tag{3.8}$$

Furthermore for every sample the isotopic difference (e) between the average of the last three measuremnts of the second sample and the first injection of the next sample was calculated eq. (3.9) which resulted in an relative memory effect (f) eq. (3.10).

$$e = (\overline{i_{16}, i_{17}, i_{18}})_k - (\overline{i_n})_j \tag{3.9}$$

$$f = \frac{e}{d} \tag{3.10}$$

To account for the constant decreasing memory effect with increasing amount of measurements, the relative memory effect of the last three measurements (c,eq. (3.9)) was considered, to determine the total memory effect (ME,eq. (3.9)) as purposed by Gröning (2011).

$$ME = \frac{f}{c} \tag{3.11}$$

$$c = f_{18} + f_{17}^2 + f_{16}^3 \tag{3.12}$$

4. Results

4.1 Results paper I - Baseflow

4.1.1 Spatial variability of isotope and hydrochemical concentrations

The snapshot campaign 2 (C-2) and 3 (C-3) baseflow water samples collected had for both campaigns a small and statistically not significant spatiotemporal variability for the selected isotopic (δ^2H) and hydrochemical concentrations (Ca, DOC, AT, pH, SO_4, Mg and H_4SiO_4) within and between the six different subcatchments. The streamwater samples at the subcatchment outlets, were similar to each other and similar to the signature of springs but different to groundwater from observation wells (detailed results are referred to **paper I - Baseflow** (Fischer et al., 2015) section *Variability in isotope and hydrochemical concentrations*). The stable isotope composition and different hydrochemical variables varied in space and between the C-2 and C-3 (Figure 4.1). The samples of springs and groundwater wells above 1400 m a.s.l. had a distinct isotopic and hydrochemical signature with more depleted δ^2H, higher Ca and lower DOC composition and was therefore defined as an "upper spring zone" (area I see Figure 4.1 and 3.1a). The signature of the stream water of WS04 and WS07 changed from the upper spring zone only slightly, where δ^2H became more enriched while Ca decreased and DOC increased. The subcatchments WS10, WS11, WS18 and WS19 had slightly lower Ca concentrations compared to WS04 and WS07 but a similar DOC composition as in area I. A second area could be derived, due to its isotopic and hydrochemical signature, which was a tributary in WS04 (drainage ditch from a wetland, see area II). This area II had more enriched δ^2H values, lower Ca and higher DOC concentrations in respect of other samples. Comparing campaign C-2 to C-3, generally all sampling locations became more enriched in their δ^2H values while the spatial patterns of Ca and DOC remained largely similar.

4.1.2 Mixing of different water samples

The variables δ^2H, Ca and DOC as a function of their catchment area and wetland percentage were selected to asses the mixing along the stream network (Figure 4.2). The variability of δ^2H, Ca and DOC composition decreased from the springs (approximate upslope area 0.001 km^2) towards 0.2 km^2 where several first order streams from springs come together which was the upper spring zone above 1400 m a.s.l.. Below the upper spring zone the streamflow composition changed only slightly towards the subcatchment outlets. Along the stream network of WS04 the variables δ^2H, Ca and DOC showed a distinctly different composition between the main stream (black lines, Figure 4.2), and the tributaries from area II the wetlands (grey lines with large symbols, Figure 4.2). For the full Figure see **paper I - Baseflow** (Fischer et al., 2015).

The mixing of different water samples was additional examined by a bivariate representation of the hydrochemical variables Ca and DOC representing geology and organic matter respectively (Figure 4.3). The stream samples from area II (WS04, draining a wetland), were significantly different from other samples for all variables in C-2 and C-3, and had their own characteristic with lower Ca and higher DOC concentrations. Because of the clear wetland signature, these available

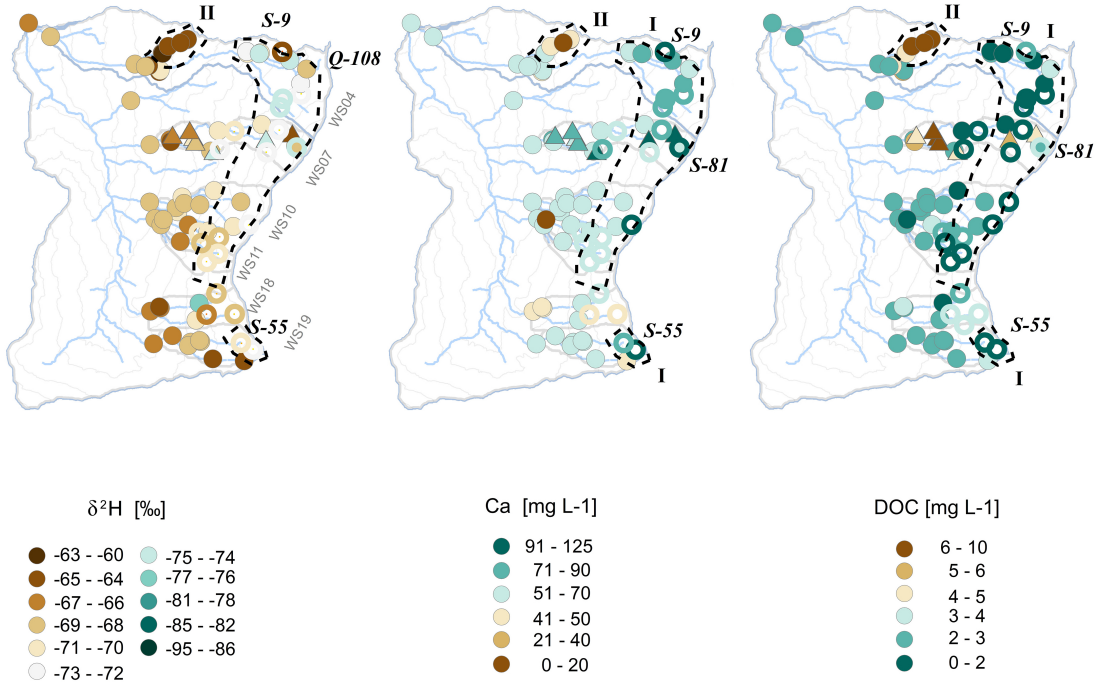

Figure 4.1: Spatial distribution of the isotopic and hydrochemical variables - δ^2H , Ca and DOC for campgain C-3: stream (filled circles), spring (open circles) and groundwater samples (triangles). Dashed lines with roman numerals I (upper spring zone) and II (tributary, i.e. drainage ditch from wetland) are regions with distinct composition. Letters indicate samples described in the text. Color scheme from ColorBrewer. Modified after Figure 4, in Fischer et al. (2015)

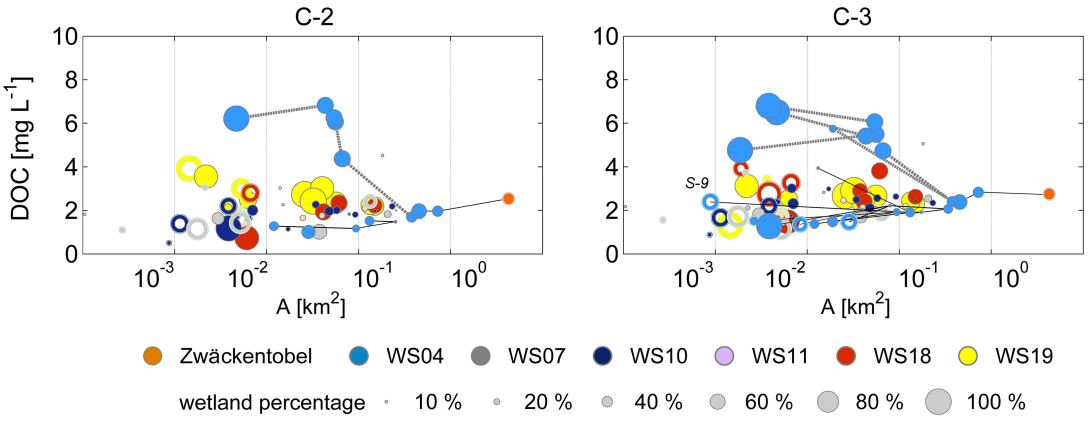

Figure 4.2: δ^2H, Ca and DOC values for snapshot campaign C-2 and C-3 - from the different sampling locations; stream (filled circles) and springs (open circles) represented as a function of their logarithmic catchment area. Symbols are scaled proportional to upslope wetland percentage. Black lines connect sampling points of WS04 along the main stream network from the water divide to the catchment outlet. Grey lines connect sampling points of WS04 along the tributaries to the main stream. Modified after Figure 5, in Fischer et al. (2015)

samples were a first indication of a third end-member from wetlands (W). The median value of these possible end-members of wetlands (W), groundwater wells (G) and springs (S) were added to the bivariate representation of Ca and DOC (Figure 4.3) to indicate possible runoff sources during baseflow. This different representation reconfirmed previous observations that for C-2 and C-3 most stream samples of the different subcatchments were clustered together and had a similar hydrochemical composition. These clustered samples were similar to deep groundwater from springs (S) from near or from bedrock with high Ca but low DOC concentrations. Groundwater samples from observation wells (G) had characteristic concentrations for the integrated soil profile, i.e., shallow groundwater with high Ca and average DOC concentrations. The pattern of C-2 and C-3 remained largely similar. Only some sampling points changed slightly from C-2 to C-3, such as in C-3 some samples of WS18 and WS19 shifted towards the wetland end-member.

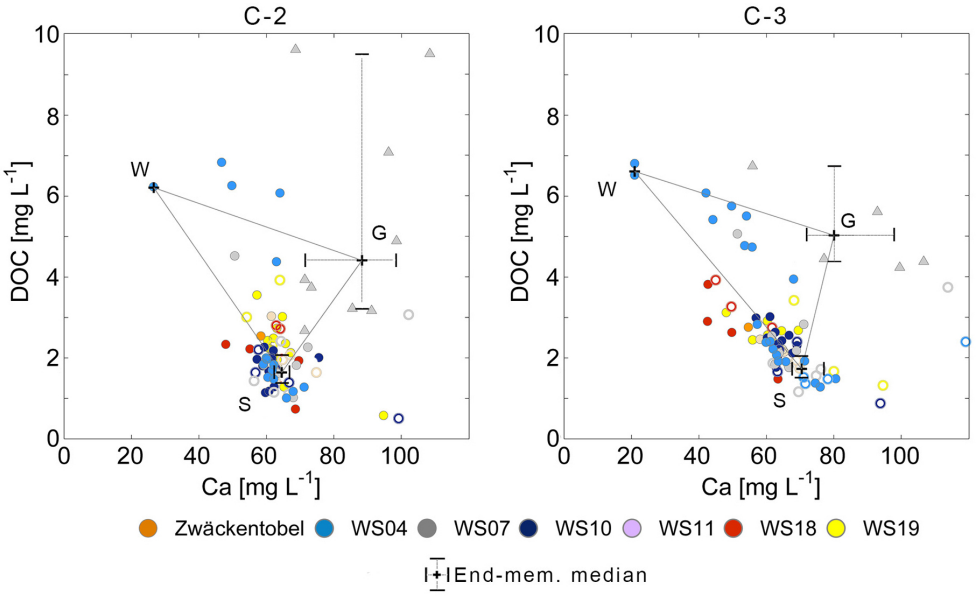

Figure 4.3: Bivariate representation of Ca and DOC for C-2 and C-3 - with different samples: stream (filled circles), springs (open circles) and groundwater (triangles). End-members (+) are median of springs (S), wetland (W) and groundwater (G) samples each with their upper and lower quartiles (error bar). Original Figure 7, in Fischer et al. (2015)

4.2 Results paper II - Runoff events

4.2.1 Sampled event characterization

Thirteen rainfall-runoff events were sampled during the snow free seasons of 2010 and 2011 with each having different event characteristics (see Table 3.3). Each of the events had different antecedent wetness conditions with differences in antecedent precipitation, groundwater level, antecedent discharge. The events covered from small up to the large rainfall and peak discharge magnitudes which were observed during the time period 1998-2011 (Table 3.3). Each event had different rainfall and spatial characteristics (Table 3.3). The discharge of WS04-WS19 responded to rainfall with a delay of 10 min up to one hour for the different events (Table 3.3).

4.2.2 Stable isotopes and hydrograph separation of sampled storm events

The isotopic composition of all collected water samples fitted along the global meteoric water line (GMWL) where the precipitation samples covered a much wider range compared to the stream samples (Figure 4.4a). Non of the samples had signs of fractionation. The IHS was performed

Table 4.1: For WS04-WS19 and event 1-12 the minimum fraction of pre-event water f_{pe} and its corresponding uncertainty $W_{f_{PE}}$. Event 13 is not displayed because it was sampled only to the first peak. The symbol np describes where an IHS was not possible.

event nr.		1	2	3	4	5	6	7	8	9	10	11	12
WS04	f_{pe}		0.83	0.1		0.28	np	0.48	0.32	0.91	0.57	0.84	0.51
	$W_{f_{PE}}$		0.1	0.87		0.16		0.3	0.8	0.35	0.3	0.16	0.24
WS07	f_{pe}	np		0.1		0.61			np				np
	$W_{f_{PE}}$			0.87		0.14							
WS10	f_{pe}	np		0.36	0.84	0.55		0.42	np	0.67	0.84	np	0.6
	$W_{f_{PE}}$			0.34	0.24	0.16		0.35		0.15	0.6		0.19
WS11	f_{pe}			0.49				np	np	0.6		0.86	0.57
	$W_{f_{PE}}$			0.25						0.1		0.17	0.17
WS19	f_{pe}	0.6	0.68	0.1	0.7	0.3	np						0.51
	$W_{f_{PE}}$	0.1	0.13	0.73	0.1	0.14							0.4

for each event separately usingδ^2H and δ^{18}O. This resulted in 30 pre-event fractions (Table 4.1) which were expected for two events not equal: WS04 event 9 and WS19 event 5 (Figure4.4b). Because both isotopes resulted in rather similar computed pre-event water contributions, only the computations based on δ^{18}O are shown in the following. The with the IHS (eq. (3.2)) derived minimum fraction of pre-event water (f_{PE}) for the different streams and events varied from 0.01 up to 0.9 and occurred half an hour before or after a maximum water level. Because for some events the isotope composition of rainfall, pre-event or streamwater were too similar an IHS was not possible. For events where an IHS was possible, the uncertainties in the minimum fraction of pre-event water calculate with eq. (3.4) varied between ±0.1 up to ±0.9.

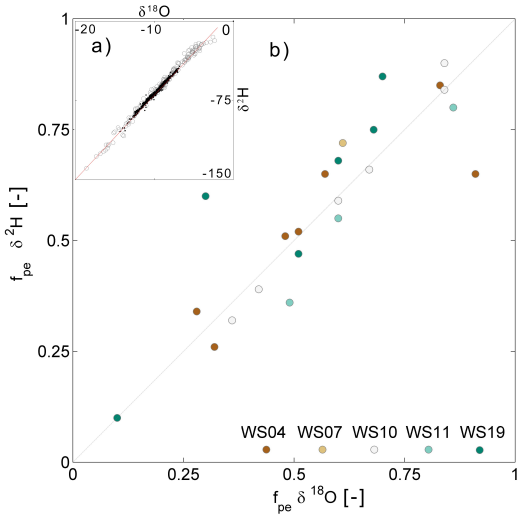

Figure 4.4: Stable isotope composition of all samples and fraction of pre-event water of all events - a, inset) All collected rainfall samples (grey circles) and stream samples (black circles) of all headwaters and events follow the global meteoric water line. b) Values of the minimum fraction of pre-event water computed based on δ^{18}O observations versus the corresponding values that were computed based on δ^2H observations for the different events and catchments (each catchment is represented by a different color). The grey line is where pre-event water computations based on δ^{18}O and δ^2H observations would be equal. Original Figure 5, in Fischer et al. (2016b)

4.2.3 Comparison of three headwaters and events

The three headwater catchments WS04, WS10 and WS19 were selected (the best data coverage and representing the different catchment properties) for a detailed analysis of event 3, 5 and 12. These three events represent a long event with high amount of rainfall and high discharge, a event with high rainfall intensity highest recorded discharge out of the 13 events sampled and the average event respectively. Generally a small spatial difference in hydrograph response and pre-event water fractions in the different headwaters could be noticed. The behaviour in the different events was largely similar. The large events had a higher event water compared to the smaller event. In event 3 the hydrograph had multiple peaks (Figure 4.5, left column). After the maximum water level was reached, the air temperature decreased to 0°C, and the rainfall changed to snowfall. Missing samples during the rain free period, just after the first peak, were due to full automatic water samplers. Due to the length of the event, all samplers were restarted two times. The fraction of pre-event water decreased rapidly after the start of rainfall for WS04, WS10 and WS19 to a minimum of 0.2, 0.36 and 0.27 respectively (Figure 4.5, left column) and reached at the second peak for WS04 and WS19 dominant event water, while WS10 had a higher fraction of pre-event water. During the recession of the hydrograph, the fraction of pre-event water rose irregularly due to short additional rainfall that instantaneously increased the fraction of event water. In event 5, the rainfall amount and intensities increased from WS04 towards WS19 and the hydrograph had two peaks (Figure 4.5, middle column). In all streams, the fraction of pre-event water decreased rapidly towards the first peak and second peak to 0.3 for WS04 and WS19. Instead in WS10, the fraction of pre-event water during the first peak was 0.72 and decreased during the second peak to 0.55. After the maximum water level the different automatic water samplers were full, and were not restarted resulting in missing observations. Event 12 had an average and evenly distributed event total rainfall and intensity and the hydrograph had multiple peaks (Figure 4.5, right column). Due to technical problems the automatic samplers didn't sample the rising limb. A manual start at the maximum water level made it possible to derive for three different headwaters the pre-event water which were ranging from 0.51 to 0.6 and increased gradually during the falling limb to 1 (Figure 4.5, right column). For the full overview of WS04, WS10 and WS19 is referred to **paper II - Runoff events** (Fischer et al., 2016b).

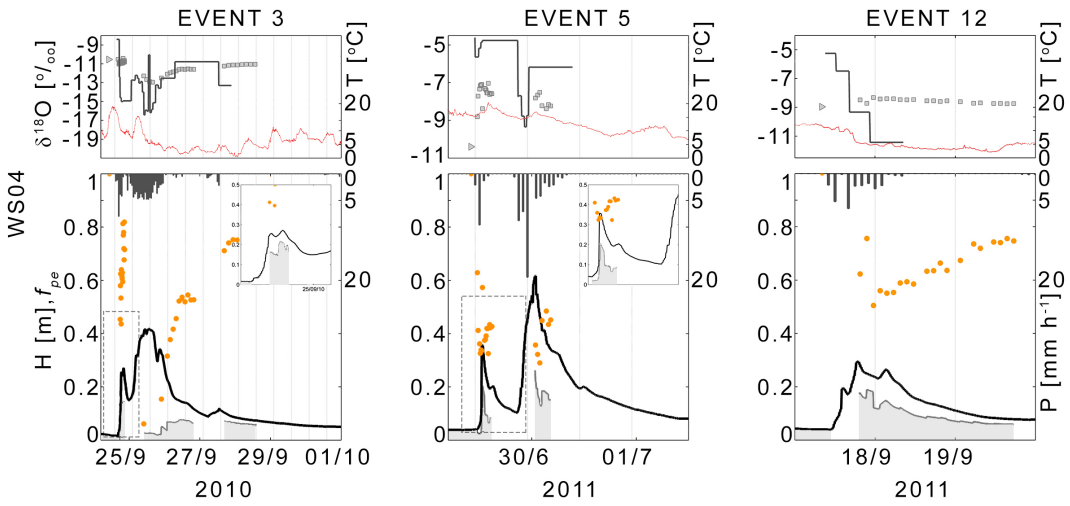

Figure 4.5: Detailed isotopic and hydrometric overview of WS04 of three different events - . The top panels show $\delta^{18}O$ in event water (line), streamwater (grey squares), pre-event water (triangle) and air temperature (red line). Bottom panels show precipitation (inverted, from the top), water level (solid dark line) and fraction of pre-event water f_{PE} (orange circles and grey area below the hydrograph). Modified from Figure 8, in Fischer et al. (2016b)

4.2.4 Explanatory factors of pre-event water fractions

All derived fractions of minimum pre-event water of WS04, WS10 and WS19 were used and represented in relation to their belonging rainfall amount and rainfall intensities (Figure 4.6). For all headwaters the minimum fraction of pre-event water decreased with increasing event total rainfall (Figure 4.6, left column). Similar but to a lesser extent, decreased the minimum fraction of pre-event water with increasing rainfall intensities (Figure 4.6, right column). All headwaters had a similar decreasing relation only WS04 and WS19 appeared to have in event 3, 5 and 12 different, i.e., lower minimum pre-event fraction compared to WS10 (Figure 4.6). The relation between the minimum fractions of pre-event water was supported by the regression analysis. The minimum fraction of pre-event water correlated best with event total rainfall while only little with rainfall intensity in all studied headwaters and for the individual headwaters. The antecedent wetness indices correlated only weakly with the minimum pre-event fraction. No significant relation between pre-event water and different catchment characteristics was found (analysis not shown).

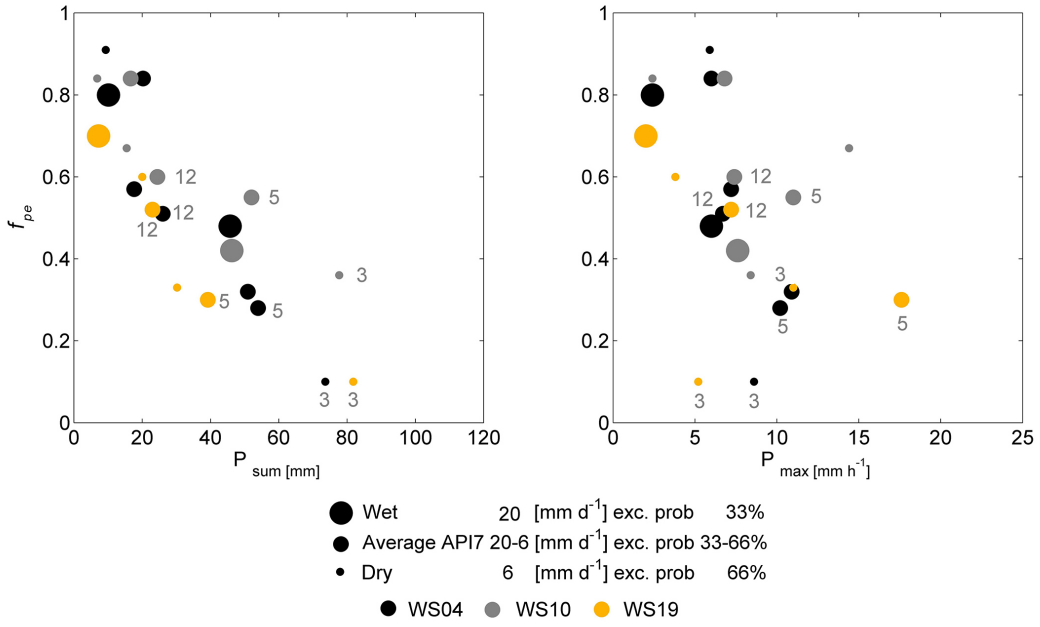

Figure 4.6: The event total rainfall related to the minimum fraction of pre-event water f_{PE} - (left) and max rainfall intensity related to the minimum fraction of pre-event water f_{PE} (right) for WS04, WS10 and WS19. Different sizes of circles indicate different antecedent conditions (wet, average and dry) and numbers refer to event 3, 5 and 12. Original Figure 9 in Fischer et al. (2016b)

4.3 Results paper III - Spatial rainfall

4.3.1 Spatial variability in event total rainfall and the weighted mean isotopic composition of rainfall

From the 13 sampled events, 10 events were selected which had the most rain samplers and represented a wide range of different rainfall and peak discharge magnitudes. The spatial patterns of event total rainfall, maximum rainfall intensity and the weighted mean δ^{18}O of rainfall varied from event to event (see Table 3.3, Figure 4.7). Large events such as event 3 and 5 had a large spatial differences of more than 60 mm across the Zwäckentobel and with average to higher rainfall intensity of 6 up to 34 mm h^{-1} (Figure 4.7c and e). Average rainfall events such as event 9 and 11 varied between 20-40 mm while the smaller events 1, 6, 10 and 12 had small

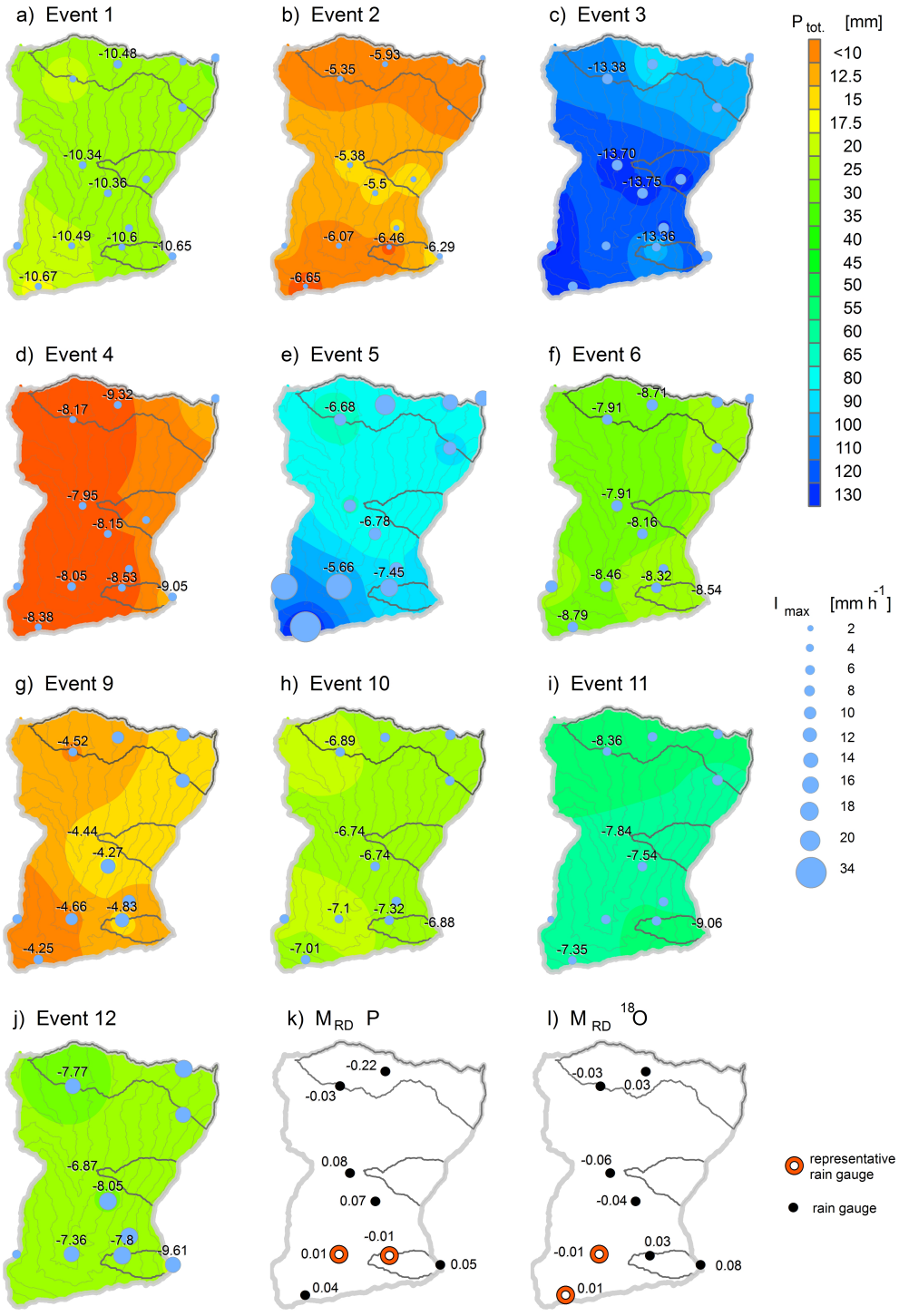

Figure 4.7: The spatial distribution total rainfall (P_{tot}., interpolated using inverse distance weighing) for different events (a-j). - The area of the circle in plots (a-j) represents the event maximum rainfall intensity. The numbers represent the weighted mean δ^{18}O of rainfall. The mean relative difference of event total rainfall (M_{RD_i} P) (k) and the mean relative difference of δ^{18}O (M_{RD} ^{18}O) at those locations where rainfall amounts and isotope composition was measured (l). The rain gauge and samplers with the lowest M_{RD} are highlighted in red in figure (k) and (l) respectively. Original Figure 5, in Fischer et al. (2016a)

spatial differences with a coefficient of variation smaller than 0.1 (<6 mm) and rainfall intensities between 2 to 6 mm h^{-1} (Figure 4.7.Beside event 5 none of these rainfall patterns of total rainfall and intensity correlated with altitude. Because the rainfall was sampled sequentially the weighted mean $\delta^{18}O$ of rainfall was used to compare the different rain samplers. For event 3 and 5 only four rain samplers were available because rain changed to snow after the maximum discharge was reached. The spatial variability of the weighted mean $\delta^{18}O$ varied for the different events between 0.3 up to 3.6 ‰ (Figure 4.7). The difference between the maximum weighted mean $\delta^{18}O$ and the minimum weighted mean $\delta^{18}O$ of all sampling locations (Spatial range of weighted mean $\delta^{18}O$ (S_R)) increased slightly with increasing event total rainfall (up to 2.7 ‰) but was very variable for the large events. There was no statistical significant relation between the spatial range of the weighted mean $\delta^{18}O$ and the maximum rainfall intensity or event duration. Different weak positive or negative correlations between the weighted mean $\delta^{18}O$ of rainfall and total rainfall or altitude were found, but only a few of these correlations were statistically significant. For two transects T1 or T2 or for two altitude classes (below or above 1350 m a.s.l.), stronger correlations between the weighted mean $\delta^{18}O$ of rainfall and event total rainfall, maximum rainfall intensity or altitude were found but only a few of these correlations were statistically significant. The results of the M_{RD} analysis showed that TB-11 was close to zero for total rainfall (Figure 4.7k) and the weighted mean $\delta^{18}O$ (Figure 4.7l) and suggest therefore that this rain sampler was the most representative location for the entire Zwäckentobel headwater catchment.

4.3.2 Temporal variability in cumulative rainfall and the isotopic composition of rainfall

The rainfall became more depleted in $\delta^{18}O$ during the events but the exact temporal pattern differed between the events. Generally the temporal variability in $\delta^{18}O$ of rainfall was relatively similar for all eight sampling locations but there were differences between the different rain samplers. The spatial variability of $\delta^{18}O$ between the different rain samplers was relatively large during the first 5 mm of rainfall, with a standard deviation of approximately 0.5-1.5 ‰. The mean of the difference between the maximum and minimum $\delta^{18}O$ for the different rain samplers (the average of the mean temporal range in $\delta^{18}O$; Mean temporal range in $\delta^{18}O$ (M_{TR})) increased with increasing event total rainfall from 1 up to 10 ‰ but didn't correlate with maximum rainfall intensity or event length. Comparing the mean temporal range in $\delta^{18}O$ (M_{TR}) with the spatial range in the incremental mean $\delta^{18}O$ (S_R) for the different events showed the temporal variability increased with total rainfall and was larger than the spatial. But the spatial range could be equal or half of the temporal variability in $\delta^{18}O$. The change in the ratio of M_{TR} and S_R did not depend on the maximal rainfall intensity and or the duration of the event.

4.3.3 Effect of different temporal weighing techniques on hydrograph separation results

The effect of the different techniques to account for the temporal variability in the isotopic composition of rainfall (technique I-IV) on the pre-event water was analysed for WS04, WS10 and WS19 for all events. In general for the small and moderate events with a small M_{TR} and a large difference between the event and pre-event water composition the different weighing techniques had a small effect on the minimum fraction of pre-event in WS04, WS10 and WS19 (4.8 Temporal weighing (T_W) and 4.9). The differences in the calculated minimum fraction of pre-event water to streamflow increased (up to 0.8) with increasing M_{TR} or a smaller difference between the event and pre-event water composition.

4.3.4 Effect of the location of the rain gauge on hydrograph separation results

The effect of the different rain sampling locations on the IHS results was assessed by determining the pre-event water fractions in streamflow for WS04, WS10 and WS19 using alternating the data of each of eight rain sampler and the incremental intensity mean (technique IV). Generally, the

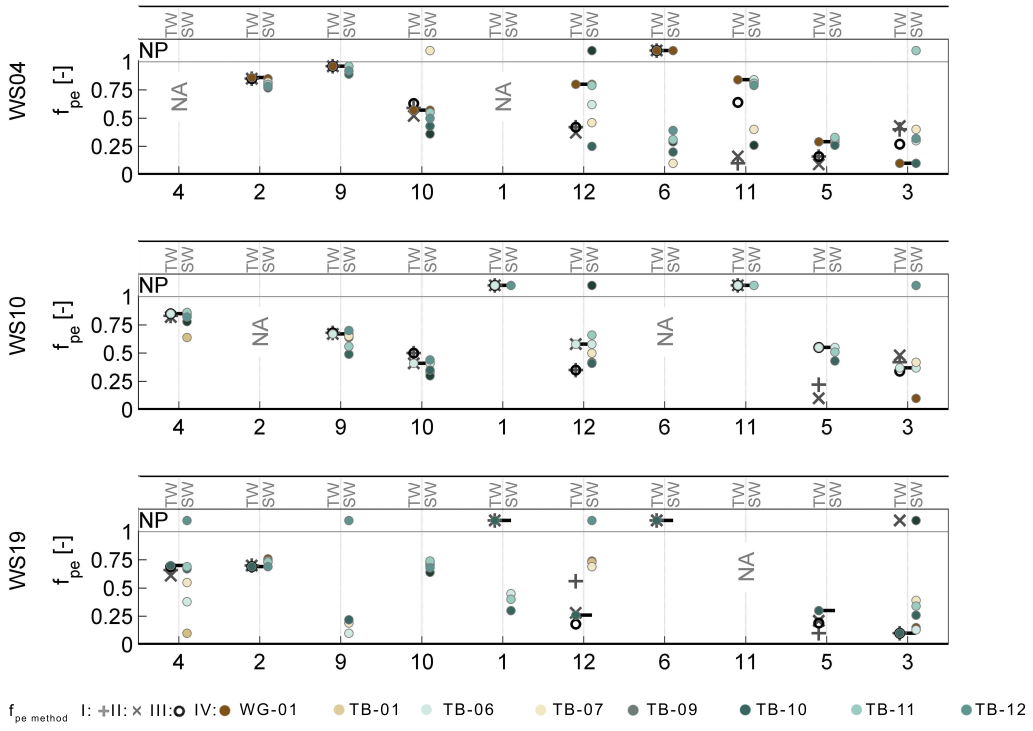

Figure 4.8: The minimum fraction of pre-event water in WS04 (top row), WS10 (middle row) and WS19 (bottom row) for the different ranked events calculated using the different weighing techniques I-IV - , to account for the temporal variation in the isotopic composition of rainfall (T_W) and using the incremental intensity mean for incremental intensity mean for the different rainfall sampling locations (S_W), different colored circles). The horizontal black line indicates the minimum fraction of pre-event water obtained using (technique IV) using the nearest rain sampler (WG-1 for WS04, TB-6 for WS10 and TB-10 for WS19). NP indicates that hydrograph separation was not possible. NA indicates that the event was not sampled. The events are orderd by total precipitation see 3.3a. Original Figure 5, in Fischer et al. (2016a)

range of the calculated minimum fraction of pre-event water was small (up to 0.3) for events with a small S_R in $\delta^{18}O$ in rainfall and the difference between event and pre-event water composition was large (4.8 ,S_R and 4.9). The range in the calculated minimum fraction of pre-event was large (up to 0.5) for events with a large spatial variability in the isotopic composition of rainfall and for which the difference between the event and pre-event water composition was small. Therefore for some events the minimum pre-event water fraction was highly dependent on the location of the event water samples while for other events the sampling location had less influence on the IHS. In some cases the sampling locations isotope composition affected whether an IHS was possible or not. The comparison of the importance of the temporal and spatial variability in the isotopic composition of rainfall on the IHS results revealed that even for large events for which the temporal variability in the isotopic composition is large, the spatial variability in the isotopic composition of rainfall still has a significant effect on the IHS results.

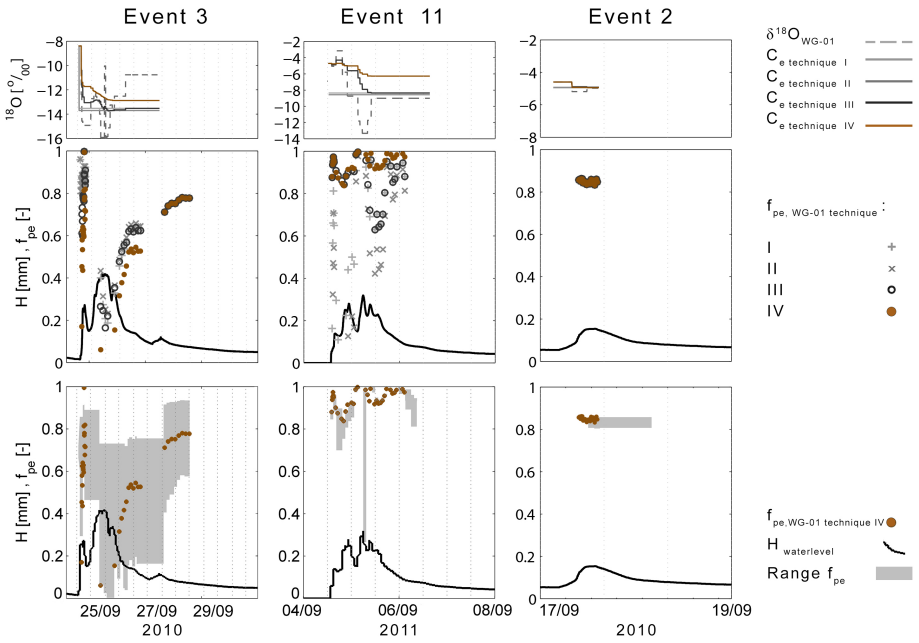

Figure 4.9: The isotopic composition of rainfall - sampled (dashed line, top row of plots), the isotopic composition of rainfall from WG-01 based on the four different weighing techniques (C_e technique I-IV) for event 3 (left column), 11 (middel column) and 2 (right column). The stream water level (black line) and the fraction of pre-event water obtained using the four different weighing techniques C_e technique I-IV in WS04 (middle row), the range in the pre-event water contribution to streamflow determined using the incremental mean technique (IV, lower row) for the the different rainfall sampling locations (shading). Original Figure 9, in Fischer et al. (2016a)

4.4 Paper IV - Spectroscopy

4.4.1 Between-sample memory effects

The representation of the isotopic composition of different measurements according to their measurement position revealed that the isotopic composition stabilized from the 7^{th} or 8^{th} injections (see Figure 4.10). The first measured standard had the most stable measurements. With increasing difference of isotope composition between antecedent vials a higher inter-vial isotopic difference occurred. The memory effect was for δ^2H larger compared to $\delta^{18}O$.

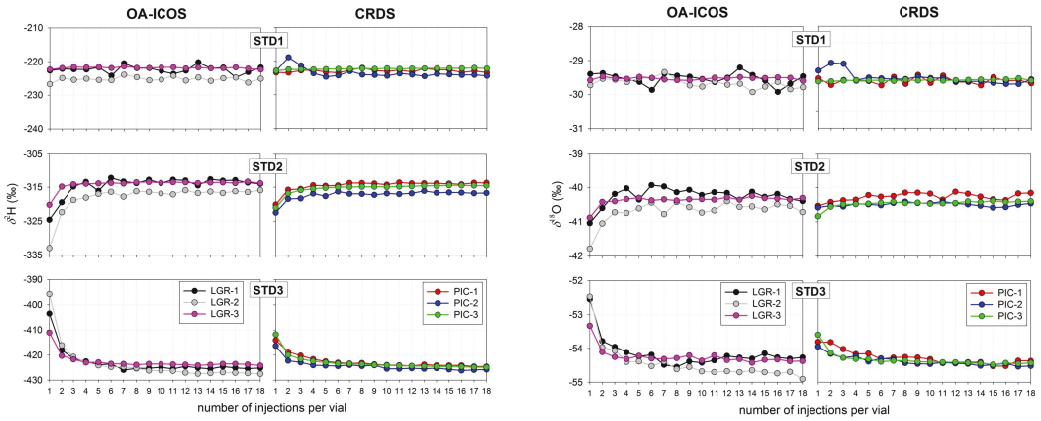

Figure 4.10: Measurement stabilisation - by sequential injection number for three laboratory measurement standards (second triplet in an analysis run) for hydrogen (left side) and oxygen (right side). Left panels: OA-ICOS instruments. Right panels: CRDS instruments. Original Figure 1a and b, in Penna et al. (2012)

The memory effect, when changing from a very isotopically, depleted to a significantly more enriched sample e.g. laboratory standard 1 and 3 and vice versa was further analysed and quantified(see Figure 4.11-left side). For OA-ICOS instruments ranged the memory effect between 6 ‰ to 14 ‰ for δ^2H and 4‰ to 9‰ for δ^{18}O measurements (see Figure 4.11-left side). The memory effect for CRDS instruments ranged between 4 ‰ to 6 ‰ for δ^2H and 2‰ to 4‰ for δ^{18}O measurements. The memory effect was on average 0.8 - 3.0 ‰ (SD: 0.8 - 3.9 ‰) when considering all measurements which decreased to 0.1‰ - 0.3‰ (SD: 0.1-0.6 ‰) when considering only the last eight injections. The intra-vial range of isotopic -values (i.e., maximum minus minimum, when all 18 injections were considered) as a function of the inter-vial range (i.e., the isotopic difference between waters analysed during the run) showed a strong relation (see Figure 4.11-rigth side). This demonstrates that when averaging all injections and large isotopic differences between adjacent vials results into a high memory effects. This effect became smaller with increasingly removing the measurements up to the last for measurements when averaging. This effect was generally more pronounced with OA-ICOS instruments compared to first generation CRDS instruments while in the latest generation instruments no difference was found.

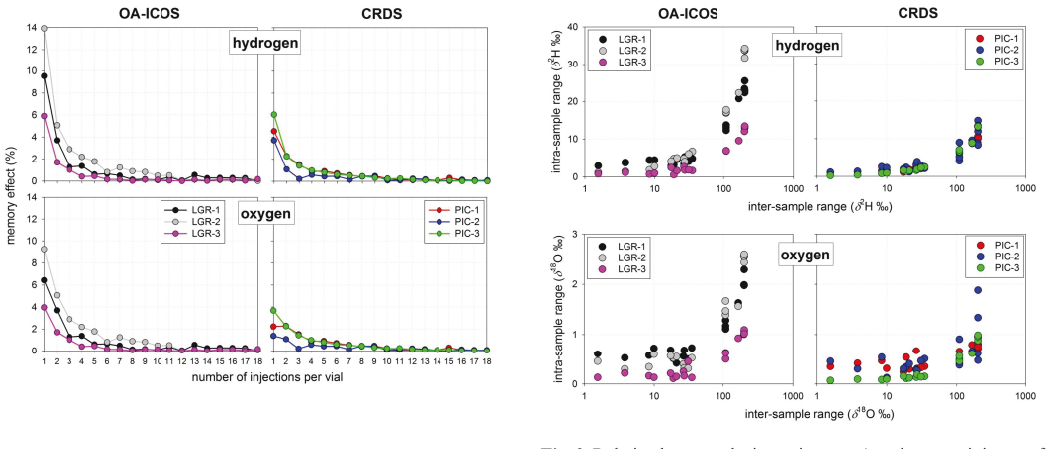

Figure 4.11: Memory effect as a function of the number of sequential injections - of the same vial for the transition between STD1 and STD3 (third triplet in an analysis run) (left side). Relation between the isotopic range (maximum–minimum of 18 injections) within each vial (either sample or measurement standard) and the absolute isotopic difference between adjacent vials in the tray (right side). Upper row: hydrogen. Lower row: oxygen. Left column: OA-ICOS instruments. Right column: CRDS instruments. Original Figure 2 and 3 in Penna et al. (2012)

5. Discussion

5.1 Discussion paper I - Baseflow

5.1.1 Spatial patterns of stream water composition in pre-alpine headwaters

The three different baseflow snapshot campaigns were a useful method to explore the newly gauged headwater. The collected water samples were useful to characterize the isotopic and hydrochemical composition of this steep and wet pre-alpine headwater catchment with different landscape units including forests, meadows and wetlands. The stable isotopic information was useful to trace the flowpath of the water while hydrochemical variables were useful to indicate sources and observe changes that the water undergoes during the runoff. The water was analysed for 15 different variables but only the isotopic ($\delta^{18}O$, $\delta^{2}H$) and hydrochemical variables (Ca, DOC, AT, pH, SO_4, Mg and H_4SiO_4) were useful and provided information. In both campaigns the different sampling locations in WS04-WS19 had different water signatures. Despite the fact that WS04-WS19 were significantly different in their landscape properties, the variability of the different sampling locations was small and statistically not significant within and between the outlet of these subcatchments. Especially the variables $\delta^{2}H$, Ca and DOC were useful for different analyses to determine the different sources and flowpath of the water. To identify the spatial patterns of streamwater composition the variables $\delta^{2}H$, Ca and DOC were represented as sampled in space by which the spatial variability emerged. The spatial representation of $\delta^{2}H$, Ca and DOC helped to visualise changes in concentrations along the stream network. Furthermore different landscape units with water of a distinct isotopic and hydrochemical signature could be identified: area I which is the upper spring zone that was near the water divide located above 1400 m a.s.l. and area II which is a tributary, i.e., a drainage ditch, from a wetland in WS04 (Figure 4.1).
By expressing the different sampling locations of each variable according to their sampling point's upstream landscape features such as catchment area, altitude, slope, topographic wetness index, land cover (forest, meadow and wetland), geological facies and shallow soils allowed the mixing of different waters to be assessed. From the different landscape features, only a clear relation of $\delta^{2}H$, Ca and DOC as a function of catchment area was found, where the variability at catchment scales of 0.2 km^2 was reduced. Other landscape features showed no strong relation with $\delta^{2}H$, Ca and DOC and therefore less important as steering features. The upslope scale of 0.2 km^2 coincided with the observed upper spring zone (area I). At scales larger than 0.2 km^2, i.e., outside the upper spring zone, the hydrochemical composition of the main stream of WS04 increased or decreased little and remained more similar to the isotopic and hydrochemical composition from the upper spring zone near the water divide.

5.1.2 Spatial patterns in relation to landscape units

Using $\delta^{2}H$ was useful to trace the flowpath of the water. From the distinct isotopic composition it was possible to observe area I (upper spring zone) and area II (wetlands). Comparing the differences in wetland and stream samples, it is likely that due to the continued saturated state,

water in wetlands is younger with shorter transit times compared to "older" water from the steeper slopes, which was also observed by Inamdar et al. (2013). High Ca and low DOC concentrations in the upper spring zone (area I) originate from deep groundwater which dissolves the carbonate bedrock. DOC concentrations increased and Ca concentrations decreased slightly downstream but maintained a signature similar to low DOC and high Ca concentrations from springs, i.e., deep groundwater. At confluences with tributaries from wetlands (area II), the composition of δ^2H, Ca and DOC changed only little due to minor streamflow contributions from the side branches, i.e., the wetlands were less connected. That stream samples at the different headwaters were more similar to springs than to groundwater from observation wells, was visible in the bivariate solute diagram where most samples were grouped together near the hydrochemical composition of deep groundwater from springs located near the water divide. Only few streamwater samples showed a signature that was similar to the samples from wetlands or shallow groundwater from observation wells. For the bivariate representation of Ca and DOC the observations were largely bounded within the degree of uncertainty by three end-members of groundwater wells (shallow groundwater), springs (deep groundwater) and wetlands. Therefore, stream samples at the different headwaters were more similar to springs than to groundwater from observation wells. Only some sampling locations appeared to be connected to different flowpaths in respect of their sampling typology.
The observed hydrochemical compositions in WS04-WS19 corresponded to the observations made by Keller (1990) and Keller et al. (1989), who studied hydrochemical variables at the outlet of WS04 together with six additional headwaters (below 1 km^2) in the larger Alptal catchment (47 km^2) and implies similarities in baseflow generation. Although streamwater contained specific hydrochemical composition for the region, which is largely affected by geology, in contrast to findings of Soulsby et al. (2007), the hydrochemical variables Ca, Mg and H_4SiO_4 gave no further information to distinguish between the three geological flysch facies. Only SO_4 was useful to distinguish between sources and weathering flysch layers such as in WS04 and WS10 (containing $CaSO_4$ (anhydrite) (Campbell et al., 1995), eroding channels high concentrations compared to more stable stream channels low concentrations). Studies with different geologies such as granitic (Likens and Buso, 2006; Zimmer et al., 2012) or schist (Asano et al., 2009) had two orders of magnitude lower Ca concentrations compared to the Zwäckentobel (Keller et al., 1989; Zobrist, 2010) by which some variables like pH could be used to obtain information. The Ca rich geology however meant that all streamwater samples were highly buffered (pH near 8.0) and potential differences in pH between different landscape units including wetland, pastures and forest were blurred. That not all tracers used were useful might have been due to the frequent rainfall and thus continuous wet state of the headwater. In situations with longer dry spells it might be that some sampling locations will disconnect and not contribute to streamflow while the signature of a water sample might show signs of fractionation in stable isotopes or more pronounced values e.g. in Ca, DOC or pH.

5.1.3 Wetland contribution in pre-alpine baseflow

Pre-alpine headwater catchments with shallow soils have a limited aquifer and are lacking a riparian zone. These headwaters with high precipitation respond quickly to rainfall and thus, therefore, according to Asano et al. (2009) and Frisbee et al. (2011) a network-mixing model with asymptotic convergence solutes would be a valid conceptualisation of these systems. However, our observations lead to a different perception. The observed isotopic and hydrochemical signatures of the Zwäckentobel did not change significantly towards the catchment outlet during baseflow. We cannot fully exclude that outside the upper spring zone (altitudes below 1400 m a.s.l.) deep groundwater or groundwater with a similar composition to the streamwater contributed to baseflow. From our analysis of δ^2H, Ca and DOC, it is more likely that the deep groundwater from the upper spring zone determines, to a large extent the isotopic and hydrochemical signatures of baseflow contribution at the subcatchment outlet. The spatially distributed baseflow generating zones (area I, consisted of two elements such as zero-order basins

described by Asano et al. (2009) or deep groundwater (form perennial springs, in the upper spring zone near the ridge) described by Zimmer et al. (2012). Despite the shallow soils with limited storage capacity, deep groundwater seeped from fractures and fissures into the zero-order basin and fed the first order stream channels and this deep groundwater seemed to be permanently connected to the stream network. The isotopic composition of deep groundwater reflected water with longer transit times, whereas spatial patterns of the hydrochemistry remained mostly similar. Less than 10% of the groundwater and spring samples changed in their composition, presumably due to a connection with a different flowpath. Within the upper spring zone, as well as for other sampling locations, we could not distinguish between the isotopic and hydrochemical composition and different landscape units such as forest, meadows and wetlands. This might be partly due to sampling design and the chosen isotopic and hydrochemical variables. However, it is more likely that the dominance of active sources from the upper spring zone explains why we did not observe, with exception of catchment area and implicit altitude (represented by the stream network), any other relations between hydrochemistry and controlling landscape features. Nevertheless, these active contributing point elements, such as seeping deep groundwater from springs with passive features are indicators of short and long flowpaths and transit times (Rodgers et al., 2005). Therefore, instead of a network-mixing model it is more likely that steep wet pre-alpine headwaters, with point sources and a landscape mosiac described by Temnerud et al. (2007); Uchida et al. (2005) and Zimmer et al. (2012), are better represented with a more complex "Tóthian", i.e., topography-energy driven flow model, as discussed by Frisbee et al. (2011). Our findings confirmed the statement of Keller et al. (1989) who postulated that baseflow originates from deep percolating water from springs which was interestingly based on sampling only at the catchment outlet.

Next to the active contributing upper spring zone (area I) the specific composition of δ^2H, Ca and DOC was useful to distinguish another baseflow contributing unit, the wetlands (area II).The wetlands are prominent landscape units with large storage capacity and areal extent (30-60% of the subcatchment area). During baseflow however these features are passive units and are not significantly contributing to baseflow. Passive units are usually found in dry regions where seasonal drying over the summer (in dry conditions) changes the connectivey of the streamnetwork and the hydrochemical composition (Inamdar et al., 2013). Contrary to this seasonal change in connectivity, our findings show that passive, in terms of being hydrologically less connected landscape units can also occur in rainfall dominated headwaters such as the Zwäckentobel catchment (2300 mm y^{-1}). Consequently, pre-alpine headwaters with similar climate, geology and topography are, during baseflow, not just the sum of different landscape units, but are rather dominated by the arrangement of connected (active) or disconnected (passive) landscape units as conceptualised by Sidle et al. (2000) and Ambroise (2004).

The explorative snapshot campaign was useful to get an comprehensive overview on hydrological processes and which sources and landscape elements contribute to baseflow in the previously ungauged headwater. The obtained information was useful to see the at the WS04 collected longterm hydrochemical data of the NADUF in a different perspective. That during baseflow the signal of the upper spring zone was collected at the catchment outlet. Extending this to stormflow, wetlands with low hydrochemcial composition (e.g., EC or Ca) can be mistakenly interpreted as event contribution due to their low concentrations when used in hydrograph separation to distinguish between different contributing sources. Hence, future studies in pre-alpine headwater catchments should focus not only on headwater mean transit times but as shown by Tetzlaff et al. (2014) on the transit times of water through the different contributing landscape units. Overall, our results confirm the usefulness need and benefits of spatially distributed snapshot sampling to increase spatial process understanding of heterogeneous headwaters during baseflow. These results underline the usefulness of nested and / or spatially distributed tracer studies to increase knowledge of the fundamental mechanisms and governing process of baseflow generation in headwater systems.

5.2 Discussion paper II - Runoff events

5.2.1 Spatiotemporal assessment of pre-event water contribution

The Zwäckentobel headwater catchment had a, common for pre-alpine region, short snow free season (Jun-Oct) with on average 25 rainfall events with rainfall amount larger than 5 mm. Generally with a rainfall amount of 5 mm, the stream responds and the water level rises. The different streams of WS04-WS19 had, for steep headwaters characteristic, fast response to rainfall with a steep rise of the water level. While only shortly after the ceasing of the rainfall the recession started. Early IHS studies were offen constrained by their sample size during an event, limited number of events to be sampled and choice between δ^{18}O and δ^{2}H and made their information value limited. The baseflow study (**paper I - Baseflow** (Fischer et al., 2015)) was constrained by the minimum of a two day dry spell which was complicated by the frequent rainfall. Instead to study stormflow, the frequent rainfall and the availability of the laser spectroscope were advantageous to study rainfall-runoff processes and collect water samples of different streams and a wide range of rare and frequently occurring rainfall and discharge events.
Because of the irregular spatiotemporal water sampling using, similar to Buttle (1994), the minimum fraction of pre-event water allowed to compare different headwaters and events during the peak discharge. The sampled events had, opposite to the common perception that humid-forested headwaters have dominant pre-event water during the peak discharge (Buttle, 1994), a temporal variable fraction of pre-event water. **Paper I - Baseflow** (Fischer et al., 2015) observed that, despite the heterogeneous catchment properties, neighboring pre-alpine headwaters at the catchment outlet had similar baseflow signatures and runoff processes. During stormflow, the different neighboring pre-alpine headwaters had irregular differences in fraction of pre-event water but followed largely a similar temporal pattern where large events had a smaller fraction of pre-event water compared to smaller events which had a dominant fraction of pre-event water. Irrespective of the isotope used, δ^{18}O or δ^{2}H, the calculated fractions of pre-event water were less than ±10%. This was much smaller compared to the large difference reported by Lyon et al. (2009) and also smaller than the IHS error propagation estimates.
Small differences in δ^{18}O between event water and pre-event water meant that it was not possible to separate the hydrograph for each event and additionally resulted in large uncertainties in the fraction of pre-event water, as also described by Genereux (1998). Therefore, to obtain large differences between δ^{18}O of event and pre-event isotopic composition, the summer months would be favorable to perform an IHS as stated by Vitvar and Balderer (1997). This large difference however did not always occurr in the Zwäckentobel events studied due to the altitude above 1100 m a.s.l.. Besides the general lower temperatures compared to low land catchments, in some summer events the temperature could decrease towards 0°C and showed that even in summer snowfall it is not uncommon in pre-alpine headwaters. In these events the isotopic composition was more depleted compared to the average seasonal isotopic compositions and with small differences event and pre-event isotopic composition meant that an IHS was not possible. In events with snowfall the precipitated water was stored on the surface as snow which dampened the flood magnitude but also affected the sampling of water and therefore the ability to perform the IHS. Technical malfunctioning of samplers led to some events not being properly sampled. Low temperatures caused problems with batteries which affected the functioning of the automatic stream samplers. While sediment and air entrapment led to the liquid level actuator not triggered or not logistically being possible to empty and restart full samplers. In events with snowfall it was not possible to sample this snowfall because the sequential rainfall samplers were designed for liquid water. A positive effect of the generally low temperatures of the study site was that in none of the collected water samples was fractionation observed. Further more the shielded sampling equipment was beneficial to prevent samples from fractionating and avoided the use of oil (which suggested by many studies to prevent fractionation but makes the sample handling and the analysis of water samples with the laser spectroscope cumbersome). Despite the incomplete sampling of events and large uncertainties in the fraction of pre-event water, the results were

analogous to observations made by Feyen et al. (1999) and Weiler et al. (1998, 1999).

5.2.2 Rainfall as a dominant factor in runoff processes

In plot scale experiments (Kienzler and Naef, 2008; Weiler et al., 1999), a single urban catchment (Pellerin et al., 2008), a single pre-alpine headwater (Penna et al., 2014) or six nordic headwaters distributed throughout Sweden with 2-6 snowmelt events per headwater (Rodhe, 1987), a decrease of pre-event water with increasing precipitation was observed. Our study confirmed this relation for wet pre-alpine headwaters and proved the validity in neighboring headwaters with different catchment characteristics (WS04-WS19) that the minimum fraction of pre-event water largely depended on the event total rainfall and to a smaller degree to the rainfall intensity. The fast hydraulic response of the streams and fast decrease of the fraction of pre-event water in the different events indicated the strong connection between the input (rainfall) and runoff processes. Therefore it is likely that the spatiotemporal distribution of rainfall explains to a large degree the spatial differences of fraction of pre-event water between the WS04-WS19.

5.2.3 Catchment characteristics as secondary factors in runoff processes

The different components of a catchment (e.g. vegetation, soil and geology) guide the rainfall input and release the water damped to the streamflow (Blume et al., 2007; Kirchner, 2006). This was demonstrated by different studies where for different scales catchment properties were found to affect runoff generation (Bonell et al., 1990; Feyen et al., 1999; Laudon et al., 2007; McCartney et al., 1998; Weiler et al., 1998) and Shanley et al. (2002). The temporal changing state of the catchments alter these guiding mechanisms as was demonstrated by Casper et al. (2003); James and Roulet (2009); McGuire and McDonnell (2010); Pellerin et al. (2008) and Shanley et al. (2002). In WS04-WS19 the minimum fraction of pre-event water was generally temporally variable and no clear differences in pre-event water contribution between the different headwaters with variable catchment properties were found. Only subtle differences in fraction of pre-event water were noticed in the rising limb of the different hydrographs. However the coarse sampling interval of 10 min and irregular sampling restricted further assessing these small differences in pre-event water. Furthermore the forested WS10 and WS11 had a slightly higher pre-event water contribution compared to headwaters with mixed landscape or meadows with larger areas of wetlands. Therefore the effect of catchment properties on runoff generation was only a secondary factor.
To better understand the secondary role of the catchment properties as a factor in the variable pre-event water contribution it was helpful to compare the Zwäckentobel to other headwaters with similar high annual precipitation amount (>2000 mm y^{-1}) such as the Maimai (McGlynn et al., 2002) or H. J. Andrews catchment (McGuire and McDonnell, 2010). The Maimai and H. J. Andrews catchment are dominantly forested compared to the variable land cover of the Zwäckentobel consisting of meadows, forests and large percentage of wetlands 20-50%. Compared to the land cover, subsurface characteristics might be a more important explanation for the difference in pre-event water contribution. Vertical cracks of the Maimai and more permeable soil types of the H. J. Andrews facilitate rain water infiltration and fill up the subsurface topography resulting in a large subsurface storage and threshold with dominant pre-event water. The Zwäckentobel instead has shallow gleysols with a low matrix permeability, small active storage and stormflow through the organic soil horizon (20-50 cm, observed by Feyen et al. (1999) and in a nearby hillslope using dye coloring of the different flowpath by Schneider et al. (2014). In these steep and shallow soils with small storage a more dominant event water would be expected. However an important spatial element providing pre-event water to stormflow as in **paper I - Baseflow** (Fischer et al., 2015) is the large area of wetlands and continues wet state (Kollegger, 2010) due to replenishing frequent rainfall. During baseflow these wetland act as passive storage element with a large volume of pre-event water, which only needs to be connected to the stream channels to become runoff. This would explain that with increasing precipitation,

the amount of runoff produced by the precipitation increases and the fraction of pre-event water decreased. The variable rainfall with additional small storage (organic soil horizon, 20-50 cm) results in a near surface dependent threshold with subsequently more variable pre-event water contribution. The Zwäckentobel could be characterized like a combination of a hydrogeomorphic model with spatially distributed passive sources progressively become active and connected with the flow network as described by Sidle et al. (2000) and an analogy of the Babinda model with fast and slow storage components as described by Bonell et al. (1998).
The effect of catchment properties was only a secondary factor and no influence of antecedent conditions or seasonal changes were observed due to the dominant and frequent rainfall which covered any potential signal. This highlight the special character of wet pre-alpine headwater catchments. The total rainfall during the in 2010 and 2011 studied events was above 1300 mm and represented the normal total rainfall during the snow free season. However from the long-term rain gauge WG-01, it is known that in some extreme dry years, the total rainfall during the snow free season was only 820 mm with longer dry-spells. It is likely that during seasons with dryer conditions, runoff generation processes of the Zwäckentobel are different compared to the one observed in this study and it is likely that catchment properties such as storage volume and antecedent conditions become more important and it is likely to observe a stronger signal. During normal-wet seasons only little differences in runoff generation between the neighboring subcatchments was noticeable using baseflow sampling and IHS. This despite the spatial baseflow samples and during events the rising limb was sampled every 10 min (high resolution in respect of many other studies). However in events where observations (stream response and runoff processes) and explanatory variables (precipitation and catchment characteristics) are both spatially variable it is difficult to determine the dominant influencing factor on runoff processes. Discharge data (subcatchment internal and at the outlet) together with a higher spatiotemporal sampling resolution would be necessary to observe small differences of processes and refine different and dominant factors in runoff processes in fast and dynamic pre-alpine headwaters.

5.3 Discussion paper III - Spatial rainfall

5.3.1 Spatial variability in rainfall and rainfall isotopic composition

The number of rain samplers in the Zwäckentobel was much lower than the national monitoring networks described by Schürch et al. (2003); Seeger and Weiler (2014) and Smith et al. (1979) and catchment studies using 38 bulk samplers as described by McGuire et al. (2005). However, the sampler density of the Zwäckentobel of 1 sampler per 0.5 km^2 vs 1 sampler per 1.6 km^2 by other studies was much higher and together with the large number of rainfall events of different magnitudes, provided new insights into the spatial pattern in rainfall and the $\delta^{18}O$ of rainfall. Fischer et al. (2016b) (**Paper II - Runoff events**) observed in the studied headwaters a large spatial variability in event total rainfall, intensity and stable isotope composition for the large events, over relatively short distances. Therefore using the nearest rain sampler for each headwater in the IHS might have introduced an incomplete accounting of event water in space and time, as described by Buttle (1994). The effect of the spatiotemporal variability of rainfall and its isotopic composition on the IHS was examined in more detail. McGuire et al. (2005) and Smith et al. (1979) observed a consistent spatial pattern in the isotopic composition of rainfall. In the Zwäckentobel however the rainfall pattern and the pattern in weighted mean $\delta^{18}O$ of rainfall changed from one event to the other and at shorter distances of only 250 meter were significant differences in rainfall of >20 mm and $\delta^{18}O$ of rainfall 0.3‰ to more than 2‰ observed (Figure 4.7). This spatial variability in the isotope composition of rainfall (event water) was much larger than the variability in the isotopic composition of baseflow (pre-event water) sampled throughout the Zwäckentobel (<0.5‰ observed in **paper I - Baseflow** (Fischer et al., 2015). The spatial

variability in the isotopic composition of rainfall increased slightly with increasing event total rainfall (up to 2.7 ‰) and was very variable for the large events. The spatial differences in the isotopic composition of rainfall were smaller than the large spatial differences reported by other studies, (e.g. McGuire et al., 2005), which was likely due to the 100 times smaller catchment size and smaller altitude range of the Zwäckentobel. The spatial variability in the stable isotope composition of rainfall has been attributed to the amount effect (Dansgaard, 1964) or altitude (Holko et al., 2012; Kern et al., 2014; McGuire and McDonnell, 2008). In the Zwäckentobel neither were rainfall nor the weighted mean δ^{18}O of rainfall correlated to altitude or rainfall amount. The lack of relations and spatial patterns of rainfall and isotopy could have been caused by the variable wind trajectories as observed by Friedman and Smith (1970) and the complex local topography of neighboring mountains affecting the mesoscale and local atmospheric circulation as described by Roe (2005). This small scale spatiotemporal variability of rainfall and its isotopic composition suggests that for each event the spatial pattern has to be characterized separately and that inter or extrapolation based on relationships with rainfall amount or altitude must be done very carefully.

5.3.2 Temporal variability in rainfall isotopic composition and its spatial differences

The benefit of using sequential rain samplers is that they not only provide information on the spatial patterns but additional insight in the temporal changes in the isotopic composition of rainfall during the event. During the first 5 mm of rainfall a large difference in δ^{18}O between the different rain samplers was observed. This spatial variability increased or decreased during the event or remained stable throughout the event. However for some events a rain burst (sudden and high increase in rainfall intensity) affected the δ^{18}O locally and increased the spatial difference in δ^{18}O. As reported by many other rainfall isotope studies (e.g. Berman et al., 2009; Lyon et al., 2009; McDonnell et al., 1990; Penna et al., 2014), the rainfall became more depleted during the event with increasing total rainfall and event duration.

5.3.3 Consequence of the spatiotemporal variability in event water composition on hydrograph separation results

Lyon et al. (2009) demonstrated that the fractions of pre-event water to streamflow were very different when using two samplers in the IHS calculations. The spatiotemporal variability observed in the Zwäckentobel showed that for many events the temporal variability in the isotopic composition was larger than the spatial variability but that the spatial and temporal ranges in isotopic composition could be, for some events almost, the same. Compared to Lyon et al. (2009), with the observed spatiotemporal variability of rainfall and its isotopic composition of 10 events of different magnitude, it was possible to asses the influence of this spatiotemporal variability on the IHS in more detail. Generally small events had a small range and large events had a large range in the calculated minimum fraction of pre-event water in all three sub-catchments (WS04, WS10 and WS19) considering the spatial and temporal variability by the different weighing techniques I-IV (Figure 4.8 and 4.9). This small or large range in the minimum fraction of pre-event water was partly due to the small or large spatiotemporal variability in stable isotope composition of rainfall. The effect of the spatial variability in event water composition was further enhanced for events with small differences between the event water and pre-event water composition, because some rainfall samplers malfunctioned during some events. In **paper II - Runoff events** Fischer et al. (2016b), the nearest rainfall sampler of the headwater (WG-1 for WS04 and WS07, TB-6 for WS10 and WS11 and TB-10 for WS19), which sampled the majority of the events, was used in the IHS eq. (3.3) and eq. (3.2). From the assessment of the spatiotemporal variability in event water composition on hydrograph separation, results demonstrated that using the nearest rain sampler was a reasonable assumption. Instead using a different, more distant rain sampler, in a different headwater would introduce an incorrect isotopic composition of rainfall resulting in unrealistic fractions of pre-event water especially in events where pre-event water and event

water compositions were similar. In such events with similar pre-event water and event water compositions, in addition to the rain sampler location, the choice of different weighing techniques became more important for the IHS calculation. The difference in the fraction of pre-event water due to different rain sampler location and temporal weighing techniques could be larger than the uncertainty in the fraction of pre-event water estimated by (Fischer et al., 2015). This large difference in fraction in pre-event water was mainly because the depleted 'not yet fallen' rainfall was already accounted for in the weighted mean (I) and weighted intensity mean (II) techniques (McDonnell et al., 1990), and resulted in unrealistic fraction of pre-event water. The high spatiotemporal sampling density was useful in events where IHS was not possible, to exchange the rainfall sampling location with other sampling locations to derive a fraction of pre-event water (e.g. event 6, Table 4.1). However from a processes point of view this practice is unsound but demonstrates that having more rain samplers is useful as a validation step to analyse the sensitivity of the IHS results for the variability in the stable isotope composition of rainfall.

5.4 Discussion paper IV - Spectroscopy

5.4.1 The memory effect between samples

Through analyzing very depleted water samples a pronounced effect from the previous water sample was observed, i.e., the memory effect. In general spectroscopes have a memory effect but especially the more depleted samples needed 8-10 measurements until the memory effect faded. This effect occurs especially if two successive samples have large differences and are larger for δ^2H compared to δ^{18}O and observed in all six spectroscopes but slight higher in OA-ICOS. A difference in memory effect between the different type of spectroscopes might be due to the differences in construction. While machines with a long transfer line are supposed the have higher memory effects due to the "stickiness" of water. A heated transfer line, higher cavity and vaporizer temperatures, amount of water per unit surface area of the laser cavity, the injection speed of the sample, the pump-out rate of the spectroscope and syringe deterioration might all reduces the memory effect. Due to the fact that spectroscopes are black boxes it was not possible to investigate each single factor and was beyond the focus of this paper. Interestingly different machine had their own "character" i.e. accuracy and memory effect. Newer spectroscopes showed a slight improvement in performance and reduced analysis time and memory effect and demonstrate the fast development of spectroscopy.

5.5 Assessing IHS assumptions from spatiotemporal baseflow and stormflow results

Combining the results of **paper I-IV** (Fischer et al., 2015, 2016a,b; Penna et al., 2012) it was possible to asses the different assumptions of Table 1.1 used in the IHS. The isotopic composition of the different waters collected in **paper I-IV** (Fischer et al., 2015, 2016a,b) are all analysed using a laser spectroscope with an optimal laboratory work flow to reduce the memory effect between samples and obtain accurate and precise isotopic compositions as described in **paper IV - Spectroscopy** (Penna et al., 2012). Inaccuracy in this trivial first analysis would propagate in further analysis steps and obscure isotopic compositions, e.g. pre-event and event water. Assumption 1 that event and pre-event water are significantly different was not always fulfilled and meant that an IHS was not possible for every sampled event. Considering assumption 5 generally no surface water storage was observed which could have contributed to stormflow and none of the water samples had a sign of fractionation which could have been caused by evaporation of surface storages.

Paper I - Baseflow (Fischer et al., 2015), made it possible to evaluate assumption 3 and 4, i.e., asses whether pre-event water maintains a constant isotopic signature in space and time and

whether the composition of soil water is different to that of groundwater respectively. The spatial snapshot campaigns provided a good overview in the spatial isotopic composition of pre-event water and distinguished between contributing sources of baseflow and covered both assumption 3 and 4 and revealed a difference in soilwater and deep groundwater composition of 1 ‰ for δ^{18}O. This difference was as large as the spatial isotopic composition of pre-event water from snapshot campaigns and temporal differences observed in grab samples before each sampled event. This difference was three times smaller than the spatial isotopic composition of pre-event water described by Buttle (1994).

From the spatiotemporal rain water collected in **paper II and III** (Fischer et al., 2016a,b), it was possible to assess assumption 2 whether event water maintains a constant isotopic signature in space and time and whether it is necessary to account for spatiotemporal differences. In the different sampled events the spatiotemporal variability of δ^{18}O of event water was up to one order of magnitude larger compared to the spatial variability of δ^{18}O in pre-event water and streamwater samples. Accordingly, in the case of the Zwäckentobel, the event water composition contributed much more to uncertainty compared to pre-event water and stream water composition in the IHS results. Therefore it is important to incrementally sample the stable isotope composition of rainfall, as already proposed by McDonnell et al. (1990) and in addition we can add that it is necessary to account for not only the temporal variability but also the spatial variability of the isotopic composition of rainfall in IHS to achieve realistic fractions of pre-event water. Goodrich et al. (1995) stated that one rain gauge can be sufficient to gain information of the temporal rainfall characteristics in small headwaters. However from combining the observations of the spatial and temporal isotopic composition of rainfall one must conclude that due to the small scale variability of rainfall and its isotopic composition in small pre-alpine headwater catchments one rain gauge would not be sufficient for the Zwäckentobel catchment, and likely also not for other pre-alpine catchments. As a consequence the IHS assumption 2 and 3 (Table 1.1) described as: the isotope signature of pre-event or event water is constant in space and time (Buttle, 1994; Klaus and McDonnell, 2013) was changed to: The isotope signature of pre-event or event water is not constant in space and time and has to be accounted for! Especially with the promising development in laser spectroscopes in the field (Berman et al., 2009), it may make it easier to better characterize the temporal variability of the isotopic composition of rainfall. However our study demonstrates the spatial aspect of rainfall and its isotopic composition must not be forgotten.

6. Conclusion

Water samples collected in the Zwäckentobel, a pre-alpine region with high precipitation (P>2000 mm y^{-1}) and heterogeneous catchment properties, contained important information on the source and flowpath of water during baseflow and the contribution of rainfall to stormflow. The Zwäckentobel water samples had a range between -20 ‰ and 0 ‰ for $\delta^{18}O$ (all samples were on the GMWL). For these samples it was sufficient to measure each sample six times with a laser spectroscope and to discard only the first three samples. However for depleted water samples and with a high inter-vial isotopic difference, as used in **paper IV**, independently of the laser spectroscope used, the memory effect was reduced only after seven to eight injections. Snapshot campaigns during baseflow, as described in **paper I**, were useful to better understand and explore the source and flowpath of baseflow in the newly gauged Zwäckentobel and six neighbouring subcatchments with variable arrangements of landscape units. The "beyond the catchment scale" collected water samples had generally a small inter- and intra catchment variability for the selected isotopic and hydrochemical variables. But it was possible to identify two landscape units: the upper spring zone located near the water divide above 1400 m a.s.l. and a wetland in WS04. Despite the large areal extent of wetlands (30-60% of the subcatchment area with characteristic large storage capacity), these elements acted as passive (disconnected) elements while deep groundwater contributed actively to baseflow runoff. These findings can help to better understand long-term hydrochemical datasets and could be used to adapt monitoring strategies to select functional tracers and to increase knowledge of the fundamental mechanisms and governing process of headwater systems. In **paper II** five subcatchments of the Zwäckentobel headwater catchment, the rainfall and streamwater of 13 different rainstorms were sampled to investigated how the spatially varying catchment properties and temporal controls influence stormflow runoff generation. Irrespective of the stable isotope used, $\delta^{18}O$ or $\delta^{2}H$, no significant difference in minimum fraction of pre-event water contribution was observed. The pre-event water contribution was found to be temporally variable. Small events had high pre-event water contribution. With increasing precipitation, the volume of runoff produced by precipitation increased and a change from pre-event to event water dominated runoff processes occurred. The variable rainfall amount and small active storage (organic soil horizon, 20–50 cm) resulted in a threshold in the upper soil horizon with subsequently more variable pre-event water contribution. Despite the differences in catchment characteristics between the neighboring streams at headwater scale, no significant difference in minimum fraction of pre-event water contribution was observed. This spatiotemporal dataset made it possible to infer that rainfall was the dominant driver and masked catchment properties or antecedent conditions in runoff processes. These findings underline that, in contrast to the conventional approach of studying one headwater with few events, it is necessary to study different neighboring headwaters and a wide range of event magnitudes (many events and many samples), to validate and better understand the dynamic character and controlling factors of runoff processes in pre-alpine headwater catchments. Using the spatial dataset from **paper II**, consisting of 8 different rainfall sampling locations and stormflow samples of different streams, it was possible to assess, as described in **paper III** the effects of spatial variability of stable isotope composition of rainfall on the results of an IHS. Contrary to the common assumption of a constant rainfall and its isotopic composition in a small

headwater, the rainfall amount and its weighted mean δ^{18}O varied significant over distances of only 250 meter and was variable from event to event. For the majority of the events, neither rainfall nor the δ^{18}O of rainfall, were correlated to altitude or rainfall amount. Therefore one sequential sampler is not enough to get robust IHS results for small headwater catchments and the spatiotemporal variability in the isotopic composition of rainfall can significantly influence the IHS results. It is thus necessary to sample rainfall at different locations, also in small headwater catchments, to understand the factors that control runoff generation.

The different findings of this doctoral thesis show the necessity and benefits of spatially distributed measurements to derive and better understand controlling factors in runoff generation in a headwater catchment with high precipitation amounts and heterogeneous catchment properties. The combination of long-term and spatially short-term hydrometeorological measurements, together with three baseflow sampling campaigns and event water sampling in different neighboring streams and multiple events, complemented each other and helped to overcome individual limitations to untangle the complexity of different temporal and spatial controls (hydrometeorological conditions and catchment properties, respectively) affecting the runoff generation during base and stormflow.

7. Future considerations

The observations of this doctoral thesis shed a new light on the spatiotemporal baseflow and stormflow processes in pre-alpine headwater catchments with high precipitation (P>2000 mm y^{-1}) and raises additional new questions for further research. The three snapshot sampling campaigns were useful as an explorative study in the newly gauged headwater. The IHS gave good qualitative information on the contribution of rainfall and the fraction of pre-event water. Nevertheless many questions on the source and flowpath of the water (Lyon et al., 2008) and thresholds (Graham et al., 2010) are unresolved. An open question is the runoff contribution, of the observed internal landscape elements of the subcatchments (**paper I** (Fischer et al., 2015)) and the response of individual streams to storm flow in space and time. Therefore, future studies should validate the connectivity, interaction and different runoff processes of the internal catchment elements (such as wetlands or forest) in the headwater catchment with specific questions

- Do the streams with similar hydrometeorological and catchment characteristics as represented in Figure 3.2 have similar spatiotemporal runoff processes?
- What are the sources, flowpath and transit times in the different landscape elements in more detail during baseflow and stormflow?
- What are the spatiotemporal runoff processes of the different landscape elements and is it possible to observe their spatial contribution in the stormflow hydrograph?
- Are these patterns of spatial contribution to stormflow coherent with the base flow patterns, can this be related to the physical system and are these stable in time?
- How does the transition of the upper spring signal change along the stream network during stormflow? At which point in the storm hydrograph, at the catchment outlet, is it possible to observe the signal of the upper spring?
- Forest interception and throughfall can result in changed isotopic signatures (Allen et al., 2015; Saxena, 1987). Since the rainfall was sampled only in the open field this might have influenced the IHS results. Therefore it would be interesting to further investigate the spatiotemporal throughfall patterns together with a higher spatiotemporal sampling e.g. in a transect in WS04 or WS07, and the effect on IHS results.
- How useful are different tracers in the separation of the hydrograph of steep pre-alpine headwaters with high precipitation?

Subcatchment internal storm sampling of key locations and a continuation of snapshot sampling campaigns during baseflow and stormflow would provide subcatchment internal information on runoff processes during different states. Using hydrometric and a multiple tracer approach (using similar tracers to those used by Fischer et al. (2015), $\delta^{18}O$, Ca and DOC) would allow a better understanding of the flowpaths and contributing sources during stormflow of headwaters. A trivial missing variable was the discharge (measurements). Being able to more accurately measure discharge would give valuable additional information and would make it possible to qualitative and quantitative compare the different headwaters.

The sampling rate of baseflow and stormflow was higher in comparison to many other studies. The sampling was done on a trail and error based approach by looking to the weather forecast and

going to the field. However even in a data rich country like Switzerland the weather forecast is not always reliable. This resulted in unnecessary traveling to the field and missed events. Remote access to all sampling equipment would have improved the data quality significantly. Not only to see whether events are or were sampled but also for trouble shooting. Furthermore, collecting more water samples at a finer spatiotemporal resolution with more events would allow processes to be observed in more detail. A finer temporal sampling resolution would help investigate subtle changes in pre-event water in relation to differences in catchment characteristics. Although the sampled events had different antecedent conditions, the Zwäckentobel was generally wet. However it would be interesting to see whether runoff processes are different after long dry spells (>14 days) such as observed in summer 2015 where certain springs ceased, resulting in extreme low baseflow.

Many studies prefer to study catchment processes from 10 km^2 to 1000 km^2, assuming homogeneity and neglecting the small scale heterogeneity of different processes. Huge investments are made in remote sensing to be able to observe the outside of the black-box in a higher resolution and from further away than what hydrologists call the catchment. Unfortunately, cost pressure forces agencies to shut down existing long term catchments and internal measurements are often neglected while studies still use point measurements and data of single catchments of >10km^2 in modeling exercises to explain future changes. However the results of this study revealed the large spatiotemporal variability of the hydrometeorological input and catchment internal processes need to be further explored by tracing the different flowpath of the water. However hydrologists should not only look at the catchment from an hydrological point of view (subsurface and runoff processes) but step out of the box and link the full spatiotemporal process chain from atmospheric processes to the point where the water becomes runoff in a spatiotemporal context by using different sampling strategies and multiple field based lasers (separate spectroscopes for precipitation and for runoff sampling). The high annual precipitation input, flashy character of stream flow dominant wet conditions and the existence of long-term data and short spatiotemporal data make the Zwäckentobel headwater catchment an exciting study area to further explore these open questions and investigate the rainfall-runoff processes in more detail. Findings should be compared and repeated in other pre-alpine headwaters (e.g. in the streams described in Figure 3.2). The results in this thesis should be tested, compared and incorporate the different findings in modeling exercises to further explore and test both field observations and existing modeling frameworks. Is the Babinda model a good conceptual model for the Zwäckentobel or are other model representations e.g. the two-box model described by Seibert et al. (2003), or learning from model testing as shown by Fenicia et al. (2008, 2014, 2016) better alternatives? Confronting field data with models and vice versa would contribute to bridging the deep and invincible canyon developed between the so called experimentalist and modelers (Seibert and McDonnell, 2002). Experimentalist and modelers should not only start to communicate but maybe even change their roles once in a while. This would contribute to more exploration and lead to improved future field data collection and modeling exercises. Only by considering the three pillars of field observations, data analysis and modeling it is possible to validate, compare and learn from the differences to better understand these important upstream headwater catchments and develop new answers of signal propagation of the system (Soulsby et al., 2007) for the right reason (Kirchner, 2006).

References

Ahmad, M., Aggarwal, P., van Duren, M., Poltenstei, L., Araguas, L., Kurttas, T., and Wassenaar, L. I.: Fourth interlaboratory comparison exercise for 2H and 18O analysis of water samples (WICO2011), Tech. rep., International Atomic Energy Agency, Wien, 2012. 2

Allen, S. T., Keim, R. F., and McDonnell, J. J.: Spatial patterns of throughfall isotopic composition at the event and seasonal timescales, Journal of Hydrology, 522, 58–66, doi:10.1016/j.jhydrol.2014.12.029, 2015. 5, 6, 47

Ambroise, B.: Variable 'active' versus 'contributing' areas or periods: a necessary distinction, Hydrological Processes, 18, 1149–1155, doi:10.1002/hyp.5536, 2004. 37

Araguás-Araguás, L., Froehlich, K., and Rozanski, K.: Deuterium and oxygen-18 isotope composition of precipitation and atmospheric moisture, Hydrological Processes, 14, 1341–1355, doi:10.1002/1099-1085(20000615)14:8<1341::AID-HYP983>3.0.CO;2-Z, 2000. 6

Asano, Y., Uchida, T., Mimasu, Y., and Ohte, N.: Spatial patterns of stream solute concentrations in a steep mountainous catchment with a homogeneous landscape, Water Resources Research, 45, W10 432, doi:10.1029/2008WR007466, 2009. 2, 3, 36, 37

Barthold, F. K., Wu, J., Vaché, K. B., Schneider, K., Frede, H.-G., and Breuer, L.: Identification of geographic runoff sources in a data sparse region: hydrological processes and the limitations of tracer-based approaches, Hydrological Processes, 24, 2313–2327, doi:10.1002/hyp.7678, 2010. 2

Bergamini, A., Peintinger, M., Fakheran, S., Moradi, H., Schmid, B., and Joshi, J.: Loss of habitat specialists despite conservation management in fen remnants 1995–2006, Perspectives in Plant Ecology, Evolution and Systematics, 11, 65 – 79, doi:10.1016/j.ppees.2008.10.001, 2009. 1

Berman, E. S. F., Gupta, M., Gabrielli, C., Garland, T., and McDonnell, J. J.: High-frequency field-deployable isotope analyzer for hydrological applications, Water Resources Research, 45, n/a–n/a, doi:10.1029/2009WR008265, 2009. 6, 41, 43

Bishop, K., Buffam, I., Erlandsson, M., Fölster, J., Laudon, H., Seibert, J., and Temnerud, J.: Aqua Incognita: the unknown headwaters, Hydrological Processes, 22, 1239–1242, doi:10.1002/hyp.7049, 2008. 1

Blume, T., Zehe, E., and Bronstert, A.: Rainfall—runoff response, event-based runoff coefficients and hydrograph separation, Hydrological Sciences Journal, 52, 843–862, doi:10.1623/hysj.52.5.843, 2007. 39

Bonell, M., Pearce, A. J., and Stewart, M. K.: The identification of runoff-production mechanisms using environmental isotopes in a tussock grassland catchment, eastern otago, New Zealand, Hydrological Processes, 4, 15–34, doi:10.1002/hyp.3360040103, 1990. 5, 39

Bonell, M., Barnes, C. J., Grant, C. R., Howard, A., and Burns, J.: Chapter 11 - High Rainfall, Response-Dominated Catchments: A Comparative Study of Experiments in Tropical Northeast Queensland with Temperate New Zealand, in: Isotope Tracers in Catchment Hydrology, edited by Kendall, C. and McDonnell, J., pp. 347–390, Elsevier, Amsterdam, doi:10.1016/B978-0-444-81546-0.50018-5, 1998. 40

Brand, W. A., Geilmann, H., Crosson, E. R., and Rella, C. W.: Cavity ring-down spectroscopy versus high-temperature conversion isotope ratio mass spectrometry; a case study on δ and δ18O of pure water samples and alcohol water mixtures, Rapid Communications in Mass Spectrometry, 23, 1879–1884, doi:10.1002/rcm.4083, 2009. 2, 21

Brönnimann, C., Stähli, M., Schneider, P., Seward, L., and Springman, S. M.: Bedrock exfiltration as a triggering mechanism for shallow landslides, Water Resources Research, 49, 5155–5167, doi:10.1002/wrcr.20386, 2013. 1, 11

Brown, V. A., McDonnell, J. J., Burns, D. A., and Kendall, C.: The role of event water, a rapid shallow flow component, and catchment size in summer stormflow, Journal of Hydrology, 217, 171–190, doi:10.1016/S0022-1694(98)00247-9, 1999. 5, 6

Burch, H.: Ein Rückblick auf die hydrologische Forschung der WSL im Alptal(A Retrospective on the hydrological research at WSL in Alptal), Beiträge zur Hydrologie der Schweiz, 35, 18–33, doi:-, 1994. 12

Burch, H., Forster, F., Schleppi, P., and Stadler, D.: Influence of forests on floods from small prealpine catchments, 1, VHB, Garmisch Partenkirchen, 1996. 19

Burns, D. A.: Stormflow-hydrograph separation based on isotopes: the thrill is gone — what's next?, Hydrological Processes, 16, 1515–1517, doi:10.1002/hyp.5008, 2002. 4

Buttle, J., Dillon, P., and Eerkes, G.: Hydrologic coupling of slopes, riparian zones and streams: an example from the Canadian Shield, Journal of Hydrology, 287, 161–177, doi:10.1016/j.jhydrol.2003.09.022, 2004. 3

Buttle, J. M.: Isotope hydrograph separations and rapid delivery of pre-event water from drainage basins, Progress in Physical Geography, 18, 16–41, 1994. 4, 5, 38, 40, 43

Campbell, D. H., Clow, D. W., Ingersoll, G. P., Mast, M. A., Spahr, N. E., and Turk, J. T.: Processes Controlling the Chemistry of Two Snowmelt-Dominated Streams in the Rocky Mountains, Water Resources Research, 31, 2811–2821, doi:10.1029/95WR02037, 1995. 36

Casper, M. C., Volkmann, H. N., Waldenmeyer, G., and Plate, E. J.: The separation of flow pathways in a sandstone catchment of the Northern Black Forest using DOC and a nested Approach, Physics and Chemistry of the Earth, Parts A/B/C, 28, 269–275, doi:10.1016/S1474-7065(03)00037-8, 2003. 4, 39

Christophersen, N. and Hooper, R. P.: Multivariate analysis of stream water chemical data: The use of principal components analysis for the end-member mixing problem, Water Resources Research, 28, 99–107, doi:10.1029/91WR02518, 1992. 2

Dansgaard, W.: The Abundance of O18 in Atmospheric Water and Water Vapour, Tellus, 5, 461–469, doi:10.1111/j.2153-3490.1953.tb01076.x, 1953. 6

Dansgaard, W.: Stable isotopes in precipitation, Tellus, 16, 436–468, doi:10.1111/j.2153-3490.1964.tb00181.x, 1964. 6, 41

Didszun, J. and Uhlenbrook, S.: Scaling of dominant runoff generation processes: Nested catchments approach using multiple tracers, Water Resources Research, 44, W02 410, doi:10.1029/2006WR005242, 2008. 3

Dooge, J. C. I.: Bringing it all together, Hydrology and Earth System Sciences, 9, 3–14, doi:10.5194/hess-9-3-2005, 2005. 1

Fenicia, F., McDonnell, J. J., and Savenije, H. H. G.: Learning from model improvement: On the contribution of complementary data to process understanding, Water Resources Research, 44, n/a–n/a, doi:10.1029/2007WR006386, w06419, 2008. 48

Fenicia, F., Kavetski, D., Savenije, H. H. G., Clark, M. P., Schoups, G., Pfister, L., and Freer, J.: Catchment properties, function, and conceptual model representation: is there a correspondence?, Hydrological Processes, 28, 2451–2467, doi:10.1002/hyp.9726, 2014. 48

Fenicia, F., Kavetski, D., Savenije, H. H. G., and Pfister, L.: From spatially variable streamflow to distributed hydrological models: Analysis of key modeling decisions, Water Resources Research, pp. n/a–n/a, doi:10.1002/2015WR017398, 2016. 48

Feyen, H., Leuenberger, J., Papritz, A., Gysi, M., Flühler, H., and Schleppi, P.: Runoff Processes in Catchments with a Small Scale Topography, Physics and Chemistry of the Earth, 21, 177–181, doi:10.1016/S0079-1946(97)85581-4, 1996. 9, 11, 12

Feyen, H., Wunderli, H., Wydler, H., and Papritz, A.: A tracer experiment to study flow paths of water in a forest soil, Journal of Hydrology, 225, 155–167, doi:dx.doi.org/10.1016/S0022-1694(99)00159-6, 1999. 12, 39

Feyen, H. M. J.: Identification of runoff processes in catchments with a small scale topography, Ph.D. thesis, ETH Zürich, 1998. 12

Fischer, B. M. C., Rinderer, M., Schneider, P., Ewen, T., and Seibert, J.: Contributing sources to baseflow in pre-alpine headwaters using spatial snapshot sampling, Hydrological Processes, pp. n/a–n/a, doi:10.1002/hyp.10529, 2015. 11, 12, 14, 15, 18, 19, 23, 24, 25, 38, 39, 40, 42, 47

Fischer, B. M. C., Meerveld van, H. J., and Seibert, J.: Effect of small scale variability in isotopic composition of precipitation on hydrograph separation results, In preparation, doi:NA, 2016a. 12, 20, 29, 31, 32, 42, 43

Fischer, B. M. C., Stähli, M., and Seibert, J.: Pre-event water contributions to runoff events of different magnitude in pre-alpine headwaters, Hydrology Research, doi:10.2166/nh.2016.176, 2016b. 12, 15, 18, 20, 26, 27, 28, 40, 41, 42, 43

Frei, C. and Schär, C.: A precipitation climatology of the Alps from high-resolution rain-gauge observations, International Journal of Climatology, 18, 873–900, doi:10.1002/(SICI)1097-0088(19980630)18:8<873::AID-JOC255>3.0.CO;2-9, 1998. 1

Friedman, I. and Smith, G. I.: Deuterium Content of Snow Cores from Sierra Nevada Area, Science, 169, 467–470, doi:10.2307/1730266, 1970. 41

Frisbee, M. D., Phillips, F. M., Campbell, A. R., Liu, F., and Sanchez, S. A.: Streamflow generation in a large, alpine watershed in the southern Rocky Mountains of Colorado: Is streamflow generation simply the aggregation of hillslope runoff responses?, Water Resources Research, 47, W06 512, doi:10.1029/2010WR009391, 2011. 2, 36, 37

Fröhlich, H. L., Breuer, L., Frede, H.-G., Huisman, J. A., and Vaché, K. B.: Water source characterization through spatiotemporal patterns of major, minor and trace element stream concentrations in a complex, mesoscale German catchment, Hydrological Processes, 22, 2028–2043, doi:10.1002/hyp.6804, 2008. 3

Gatz, D. F., Selman, R. F., Langs, R. K., and Holtzman, R. B.: An Automatic Sequential Rain Sampler, Journal of Applied Meteorology, 10, 341–344, doi:10.1175/1520-0450(1971)010<0341:AASRS>2.0.CO;2, 1971. 6

Genereux, D.: Quantifying uncertainty in tracer-based hydrograph separations, Water Resources Research, 34, 915–919, doi:10.1029/98WR00010, 1998. 19, 38

Geris, J., Tetzlaff, D., McDonnell, J., and Soulsby, C.: The relative role of soil type and tree cover on water storage and transmission in northern headwater catchments, Hydrological Processes, 29, 1844–1860, doi:10.1002/hyp.10289, 2015. 5

Gerrits, A. M. J., Pfister, L., and Savenije, H. H. G.: Spatial and temporal variability of canopy and forest floor interception in a beech forest, Hydrological Processes, 24, 3011–3025, doi:10.1002/hyp.7712, 2010. 5

Gkinis, V., Popp, T. J., Johnsen, S. J., and Blunier, T.: A continuous stream flash evaporator for the calibration of an IR cavity ring-down spectrometer for the isotopic analysis of water, Isotopes in Environmental and Health Studies, 46, 463–475, doi:10.1080/10256016.2010.538052, 2010. 21

Goodrich, D. C., Faurès, J.-M., Woolhiser, D. A., Lane, L. J., and Sorooshian, S.: Measurement and analysis of small-scale convective storm rainfall variability, Journal of Hydrology, 173, 283–308, doi:10.1016/0022-1694(95)02703-R, 1995. 6, 43

Graham, C. B., Woods, R. A., and McDonnell, J. J.: Hillslope threshold response to rainfall: (1) A field based forensic approach, Journal of Hydrology, 393, 65–76, doi:10.1016/j.jhydrol.2009.12.015, 2010. 47

Gröning, M.: Improved water δ2H and δ18O calibration and calculation of measurement uncertainty using a simple software tool, Rapid Communications in Mass Spectrometry, 25, 2711–2720, doi:10.1002/rcm.5074, 2011. 21, 22

Hagedorn, F., Bucher, J. B., and Schleppi, P.: Contrasting dynamics of dissolved inorganic and organic nitrogen in soil and surface waters of forested catchments with Gleysols, Geoderma, 100, 173–192, doi:10.1016/S0016-7061(00)00085-9, 2001. 11

Hantke, R.: Geological map of the Canton of Zurich and its neighboring areas, Quarterly journal of the Natural History Society in Zurich, 112, doi:NA, 1967. 11

Hegg, C., McArdell, B. W., and Badoux, A.: One hundred years of mountain hydrology in Switzerland by the WSL, Hydrological Processes, 20, 371–376, doi:10.1002/hyp.6055, 2006. 1, 12

Hinton, M. J., Schiff, S. L., and English, M. C.: Examining the contributions of glacial till water to storm runoff using two- and three-component hydrograph separations, Water Resources Research, 30, 983–993, doi:10.1029/93WR03246, 1994. 4

Holko, L.: Syringe life and memory effects in isotopic analyses performed by liquid water isotopic analysers – a case study for natural waters from central Europe, Isotopes in Environmental and Health Studies, 0, 1–7, doi:10.1080/10256016.2015.1090987, 2015. 2

Holko, L., Dóša, M., Michalko, J., and Kostka, Z.: Isotopes of oxygen-18 and deuterium in precipitation in Slovakia, ournal of Hydrology and Hydromechanics, 60, 265–276, doi:10.2478/v10098-012-0023-2, 2012. 6, 41

Hooper, R. P., Christophersen, N., and Peters, N. E.: Modelling streamwater chemistry as a mixture of soilwater end-members — An application to the Panola Mountain catchment, Georgia, U.S.A., Journal of Hydrology, 116, 321–343, doi:10.1016/0022-1694(90)90131-G, 1990. 3

Hrachowitz, M., Bohte, R., Mul, M. L., Bogaard, T. A., Savenije, H. H. G., and Uhlenbrook, S.: On the value of combined event runoff and tracer analysis to improve understanding of catchment functioning in a data-scarce semi-arid area, Hydrology and Earth System Sciences, 15, 2007–2024, doi:10.5194/hess-15-2007-2011, 2011. 2, 4, 5, 6

Hsü, K. J. and Briegel, U.: The Flysch, in: Geology of Switzerland SE - 6, pp. 65–82, Birkhäuser, Basel, doi:10.1007/978-3-0348-8663-5{_}6, 1991. 11

IAEA: Laser Spectroscopy Analysis of Liquid Water Samples for Stable Hydrogen and Oxygen Isotopes, Performance Testing and Procedures for Installing and Operating the LGR DT-100 Liquid Water Isotope Analyzer. International Atomic Energy Agency, Tech. rep., IAEA, Vienna, doi:ISSN1018-5518, 2009. 21

Inamdar, S., Dhillon, G., Singh, S., Dutta, S., Levia, D., Scott, D., Mitchell, M., Van Stan, J., and McHale, P.: Temporal variation in end-member chemistry and its influence on runoff mixing patterns in a forested, Piedmont catchment, Water Resources Research, 49, 1828–1844, doi:10.1002/wrcr.20158, 2013. 2, 36, 37

James, A. L. and Roulet, N. T.: Investigating the applicability of end-member mixing analysis (EMMA) across scale: A study of eight small, nested catchments in a temperate forested watershed, Water Resources Research, 42, doi:10.1029/2005WR004419, 2006. 2

James, A. L. and Roulet, N. T.: Antecedent moisture conditions and catchment morphology as controls on spatial patterns of runoff generation in small forest catchments, Journal of Hydrology, 377, 351–366, doi:10.1916/j.jhydrol.2009.08.039, 2009. 4, 5, 6, 39

Jordan, J.: Spatial and temporal variability of stormflow generation processes on a Swiss catchment, Journal of Hydrology, 153, 357–382, doi:10.1016/0022-1694(94)90199-6, 1994. 4, 5, 6

Keller, H. M.: Factors Affecting Water Quality of Small Mountain Catchments, Journal of Hydrology (NZ), 9, 133–141, 1970. 2, 11, 12

Keller, H. M.: Extreme conditions of streamwater chemistry in a partly forested mountainous region, IAHS PUBLICATION Proceedings of two LausanneSymposia, August 1990, pp. 477–486, 1990. 2, 12, 36

Keller, H. M., Burch, H. J., and Guecheva, M.: The variability of water quality in a small mountainous region, IAHS PUBLICATION Regional Characterization of Water Quality(Proceedings of the Baltimore Symposium, May 19), pp. 305–312, 1989. 2, 36, 37

Kennedy, V., Kendall, C., Zellweger, G., Wyerman, T., and Avanzino, R.: Determination of the components of stormflow using water chemistry and environmental isotopes, Mattole River basin, California, Journal of Hydrology, 84, 107 – 140, doi:http://dx.doi.org/10.1016/0022-1694(86)90047-8, 1986. 6

Kennedy, V. C., Zellweger, G. W., and Avanzino, R. J.: Variation of rain chemistry during storms at two sites in northern California, Water Resources Research, 15, 687–702, doi:10.1029/WR015i003p00687, 1979. 15

Kern, Z., Kohán, B., and Leuenberger, M.: Precipitation isoscape of high reliefs: interpolation scheme designed and tested for monthly resolved precipitation oxygen isotope records of an Alpine domain, Atmos. Chem. Phys., 14, 1897–1907, doi:10.5194/acp-14-1897-2014, 2014. 6, 41

Kienzler, P. M. and Naef, F.: Subsurface storm flow formation at different hillslopes and implications for the 'old water paradox', Hydrological Processes, 116, 104–116, doi:10.1002/hyp.6687, 2008. 4, 39

Kirchner, J. W.: Getting the right answers for the right reasons: Linking measurements, analyses, and models to advance the science of hydrology, Water Resources Research, 42, n/a–n/a, doi:10.1029/2005WR004362, w03S04, 2006. 1, 39, 48

Klaus, J. and McDonnell, J. J.: Hydrograph separation using stable isotopes: Review and evaluation, Journal of Hydrology, 505, 47–64, doi:10.1016/j.jhydrol.2013.09.006, 2013. 2, 3, 4, 5, 43

Kollegger, A.: Untersuchung der räumlichen und zeitlichen Verteilung der Bodenfeuchtigkeit am Beispiel des Erlenbaches (Alptal/Schweiz). Vergleich einer quantitativen und einer qualitativen Messmethode, Master thesis, University of Zurich, 2010. 13, 39

Kosugi, K., Katsura, S., Katsuyama, M., and Mizuyama, T.: Water flow processes in weathered granitic bedrock and their effects on runoff generation in a small headwater catchment, Water Resources Research, 42, W02 414, doi:10.1029/2005WR004275, 2006. 3

Krupa, S. V.: Sampling and physico-chemical analysis of precipitation: a review, Environmental Pollution, 120, 565–594, doi:10.1016/S0269-7491(02)00165-3, 2002. 6

Laquer, F. C.: Sequential precipitation samplers: A literature review, Atmospheric Environment. Part A. General Topics, 24, 2289–2297, doi:10.1016/0960-1686(90)90322-E, 1990. 6

Laudon, H. and Slaymaker, O.: Hydrograph separation using stable isotopes, silica and electrical conductivity: an alpine example, Journal of Hydrology, 201, 82 – 101, doi:10.1016/S0022-1694(97)00030-9, 1997. 2, 5

Laudon, H., Sjöblom, V., Buffam, I., Seibert, J., and Mörth, M.: The role of catchment scale and landscape characteristics for runoff generation of boreal streams, Journal of Hydrology, 344, 198–209, doi:10.1016/j.jhydrol.2007.07.010, 2007. 4, 5, 39

Liechti, K., Zappa, M., Fundel, F., and Germann, U.: Probabilistic evaluation of ensemble discharge nowcasts in two nested Alpine basins prone to flash floods, Hydrological Processes, 27, 5–17, doi:10.1002/hyp.9458, 2013. 1

Likens, G. and Buso, D. .: Variation in Streamwater Chemistry Throughout the Hubbard Brook Valley, Biogeochemistry, 78, 1–30, doi:10.1007/s10533-005-2024-2, 2006. 2, 3, 36

Lis, G., Wassenaar, L. I., and Hendry, M. J.: High-precision laser spectroscopy D/H and 18O/16O measurements of microliter natural water samples., Analytical chemistry, 80, 287–93, doi:10.1021/ac701716q, 2008. 2

Lu, H.-Y.: Application of water chemistry as a hydrological tracer in a volcano catchment area: A case study of the Tatun Volcano Group, North Taiwan, Journal of Hydrology, 511, 825–837, doi:10.1016/j.jhydrol.2014.02.036, 2014. 2

Lyon, S. W., Desilets, S. L. E., and Troch, P. A.: Characterizing the response of a catchment to an extreme rainfall event using hydrometric and isotopic data, Water Resources Research, 44, doi:10.1029/2007WR006259, 2008. 4, 6, 47

Lyon, S. W., Desilets, S. L. E., and Troch, P. A.: A tale of two isotopes: differences in hydrograph separation for a runoff event when using δD versus δ18O, Hydrological Processes, 23, 2095–2101, doi:10.1002/hyp.7326, 2009. 6, 38, 41

Lyon, S. W., Nathanson, M., Spans, A., Grabs, T., Laudon, H., Temnerud, J., Bishop, K. H., and Seibert, J.: Specific discharge variability in a boreal landscape, Water Resources Research, 48, W08 506, doi:10.1029/2011WR011073, 2012. 3

McCartney, M. P., Neal, C., and Neal, M.: Use of deuterium to understand runoff generation in a headwater catchment containing a dambo, doi:10.5194/hess-2-65-1998, 1998. 5, 39

McDonnell, J. J.: Where does water go when it rains? Moving beyond the variable source area concept of rainfall-runoff response, Hydrological Processes, 17, 1869–1875, doi:10.1002/hyp.5132, 2003. 1, 2

McDonnell, J. J. and Beven, K.: Debates—The future of hydrological sciences: A (common) path forward? A call to action aimed at understanding velocities, celerities and residence time distributions of the headwater hydrograph, Water Resources Research, 50, 5342–5350, doi:10.1002/2013WR015141, 2014. 1, 6

McDonnell, J. J., Bonell, M., Stewart, M. K., and Pearce, A. J.: Deuterium Variations in Storm Rainfall: Implications for Stream Hydrograph Separation, Water Resources Re, 26, 455–458, doi:10.1029/WR026i003p00455, 1990. 4, 6, 19, 20, 41, 42, 43

McDonnell, J. J., Sivapalan, M., Vaché, K., Dunn, S., Grant, G., Haggerty, R., Hinz, C., Hooper, R., Kirchner, J., Roderick, M. L., Selker, J., and Weiler, M.: Moving beyond heterogeneity and process complexity: A new vision for watershed hydrology, Water Resources Research, 43, W07 301, doi:10.1029/2006WR005467, 2007. 3

McGlynn, B. L., McDonnel, J. J., and Brammer, D. D.: A review of the evolving perceptual model of hillslope flowpaths at the Maimai catchments, New Zealand, Journal of Hydrology, 257, 1–26, doi:10.1016/S0022-1694(01)00559-5, 2002. 39

McGlynn, B. L., McDonnell, J. J., Seibert, J., and Kendall, C.: Scale effects on headwater catchment runoff timing, flow sources, and groundwater-streamflow relations, Water Resources Research, 40, W07 504, doi:10.1029/2003WR002494, 2004. 4, 5

McGuire, K. and McDonnell, J.: Stable Isotope Tracers in Watershed Hydrology, in: Stable Isotopes in Ecology and Environmental Science, pp. 334–374, Blackwell Publishing Ltd, doi:10.1002/9780470691854.ch11, 2008. 6, 41

McGuire, K. J. and McDonnell, J. J.: Hydrological connectivity of hillslopes and streams: Characteristic time scales and nonlinearities, Water Resources Research, 46, W10 543, doi:10.1029/2010WR009341, 2010. 39

McGuire, K. J., McDonnell, J. J., Weiler, M., Kendall, C., McGlynn, B. L., Welker, J. M., and Seibert, J.: The role of topography on catchment-scale water residence time, Water Resources Research, 41, 1–14, doi:10.1029/2004WR003657, 2005. 6, 40, 41

Menzel, L., Lang, H., and Martin, R.: Mean Annual Actual Evaporation 1973–1992, in: Hydrological Atlas of Switzerland, chap. 4.1, p. 4.1, Federal Office for the Environment FOEN, Bern, 9 edn., 2007. 9

Molnar, P., Densmore, A. L., McArdell, B. W., Turowski, J. M., and Burlando, P.: Analysis of changes in the step-pool morphology and channel profile of a steep mountain stream following a large flood, Geomorphology, 124, 85–94, doi:10.1016/j.geomorph.2010.08.014, 2010. 11

Munksgaard, N. C., Wurster, C. M., Bass, A., and Bird, M. I.: Extreme short-term stable isotope variability revealed by continuous rainwater analysis, Hydrological Processes, 26, 3630–3634, doi:10.1002/hyp.9505, 2012. 6

Onda, Y., Tsujimura, M., Fujihara, J., and Ito, J.: Runoff generation mechanisms in high-relief mountainous watersheds with different underlying geology, Journal of Hydrology, 331, 659–673, doi:10.1016/j.jhydrol.2006.06.009, 2006. 4, 5

Pearce, a. J., Stewart, M. K., and Sklash, M. G.: Storm Runoff Generation in Humid Headwater Catchments: 1. Where Does the Water Come From?, Water Resources Research, 22, 1263–1272, doi:10.1029/WR022i008p01263, 1986. 5

Pellerin, B. A., Wollheim, W. M., Feng, X., and Vörösmarty, C. J.: The application of electrical conductivity as a tracer for hydrograph separation in urban catchments, Hydrological Processes, doi:10.1002/hyp, 2008. 4, 6, 39

Penna, D., Stenni, B., Šanda, M., Wrede, S., Bogaard, T. a., Gobbi, A., Borga, M., Fischer, B. M. C., Bonazza, M., and Chárová, Z.: On the reproducibility and repeatability of laser absorption spectroscopy measurements for δ2H and δ18O isotopic analysis, Hydrology and Earth System Sciences, 14, 1551–1566, doi:10.5194/hess-14-1551-2010, 2010. 2, 16, 21, 22

Penna, D., Stenni, B., Šanda, M., Wrede, S., Bogaard, T. a., Michelini, M., Fischer, B. M. C., Gobbi, A., Mantese, N., Zuecco, G., Borga, M., Bonazza, M., Sobotková, M., Čejková, B., and Wassenaar, L. I.: Technical Note: Evaluation of between-sample memory effects in the analysis of δ2H and δ18O of water samples measured by laser spectroscopes, Hydrology and Earth System Sciences, 16, 3925–3933, doi:10.5194/hess-16-3925-2012, 2012. 16, 33, 34, 42

Penna, D., van Meerveld, H. J., Oliviero, O., Zuecco, G., Assendelft, R. S., Dalla Fontana, G., and Borga, M.: Seasonal changes in runoff generation in a small forested mountain catchment, Hydrological Processes, 29, 2027–2042, doi:10.1002/hyp.10347, 2014. 2, 4, 6, 39, 41

Renshaw, C. E., Feng, X., Sinclair, K. J., and Dums, R. H.: The use of stream flow routing for direct channel precipitation with isotopically-based hydrograph separations: the role of new water in stormflow generation, Journal of Hydrology, 273, 205–216, doi:10.1016/S0022-1694(02)00392-X, 2003. 4

Rinderer, M., Kollegger, A., Fischer, B. M. C., Stähli, M., and Seibert, J.: Sensing with boots and trousers — qualitative field observations of shallow soil moisture patterns, Hydrological Processes, 26, 4112–4120, doi:10.1002/hyp.9531, 2012. 11, 13, 14

Rinderer, M. O.: Patterns of groundwater and soil moisture variablity: Hard data, soft data and dominant controls, Ph.D. thesis, University of Zürich, 2015. 13

Roa-García, M. C. and Weiler, M.: Integrated response and transit time distributions of watersheds by combining hydrograph separation and long-term transit time modeling, Hydrology and Earth System Sciences, 14, 1537–1549, doi:10.5194/hess-14-1537-2010, 2010. 4, 5, 6

Rodgers, P., Soulsby, C., Waldron, S., and Tetzlaff, D.: Using stable isotope tracers to assess hydrological flow paths, residence times and landscape influences in a nested mesoscale catchment, Hydrol. Earth Syst. Sci., 9, 139–155, doi:10.5194/hess-9-139-2005, 2005. 2, 37

Rodhe, A.: The Origin of Streamwater Traced by Oxygen-18, Report series a 41, University of Uppsala, 1987. 4, 39

Roe, G. H.: Orographic precipitation, Annual review of earth and planetary sciences, 33, 645–671, doi:10.1146/annurev.earth.33.092203.122541, 2005. 41

Ruette, J. V., Lehmann, P., and Or, D.: Effects of rainfall spatial variability and intermittency on shallow landslide triggering patterns at a catchment scale, Water Resources Research, pp. 1–57, doi:10.1002/2013WR015122, 2014. 1

Saxena, R.: Oxygen-18 fractionation in nature and estimation of groundwater recharge, Ph.D. thesis, University of Uppsala, 1987. 5, 47

Sayres, D. S., Moyer, E. J., Hanisco, T. F., St. Clair, J. M., Keutsch, F. N., O'Brien, A., Allen, N. T., Lapson, L., Demusz, J. N., Rivero, M., Martin, T., Greenberg, M., Tuozzolo, C., Engel, G. S., Kroll, J. H., Paul, J. B., and Anderson, J. G.: A new cavity based absorption instrument for detection of water isotopologues in the upper troposphere and lower stratosphere, Review of Scientific Instruments, 80, 044102, doi:http://dx.doi.org/10.1063/1.3117349, 2009. 21

Schaffner, M., Pfaundler, M., Goggel, W., Helg, U., and Aschwanden, H.: Fliessgewaessertypisierung der Schweiz. Eine Grundlage für Gewasserbeurteilung und-entwicklung (Watercourses typing Switzerland. A basis for water assessment and development), Tech. Rep. Umwelt-Wissen Nr. 1329, Bafu, Bern, doi:-, 2013. 11

Schleppi, P., Waldner, P. a., and Stähli, M.: Errors of flux integration methods for solutes in grab samples of runoff water, as compared to flow-proportional sampling, Journal of Hydrology, 319, 266–281, doi:10.1016/j.jhydrol.2005.06.034, 2006. 12

Schmidli, J. and Frei, C.: Trends of heavy precipitation and wet and dry spells in Switzerland during the 20th century, International Journal of Climatology, 25, 753–771, doi:10.1002/joc.1179, 2005. 1

Schneider, P., Pool, S., Strouhal, L., and Seibert, J.: True colors-experimental identification of hydrological processes at a hillslope prone to slide, Hydrology and Earth System Sciences, 18, 875–892, doi:10.5194/hess-18-875-2014, 2014. 39

Schürch, M., Kozel, R., Schotterer, U., and Tripet, J.-P.: Observation of isotopes in the water cycle—the Swiss National Network (NISOT), Environmental Geology, 45, 1–11, doi:10.1007/s00254-003-0843-9, 2003. 6, 40

Seeger, S. and Weiler, M.: Reevaluation of transit time distributions, mean transit times and their relation to catchment topography, Hydrol. Earth Syst. Sci., 18, 4751–4771, doi:10.5194/hess-18-4751-2014, 2014. 6, 40

Segura, C., James, A. L., Lazzati, D., and Roulet, N. T.: Scaling relationships for event water contributions and transit times in small-forested catchments in Eastern Quebec, Water Resources Research, 48, W07 502, doi:10.1029/2012WR011890, 2012. 4

Seibert, J. and McDonnell, J. J.: On the dialog between experimentalist and modeler in catchment hydrology: Use of soft data for multicriteria model calibration, Water Resources Research, 38, 23–1–23–14, doi:10.1029/2001WR000978, 1241, 2002. 1, 48

Seibert, J. and McDonnell, J. J.: Gauging the Ungauged Basin: Relative Value of Soft and Hard Data, Journal of Hydrologic Engineering, 20, A4014 004, doi:10.1061/(ASCE)HE.1943-5584.0000861, 2015. 1

Seibert, J., Rodhe, A., and Bishop, K.: Simulating interactions between saturated and unsaturated storage in a conceptual runoff model, Hydrological Processes, 17, 379–390, doi:10.1002/hyp.1130, 2003. 48

Seneviratne, S. I., Lehner, I., Gurtz, J., Teuling, A. J., Lang, H., Moser, U., Grebner, D., Menzel, L., Schroff, K., Vitvar, T., and Zappa, M.: Swiss prealpine Rietholzbach research catchment and lysimeter: 32 year time series and 2003 drought event, Water Resources Research, 48, n/a–n/a, doi:10.1029/2011WR011749, w06526, 2012. 1

Shaman, J., Stieglitz, M., and Burns, D.: Are big basins just the sum of small catchments?, Hydrological Processes, 18, 3195–3206, doi:10.1002/hyp.5739, 2004. 3

Shanley, J. B., Kendall, C., Smith, T. E., Wolock, D. M., and McDonnell, J. J.: Controls on old and new water contributions to stream flow at some nested catchments in Vermont, USA, Hydrological Processes, 16, 589–609, doi:10.1002/hyp.312, 2002. 5, 39

Sidle, R., Tsuboyama, Y., Noguchi, S., Hosoda, I., Fujieda, M., and Shimizu, T.: Stormflow generation in steep forested headwaters: a linked hydrogeomorphic paradigm, Hydrological Processes, 14, 369–385, doi:10.1002/(SICI)1099-1085(20000228)14:3<369::AID-HYP943>3.0.CO;2-P, 2000. 2, 37, 40

Sklash, M. G. and Farvolden, R. N.: The role of groundwater in storm runoff, Journal of Hydrology, 43, 45–65, doi:10.1016/0022-1694(79)90164-1, 1979. 18

Sklash, M. G., Farvolden, R. N., and Fritz, P.: A conceptual model of watershed response to rainfall, developed through the use of oxygen-18 as a natural tracer, Canadian Journal of Earth Sciences, 13, 271–283, doi:10.1139/e76-029, 1976. 2, 4, 6

Smith, G. I., Friedman, I., Klieforth, H., and Hardcastle, K.: Areal Distribution of Deuterium in Eastern California Precipitation, 1968–1969, Journal of Applied Meteorology, 18, 172–188, doi:10.1175/1520-0450(1979)018<0172:ADODIE>2.0.CO;2, 1979. 6, 40

Soulsby, C., Tetzlaff, D., van den Bedem, N., Malcolm, I. A., Bacon, P. J., and Youngson, A. F.: Inferring groundwater influences on surface water in montane catchments from hydrochemical surveys of springs and streamwaters, Journal of Hydrology, 333, 199–213, doi:10.1016/j.jhydrol.2006.08.016, 2007. 2, 36, 48

Spreafico, M. and Weingartner, R.: Hydrologie der Schweiz, Tech. Rep. 7, Federal Office for Water and Geology, Bern, doi:1660-0746, 2005. 11

Stähli, M. and Gustafsson, D.: Long-term investigations of the snow cover in a subalpine semi-forested catchment, Hydrological Processes, 20, 411–428, doi:10.1002/hyp.6058, 2006. 9

Suecker, J. K., Ryan, J. N., Kendall, C., and Jarrett, R. D.: Determination of hydrologic pathways during snowmelt for alpine/subalpine basins, Rocky Mountain National Park, Colorado, Water Resources Research, 36, 63–75, doi:10.1029/1999WR900296, 2000. 5

SZNG, S. N. G.: Geology and Geotopes in Canton of Schwyz, SZNG, Einsiedeln, 2003. 11

Temnerud, J., Seibert, J., Jansson, M., Bishop, K., and Carlo, M.: Spatial variation in discharge and concentrations of organic carbon in a catchment network of boreal streams in northern Sweden, Journal of Hydrology, 342, 72–87, doi:10.1016/j.jhydrol.2007.05.015, 2007. 2, 3, 37

Tetzlaff, D. and Soulsby, C.: Sources of baseflow in larger catchments – Using tracers to develop a holistic understanding of runoff generation, Journal of Hydrology, 359, 287–302, doi:10.1016/j.jhydrol.2008.07.008, 2008. 2, 3

Tetzlaff, D., Birkel, C., Dick, J., Geris, J., and Soulsby, C.: Storage dynamics in hydropedological units control hillslope connectivity, runoff generation, and the evolution of catchment transit time distributions, Water Resources Research, 50, 969–985, doi:10.1002/2013WR014147, 2014. 37

Turowski, J. M., Yager, E. M., Badoux, A., Rickenmann, D., and Molnar, P.: The impact of exceptional events on erosion, bedload transport and channel stability in a step-pool channel, Earth Surface Processes and Landforms, 34, 1661–1673, doi:10.1002/esp.1855, 2009. 1, 11

Uchida, T., Asano, Y., Onda, Y., and Miyata, S.: Are headwaters just the sum of hillslopes ?, Hydrological Processes, 19, 3251–3261, doi:10.1002/hyp.6004, 2005. 3, 37

Vachaud, G., Passerat De Silans, A., Balabanis, P., and Vauclin, M.: Temporal Stability of Spatially Measured Soil Water Probability Density Function, Soil Science Society of America Journal, 49, doi:10.2136/sssaj1985.03615995004900040006x, 1985. 20

Vitvar, T. and Balderer, W.: Estimation of mean water residence times and runoff generation by180 measurements in a Pre-Alpine catchment (Rietholzbach, Eastern Switzerland), Applied Geochemistry, 12, 787–796, doi:10.1016/S0883-2927(97)00045-0, 1997. 2, 4, 6, 38

Viviroli, D. and Weingartner, R.: The hydrological significance of mountains: from regional to global scale, Hydrology and Earth System Sciences, 8, 1016–1029, doi:10.5194/hess-8-1017-2004, 2004. 1

Wagener, T., Sivapalan, M., Troch, P., and Woods, R.: Catchment Classification and Hydrologic Similarity, Geography Compass, 1, 901–931, doi:10.1111/j.1749-8198.2007.00039.x, 2007. 3

Wang, L., Caylor, K. K., and Dragoni, D.: On the calibration of continuous, high-precision δ18O and δ2H measurements using an off-axis integrated cavity output spectrometer, Rapid Communications in Mass Spectrometry, 23, 530–536, doi:10.1002$/$rcm.3905, 2009. 21

Wassenaar, L. I., Coplen, T. B., and Aggarwal, P. K.: Approaches for Achieving Long-Term Accuracy and Precision of δ18O and δ2H for Waters Analyzed using Laser Absorption Spectrometers, Environmental Science & Technology, 48, 1123–1131, doi:10.1021/es403354n, 2014. 2, 16

Weiler, M., Naef, F., and Leibundgut, C.: Study of runoff generation on hillslopes using tracer experiments and a physically based numerical hillslope model, IAHS, 248, 353–362, 1998. 5, 13, 39

Weiler, M., Scherrer, S., Naef, F., and Burlando, P.: Hydrograph separation of runoff components based on measuring hydraulic state variables, tracer experiments, and weighting methods, IAHS, 258, 249–255, 1999. 13, 39

Weiler, M., McGlynn, B. L., McGuire, K. J., and McDonnell, J. J.: How does rainfall become runoff? A combined tracer and runoff transfer function approach, Water Resources Research, 39, n/a–n/a, doi:10.1029/2003WR002331, 1315, 2003. 2

Werner, M. and Cranston, M.: Understanding the Value of Radar Rainfall Nowcasts in Flood Forecasting and Warning in Flashy Catchments, Meteorological Applications, 16, 41–55, doi:10.1002/met, 2009. 1

West, A. G., Goldsmith, G. R., Brooks, P. D., and Dawson, T. E.: Discrepancies between isotope ratio infrared spectroscopy and isotope ratio mass spectrometry for the stable isotope analysis of plant and soil waters, Rapid Communications in Mass Spectrometry, 24, 1948–1954, doi:10.1002/rcm.4597, 2010. 2

Wolock, D. M., Fan, J., and Lawrence, G. B.: Effects of basin size on low-flow stream chemistry and subsurface contact time in the Neversink River watershed, New York, Hydrological Processes, 11, 1273–1286, doi:10.1002/(SICI)1099-1085(199707)11:9<1273::AID-HYP557>3.0.CO;2-S, 1997. 3

Wood, E. F., Sivapalan, M., Beven, K., and Band, L.: Effects of spatial variability and scale with implications to hydrologic modeling, Journal of Hydrology, 102, 29–47, doi:10.1016/0022-1694(88)90090-X, 1988. 3

Woods, R., Sivapalan, M., and Duncan, M.: Investigating the representative elementary area concept: An approach based on field data, Hydrological Processes, 9, 291–312, doi:10.1002/hyp.3360090306, 1995. 3

Zimmer, M. A., Bailey, S. W., McGuire, K. J., and Bullen, T. D.: Fine scale variations of surface water chemistry in an ephemeral to perennial drainage network, Hydrological Processes, 27, 3438–3451, doi:10.1002/hyp.9449, 2012. 2, 3, 36, 37

Zobrist, J.: Water Chemistry of Swiss Alpine Rivers, in: Alpine Waters, chap. Water Chem, pp. 95–118, Springer-Verlag, Heidelberg, doi:10.1007/978-3-540-88275-6{_}5, 2010. 36
[1]

[1]Numbers behind a reference indicate the page number in the document.

8. Appendix

8.1 Paper I - Baseflow

Contributing sources to baseflow in pre-alpine headwaters using spatial snapshot sampling

HYDROLOGICAL PROCESSES
Hydrol. Process. (2015)
Published online in Wiley Online Library
(wileyonlinelibrary.com) DOI: 10.1002/hyp.10529

Contributing sources to baseflow in pre-alpine headwaters using spatial snapshot sampling

Benjamin M. C. Fischer,[1]* Michael Rinderer,[1] Philipp Schneider,[1] Tracy Ewen[1] and Jan Seibert[1,2]

[1] *Department of Geography, University of Zurich, Winterthurerstrasse 190, CH-8057 Zurich, Switzerland*
[2] *Department of Earth Sciences, Uppsala University, Sweden*

Abstract:

Mountainous headwaters consist of different landscape units including forests, meadows and wetlands. In these headwaters it is unclear which landscape units contribute what percentage to baseflow. In this study, we analysed spatiotemporal differences in baseflow isotope and hydrochemistry to identify catchment-scale runoff contribution. Three baseflow snapshot sampling campaigns were performed in the Swiss pre-alpine headwater catchment of the Zwäckentobel (4.25 km^2) and six of its adjacent subcatchments. The spatial and temporal variability of δ^2H, Ca, DOC, AT, pH, SO_4, Mg and H_4SiO_4 of streamflow, groundwater and spring water samples was analysed and related to catchment area and wetland percentage using bivariate and multivariate methods. Our study found that in the six subcatchments, with variable arrangements of landscape units, the inter- and intra catchment variability of isotopic and hydrochemical compositions was small and generally not significant. Stream samples were distinctly different from shallow groundwater. An upper spring zone located near the water divide above 1,400 m and a larger wetland were identified by their distinct spatial isotopic and hydrochemical composition. The upstream wetland percentage was not correlated to the hydrochemical streamflow composition, suggesting that wetlands were less connected and act as passive features with a negligible contribution to baseflow runoff. The isotopic and hydrochemical composition of baseflow changed slightly from the upper spring zone towards the subcatchment outlets and corresponded to the signature of deep groundwater. Our results confirm the need and benefits of spatially distributed snapshot sampling to derive process understanding of heterogeneous headwaters during baseflow. Copyright © 2015 John Wiley & Sons, Ltd.

KEY WORDS headwater catchments; snapshot sampling; spatiotemporal patterns; scaling; surface and groundwater chemistry; stable isotopes and catchment characteristics

Received 14 February 2014; Accepted 29 April 2015

INTRODUCTION

Despite their importance for water resources, headwaters are still largely unmeasured (Bishop *et al*., 2008). This is especially true for mountainous headwaters where hydrological and hydrochemical observations are often difficult and, thus, rare. Many mountainous headwaters are characterized by high amounts of precipitation, steep gradients, shallow soils and a mosaic of different landscape units such as forests, meadows and wetlands. Along the steep and deeply incised mountainous stream channels the riparian zone is generally missing (Sidle *et al*., 2000). For these heterogeneous mountainous headwaters it is still not fully clear which landscape units predominantly contribute to streamflow, and in particular sustain baseflow. Mountainous headwaters can contribute significantly to downstream runoff and in particular to baseflow (Tetzlaff and Soulsby, 2008). It is therefore important to understand where and how baseflow is generated to be able to make predictions on how baseflow might be affected by climate or land-cover changes. Besides baseflow quantity, water quality is also controlled by the pattern of different landscape units. To predict potential changes, it is important to understand water sources and transit times along the various flow paths. Tracer approaches are commonly used to study sources and flow paths of water (Christophersen and Hooper, 1992; Rodgers *et al*., 2004; Soulsby *et al*., 2007; Barthold *et al*., 2010; Hrachowitz *et al*., 2011; Inamdar *et al*., 2013; Lu, 2014; Penna *et al*., 2014).

Of the different environmental tracers, the isotopes ^2H and ^{18}O have been found to be especially useful to identify sources of streamflow based on differences in the isotopic composition of the sources, e.g. rainfall and groundwater (Tetzlaff and Soulsby, 2008; Hrachowitz *et al*., 2011). Hydrochemical tracers such as Ca or DOC, on the other hand, provide information on flow pathways as the

*Correspondence to: Benjamin M. C. Fischer, Department of Geography, University of Zurich, Winterthurerstrasse 190, CH-8057 Zurich, Switzerland.
E-mail: benjamin.fischer@geo.uzh.ch

concentrations depend on what the water encounters on its way from rain to stream (Lyon *et al.*, 2012; Likens and Buso, 2006; James and Roulet, 2006; Inamdar *et al.*, 2013).

Streamflow integrates water from different sources. A common approach to study spatial variations in runoff contribution during streamflow is by synoptic, spatially distributed sampling to determine the isotopic and hydrochemical composition of water at various locations throughout a catchment (Fröhlich *et al.*, 2008; Tetzlaff and Soulsby, 2008). Several studies have used baseflow snapshot campaigns to obtain information about spatial patterns of major baseflow controls. Temnerud *et al.* (2007), for instance, analysed the mixing of TOC (total organic carbon) along the stream network in a boreal catchment and found that the decrease of variability with scale could not be explained by mixing alone, but was a result of the spatial pattern of landscape units. Likens and Buso (2006) mapped the hydrochemical patterns of the Hubbard Brook Experimental Forest during two snapshot campaigns and found minor changes between the two seasons, but a large change in hydrochemistry along the stream network. Here, hydrochemical patterns were attributed to differences in vegetation, geologic substrates and wetland areas. Other studies found soil depth (Buttle *et al.*, 2004; Kosugi *et al.*, 2006) or active zones of seeping deep groundwater (Asano *et al.*, 2009; Zimmer *et al.*, 2012) to be important factors for baseflow generation. However, the importance of different spatial controls varies with geographic settings and especially steep pre-alpine regions with high precipitation amounts ($P > 2{,}000\,mm\,year^{-1}$) are not yet fully understood.

In this study we conducted three baseflow snapshot sampling campaigns in a steep and wet pre-alpine headwater and used the observed isotopic and hydrochemical signatures to assess which sources contribute to baseflow. We asked whether any spatial patterns of streamwater composition could be observed and whether there was any relation to (sub)catchment landscape units. In particular we addressed the role of wetlands in these wet headwater catchments.

MATERIALS AND METHODS

Study area

The Zwäckentobel (4.25 km^2) is a Swiss pre-alpine headwater located in the Alptal 40 km south of Zurich (see Figure 1a). The south–north oriented catchment consists of approximately ten perennial streams. In the Erlenbach subcatchment (WS04) long-term observations of discharge and different hydrochemical variables exist (Hegg *et al.*, 2006; Schleppi *et al.*, 2006). Subcatchment characteristics such as area (km^2), altitude (m) and slope (°) were derived from a digital elevation model (DEM; swissALTI3D; Federal Office of Topography Swisstopo, Bern) using the Whitebox Geospatial Analysis-D8 flow pointer tool (Lindsay, 2009) (Table I). All subcatchments have alternating steep slopes of more than 20° and flatter areas along the main axis, originating from erosion deposits such as soil creep and landslides.

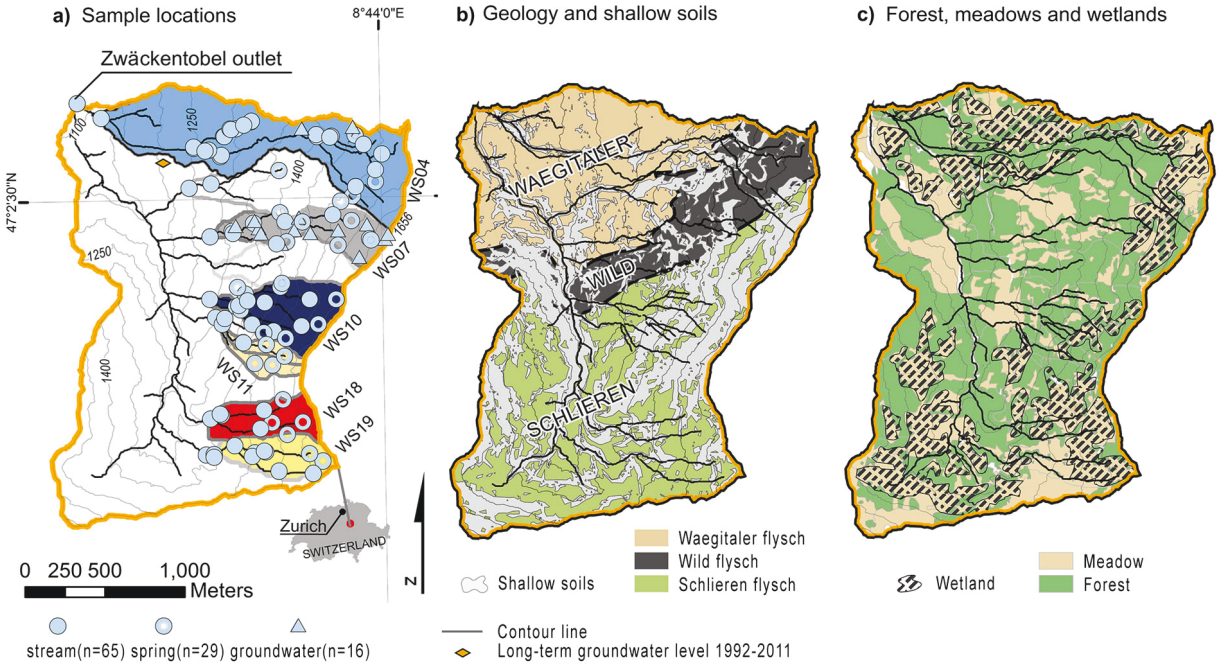

Figure 1. Maps of the Zwäckentobel with a) sampling locations in selected subcatchments WS04, WS07, WS10, WS11, WS18 and WS19, b) geology: three different types of flysch with shaded gray areas indicate shallow soils located on slopes >20° and c) land use: forest and meadows with hatched areas indicating wetlands. Color scheme Figure 1b and 1c from www.ColorBrewer.org

Table I. Sample number for the three snapshot campaigns of the Zwäckentobel outlet (ZT) and its subcatchments WS04 to WS19 with its topographic, geology and land use characteristics

				Subcatchment						
			∑n	ZT	WS04	WS07	WS10	WS11	WS18	WS19
Campaign samples	C-1 (19.11.2010)		46	1	7	14	12	5	0	7
	C-2 (07.06.2011)		82	1	16	20	16	8	6	15
	C-3 (18.10.2011)		84	1	24	20	14	7	8	10
Topography	Area		km^2	4.25	0.73	0.21	0.23	0.09	0.15	0.15
	Altitude	*Max*		1656	1656	1656	1598	1583	1598	1598
		Mean	m	1360	1342	1468	1432	1421	1476	1494
		Min		1084	1109	1262	1276	1292	1351	1384
	Slope	*Mean*	°	19	17	21	23	24	20	18
		Max		56	49	47	53	45	42	43
Geology	Waegitaler flysch		%	29	64	16	0	0	0	0
	Wild flysch			17	29	42	0	0	0	0
	Schlieren flysch			54	7	42	100	100	100	100
	Shallow soils<1 m		%	29	44	55	73	74	59	49
Land use	Forest		%	55	53	53	72	81	38	18
	Partly forested			21	22	27	14	10	10	1
	Meadow			24	25	20	14	9	52	81
	Wetland		%	29	33	28	23	21	57	51

The geology of the region is tertiary flysch consisting of different calcarius sedimentary layers of schist, marl or sandstone (Hantke, 1967; Hsü and Briegel, 1991) (Figure 1b). Ontop of the flysch parent material are shallow and creeping gleysols (0.5–2.5 m in depth). These gleysols consist of a B_g-horizon with high silt and clay content and the A-horizon of 20–50 cm Muck or Mor humus (Feyen *et al*., 1996). The clay layer has low matrix permeability but high drainage capacity in macropores (see Feyen *et al*. (1996) for a more detailed soil description). The landscape units of the Zwäckentobel are light to dense spruce forest, wetland or meadows. During the summer months, the meadows of WS18, WS19 and the upper part of WS04 and WS07 are used as alpine pastures. The different land cover was delineated from an aerial photo (Spot Mosaic; Federal Office of Topography Swisstopo, Bern) and divided into three classes: forest, partly forested and meadow (Figure 1c). Wetlands were derived from the available Federal inventory of wetlands of national importance (Swiss Federal Office for Environment, Bern).

The Zwäckentobel has a humid-temperate climate with a mean annual temperature of 6 °C (Feyen *et al*., 1996). The annual precipitation is 2,300 mm $year^{-1}$ and is relatively equally distributed but slightly skewed to the summer season (Turowski *et al*., 2009). On average there is precipitation on almost every second day. About one third of the annual precipitation falls as snow (Stähli and Gustafsson, 2006). During rainfall events, streams respond quickly and flow increases by several orders of magnitude, but returns to baseflow within approximately one day.

Field sampling design

Three spatially distributed snapshot campaigns were carried out: Campaign C-1 on 19 November 2010, at the end of the summer season had an early snow cover and was representative of early winter baseflow conditions; C-2 on 7 June 2011, shortly after all snow cover had melted was characterized by short dry spells and higher groundwater levels; and C-3 on 18 October 2011, in autumn, had longer dry spells with lower groundwater levels (see Figure 2). These dates were chosen to represent the preceding hydro-meteorological period, i.e. spring with typically high groundwater levels (C-2) and autumn with typically low groundwater levels (C-1 and C-3). The campaigns were planned such that the system was in a baseflow state with at least two antecedent days without precipitation (Figure 2) ensuring stable flow conditions to more easily identify sources (Temnerud *et al*., 2007).

Because of frequent precipitation events it was important to collect all samples in one day. Therefore, the number of sampling locations was restricted to 110 and distributed discharge measurements could not be performed for practical reasons. The actual number of samples taken was less than the 110 predefined sampling points as there was too little or no water at all at some of the points (Table I). During each campaign five sampling teams visited 10–20 sample points with a handheld GPS (Garmin GPSMAP 60CS,

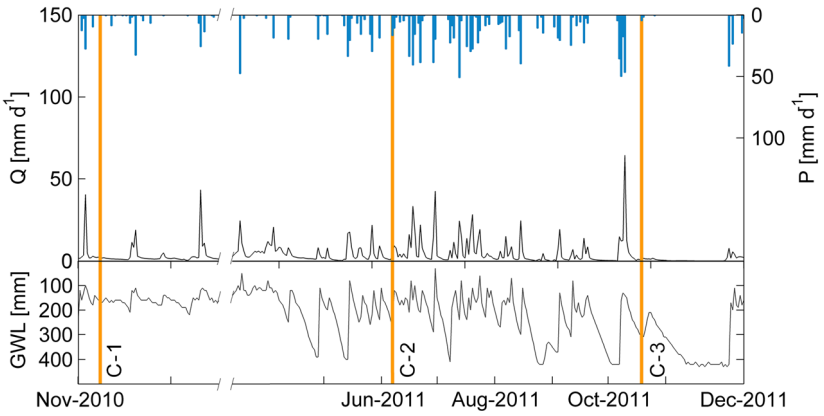

C-1 (19.11.2010): Q= 2 mm d^{-1} ≈ 18 L s^{-1} | GWL= -160 mm | API_2= 0 mm | API_7= 54 mm
C-2 (07.06.2011): Q= 0.5 mm d^{-1} ≈ 5 L s^{-1} | GWL= -120 mm | API_2= 0 mm | API_7= 20 mm
C-3 (18.10.2011): Q= 0.7 mm d^{-1} ≈ 6 L s^{-1} | GWL= -300 mm | API_2= 0 mm | API_7= 0 mm

Figure 2. Precipitation (P), discharge (Q) and groundwater level (GWL) of WS04 between fall 2010 and 2011 with the sampling campaigns C-1, C-2 and C-3 (vertical lines). Text below is sampling campaign information on discharge, groundwater level relative to the surface and antecedent precipitation index (API) for 2 and 7 days

field accuracy ±8 m). For each sampling location, two grab water samples were taken; 20 ml for stable isotope analyses (20-ml glass vial with cap and additional Teflon/rubber septum) and 250 ml for hydrochemical analyses (250-ml PE bottle with cap).

The sampling locations were selected by following the stream network of the different subcatchment outlets upslope to the water divide. Perennial key locations were chosen such as confluences of different branches (n = 65 of which eight samples were taken along an artificial drainage ditch from a wetland (W) within WS04), springs (n = 29) and groundwater wells (n=16) (Figure 1a). Groundwater samples were taken from fully screened wells with an average depth of about 1 m (for details on the groundwater observation network see Rinderer *et al.*, 2014).

Similar to the subcatchment characteristics, for every sampling location different upslope controlling landscape features were derived such as the area (km^2), altitude (m), slope (°) and topographic wetness index (TWI) within a Geographic Information System (GIS) framework. Additionally, for each sampling location the upslope percentage of forest, meadow and wetlands were derived from the land use map see Figure 1c and Table I. The percentage of the different types of geology and shallow soils was derived from the geological map with an additional DEM-analysis where slopes >20° were set to a soil depth of 1 m see Figure 1b and Table I. This was then spot checked with a hand auger in the field and resulted in an estimate of the shallow soil information (depth larger than or less than 1 m).

Laboratory methods

For the isotopic composition the water samples were analysed in the stable isotope laboratory of the University of Zurich, Department of Geography. The samples were filtered prior to analysis with a 0.45-µm filter (25-mm PTFE Syringe Filter, Simplepure USA) from which 1 ml was pipetted in a vial (1.5-ml 32 × 11.6-mm screw neck vials with cap and PTFE/silicone/PTFE septa). Samples were analysed with a Cavity Ring-Down Spectroscope-Picarro L1102-i Liquid Analyser (first generation analyser with a manufacturer's precision of $\delta^2H < 0.5‰$ and $\delta^{18}O < 0.1‰$) and the analysis scheme of Penna *et al.* (2010).

The 250-ml water samples were analysed for hydrochemical variables Ca, DOC, (electrical conductivity (CT), pH, alkalinity (AT), total hardness (TH), Cl, NO_3, SO_4, Na, K, Mg and H_4SiO_4) at the laboratory of the Swiss Federal Institute of Aquatic Science and Technology (EAWAG; see Table II for instruments used). All samples were filtered prior to analysis with a 0.45-µm filter (Ø 47-mm cellulose filter paper, Whatman Germany).

Data analysis

The three snapshot campaigns resulted in datasets consisting of selected isotopic and hydrochemical variables. A selection of isotopic and hydrochemical variables (δ^2H, Ca, DOC AT, pH, SO_4, Mg and H_4SiO_4) was made based on their value for identifying processes, detection limit of the instruments and the correlation between different variables to avoid redundancies. For each campaign, the different variables were summarized for stream samples taken in the subcatchments (WS04 to WS19), at the different subcatchment outlets (O), in groundwater wells (G) and at springs (S). Spatiotemporal differences were tested with the Tukey's honestly significant difference criterion $\alpha = 0.05$ (Hochberg and

Table II. Overview of different variables and instruments used for stable isotope and hydrochemical analysis: electrical conductivity (CT), pH, alkalinity (AT), total hardness (TH), chloride (Cl), nitrate (NO_3), sulphate (SO_4), sodium (Na), potassium (K), calcium (Ca), magnesium (Mg), dissolved organic carbon (DOC) and silicic acid (H_4SiO_4)

Variable	Instrument	Manufacturer	Precision
δ^2H and $\delta^{18}O$	Cavity Ring-Down Spectroscope-Picarro L1102-i liquid analyser	Picarro, Inc., USA	0.5‰ and 0.1‰ for (δ^2H and $\delta^{18}O$)
CT	Metrohm 712 conductometer		$2\,\mu S\,cm^{-1}$
pH	Metrohm 809 Titrando with pH-electrode		0.05 pH
AT			$0.1\,mmol\,l^{-1}$
TH	Metrohm 809 Titrando with ion selective electrode		$0.1\,mmol\,l^{-1}$
Cl	Metrohm 761 Compact IC with chem. Suppression	Metrohm Schweiz AG, Switzerland	$0.2\,mg\,l^{-1}$
NO_3	with Metrosep A Supp 5 100/4 mm column		$0.1\,mg\,l^{-1}$
SO_4			$2.0\,mg\,l^{-1}$
Na	Metrohm 761 Compact IC with chem. Suppression		$0.8\,mg\,l^{-1}$
K	with Metrohm C 4—100/4.0 column		$0.3\,mg\,l^{-1}$
Ca			$1.7\,mg\,l^{-1}$
Mg			$0.8\,mg\,l^{-1}$
H_4SiO_4	Autoanalyser AA3, Bran+Luebbe and method no. G-177-96 (Methods of Seawater Analysis, K. Grasshoff, M. Ehrhard, K. Kremling 1983)	Bran + *Luebbe*, Germany	$0.2\,mg\,l^{-1}$
DOC	Shimadzu TOC-V CPH	Shimadzu Corporation, Japan	$0.2\,mg\,l^{-1}$

Tamhane, 1987) for different variables and campaigns. The spatial variability of different hydrochemical variables and sampling locations were visually assessed by representing the streamflow, geology, organic matter (δ^2H, Ca and DOC, respectively) as sampled in space. Changes in variability were further assessed by expressing each sample point δ^2H, Ca or DOC as a function of different upslope controlling landscape features such as the catchment area, altitude, slope, topographic wetness index, land use (forest, meadow and wetland), geological facies and shallow soils.

Hydrochemical mixing was further examined with bivariate solute diagrams and a PCA was performed to investigate the spatiotemporal patterns of the isotopic and hydrochemical variables (δ^2H, Ca, DOC, AT, SO_4, Mg, and H_4SiO_4). The resulting patterns for each campaign were compared to give an indication of hydrochemical compositions. From the chosen sampling design (springs, stream and groundwater well samples) only two end-members were available to explain streamflow. Therefore instead of a full geographical end-member mixing analysis (EMMA), the end-member groundwater from wells and springs were used as an explorative element to explain the contribution to streamflow. The median values of sampled end-members were projected together with their upper and lower quartiles into the bivariate solute diagrams and PCA-biplots.

A summary of the data and spatial representation for campaign C-1 can be found in the Supporting Information, but because of the snow cover and the reduced number of sampling points, campaign C-1 is not included in the analyses presented in this paper.

RESULTS

Variability in isotope and hydrochemical concentrations

Figure 3 shows the variability of δ^2H, Ca, DOC, AT, pH, SO_4, Mg, and H_4SiO_4 for each campaign (C-2, C-3) and for stream samples of the subcatchments (WS04 to WS19), subcatchment outlet samples (O), groundwater wells (G) and spring samples (S). The results of significance tests are indicated in italic letters inside each box for campaigns, and on top of each box subcatchments and outlets refer to: (1) the spatial comparison for each source (O, G and S) and subcatchment WS04 to WS19; (2) the intra-comparison of watershed samples to the respective subcatchment outlets; where mixing of each subcatchment towards the subcatchment outlet was separately assessed with the Wilcoxon signed rank test ($\alpha = 0.05$; shown as a gray box); and (3) a comparison for each snapshot campaign (C-2, C-3).

For δ^2H, the spatial comparison of the different groups (WS04-WS19, O, G and S) shows for groundwater (sampled from wells), significantly lower δ^2H values compared to stream samples from WS19 and the outlets for campaign C-2. For C-3 on the other hand, there were no significant differences (Figure 3, δ^2H), and only the outlet of WS10 was significantly different to the internal sampling points. For the comparison between campaigns C-2 and C-3, there were significant differences with enriched δ^2H for WS04, WS10, WS18, O, G and S in C-3 compared to C-2.

For campaign C-2 the spatial comparison shows significantly higher Ca concentrations for groundwater from wells compared to stream samples from WS04,

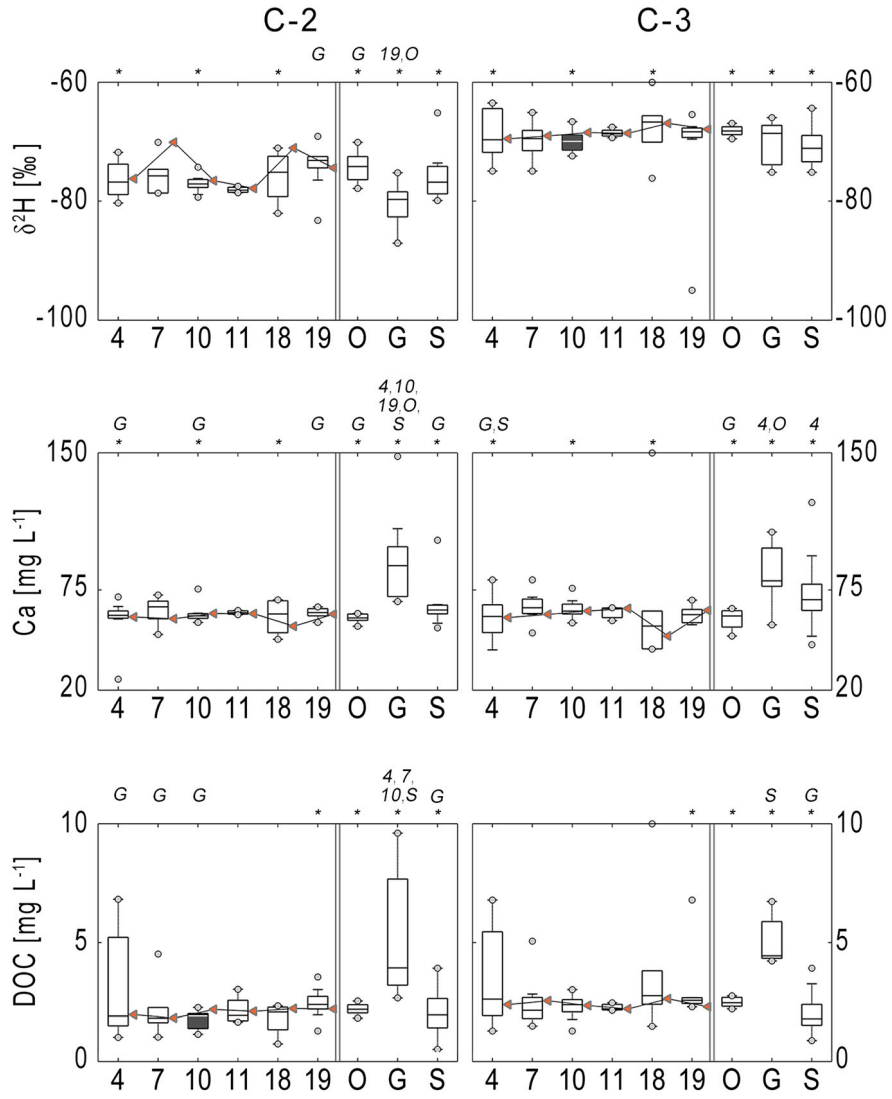

Figure 3. Isotopic and hydrochemical variables (rows) for each sampling campaign (columns: C2, C3). The x-axis indicates different groups, WS04 to WS19 (4 to 19), followed by outlets of all subcatchments (O), groundwater (G) and springs (S). The boxes show the range of values for different sample groups (showing the 25th, median, 75th percentile with whiskers of 10th and 90th percentile, and minimum and maximum as gray circles). The orange triangles, connected by a black line, indicate the values at the subcatchment outlet (missing triangles or lines are because of missing values). Italic letters in or on top of each box indicate significant difference in means ($p < 0.05$) of the different datasets for: (I) temporal comparison of the means where the * above the box plot indicated a significant difference compared to the other sampling campaign and (II) spatial comparison of WS, O, G and S. Black shaded boxes indicate a significant difference in means ($p < 0.05$) of all stream samples of a subcatchment compared to its respective subcatchment outlet

WS10, WS19, the outlets and the springs. For C-3 the groundwater from wells had significantly higher concentrations compared to the stream samples from WS04 and outlets (Figure 3, Ca). For the comparison between campaigns, the concentrations were significantly lower for C-3 compared to C-2 for WS04, WS18 and G whereas the concentrations were significantly higher for C-3 compared to C-2 for WS10, O and S.

For DOC, the spatial comparison shows significantly higher concentrations for groundwater from wells compared to the stream samples of WS04, WS07, WS10 and the springs for C-2 (Figure 3, DOC). For C-3 the groundwater from wells had significantly higher concentrations compared to the springs. In both C-2 and C-3, stream samples of WS04 had the largest interquartile range (IQR). For the intra-comparison to the outlet, a significant difference was found for WS10. For the comparison between campaigns, there was a higher concentration and significant difference for WS19 and O, G and S for C-3 compared to C-2.

For each of the remaining hydrochemical variables, the IQR among groundwater samples was high for AT, Mg and H_4SiO_4 for both C-2 and C-3 (Figure 3). Groundwater samples from wells were significantly different for C-2 from WS04, WS10, and samples from O and S were significantly different for AT, SO_4 and H_4SiO_4. For

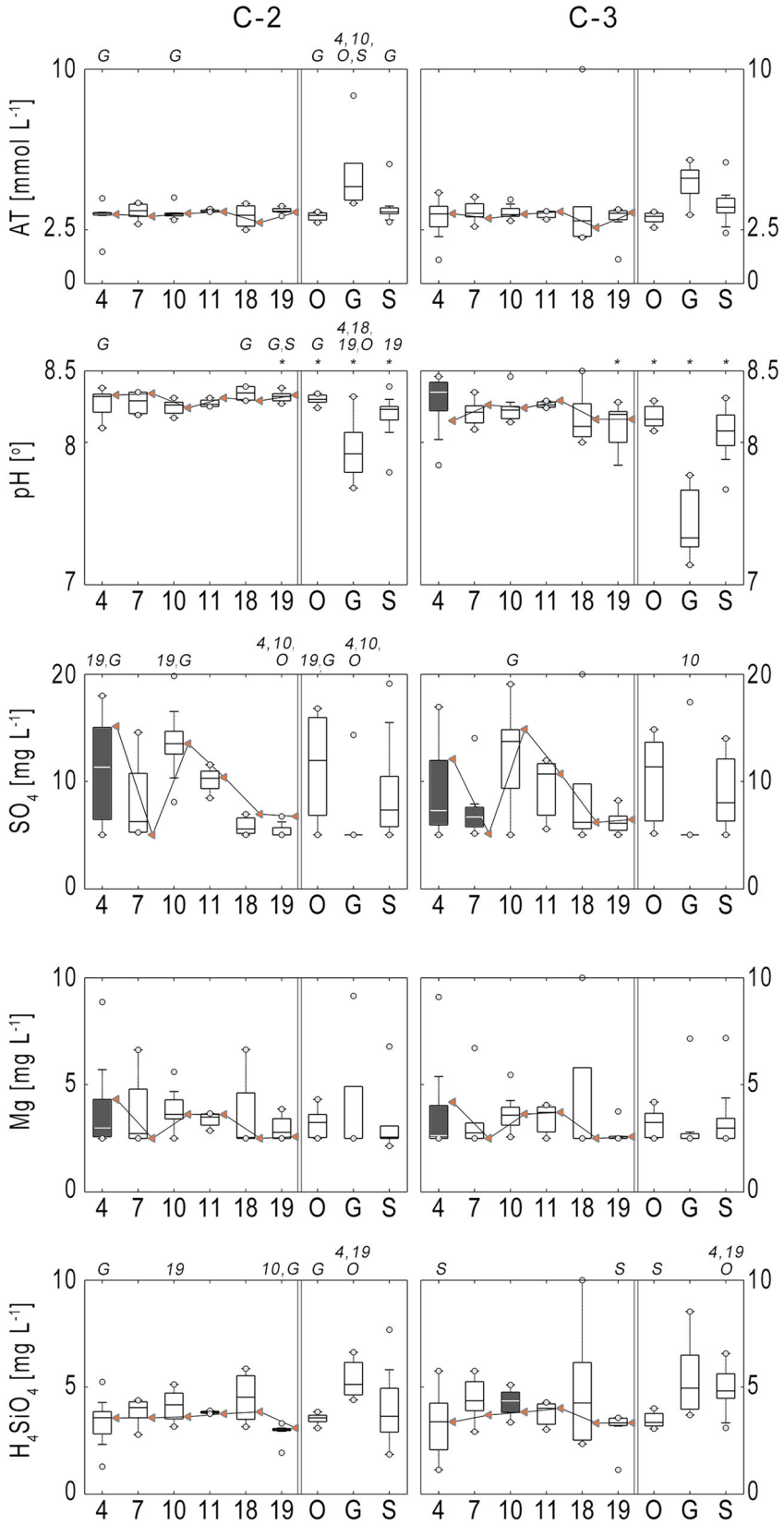

Figure 3. (Continued)

springs, IQR was high for SO_4 and H_4SiO_4 in C-2 and C-3 and high for AT in C-3. The outlets showed less variability for AT, SO_4, Mg and H_4SiO_4 during both C-2 and C-3. For the subcatchment variability there were no significant differences found except for SO_4 which had a high IQR in stream samples of WS04 and WS10 in C-2 (significantly different) and C-3. For pH, only groundwater from wells differed significantly while other differences were near or within the instrument precision of ±0.05 and therefore not significant. For the intra-comparison to outlets, only SO_4 and Mg for WS04 in C-2 and C-3 show a significant difference, as well as SO_4 for stream samples of WS07 in C-3. For the differences between campaigns, there were no significant differences found.

Ca, DOC, AT and H_4SiO_4 in groundwater from wells and spring samples were quite variable during the two campaigns (C-2, C-3), whereas the outlets show less variability overall. Additionally, samples from groundwater wells had a distinct composition with higher Ca, DOC, AT and low SO_4 concentrations while springs had high Ca, SO_4, H_4SiO_4 but low DOC.

Isotopic and hydrochemical patterns

The δ^2H, Ca and DOC composition varied in space and time (Figure 4). For δ^2H (top row) in sampling campaign C-2 the springs near the water divide had generally lighter δ^2H compared to stream samples, with some exceptions in WS07, WS10 and WS19. A more variable pattern of δ^2H in stream, groundwater wells and spring samples occurred in C-3. Large differences can be seen in δ^2H between C-2 and C-3 with the exception of spring S-55. Generally the springs near the water divide had more depleted δ^2H values compared to the stream samples, which had more enriched values δ^2H downslope.

The spatial patterns of Ca (middle row) remained similar for the three campaigns. Springs and groundwater well samples of area I had higher Ca concentrations compared to most stream samples. This area I lies above 1400 m and can be defined as an 'upper spring zone' (see Figure 1a). In WS04 and WS07 the Ca concentrations decreased from the springs near the water divide from 80 mg l^{-1}, towards the subcatchment outlet to 60 mg l^{-1}. Compared to WS04 and WS07 the subcatchments WS10 and WS11 had 5–10 mg l^{-1} lower Ca concentrations.

The spatial patterns of DOC (bottom row) showed a similar pattern for the campaigns with increasing concentrations from the upper springs in area I (1.3 mg l^{-1}) towards the catchment outlet (2.8 mg l^{-1}). DOC values of some springs had 1–2 mg l^{-1} higher concentrations (see S-55 and S-81). Water samples from groundwater wells tended to have DOC concentrations of 5 up to 7 mg l^{-1}. In both C-2 and C-3 a tributary in WS04, which is a drainage ditch from a wetland (see area II), stood out by having distinctly different concentrations with DOC concentrations similar to groundwater well samples (7 mg l^{-1}) but approximately 5 mg l^{-1} higher compared to springs and stream samples. The δ^2H values observed for this tributary were 4‰ higher compared to the main stream and Ca concentrations were approximately 20 mg l^{-1}, which was 20–50 mg l^{-1} lower than the other stream, spring and groundwater well samples. Furthermore WS18 had slightly lower Ca concentrations and higher DOC concentrations with respect to the neighbouring spring area I.

Controlling landscape characteristics

The effect of mixing along the stream network for the selected variables δ^2H, Ca and DOC is shown by expressing the different concentrations as a function of their catchment area and wetland percentage in Figure 5. The variability of δ^2H, Ca and DOC composition decreased from the springs (approximate upslope area 0.001 km^2) towards 0.2 km^2 where several first order streams from springs come together and defined the upper spring zone above 1400 m. Below this upper spring zone the streamflow composition changed only slightly towards the subcatchment outlets. Along the stream network of WS04 the variables δ^2H, Ca and DOC showed a distinctly different composition between the main stream (black lines, Figure 5), and its tributaries from wetlands (gray lines with large symbols, Figure 5). The δ^2H of the main stream increased slightly towards the subcatchment outlet (C-2; −80 to −76‰ and C-3; from −74 to −70‰), Ca concentrations decreased (C-2 and C-3; from 80 to 60 mg l^{-1}) while DOC increased (C-2 and C-3; from 1.3 to 2.8 mg l^{-1}). The tributary draining a wetland (area II in Figure 3) had high δ^2H, low Ca and high DOC concentrations. Furthermore spring S-9 was distinctly different in its signature (enriched δ^2H, higher Ca and marginally higher DOC concentrations) compared to neighbouring springs in WS04.

The role of wetlands as a potential controlling element on the hydrochemistry was further examined by expressing Ca and DOC as a function of upslope wetland percentages (see Figure 6). For both C-2 and C-3 the tributaries of WS04 had lower Ca (20–50 mg l^{-1}) and higher DOC concentrations (6 mg l^{-1}) compared to most streams (Ca 65 mg l^{-1} and DOC 3 mg l^{-1}) and springs (Ca >70 mg l^{-1} and DOC 2 mg l^{-1}). Exceptions were groundwater samples from wells (Ca >70 mg l^{-1} and DOC 7 mg l^{-1}) and springs of WS18 with slightly increased DOC concentrations (4 mg l^{-1}) as compared to other springs.

The hydrochemical variables Ca and DOC were selected as representing geology and organic matter respectively, to assess the mixing of the different water samples (Figure 7). The bivariate representation of Ca and DOC of C-2 and C-3 showed that most stream samples of the different subcatchments had a similar hydrochemical

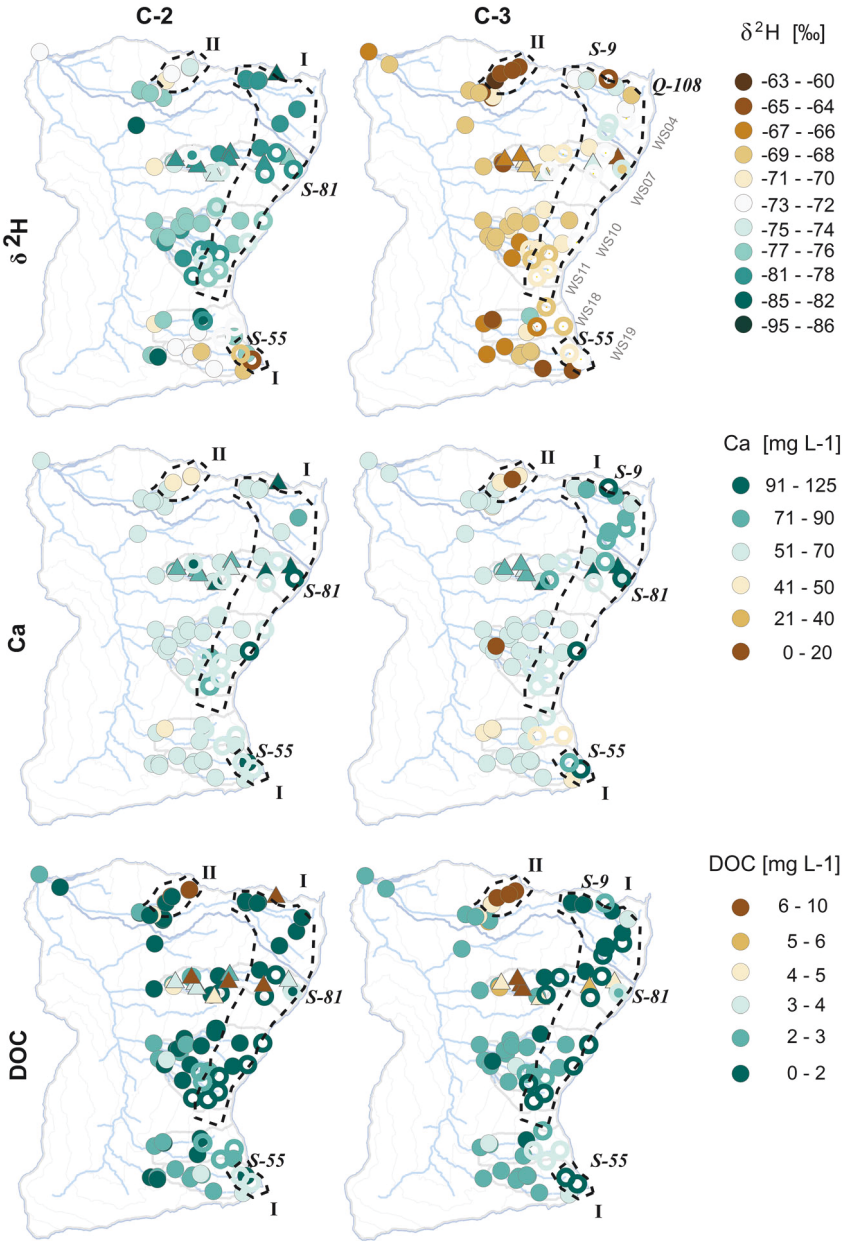

Figure 4. Spatial distribution of the isotopic and hydrochemical variables δ^2H, Ca and DOC for C-2 and C-3: stream (filled circles), spring (open circles) and groundwater samples (triangles). Dashed lines with roman numerals I (upper spring zone) and II (tributary, i.e. drainage ditch from wetland) are regions with distinct composition. Letters indicate samples described in the text. Color scheme from www.ColorBrewer.org

composition and were clustered near Ca ±60 mg l^{-1} and DOC ±2.5 mg l^{-1}. These samples were similar to deep groundwater from springs (S) from near or from bedrock with high Ca but low DOC concentrations. Groundwater samples from observation wells (G) had characteristic concentrations for the integrated soil profile, i.e. shallow groundwater with high Ca and average DOC concentrations. Stream samples from WS04, draining a wetland (Figures 5 and 6), were significantly different from other samples for all variables in C-2 and C-3, and had their own characteristic, e.g. enriched δ^2H values as well as lower Ca and higher DOC concentrations. Even though this is a low number of sampling points with a clear wetland signature, these available samples were a first indication of a third end-member from wetlands (W). The median value of these possible end-members of wetlands (W), groundwater wells (G) and springs (S) was added to the bivariate representation of Ca and DOC (Figure 7) to indicate possible runoff sources during baseflow. For C-2 most stream samples had signatures of the deep groundwater from springs while in C-3 some samples of WS18 and WS19 shifted towards the wetland end-

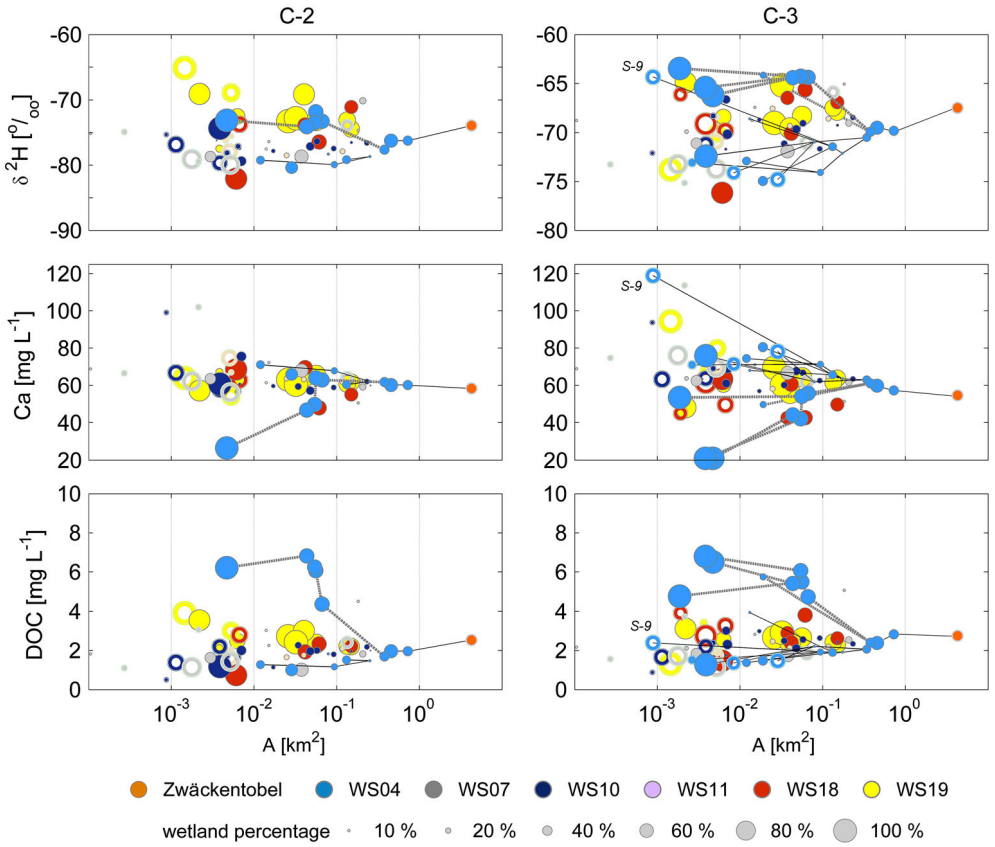

Figure 5. δ^2H, Ca and DOC values for snapshot campaign C-2 and C-3 from the different sampling locations; stream (filled circles) and springs (open circles) represented as a function of their logarithmic catchment area. Symbols are scaled proportional to upslope wetland percentage. Black lines connect sampling points of WS04 along the main stream network from the water divide to the catchment outlet. Gray lines connect sampling points of WS04 along the tributaries to the main stream

member. In both C-2 and C-3 the samples that were identified as tributaries in WS04 draining a wetland (Figures 5 and 6), had higher DOC concentrations and therefore a wetland signature. These results are consistent with the descriptive statistics and spatial and longitudinal representation of different variables (shown in Figures 3–5), indicating spatial differences and potential end-members (springs, groundwater wells and wetlands).

The isotopic and hydrochemical dataset was additionally explored with a PCA for sampling campaign C-2 and C-3 (Figure 8). From the Kaiser's rule (Kaiser, 1960) it followed that for the PCA, two principal components were sufficient to explain between 60% (C-2) and 80% (C-3) of the variance. The different isotopic and hydrochemical factor loadings were located in different quadrants (numbered with roman numerals, see Figure 8). From the scores of PCA of sampling campaigns C-2 and C-3, it appeared that the different sampling points for each subcatchment (grouped in different quadrants) were correlated with different isotopic and hydrochemical variables. The sampling points of the smaller subcatchments WS10 and WS11 were in quadrant II, while WS18 and WS19 were in quadrant III. The larger subcatchments WS04 and WS07 were similarly distributed over quadrant I, II and IV. Similar to the bivariate representation of Ca and DOC for C-2, the different samples were closer together and showed an increase in spread for C-3. The possible end-members W, G and S (observed in the bivariate analysis) were added by their median values to the PCA-biplot. For both campaigns, WS04 and WS07 had a dominant spring and wetland signature, while WS10 and WS11 were marked by a spring signature. WS18 and WS19 were bounded by the end-member groundwater from wells and wetlands. Compared to bivariate representation in the PCA-biplot more samples were not bound by the three different end-members of spring, groundwater wells and wetland.

DISCUSSION AND CONCLUSIONS

Spatiotemporal variability of hydrochemical variables

We demonstrated with three snapshot campaigns during baseflow that such an analysis of hydrochemical variables and isotopic composition can be applied to steep and wet pre-alpine headwaters with different landscape units including forests, meadows and wetlands. Observ-

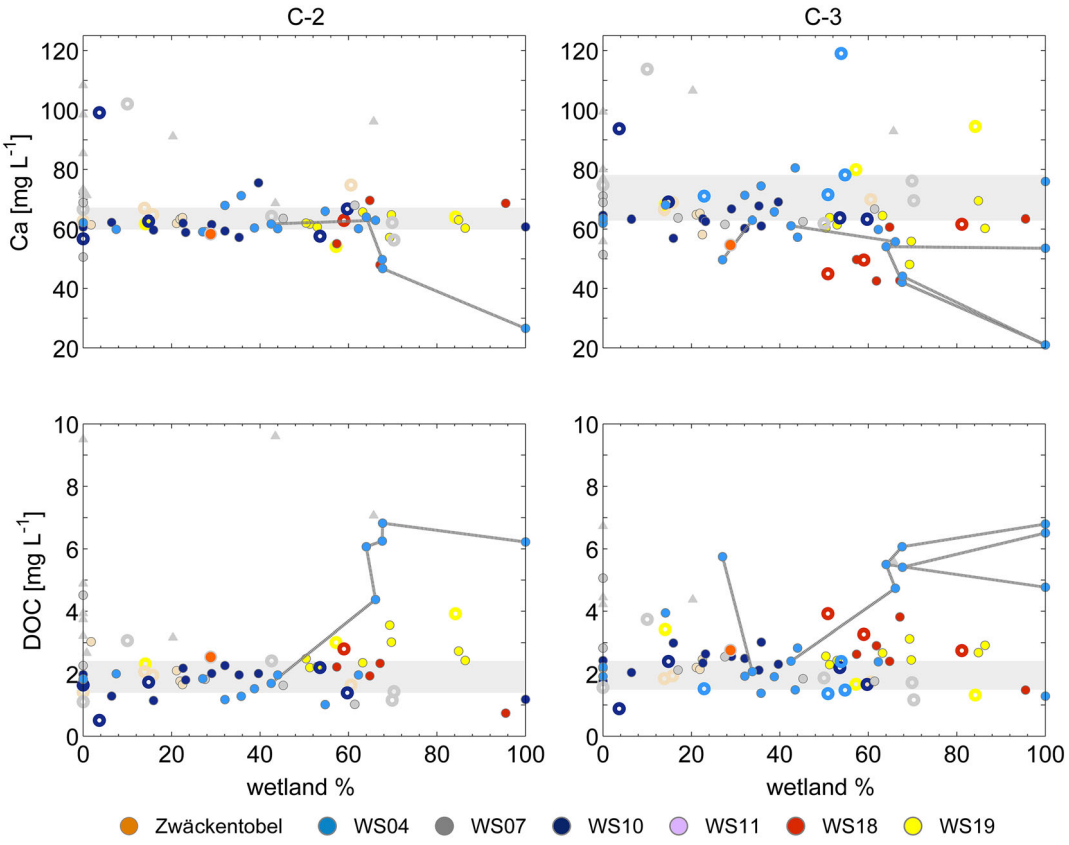

Figure 6. Ca and DOC concentrations for snapshot campaigns C-2 and C-3 as a function of their upstream wetland percentage for the different samples: stream (filled circles), springs (open circles) and groundwater (triangles). Gray lines connect sampling points WS04 along the tributaries to the main stream. The gray shaded area indicates the variability of the spring signature based on the 25th and 75th percentile of Figure 3

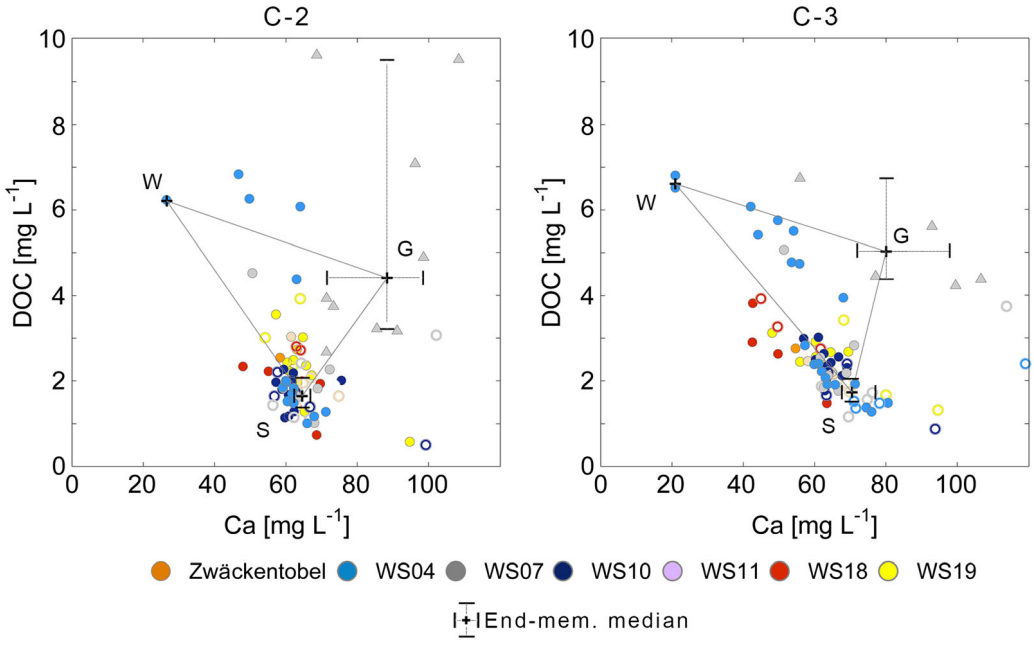

Figure 7. Bivariate representation of Ca and DOC for C-2 and C-3 with different samples: stream (filled circles), springs (open circles) and groundwater (triangles). End-members (+) are median of springs (S), wetland (W) and groundwater (G) samples each with their upper and lower quartiles (error bar)

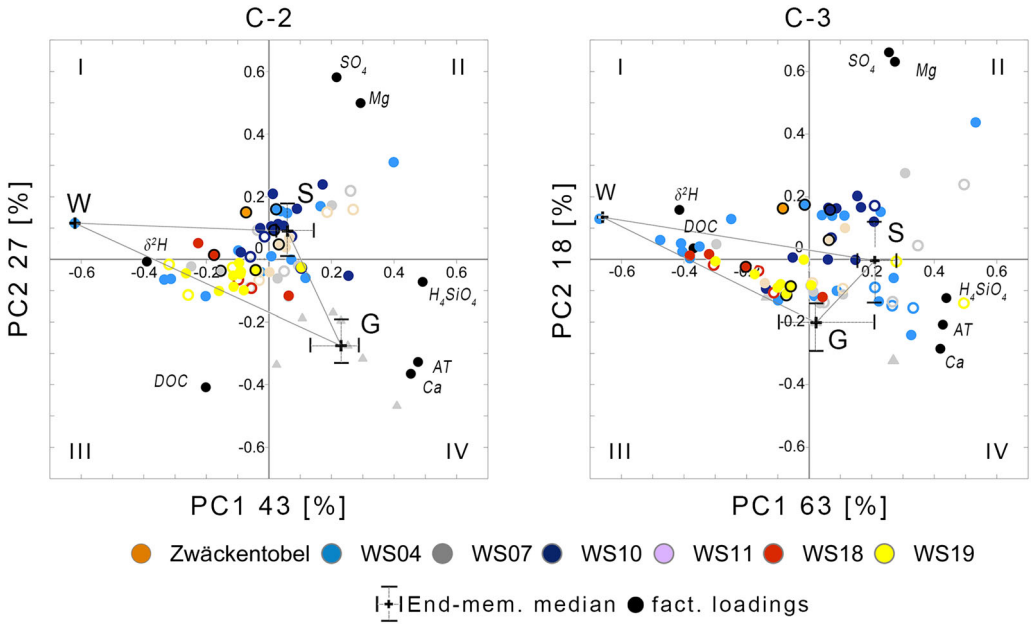

Figure 8. PCA-biplot of C-2 and C-3 with scores stream (filled circles), springs (open circle), groundwater samples (triangle) and correlated isotopic and hydrochemical loadings. ZT is the Zwäckentobel outlet. Quadrants are numbered with roman numerals. End-members (+) are median of springs (S), wetland (W) and groundwater (G) samples each with their upper and lower quartiles (error bar)

ing isotopic and hydrochemical signature dynamics during baseflow, we investigated which sources contribute to baseflow. We further identified the spatial patterns of streamwater composition and their relation to (sub) catchment landscape units and stream chemistry. An additional focus was on understanding the role of wetlands in these types of wet headwater catchments.

In the analysis of the spatiotemporal variability for selected isotopic (δ^2H) and hydrochemical (Ca, DOC, AT, pH, SO_4, Mg and H_4SiO_4) components, the variability of the concentrations was small and statistically not significant within and between these subcatchments, despite the differences in landscape characteristics of the six adjacent subcatchments. Streamwater samples at the subcatchment outlets, however, were more similar to springs than to groundwater from observation wells.

From the selected variables, the combination δ^2H, Ca and DOC proved to be most useful for distinguishing different sources. Although we observed the influence of geology on the hydrochemical composition of streamwater, in contrast to findings of Soulsby *et al.* (2007), the hydrochemical variables Ca, Mg and H_4SiO_4 gave no further information to distinguish between the three geological flysch facies. The spatial difference in SO_4 concentrations between the different subcatchments could neither be explained with a geological map, or as indicated by Keller *et al.* (1989), by atmospheric deposition. From our observations it is likely that during baseflow subcatchments with high SO_4 concentrations are dominantly fed by deep groundwater from springs with slightly higher SO_4 concentrations compared to shallow groundwater and wetlands. An additional increase in SO_4 concentrations of WS04 and WS10 are likely because of both their steep and erosive stream networks. This additional weathering of flysch layers containing $CaSO_4$ (anhydrite) might have increased the concentration of SO_4 (Campbell *et al.*, 1995). This is also in agreement with low SO_4 concentrations for the flatter more stable stream network of WS07 and WS19. These first results could be further examined in a more detailed study to gain insight into the poorly understood and complex interaction of SO_4 from atmosphere, weathering, terrestrial processes and limnology, as previously stated by Campbell *et al.* (1995). Studies with different geologies such as granitic (Likens and Buso, 2006; Zimmer *et al.*, 2012) or schist (Asano *et al.*, 2009) had two orders of magnitude lower Ca concentrations compared to the Zwäckentobel (Keller *et al.*, 1989; Zobrist, 2010). The Ca-rich geology resulted in that all streamwater samples were highly buffered (pH near 8.0). This blurred potential differences in pH between different landscape units including wetland, pastures and forest. Comparing our Ca concentrations with observations made by Keller (1990) and Keller *et al.* (1989), who studied hydrochemical variables at the outlet of WS04 together with six additional headwaters (below 1 km^2) in the larger Alptal catchment (47 km^2), they found spatial variabilities of baseflow concentrations for Ca, of 50–80 $mg\,l^{-1}$; H_4SiO_4, of 1–3 $mg\,l^{-1}$; and SO_4 of 3-25 $mg\,l^{-1}$. These concentrations corresponded to the spatial variability observed in our adjacent subcatchments, WS04–WS19, which implies similarities in baseflow generation. On the other hand, Schleppi *et al.* (2006)

showed the long-term temporal variability of Ca for WS04 (for 15 years of weekly discharge with proportional sampling at the catchment-scale) and found that Ca was approximately 60 mg l^{-1} during baseflow while for higher flows the concentration decreased exponentially to 20 mg l^{-1}. This long-term temporal variability is of the same order of magnitude as the spatial variability of deep groundwater and wetlands during baseflow found in our study. This overlap of the sampled concentrations is a potential source of error when used in hydrograph separation to distinguish between different sources, e.g. pre-event water from groundwater and wetlands (Ca >50 and 20 mg l^{-1}, respectively) compared to event water (Ca 0 mg l^{-1}).

Spatial differences of δ^2H, Ca and DOC became visible by mapping the measured chemical variables to the respective sampling locations. Different landscape units with water of a distinct isotopic and hydrochemical signature could be identified: a tributary, i.e. a drainage ditch, from a wetland in WS04, and the upper spring zone that was near the water divide located above 1400 m. The spatial representation of δ^2H, Ca and DOC also helped to visualize changes in concentrations along the stream and distinguish deep groundwater from springs which were connected to different flowpaths, as in the case of springs S-81, S-55 and S-9.

The role of landscape units in sustaining baseflow

Several studies found evidence of hydrochemical changes along the stream network, e.g. Asano *et al.* (2009) pointed to the signal propagation along the longitudinal stream network while Zimmer *et al.* (2012) discussed the dominance of small active sources from upstream areas of a catchment. Other studies found relations with different landscape characteristics (Rodgers *et al.*, 2004; Frisbee *et al.*, 2011). Temnerud *et al.* (2007) stated that the dampening of the hydrochemical variability originates not from conservative mixing but from a structured mosaic of landscape units. Our study supports these previous findings. From the isotopic and hydrochemical variables we gained insight into the baseflow generation processes and the contributing sources in steep and wet pre-alpine headwaters with a heterogeneous landscape.

The water composition (δ^2H, Ca and DOC) varied considerably. This variability was examined by representing each variable according to their sampling point's upstream landscape features such as catchment area, altitude, slope, topographic wetness index, land use (forest, meadow and wetland), geological facies and shallow soils. However, only a clear relation of δ^2H, Ca and DOC as a function of catchment area was found, where the variability at catchment scales of 0.2 km^2 was reduced (analysis of the other landscape features showed no strong relationships). The upslope scale of 0.2 km^2 coincided with the observed upper spring zone. At scales larger than 0.2 km^2, i.e. outside the upper spring zone, the hydrochemical composition of the main stream increased or decreased little and remained more similar to the isotopic and hydrochemical composition from the upper spring zone near the water divide. In the case of WS04, the upper spring zone had the lightest δ^2H composition, with heavier δ^2H concentrations downstream and with decreasing altitude. In contrast, wetlands had enriched δ^2H, indicating different water and flowpaths compared to the spring zone or groundwater from wells. Comparing the differences in wetland and stream samples, it is likely that because of the continued saturated state, water in wetlands is younger with shorter transit times compared to 'older' water from the steeper slopes, which was also observed by Inamdar *et al.* (2013). High Ca concentrations in the upper spring zone originate from deep groundwater which dissolves the carbonate bedrock. Once at the surface and in the stream, stabilizing processes (e.g. chemical precipitation) and mixing with water of lower concentration may have led to decreasing Ca concentrations further downstream. Another typical hydrochemical characteristic of deep groundwater from springs was the low DOC concentrations. DOC concentrations increased and Ca concentrations decreased slightly downstream but maintained a signature similar to low DOC and high Ca concentrations from springs, i.e. deep groundwater. At confluences with tributaries from wetlands, the composition of δ^2H, Ca and DOC changed little, and any changes were likely because of only minor contributions from the side branches to baseflow in the main stream, i.e. the wetlands were less connected. This was supported by Ca or DOC concentrations of sampling locations represented according to their upstream wetland percentage. In a situation where wetlands and other areas contribute equally to baseflow the different sampling points would resemble a line between low wetland percentage with high Ca and low DOC concentrations (i.e. wetland 20%; Ca 75 mg l^{-1}; DOC 2 mg l^{-1}) and high wetland percentage with low Ca and high DOC concentrations (i.e. wetland 100%; Ca 20 mg l^{-1}; DOC >6 mg l^{-1}). From our sampling design most sampling locations, including sites with high wetland percentage, had high Ca and low DOC concentrations, and we concluded that their streamwater originated from runoff sources other than wetlands. The DOC concentrations in this study were in the same range as at other headwaters (James and Roulet, 2006; Likens and Buso, 2006; Tetzlaff and Soulsby, 2008) but one order of magnitude lower compared to Swedish headwaters (Temnerud *et al.*, 2007).

Bivariate solute diagrams and multivariate principal component analysis are established methods to distinguish between different spatiotemporal patterns of streamwater composition and characterize specific geo-

graphic water sources of different catchments in relation to their multiple variables (Christophersen and Hooper, 1992; Fröhlich *et al*., 2008; Barthold *et al*., 2010). In our study the bivariate representation of Ca and DOC was useful to identify three runoff sources: deep groundwater from springs, shallow groundwater and wetlands sampled in the drainage ditch of WS04. Although our sampling design had only few stream samples that were directly sampled and a distinct wetland signature (low Ca, high DOC), the bivariate representation with end-members gave a first impression of the origin of runoff during baseflow. Most samples were grouped together near the hydrochemical composition of deep groundwater from springs located near the water divide. Only few streamwater samples showed a signature that was similar to the samples from wetlands or shallow groundwater from observation wells. For the bivariate representation of Ca and DOC the observations were largely bounded within the degree of uncertainty by three end-members of groundwater wells (shallow groundwater), springs (deep groundwater) and wetlands.

In contrast to the bivariate representation of Ca and DOC, the PCA-biplot gave more insight into differences of the spatial isotopic and hydrochemical compositions. Fröhlich *et al*. (2008) observed that different subcatchments can have a unique hydrochemical composition at a larger catchment scale (692 km^2). Similarly, Hrachowitz *et al*. (2011) showed this for a semi-arid catchment and Lu (2014), for a volcanic catchment. From the PCA-biplot we made similar observations for the studied headwaters. Subcatchments had distinct isotopic and hydrochemical compositions, where neighbouring subcatchments formed pairs with comparable hydrochemical compositions: WS04 and WS07, WS10 and WS11 and WS18 and WS19. These spatial patterns of isotopic and hydrochemical composition were coherent and combined the analyses (boxplot and bivariate representation of Ca and DOC) into one analysis to give a comprehensive overview of the multivariate data (δ^2H, Ca, DOC AT, pH, SO_4, Mg, and H_4SiO_4). Compared to the bivariate representation with end-members, for the PCA-biplot, not all observations were bounded by the end-members. This might be because of the unique hydrochemical composition of subcatchments, with single or other (not sampled) end-members. Besides this limitation of the available end-members, these extreme signatures proved to be useful as a first indicator for baseflow runoff processes and source areas.

Wider implications on pre-alpine baseflow

Pre-alpine headwaters with shallow soils and high precipitation respond quickly to rainfall and therefore, according to Frisbee *et al*. (2011), a network-mixing model would be a valid conceptualization of these systems. Shallow soils, however, have a limited aquifer while glacial valley bottom deposits can sometimes store groundwater from upslope areas and sustain baseflow (Tetzlaff and Soulsby, 2008). Other studies showed that during baseflow conditions the riparian zone acts as the main input to streamflow generation (Sidle *et al*., 2000; Penna *et al*., 2014). Our studied headwaters were lacking such a valley aquifer and riparian zone. We rather observed different spatially distributed baseflow generating zones similar to the work of Asano *et al*. (2009) and Zimmer *et al*. (2012), from the deep groundwater (perennial springs, in the upper spring zone near the ridge). Despite the shallow soils with limited storage capacity, deep groundwater seeped from fractures and fissures into the zero-order basin and fed the first order stream channels, and this deep groundwater seemed to be permanently connected to the stream network. The C-2 and C-3 campaigns showed a seasonal change for stable isotopes, indicating water with longer transit times, whereas spatial patterns of the hydrochemistry remained mostly similar. Less than 10% of the groundwater and spring samples changed in their composition, presumably because of a connection with a different flowpath. Our findings confirmed the statement of Keller *et al*. (1989) who postulated that baseflow originates from deep percolating water from springs based on sampling at the catchment outlet. Uchida *et al*. (2005) made similar observations in steep, homogeneous and forested headwaters in Japan. Inamdar *et al*. (2013) found from changes in hydrochemistry that during seasonal drying over the summer (in dry conditions), portions of the drainage network were disconnected and did not contribute to streamflow. Contrary to this seasonal change in connectivity, our findings show that passive, in terms of being hydrologically less connected landscape units, can also occur in rainfall dominated headwaters such as the Zwäckentobel catchment (2,300 mm $year^{-1}$). The wetlands are prominent landscape units with large storage capacity and areal extent (30–60% of the subcatchment area), but during baseflow these features mostly act as passive units not significantly contributing to baseflow. Consequently, pre-alpine headwaters with similar climate, geology and topography are, during baseflow, not just the sum of different landscape units, but are rather dominated by the arrangement of connected (active) or disconnected (passive) landscape units as conceptualized by Sidle *et al*. (2000) and Ambroise (2004).

The Zwäckentobel headwater is dominated by deep groundwater from the upper spring zone near the water divide. The isotopic and hydrochemical composition does not change significantly during baseflow towards the catchment outlet. We cannot fully exclude that outside the upper spring zone (altitudes below 1,400 m) deep groundwater or groundwater with a similar composition to the streamwater contributed to baseflow. From our analysis of

δ^2H, Ca and DOC, it is more likely that the deep groundwater from the upper spring zone determines to a large extent the isotopic and hydrochemical signatures of baseflow contribution at the subcatchment outlet. Within the upper spring zone, as well as for other sampling locations, we could not distinguish between the isotopic and hydrochemical composition and different landscape units such as forest, meadows and wetlands. This might be partly because of sampling design and the chosen isotopic and hydrochemical variables. However, it is more likely that the dominance of active sources from the upper spring zone explains why we did not observe, with exception of catchment area and implicit altitude (represented by the stream network), any other relations between hydrochemistry and controlling landscape features. Nevertheless, these active contributing point elements, such as seeping deep groundwater from springs with passive features are indicators short and long flowpaths and transit times (Rodgers *et al*., 2004). Therefore, instead of a network-mixing model it is more likely that steep wet pre-alpine headwaters are better represented with a more complex 'Tóthian', i.e. topography-energy driven flow model, as discussed by Frisbee *et al*. (2011).

Hence, future studies in pre-alpine headwater catchments should focus not only on headwater mean transit times but as shown by Tetzlaff *et al*. (2014) on the transit times of water through the different contributing landscape units. Overall, our results confirm the need for and benefits of spatially distributed snapshot sampling to increase spatial process understanding of heterogeneous headwaters during baseflow. These results underline the usefulness of nested and/or spatially distributed tracer studies to increase knowledge of the fundamental mechanisms and governing process of baseflow generation in headwater systems.

ACKNOWLEDGEMENTS

This research project could not have been performed without the support of many people who helped in the field and the laboratory -a great thank you to all of them. Especially we thank Ilaria Clemenzi, Nans Addor, Georgie Bennett, Ellen Cerwinka, Daniel Furrer, Inge Juszak, Seraina Kauer, Käthi Liechti, Bernardo Maestrini, Andri Moll, Isabelle Nanz, Paribesh Pradhan, Silvan Ragettli, Maarten Smoorenburg, Maria Staudinger, Karl Steiner, Marc Vis, Annagreth Schuler, Werni Ruhstaller and the AUA Laboratory at EAWAG for chemical analyses. We also thank Manfred Stähli (WSL), the Oberallmeindkorporation Schwyz (OAK), the Department of Environment of the Canton of Schwyz and the municipality Alpthal for the good cooperation. The constructive comments of the editor and three anonymous reviewers helped to improve the manuscript.

REFERENCES

Ambroise B. 2004. Variable "active" versus "contributing" areas or periods: a necessary distinction. *Hydrological Processes* **18**: 1149–1155. DOI:10.1002/hyp.5536.

Asano Y, Uchida T, Mimasu Y, Ohte N. 2009. Spatial patterns of stream solute concentrations in a steep mountainous catchment with a homogeneous landscape. *Water Resources Research* **45**, W10432. DOI: 10.1029/2008WR007466.

Barthold FK, Wu J, Vaché KB, Schneider K, Frede H-G, Breuer L. 2010. Identification of geographic runoff sources in a data sparse region: hydrological processes and the limitations of tracer-based approaches. *Hydrological Processes* **24**: 2313–2327. DOI:10.1002/hyp.7678.

Bishop K, Buffam I, Erlandsson M, Fölster J, Laudon H, Seibert J, Temnerud J. 2008. Aqua Incognita: the unknown headwaters. *Hydrological Processes* **22**: 1239–1242. DOI:10.1002/hyp.7049.

Buttle JM, Dillon PJ, Eerkes GR. 2004. Hydrologic coupling of slopes, riparian zones and streams: an example from the Canadian Shield. *Journal of Hydrology* **287**: 161–177. DOI:10.1016/j.jhydrol.2003.09.022.

Campbell DH, Clow DW, Ingersoll GP, Mast MA, Spahr NE, Turk JT. 1995. Processes controlling the chemistry of two snowmelt-dominated streams in the rocky mountains. *Water Resources Research* **31**: 2811–2821. DOI:10.1029/95WR02037.

Christophersen N, Hooper RP. 1992. Multivariate analysis of streamwater chemical data: the use of principal components analysis for the end-member mixing problem. *Water Resources Research* **28**: 99–107. DOI:10.1029/91WR02518.

Feyen H, Leuenberger J, Papritz A, Gysi M, Flühler H, Schleppi P. 1996. Runoff processes in catchments with a small scale topography. *Physics and Chemistry of the Earth* **21**: 177–181. DOI:10.1016/S0079-1946(97)85581-4.

Frisbee MD, Phillips FM, Campbell AR, Liu F, Sanchez SA. 2011. Streamflow generation in a large, alpine watershed in the southern Rocky Mountains of Colorado: is streamflow generation simply the aggregation of hillslope runoff responses? *Water Resources Research* **47**, W06512. DOI: 10.1029/2010WR009391.

Fröhlich HL, Breuer L, Frede H-G, Huisman JA, Vaché KB. 2008. Water source characterization through spatiotemporal patterns of major, minor and trace element stream concentrations in a complex, mesoscale German catchment. *Hydrological Processes* **22**: 2028–2043. DOI:10.1002/hyp.6804.

Hantke R. 1967. Geological map of the Canton of Zurich and its neighboring areas. *Q. J. Nat. Hist. Soc. Zurich*.

Hegg C, McArdell BW, Badoux A. 2006. One hundred years of mountain hydrology in Switzerland by the WSL. *Hydrological Processes* **20**: 371–376. DOI:10.1002/hyp.6055.

Hochberg Y, Tamhane AC. 1987. Frontmatter. In *Multiple Comparison Procedures*. John Wiley & Sons, Inc: Hoboken, NJ, USA. DOI: 10.1002/9780470316672.fmatter.

Hrachowitz M, Bohte R, Mul ML, Bogaard TA, Savenije HHG, Uhlenbrook S. 2011. On the value of combined event runoff and tracer analysis to improve understanding of catchment functioning in a data-scarce semi-arid area. *Hydrology and Earth System Sciences* **15**: 2007–2024. DOI:10.5194/hess-15-2007-2011.

Hsü KJ, Briegel U. 1991. The Flysch. In *Geology of Switzerland SE - 6*. Birkhäuser: Basel; 65–82. DOI: 10.1007/978-3-0348-8663-5_6.

Inamdar S, Dhillon G, Singh S, Dutta S, Levia D, Scott D, Mitchell M, Van Stan J, McHale P. 2013. Temporal variation in end-member chemistry and its influence on runoff mixing patterns in a forested, Piedmont catchment. *Water Resources Research* **49**: 1828–1844. DOI:10.1002/wrcr.20158.

James AL, Roulet NT. 2006. Investigating the applicability of end-member mixing analysis (EMMA) across scale: a study of eight small, nested catchments in a temperate forested watershed. *Water Resources Research* **42**: . DOI:10.1029/2005WR004419.

Kaiser HF. 1960. The application of electronic computers to factor analysis. *Educational and Psychological Measurement* **20**: 141–151.

Keller HM. 1990. Extreme conditions of streamwater chemistry in a partly forested mountainous region. IAHS Publ. Proceedings of two Lausanne Symp. August 1990, 477–486.

Keller HM, Burch HJ, Guecheva M. 1989. The variability of water quality in a small mountainous region. IAHS Publ. Reg. Charact. Water Quality (Proceedings Balt. Symp. May 19), 305–312.

Kosugi K, Katsura S, Katsuyama M, Mizuyama T. 2006. Water flow processes in weathered granitic bedrock and their effects on runoff generation in a small headwater catchment. *Water Resources Research* **42**, W02414. DOI: 10.1029/2005WR004275.

Likens G, Buso D. 2006. Variation in streamwater chemistry throughout the Hubbard brook valley. *Biogeochemistry* **78**: 1–30. DOI:10.1007/s10533-005-2024-2.

Lindsay JB. 2009. *Whitebox Geospatial Analysis Tools*. The University of Guelph: Canada.

Lu H-Y. 2014. Application of water chemistry as a hydrological tracer in a volcano catchment area: a case study of the Tatun Volcano Group, North Taiwan. *Journal of Hydrology* **511**: 825–837. DOI:10.1016/j.jhydrol.2014.02.036.

Lyon SW, Nathanson M, Spans A, Grabs T, Laudon H, Temnerud J, Bishop KH, Seibert J. 2012. Specific discharge variability in a boreal landscape. *Water Resources Research* **48**, W08506. DOI: 10.1029/2011WR011073.

Penna D, Stenni B, Šanda M, Wrede S, Bogaard TA, Gobbi A, Borga M, Fischer BMC, Bonazza M, Chárová Z. 2010. On the reproducibility and repeatability of laser absorption spectroscopy measurements for δ^2H and δ^{18}O isotopic analysis. *Hydrology and Earth System Sciences* **14**: 1551–1566. DOI:10.5194/hesC-14-1551-2010.

Penna D, van Meerveld HJ, Oliviero O, Zuecco G, Assendelft RS, Dalla Fontana G, Borga M. 2014. Seasonal changes in runoff generation in a small forested mountain catchment. *Hydrological Processes*. DOI:10.1002/hyp.10347.

Rinderer M, van Meerveld HJ, Seibert J. 2014. Topographic controls on shallow groundwater levels in a steep, prealpine catchment: when are the TWI assumptions valid? *Water Resources Research* **50**: 6067–6080. DOI:10.1002/2013WR015009.

Rodgers P, Soulsby C, Petry J, Malcolm I, Gibbins C, Dunn S. 2004. Groundwater-surface-water interactions in a braided river: A tracer-based assessment. *Hydrological Processes* **18**: 1315–1332. DOI:10.1002/hyp.1404.

Schleppi P, Waldner PA, Stähli M. 2006. Errors of flux integration methods for solutes in grab samples of runoff water, as compared to flow-proportional sampling. *Journal of Hydrology* **319**: 266–281. DOI:10.1016/j.jhydrol.2005.06.034.

Sidle RC, Tsuboyama Y, Noguchi S, Hosoda I, Fujieda M, Shimizu T. 2000. Stormflow generation in steep forested headwaters: a linked hydrogeomorphic paradigm. *Hydrological Processes* **14**: 369–385. DOI:10.1002/(SICI)1099-1085(20000228)14:3<369::AID-HYP943>3.0.CO;2-P.

Soulsby C, Tetzlaff D, van den Bedem N, Malcolm IA, Bacon PJ, Youngson AF. 2007. Inferring groundwater influences on surface water in montane catchments from hydrochemical surveys of springs and streamwaters. *Journal of Hydrology* **333**: 199–213. DOI:10.1016/j.jhydrol.2006.08.016.

Stähli M, Gustafsson D. 2006. Long-term investigations of the snow cover in a subalpine semi-forested catchment. *Hydrological Processes* **20**: 411–428. DOI:10.1002/hyp.6058.

Temnerud J, Seibert J, Jansson M, Bishop K, Carlo M. 2007. Spatial variation in discharge and concentrations of organic carbon in a catchment network of boreal streams in northern Sweden. *Journal of Hydrology* **342**: 72–87. DOI:10.1016/j.jhydrol.2007.05.015.

Tetzlaff D, Soulsby C. 2008. Sources of baseflow in larger catchments—using tracers to develop a holistic understanding of runoff generation. *Journal of Hydrology* **359**: 287–302. DOI:10.1016/j.jhydrol.2008.07.008.

Tetzlaff D, Birkel C, Dick J, Geris J, Soulsby C. 2014. Storage dynamics in hydropedological units control hillslope connectivity, runoff generation, and the evolution of catchment transit time distributions. *Water Resources Research* **50**: 969–985. DOI:10.1002/2013WR014147.

Turowski JM, Yager EM, Badoux A, Rickenmann D, Molnar P. 2009. The impact of exceptional events on erosion, bedload transport and channel stability in a step-pool channel. *Earth Surface Processes and Landforms* **34**: 1661–1673. DOI:10.1002/esp.1855.

Uchida T, Asano Y, Onda Y, Miyata S. 2005. Are headwaters just the sum of hillslopes? *Hydrological Processes* **19**: 3251–3261. DOI:10.1002/hyp.6004.

Zimmer MA, Bailey SW, McGuire KJ, Bullen TD. 2012. Fine scale variations of surface water chemistry in an ephemeral to perennial drainage network. *Hydrological Processes* **27**: 3438–3451. DOI:10.1002/hyp.9449.

Zobrist J. 2010. Water chemistry of Swiss Alpine Rivers. In *Alpine Waters*. Springer-Verlag: Heidelberg; 95–118. DOI: 10.1007/978-3-540-88275-6_5.

SUPPORTING INFORMATION

Additional supporting information may be found in the online version of this article at the publisher's web site.

8.2 Paper II - Runoff events

Pre-event water contributions to runoff events of different magnitude in pre-alpine headwaters

Pre-event water contributions to runoff events of different magnitude in pre-alpine headwaters

Benjamin M. C. Fischer, Manfred Stähli and Jan Seibert

ABSTRACT

Precipitation and catchment characteristics of mountainous headwaters can vary largely within short distances. It remains unclear how these two factors determine the contribution of event water and pre-event water to stormflow. We investigated this in five neighboring headwaters with high annual precipitation amounts (>2,000 mm y^{-1}) in a steep pre-alpine region in Switzerland. Rainfall and streamwater of 13 different rainstorms were sampled (P: 5 mm intervals, Q: 12 to 51 samples per events) to perform a two-component isotope hydrograph separation. Pre-event water contributions based on $\delta^{18}O$ or $\delta^{2}H$ computation were similar. The pre-event water contributions of headwaters depended largely on rainfall (amount and intensity) and varied more between events than between catchments, despite clear differences in land cover between the catchments. Furthermore, antecedent wetness was not found to control pre-event water contribution. With increasing rainfall amount, the proportion of rainfall in runoff increased and changed from pre-event to event water dominated. The variable rainfall amount and small active storage (organic soil horizon, 20–50 cm) resulted in a threshold in the upper soil horizon with subsequently more variable pre-event water contribution. Our results show the necessity of sampling in different headwaters and events to better understand controlling factors in runoff generation.

Key words | catchment comparison, headwater catchments, hydrograph separation, isotope hydrology, runoff generation

Benjamin M. C. Fischer (corresponding author)
Jan Seibert
Department of Geography,
University of Zurich,
Winterthurerstrasse 190,
CH-8057 Zurich,
Switzerland
E-mail: *benjamin.fischer@geo.uzh.ch*

Manfred Stähli
Swiss Federal Institute for Forest,
Snow and Landscape Research WSL,
Birmensdorf,
Switzerland

Jan Seibert
Department of Earth Sciences,
Uppsala University,
Uppsala, Sweden

INTRODUCTION

Runoff generation processes vary in space and time. The spatial variation is controlled by catchment properties such as land-use/cover and geology, while the temporal variation is mainly controlled by hydrometeorological conditions such as precipitation and soil moisture. Understanding this spatiotemporal variability of runoff processes as a function of precipitation and catchment characteristics is important for predictions of streamflow quantity and quality.

As part of the water itself, the stable isotopes $\delta^{18}O$ and $\delta^{2}H$, are valuable conservative tracers in the two end-member mass balance approach (also called two-component isotope hydrograph separation (IHS)) to study how catchments transform rainfall into runoff. Using IHS allows the stormflow hydrograph to be separated, and to discern to what degree rainfall (event water) and water, that has been stored in the catchment before the event (pre-event water), contribute to stormflow (Sklash *et al.* 1976; Klaus & McDonnell 2013).

IHS has, however, frequently been performed only in single headwaters (e.g., McDonnell *et al.* 1990; Jordan 1994; Vitvar & Balderer 1997; Renshaw *et al.* 2003; Pellerin *et al.* 2007; Lyon *et al.* 2008; Penna *et al.* 2014). From several IHS studies in forested headwaters, the general perception developed that pre-event water dominates the peak discharge (Buttle 1994; Klaus & McDonnell 2013). However, the value of an IHS study in one catchment and one event is limited. Such studies are criticized for not providing further

doi: 10.2166/nh.2016.176

insights into hydrological processes (Burns 2002). With advances in laser spectroscopes, measuring the composition of both stable isotopes $\delta^{18}O$ and $\delta^{2}H$ has become relatively easy and the price per sample has decreased (Lis *et al.* 2008; Penna *et al.* 2010). This development has made it possible to investigate more catchments or events. Few early IHS studies compared different catchments (Rodhe 1987) and only recently has IHS been used to compare neighboring headwaters (Onda *et al.* 2006; Laudon *et al.* 2007) and/or many events (McGlynn *et al.* 2004; Lyon *et al.* 2008; James & Roulet 2009; Roa-García & Weiler 2010; Hrachowitz *et al.* 2011; Segura *et al.* 2012). Several of these runoff generation studies found a more variable event and pre-event water contribution, contrary to the presumed dominance in pre-event water found in the single headwater studies. Casper *et al.* (2003), Pellerin *et al.* (2007), Kienzler & Naef (2008), James & Roulet (2009), and Penna *et al.* (2014), could relate an increase of event water to rainfall sum, intensities, and duration (see also Klaus & McDonnell 2013). In forested headwaters, trees not only affect the amount of spatiotemporal throughfall (Gerrits *et al.* 2010) and isotopic composition (Allen *et al.* 2015), but also affect the subsurface connectivity (Weiler *et al.* 1998). Interception and transpiration of trees together with higher infiltration capacities of the soils can have a delaying effect on stream response, and pre-event water dominates the stormflow (Buttle 1994; Roa-García & Weiler 2010; Klaus & McDonnell 2013). Roa-García & Weiler (2010) observed higher pre-event water fractions in wetlands compared to forest and grasslands. Other studies have also observed higher event water fractions in wetlands (McCartney *et al.* 1998; Laudon *et al.* 2007) and in grasslands (Bonell *et al.* 1990). Infiltration capacity, soil type, storage potential of soils (Geris *et al.* 2015), and macropore distribution (Buttle 1994) are important controlling factors in runoff generation processes. High responsive headwaters with shallow soils of less than a meter have generally limited water storage in the soil mantel (Pearce *et al.* 1986). Suecker *et al.* (2000) observed higher event water contributions on steep slopes. In different studies from around the world, described in Buttle (1994) or Jordan (1994), it is difficult to observe a relationship between event water contribution and geology. On the other hand, Onda *et al.* (2006) however did not observe a significant relation between soil depth and event water, but found that headwaters with 'permeable' geologies (larger number of cracks and fissures) had a lower event water contribution.

Brown *et al.* (1999) and Shanley *et al.* (2002) observed that event water contribution increases with catchment size, while no relation was found by either McGlynn *et al.* (2004) or James & Roulet (2009). Seasonality and the state of the system affect flow pathways (Hinton *et al.* 1994; Penna *et al.* 2014). Jordan (1994), Casper *et al.* (2003), and James & Roulet (2009) found that dry antecedent conditions with low connectivity result in higher event water contribution while McGlynn *et al.* (2004) found the opposite.

Pre-alpine headwaters are characterized by a large spatiotemporal variability of precipitation and variation in land cover, topography, and geology (Gurtz *et al.* 1999). Despite the heterogeneous catchment characteristics, baseflow processes in neighboring pre-alpine headwaters can be similar (Fischer *et al.* 2015). During stormflow however, it remains to be quantified how the variability of precipitation and catchment characteristics controls runoff processes in these headwaters.

In this study we investigated a steep pre-alpine region with high annual precipitation amounts (>2,000 mm y^{-1}) in Switzerland using IHS for five neighboring headwaters and 13 different rainstorm events. The objective was: (1) to assess differences in pre-event water contribution between headwaters and different events, and (2) to relate these differences to rainfall, catchment, and antecedent characteristics.

METHODS

Study area

The study area, the Zwäckentobel, is a pre-alpine catchment in Switzerland and approximately 40 km south of Zurich. The climate is humid with a mean annual temperature of 6 °C. The mean annual precipitation is 2,300 mm y^{-1}, of which half falls during the snow-free season (June–October). It rains approximately every second day and about one-third of the annual precipitation falls as snow (Stähli & Gustafsson 2006). The mean annual actual evaporation is approximately 300 mm y^{-1} (Menzel *et al.* 2007). The mountain streams respond quickly and can have high discharges

with large amounts of sediment transport (Turowski *et al.* 2009). After rainfall events, the streams return to baseflow within approximately 1 day.

The Zwäckentobel is a 4.3 km^2 south–north oriented headwater catchment. The east facing side of the catchment is steep with frequent landslides and an ephemeral stream network. Approximately ten perennial streams drain the remaining part of the Zwäckentobel. One of the streams is the 0.7 km^2 Erlenbach catchment (WS04) which has been the subject of numerous studies since 1964 (Hegg *et al.* 2006). In 2009, the streams of WS07, WS10, WS11, and WS19 (0.09 to 0.21 km^2) were additionally gauged (Figure 1(a) and Table 1). Common features for all headwaters (WS04–WS19) are alternating steep slopes of more than 20° and flatter areas along the main axis, originating from erosion deposits like soil creep and landslides. The steep terrain and high transport capacity of streams created step-pool channels (Molnar *et al.* 2010) cutting into the alluvium of weathered bedrock (Keller 1970). As a consequence, a riparian zone is lacking (Hagedorn *et al.* 2001).

The geology of the Zwäckentobel has three different types of tertiary flysch: Wild, Waeggitaler, and Schlieren flysch. The different facies consist of different calcareous sedimentary layers of schist, marl or sandstone (Hantke 1967; Hsü & Briegel 1991) with creeping gleysols (0.5–2.5 m) on top (Figure 1(b)). The spatial distribution of shallow soils (depth ≤1 m) was taken from Fischer *et al.* (2015). The soils have a high silt and clay content resulting in a low matrix permeability but a high drainage capacity in macropores and the organic layer of 20–50 cm (Feyen *et al.* 1999).

The land cover of the Zwäckentobel was classified by Fischer *et al.* (2015) into forest, partly forested, meadows, and wetlands (Figure 1(c)). The dominant tree species in the Zwäckentobel is Norway spruce with a plate-shaped root network with an approximate root depth of 1 meter, in wet areas. Non-forested locations within the catchment are generally wetter and consist of bushed and/or swampy meadows or wetlands (Rinderer *et al.* 2012). During the summer months, meadows in the upper part (above 1,450 m) of WS04 and WS19 are used as alpine pastures.

Instrumentation

Precipitation was measured at 14 locations (Figure 1(a)). Two of the rain gauges are situated in the Erlenbach catchment (WS04) and have been measuring precipitation since 1964

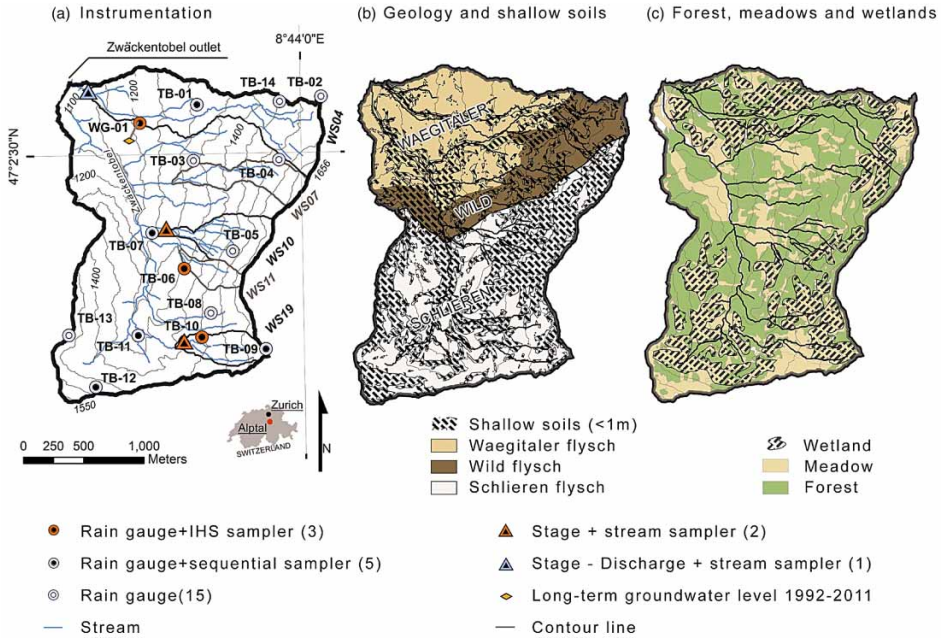

Figure 1 | Map of the Zwäckentobel: (a) sampling locations in selected headwaters WS04 to WS19; (b) geology: three different types of flysch and on top the shallow soils ≤1 m indicated as hatched areas; (c) land cover: forest and meadows with hatched areas indicating wetlands. Color scheme of Figures 1(b) and 1(c) adapted from www.ColorBrewer.org.

Table 1 | Catchment characteristics of the Zwäckentobel and its five headwaters

				ZT	WS04	WS7	WS10	WS11	WS19
Shape	Size		km	4.25	0.7	0.21	0.23	0.09	0.15
	Altitude	Max		1,656	1,656	1,656	1,598	1,583	1,598
		Mean		1,360	1,342	1,468	1,432	1,421	1,494
		Min		1,084	1,109	1,262	1,276	1,292	1,384
	Slope	Mean		19	17	21	23	24	18
		Max		56	49	47	53	45	43
Geology		Waegitaler		29	64	16	0	0	0
	Flysch	Wild	%	17	29	42	0	0	0
		Schlieren		54	7	42	100	100	100
	Soil depth	<1 m	%	29	44	55	73	74	49
Land cover	Forest			55	53	53	72	81	18
	Partly	forested	%	21	22	27	14	10	1
	Meadow			24	25	20	14	9	81
	Wetland		%	29	33	28	23	21	51

(WG-01: Ott Pluvio, OTT Hydrometrie AG, Switzerland and TB-14: Joss-Tognini tipping bucket, Lamprecht meteo, Germany). The remaining 12 rain gauges (Davis II rain collector-tipping bucket; Davis Instruments Corp., USA with Odyssey data logger; Dataflow Systems, New Zealand) were distributed over the Zwäckentobel in the open field at a height of 1.5 m above ground level and measured rainfall during the period 2009–2011. Barometric pressure and air temperature were measured at WG-01 and WS19 (Keller DCX-22, Keller AG, Switzerland; Figure 1(a)).

In the Erlenbach catchment (WS04), stage/discharge has been measured with a concrete flume from 1984 to the present (Hegg *et al.* 2006). The headwaters WS07, WS10, WS11, and WS19 and the Zwäckentobel outlet (ZT) were gauged in 2009 (Keller DCX-22 pressure and temperature sensors, Keller AG, Switzerland, Figure 1(a)). Due to the frequently changing stream morphologies it was impossible to derive rating curves. In the vicinity of WG-01, groundwater levels have been measured since 1992 in a screened groundwater well and with an Ott-groundwater data logger (OTT Hydrometrie AG, Switzerland; Figure 1(a)).

Event sampling

In headwaters WS04, WS07, WS10, WS11, and WS19, different rainfall–runoff events were sampled during the snow-free season of 2010 and 2011 (Tables 2–4). Before each rainfall event, a grab sample was taken from each stream to determine the pre-event water composition. Rainwater samples for isotope analysis were collected with eight sequential rainfall samplers (adapted after Kennedy *et al.* 1979 containing 12×100 mL honey jars, each representing 5 mm of liquid precipitation, Figure 1(a)). At the catchment outlets of WS04, WS07, WS10, WS11, and WS19, automatic samplers collected streamwater samples (ISCO 6712 with 24×1 L bottles and Liquid Level Actuator, Teledyne Isco, USA; Figure 1(a)). The different automatic samplers started after the water level of the streams rose more than 1 cm and sampled six samples every 10 min during the rising limb, followed by 18 samples every 60 min. This sampling scheme allowed the rising limb to be sampled with a high temporal resolution, while taking at least one sample as close as possible to the maximum discharge peak, such as in event 2 (Figure 2, left). For large events, it was attempted to collect the water samples from the full automatic samplers. These samplers were reprogrammed and restarted (sampling interval 120 or 240 min) to capture parts of the falling limb of the hydrograph, such as in event 11 (Figure 2, right). To improve sample handling and avoid sample contamination (Wassenaar *et al.* 2014), we chose not to use mineral oil in rain and stream water sample bottles, and rather collected all samples directly after a rainfall event to

Table 2 | Hydrometeorological characteristics of the 13 sampled events

Event nr.	1	2	3	4	5	6	7	8	9	10	11	12	13
Year	2010				2011								
Day, month	8 Sep	17 Sep	24 Sep	4 Oct	29 Jun	8 Jul	14 Jul	15 Aug	24 Aug	27 Aug	4 Sep	18 Sep	6 Oct
A_{DS} *[d]*	7	1	5	2	3	5	1	2	3	0	0	1	14
A_{PI7} [mm]	2	50	6	10	24	5	41	23	2	10	9	26	0
A_{GL1} *[cm]*	−34	−23	−28	−19	−28	−36	−12	−28	−38	−41	−37	−23	−42
A_{Q1} [l s^{-1} km^{-2}]	7	16	3	7	10	7	11	7	1	4	0	13	1
P length [h]	10	8	70	10	23	11	30	37	2	19	11	11	33
P_{sum} [mm]	22 (2.6)	11 (1.4)	109 (16)	10 (1)	84 (19)	25 (1.5)	56 (17)	50 (15)	11.8 (2)	20.4 (1)	51 (11)	25 (2)	31(12)
P [mm h^{-1}]	2.2(0.3)	1.3 (0.2)	1.5 (0.2)	0.9 (0.1)	3.6 (0.9)	2.5 (0.2)	2 (0.6)	1.4 (0.4)	6 (1)	1 (0.1)	1.9 (0.4)	1.6 (0.2)	0.9 (0.4)
P_{max} [mm h^{-1}]	4.5 (0.6)	2.3 (0.3)	7.6 (1.1)	2.4 (0.4)	18 (8.4)	9 (0.9)	6.7 (1.6)	10 (2.7)	10 (3)	7.3 (0.7)	7 (1.4)	6 (1.4)	8.6 (3.5)
$H_{responds}$ [h]	0.6 (1)	1 (0.6)	0.2 (0)	0.3 (0.3)	0.2 (0.1)	0.1 (0.1)	0.3 (0.2)	0.7 (0.3)	0.1 (0.1)	0.4 (0.3)	0.3 (0.2)	0.3 (0.2)	1.3 (0.5)
Q_{peak} [l s^{-1} km^{-2}]	353	106	1,010	53	3,004	390	1,197	1,287	86	334	589	504	509
Q/P [-]	0.35	0.36	0.7	0.29	0.6	0.25	0.68	0.55	0.12	0.25	0.52	0.52	0.28

Antecedent dryspell (A_{DS}), antecedent precipitation index with 7 days prior to an event (A_{PI7}), antecedent groundwater level (A_{GL1}), antecedent discharge (A_{Q1}), rainfall duration (P length), mean event rainfall sum all rain gauges (P_{sum}), mean average hourly rainfall intensity of all rain gauges (P), maximum hourly rainfall intensity of all rain gauges (P_{max}), mean stream responds to rainfall of all headwaters (H responds), maximum specific discharge of WS04 (Q_{peak}), runoff coefficient (Q/P). Spatial standard deviation is in brackets.

Table 3 | For WS04–WS19 and event 1–13 the number of stream samples n_{Cs}, $\delta^{18}O$ [‰] of pre-event water *Cpe,* maximum and minimum event water *Ce* and maximum and minimum streamwater, IHS based minimum fraction of pre-event water f_{PE} and its corresponding uncertainty $W f_{PE}$. The letters np indicate events where an IHS was not possible

Event		1	2	3	4	5	6	7	8	9	10	11	12	13
Year		2010				2011								
Day, month		8 Sep	17 Sep	24 Sep	4 Oct	29 Jun	8 Jul	14 Jul	15 Aug	24 Aug	27 Aug	4 Sep	18 Sep	6 Oct
WS04	C_{pe}		−10.5	−10.4		−10.7	−8.45	−9.12	−8.5	−8.5	−8.51	−8.96	−9.01	−9.41
	C_{e-WG01}		−4.6	−8.39		−4.61	−6.89	−6.89	−4.26	−2.9	−5.39	−3.15	−4.37	−8.89
			−6.63	−16.4		−9.35	−8.95	−8.95	−15.22	−5.27	−7.59	−13.33	−11.77	−10.47
	n_{Cs}		23	46		23	15	26	45	10	20	26	29	21
	C_s		−9.59	−10.4		−7.03	−8.67	−8.67	−8.76	−8.51	−8.08	−8.3	−8.01	−9.39
			−10.53	−12.94		−8.81	−9.73	−9.73	−10.32	−8.82	−9.23	−9.28	−9.07	−9.8
	f_{PE}		0.83	0.1		0.28	np	0.48	0.32	0.91	0.57	0.84	0.51	np
	$W f_{PE}$		±0.1	±0.87		±0.16		±0.3	±0.8	±0.35	±0.3	±0.16	±0.24	
WS07	C_{pe}	−10.64		−10.6		−9.39			−9.39				−9.49	−9.39
	n_{Cs}	24		49		34			9				24	20
	C_s	−8.84		−8.84		−8.84			−9.08				−8.31	−9.33
		−10.48		−10.48		−10.48			−10.13				−9.49	−9.85
	f_{PE}	np		0.1		0.61			np				np	0.29
	$W f_{PE}$			±0.87		±0.14								
WS10	C_{pe}	−10.64		−10.42	−10.7	−9.43		−9.35	−9.36	−10.24	−8.45	−8.95	−9.756	−9.73
	C_{e-TB07}	−8.32		−8.87	−7.35	−4.61		−3.43	−3.75	−2.36	−4.96	−3.75	−4.64	−5.36
		−11.63		−20.4	−8.7	−9.35		−9.05	−14.19	−5.68	−7.52	−12.67	−11.88	−10.43
	n_{Cs}	24		53	24	35		7	6	8	10	20	23	24
	C_s	−10.35		−10.42	−10.27	−7.38		−7.86	−8.95	−8.4	−8.27	−8.17	−8.65	−9.19
		−10.79		−12.42	−10.88	−9.44		−9.82	−10.03	−10.24	−8.75	−9.52	−9.76	−10.19
	f_{PE}	np		0.36	0.84	0.55		0.42	np	0.67	0.84	np	0.6	np
	$W f_{PE}$			±0.34	±0.24	±0.16		±0.35		±0.15	±0.6		±0.19	
WS11	C_{pe}			−10.52				−9.964	−9.11	−10.5		−9	−9.89	−9.7
	n_{Cs}			54				15	15	20		23	18	24
	C_s			−10.16				−8.99	−8.95	−7.92		−8.35	−8.65	−9.16
				−12.29				−9.33	−9.85	−10.5		−9.33	−9.18	−10.18
	f_{PE}			0.49				np	np	0.6		0.86	0.57	0.74
	$W f_{PE}$			±0.25						±0.1		±0.17	±0.17	±0.29
WS19	C_{pe}	−10.46	−10.19	−10.26	−11.3	−9.1	−8.9						−8.79	−8.4
	C_{e-TB10}	−8.13	−5.74	−8.88	−7.72	−5.3	−5.7						−4.75	−6.32
		−11.8	−7.87	−17.33	−9.06	−9.56	−9.66						−10.88	−12.14
	n_{Cs}	24	23	54	24	34	13						22	23
	C_s	−9.8	−8.92	−10.26	−10.35	−6.82	−8.55						−7.08	−8.71
		−11.04	−10.46	−14.32	−10.89	−8.54	−8.75						−8.8	−9.73
	f_{PE}	0.6	0.68	0.1	0.7	0.3	np						0.51	0.33
	$W f_{PE}$	±0.1	±0.13	±0.73	±0.1	±0.14							±0.4	±0.2

Table 4 | For WS04–WS19 and event 1–13 the number of stream samples n_{Cs}, δ^2H [‰] of pre-event water *Cpe,* maximum and minimum event water *Ce* and maximum and minimum streamwater, IHS based minimum fraction of pre-event water f_{PE} and its corresponding uncertainty $W f_{PE}$. The letters np indicate events where an IHS was not possible

Event		1	2	3	4	5	6	7	8	9	10	11	12	13
Year		2010				2011								
Day, month		8 Sep	17 Sep	24 Sep	4 Oct	29 Jun	8 Jul	14 Jul	15 Aug	24 Aug	27 Aug	4 Sep	18 Sep	6 Oct
WS04	C_{pe}		−66.8	−72.4		−68.7	−66.5	−62.1	−64.6	−57.1	−60.6	−59.8	−56.9	−61
	C_{e-WG01}		−26.1	−53.6		−25.4	−46.1	−21.8	−25.6	−19.7	−29.7	−17.3	−20.8	−60.3
			−45.1	−123.0		−64.1	−59.8	−52.6	−115.6	−24.9	−47.6	−96.0	−103.6	−73.2
	n_{Cs}		23	46		23	15	26	45	10	20	26	29	21
	C_s		−64.5	−71.2		−47.3	−57.6	−46.8	−59.7	−57.4	−53.8	−55.6	−52.9	−62.6
			−72.3	−92.4		−61.4	−66.5	−62.1	−73.6	−59.5	−62.4	−62.98	−61.0	−66.4
	f_{PE}		0.85	0.1		0.34	np	0.51	0.26	0.65	0.65	0.9	0.52	np
	$W f_{PE}$		±0.12	±0.88		±0.17		±0.26	±0.9	±0.35	±0.34	±0.2	±0.24	
WS07	C_{pe}	−71		−73.2		−58.7			−64.6				−60.9	−60.9
	n_{Cs}	24		49		34			9				24	20
	C_s	−69.8		−72.5		−51.4			−62.4				−54.9	−62.4
		−74.2		−90.6		−62.6			−69.6				−64.4	−67.4
	f_{PE}	np		0.1		0.72			np				np	0.29
	$W f_{PE}$			±0.8		±0.18								
WS10	C_{pe}	−73.8		−72.3	−71.3	−72.1		−68.5	−64.6	−70.9	−57.5	−63.3	−60.9	−66.7
	C_{e-TB07}	−54.1		−29	−55.1	−49.5		−29.3	−20.3	−18.3	−28.1	−23.2	−23.8	−32.8
		−77.8		−34.4	−153.7	−62.9		−60.9	−107.7	−27.9	−45.7	−89.6	−82.6	−68.8
	n_{Cs}	24		53	24	35		7	6	8	10	20	23	24
	C_s	−69.9												
		−71.3	−71.1	−47.5		−51.6	−62.4	−54.5	−55.2	−56.1	−64.2	−60.6		
		−75.1		−89.1	−74.7	−63.8		−68.5	−69.3	−70.9	−58.9	−64.2	−57.1	−63.8
	f_{PE}	np		0.32	0.9	0.55		0.39	np	0.66	0.84	np	0.59	np
	$W f_{PE}$			±0.58	±0.37	±0.16		±0.36		±0.1	±0.39		±0.19	
WS11	C_{pe}			−72.2				−62.2	−64.6	−72.1		−58.3	−57.6	−60.3
	n_{Cs}			54				15	15	20		23	18	24
	C_s			−70.8				−60.9	−65	−48.3		−55.7	−57.1	−60.8
				−88.5				−64.1	−68.7	−72.1		−63.4	−67.7	−69.8
	f_{PE}			0.36				np	np	0.55		0.8	0.57	0.74
	$W f_{PE}$			±0.53						±0.1		±0.28	±0.17	±0.29
WS19	C_{pe}	−69.8	−69.4	−70.2	−74.9	−47.2	−66.5						−46.6	−57.5
	C_{e-TB10}	−50.7	−33.6	−55.3	−50.3	−31	−15						−23.9	−39.2
		−77.1	−49.4	−127.9	−63.9	−67.6	−61.8						−70.2	−82.5
	n_{Cs}	24	23	54	24	34	13						22	23
	C_s	−67.7	−60.7	−69.9	−71.8	−42.6	−55.9						−46.7	−57.8
		−72.8	−71.7	−104.3	−75.4	−57.3	−58.7						−60.1	−65.9
	f_{PE}	0.68	0.75	0.1	0.87	0.6	np						0.47	0.33
	$W f_{PE}$	±0.1	±0.14	±0.8	±0.27	±0.35							±0.15	±0.2

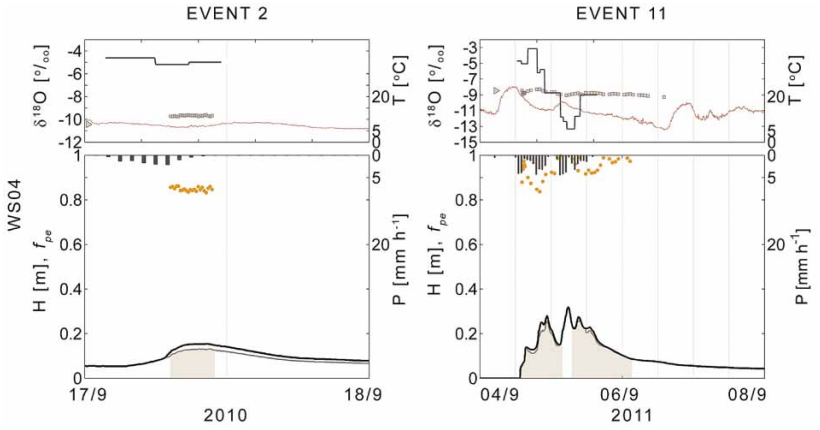

Figure 2 | For WS04, sampled events 2 and 11. The top panels show the the $\delta^{18}O$ in event water (dark line), streamwater (grey squares), pre-event water (triangle), and air temperature (dashed line). Bottom panels show precipitation (inverted, from the top), water level (solid dark line), and fraction of pre-event water *fpe* (circles and grey area below the hydrograph).

prevent fractionation. In the field, rainfall and stream samples were filled in a 20 mL glass for transport and storage (20 mL glass with cap and additional Teflon/rubber septum). Excess water from all sampler tubing, bottles, and tipping buckets was removed, i.e., dried as well as possible to prevent inter-event contamination. Due to malfunctioning of some automatic samplers (e.g., air bubbles or sediment in the water level actuators or power failures when temperatures fell below 5 °C), not all events were sampled equally for all streams. The number of water samples for stable isotope analysis per stream and event ranged from 7 samples (short events) up to 54 samples (for long events). The number of sampled events varied per stream from 6 to 11 (Table 3).

Water sample analysis

The collected water samples were analyzed for their stable isotope composition at the stable isotope laboratory of the University of Zurich, Department of Geography. All water samples were filtered (0.45 µm filter 25 mm PTFE Syringe Filter, Simplepure USA) and pipetted in a vial (1 mL into a 1.5 mL 32 × 11.6 mm screw neck vials with cap and PTFE/silicone/PTFE septa) prior to analysis. Samples were analyzed with a Cavity Ring-Down Spectroscope-Picarro L1102-i Liquid Analyser (1st generation analyser, Picarro Inc. 2008). The analysis scheme of Penna *et al.* (2010) was followed, and values were reported as δ-values in per mille (‰) relative to Vienna Standard Mean Ocean Water. Most samples could be measured with a precision for δ^2H of <0.5‰ and for $\delta^{18}O$ of <0.1‰. Due to some technical issues with the spectroscope, for some samples the accuracy for δ^2H was >1‰ while for $\delta^{18}O$ it remained <0.1‰.

IHS

For the different rainfall–runoff events a IHS was used to quantify the fraction of pre-event water in storm runoff, f_{PE} (Equations (1) and (2)) (Sklash & Farvolden 1979):

$$Q_s = Q_E + Q_{PE} \tag{1}$$

$$f_{PE} = \frac{C_S - C_E}{C_{PE} - C_E} \tag{2}$$

The symbol C describes the stable isotope composition of stormflow (streamwater), baseflow (pre-event water), and rainfall (event water) indicated with subscripts *S, PE*, and *E*, respectively. The incremental intensity mean (McDonnell *et al.* 1990) was used to account for the event water (Equation (3)). Here, I_i is the rainfall intensity and δ_i is the stable isotope composition of the accompanying precipitation. Some sequential rainfall samplers malfunctioned during some events. Therefore the nearest sequential rainfall sampler, which sampled the majority of the events, was assigned to each headwater (WG-1 for WS04 and WS07, TB-6 for WS10 and WS11, and TB-10 for WS19) to be

used in the IHS.

$$C_E = \frac{\sum_{i=1}^{n} I_i \delta_i}{\sum_{i=1}^{n} I_i} \tag{3}$$

For each of the 13 events, the uncertainty of the pre-event water contributions was quantified based on Equation (4) (Genereux 1998) with a confidence level of 0.05. The symbols $W_{f_{PE}}$, f_{PE}, and f_E represent the uncertainty in the pre-event water, and the fraction of pre-event and event water, respectively. W_{CE} is the uncertainty in event water and estimated using the standard deviation of the collected stable isotope composition of the nearest sequential rainfall sampler. A data set that had been collected during a previous baseflow snapshot campaign by Fischer *et al.* (2015) was used to quantify the uncertainty of pre-event water W_{CP}. For each headwater catchment the baseflow samples within the catchment were used to calculate the standard deviation of the stable isotope composition. Streamwater uncertainty, W_{CS}, was based on the laboratory precision of repeat measurements:

$$W_{f_{PE}} = \left\{ \left[\frac{f_E}{(C_E - C_{PE})} W_{CE} \right]^2 + \left[\frac{f_{PE}}{(C_E - C_{PE})} W_{CPE} \right]^2 + \left[\frac{-1}{(C_E - C_{PE})} W_{CS} \right]^2 \right\}^{1/2} \tag{4}$$

Data analysis

For each sampled event, three proxies were used to describe the antecedent conditions of the study area (Table 2). Based on rain gauge WG-01 (1998–2011), the antecedent precipitation index, with 7 days prior to an event (A_{PI7}), was calculated. Additionally, the antecedent discharge (A_{Q1}; WS04) and groundwater level (A_{GL1}; long-term groundwater well near WG-01) were derived, both for 1 day prior to an event. From 14 rain gauges, the mean and standard deviation of different rainfall characteristics were derived for each event. In WS04, the maximum discharge Q_{max} was derived and the runoff coefficient was additionally computed by subtracting the baseflow from the total stormflow divided by the event rainfall sum, analogous to Burch *et al.* (1996). Baseflow was defined as a straight line from the rise of the hydrograph to the inflection point where the hydrograph in the semi-logarithmic domain flattens. For every event, the exceedance probabilities of maximum event discharge (WS04, 1998–2011) and event rainfall sum (WG-1, 1998–2011) were determined (Figure 3).

In addition to standard representation of the IHS (hydrograph, precipitation, air temperature, stable isotope, and calculated pre-event water), we related the rainfall characteristics, antecedent conditions, and baseflow, 1 day before an event (WS04), to the observed minimum f_{PE} (near the maximum discharge) using a linear relation to explain differences in pre-event water. Additionally, five types of multiple linear regression were performed, where for each type, the rainfall characteristics, antecedent conditions, and baseflow 1 day before an event (WS04), were added stepwise to relate to the observed minimum f_{PE} to explain differences in pre-event water.

RESULTS

Sampled event characterization

Thirteen rainfall–runoff events were sampled during the snow-free seasons of 2010 and 2011 (see Table 2). The

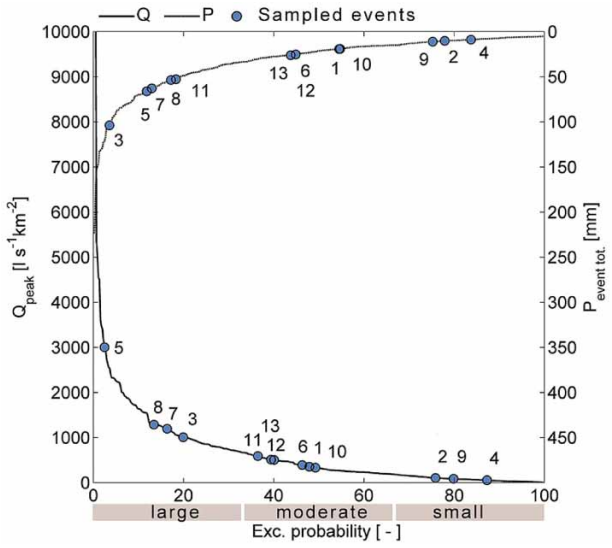

Figure 3 | Peakflow exceedance curve (WS04, Q_{peak} >33 l s^{-1} km^{-2}), event rainfall sum distribution (WG-01, P_{sum} >5 mm) for the period 1998–201,1 and where circles indicate the sampled events 1–13.

events covered a wide range of different rainfall and peak discharge magnitudes observed during the time period 1998–2011 (Figure 3). The mean hourly rainfall intensities of all rain gauges of the Zwäckentobel varied between 1 and 6 mm h^{-1} with a maximum of up to 18 mm h^{-1} and a large spatial variability (Table 2). The discharge of WS04–WS19 responded to rainfall with a delay of 10 min up to 1 hour for the different events (Table 2). Each of the events had different antecedent wetness conditions with A_{PI7} ranging from wet to dry (Figure 4). The baseflow 1 day before an event (A_{Q1}) was below 0.1 up to 16 l s^{-1} km^{-2}. The groundwater levels before an event (A_{GL1}) were between −12 and −42 cm below ground surface.

Stable isotopes and hydrograph separation of sampled storm events

The isotopic composition of all isotope water samples followed the global meteoric water line (GMWL) and no fractionation was observed (Figure 5(a)). The IHS was performed using both δ^2H and $\delta^{18}O$, which mainly resulted in 60 similar pre-event fractions with only two exceptions: WS04 event 9 and WS19 event 5 (Tables 3 and 4, and Figure 5(b)). Since both isotopes resulted in rather similar computed pre-event water contributions, only the computations based on $\delta^{18}O$ are shown in the following.

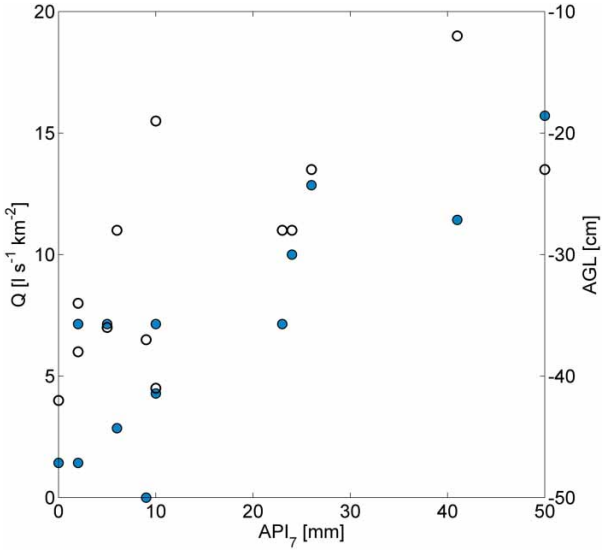

Figure 4 | Antecedent discharge (closed circles) and antecedent groundwater level (open circles) against antecedent precipitation index for the sampled events 1–13.

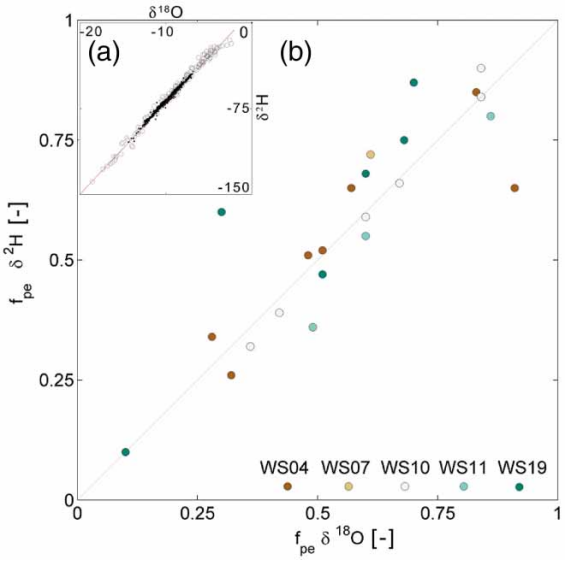

Figure 5 | (a) Inset: all collected rainfall samples (grey circles) and stream samples (black circles) of all headwaters and events follow the global meteoric water line. (b) Values of the minimum fraction of pre-event water computed based on $\delta^{18}O$ observations versus the corresponding values that were computed based on δ^2H observations for the different events and catchments (each catchment is represented by a different color). The grey line is where pre-event water computations based on $\delta^{18}O$ and δ^2H observations would be equal.

The $\delta^{18}O$ in pre-event water varied for the different streams and the different events by 0.5–1‰ (Table 3 and Figure 6). The $\delta^{18}O$ in event water varied for the different sampling locations by 0.5 and 2‰ and the temporal variability of events was 2 up to 12‰ (Table 3 and Figure 6). The $\delta^{18}O$ difference between pre-event water and streamwater samples near the peak was about 0.5–2‰ and up to 0.5–4‰ for some larger events (Table 3 and Figure 6).

The minimum fraction of pre-event water (f_{PE}) for the different streams and events varied from 0.01 up to 0.9 and occurred half an hour before or after a maximum water level (Figure 6). For some events, the rainfall, pre-event, or streamwater sample compositions were too similar to allow the fraction of pre-event water to be calculated (Table 3). In events where IHS was possible, the uncertainties in the minimum fraction of pre-event water (Wf_{PE}) were between ±0.1 up to ±0.9 (Table 3).

Comparison of three headwaters and events

The three headwater catchments with the best data coverage (WS04, WS10, and WS19) were selected for a more detailed

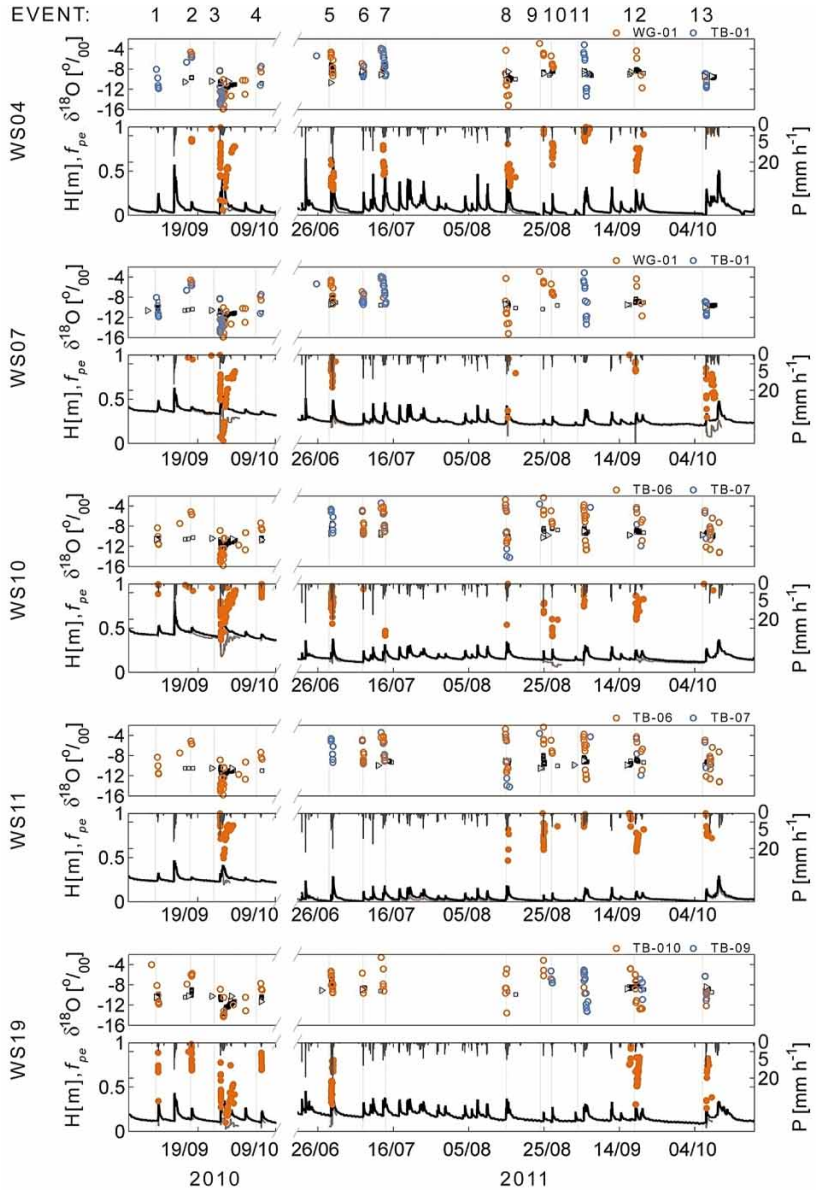

Figure 6 | Hydrometric and $\delta^{18}O$ overview of WS04–W19 and events 1–13. The top panels show $\delta^{18}O$ in event water (open circles and colors indicate different rain gauges), streamwater (grey squares) and pre-event water (triangle). Bottom panels show precipitation (inverted, from the top), water level (solid dark line), and fraction of pre-event water *fpe* (circles).

comparison. In event 3, the maximum event rainfall sum was recorded above WS10, while different rainfall gradients were observed in WS04 and WS19 (Figure 7(a) and 7(d)). The rainfall intensities were moderate and spatially equal (Table 2 and Figure 7(a)) and the hydrograph had multiple peaks (Figure 8, left column). After the maximum water level was reached, the air temperature decreased to 0 °C, and the rainfall changed to snowfall. The $\delta^{18}O$ in event water of sampler WG-1, TB-6, and TB-10 started with a similar value but decreased to different minimums (Table 3 and Figure 8, left column). During the rain-free period after the first peak, streamwater samples were missing because the automatic water samplers were full. Shortly before the maximum water level, all samplers were restarted two times. The $\delta^{18}O$ in pre-event water and streamwater were similar for WS04 and WS10 while for WS19 it was slightly more

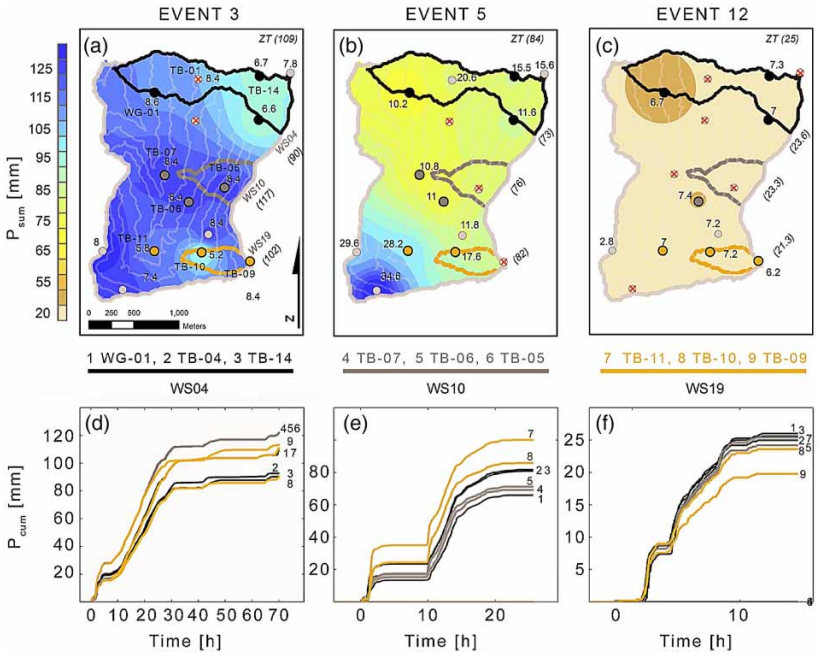

Figure 7 | Spatial distribution of event rainfall [mm] for (a) event 3, (b) event 5, and (c) event 12. Circles indicate rain gauges where text indicates the maximum event rainfall intensity [mm h^{-1}]. The headwater areal event rainfall [mm] is listed in between brackets. Crosses indicate technical failures of rain gauges or sequential samplers. (d), (e), and (f) indicate the accumulated event rainfall [mm] of the different rain gauges in WS04, WS10, and WS19.

depleted (Table 3 and Figure 8, left column). The fraction of pre-event water decreased rapidly after the start of rainfall to a minimum of 0.2, 0.36, and 0.27, respectively (Figure 8, left column). During the second peak, WS04 and WS19 had dominant event water, while WS10 had a higher fraction of pre-event water. During the recession of the hydrograph, the fraction of pre-event water rose irregularly due to short additional rainfall that instantaneously increased the fraction of event water.

In event 5, the rainfall amount and intensities increased from WS04 towards WS19 (Table 2 and Figure 7(b) and 7(e)) and the hydrograph had two peaks (Figure 8, middle column). The $\delta^{18}O$ in event water of sampler WG-1 and TB-6 had a similar range, but were temporally different, while TB-10 was more depleted (Table 3 and Figure 8, middle column). The $\delta^{18}O$ in pre-event water and streamwater samples in WS04 and WS10 were alike and became more enriched towards the first peak of the hydrograph, while WS19 was more depleted. In all streams, the fraction of pre-event water decreased rapidly towards the first peak and increased during the intra-event of 6 hours. With the onset of the rain, the streams responded fast and WS04 had the highest recorded discharge of the 13 events sampled (Figure 2). The fraction of pre-event water was 0.3 for WS04 and WS19, during the first and second peak. In WS10, the fraction of pre-event water during the first peak was 0.72 and decreased during the second peak to 0.55. After the maximum water level the different automatic water samplers were full, and were not restarted, and therefore further observations were missing.

Event 12 had an average and evenly distributed event rainfall sum and intensity (Table 2 and Figure 7(c) and 7(f)) and the hydrograph had multiple peaks (Figure 8, right column). The $\delta^{18}O$ in event water of sampler WG-1 and TB-10 were alike, while more depleted in TB-06 (Table 3 and Figure 8, right column). The $\delta^{18}O$ in pre-event water in WS04, WS10, and WS19 were alike and the streamwater increased on average 1‰ during events. The rising limb was not sampled due to technical problems and started just at the maximum water level. The three different headwaters had fractions of pre-event water ranging from 0.51 to 0.6 and increased gradually during the falling limb to 1 (Table 3 and Figure 8, right column).

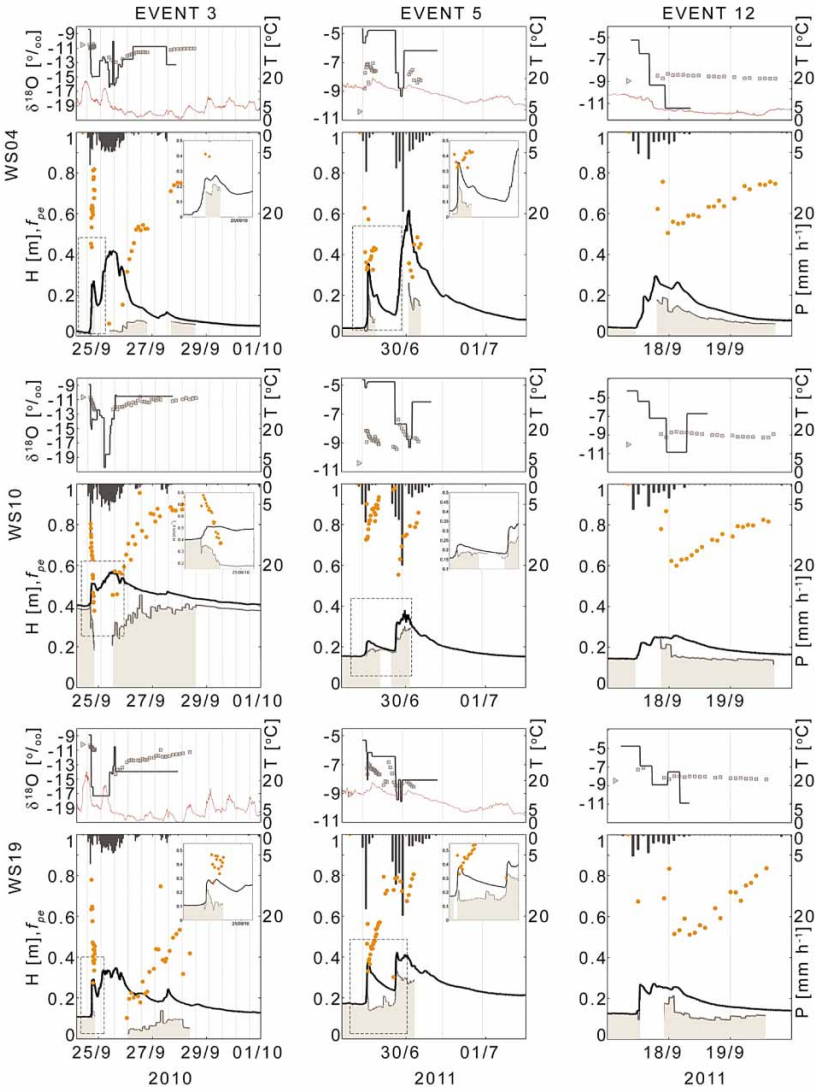

Figure 8 | Detailed hydrometric and $\delta^{18}O$ overview of headwaters WS04, WS10, and W19 and event 3, 5, and 12. The top panels show $\delta^{18}O$ in event water (line), streamwater (grey squares), pre-event water (triangle), and air temperature (dashed line). Bottom panels show precipitation (inverted, from the top), water level (solid dark line), and fraction of pre-event water *fpe* (circles and grey area below the hydrograph).

Explanatory factors of pre-event water fractions

In WS04, WS10, and WS19 the minimum fraction of pre-event water decreased with increasing event rainfall sum (Figure 9, left column). To a lesser extent, the minimum fraction of pre-event water decreased with increasing maximum hourly rainfall intensities (Figure 9, right column). For both WS04 and WS19, the fraction of pre-event water in event 3, 5 s and 12 was lower compared with WS10 (Figure 9). In addition, no relation between antecedent wetness and minimum fraction of pre-event water was observed (Figure 9). The relation between the minimum fractions of pre-event water was supported by the regression analysis. The rainfall sum correlated best with the minimum fraction of pre-event water in studied headwaters and for the individual headwaters (Table 5). Rainfall intensity correlated less with the minimum fraction of pre-event water and added little information in combination with rainfall sum to explain the pre-event water. The antecedent wetness indices A_{PI7}, A_{GL1}, and A_{Q1} correlated only weakly with the

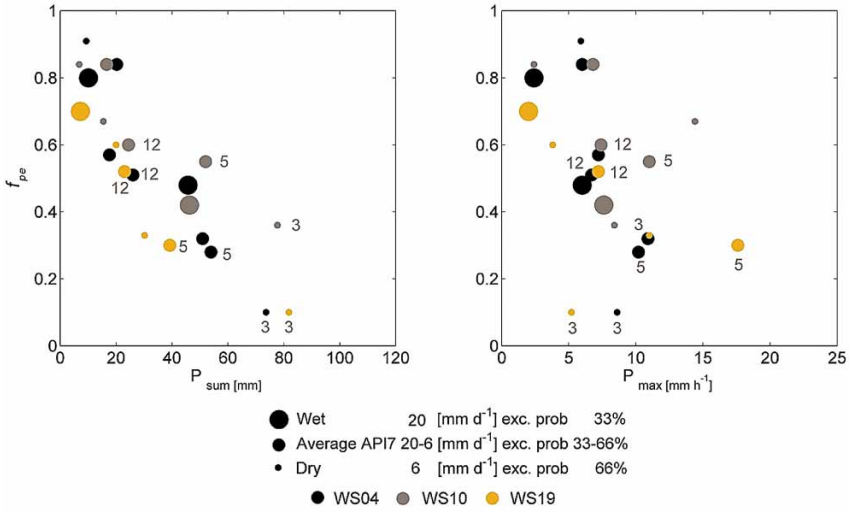

Figure 9 | The event rainfall sum related to the minimum fraction of pre-event water f_{pe} (left) and max rainfall intensity related to the minimum fraction of pre-event water *fpe* (right) for WS04, WS10, and WS19. Different sizes of circles indicate different antecedent conditions (wet, average, and dry) and numbers refer to event 3, 5, and 12.

Table 5 | Multiple linear relation of pre-event water and different predictors

	R^2	F	p
WS04, WS07, WS10, WS11, WS19			
$f_{PE\ min} = 0.80–0.01\ P_{sum}$	0.50	30	<0.001
$f_{PE\ min} = 0.71–0.02\ P_{max}$	0.13	4.25	0.04
$f_{PE\ min} = 0.43–0.06\ A_{PI7}$	0.03	1.1	0.3
$f_{PE\ min} = 0.42–0.004\ A_{GL1}$	0.02	0.7	0.4
$f_{PE\ min} = 0.52–0.003\ A_{Q1}$	0.002	6.2	0.02
$f_{PE\ min} = 0.91–0.01\ P_{sum}–0.02\ P_{max}$	0.53	16.2	<0.001
$f_{PE\ min} = 0.91–0.01\ P_{sum}–0.02\ P_{max}–0.004\ A_{PI7}$	0.53	10.4	<0.001
$f_{PE\ min} = 0.91–0.01\ P_{sum}–0.02\ P_{max}–0.004\ A_{PI7} + 0.001A_{GL1}$	0.58	9.3	<0.001
$f_{PE\ min} = 0.87–0.01\ P_{sum}–0.02\ P_{max}–0.001\ A_{PI7} + 0.004A_{GL1}–0.002A_{Q1}$	0.64	8.9	<0.001
WS04 $f_{PE\ min} = 0.92–0.01\ P_{sum}$	0.87	49.9	<0.001
$f_{PE\ min} = 0.99–0.01\ P_{sum}–0.01\ P_{max}$	0.88	24.7	<0.001
WS07 $f_{PE\ min} = 1.1–0.01\ P_{sum}$	np		
$f_{PE\ min} = 1.1–0.01\ P_{sum}\ {}_{+}0.01\ P_{max}$	np		
WS10 $f_{PE\ min} = 0.83–0.01\ P_{sum}$	0.80	20.2	<0.001
$f_{PE\ min} = 0.88–0.001\ P_{sum}–0.01\ P_{max}$	0.82	9.07	<0.1
WS11 $f_{PE\ min} = 0.8–0.003\ P_{sum}$	0.02	0.04	0.85
$f_{PE\ min} = 0.85–0.003\ P_{sum}–0.001\ P_{max}$	0.02	0.01	0.98
WS19 $f_{PE\ min} = 0.73–0.01\ P_{sum}$	0.94	65	<0.001
$f_{PE\ min} = 0.78–0.001\ P_{sum}–0.02\ P_{max}$	0.99	>100	<0.001

Minimum fraction of pre-event water ($f_{PE\ min}$), event rainfall sum (P_{sum}), maximum hourly rainfall intensity (P_{max}), antecedent precipitation index with 7 days prior to an event (A_{PI7}), antecedent groundwater level (A_{GL1}), antecedent discharge (A_{Q1}) of WS04.

minimum pre-event fraction. No significant relation between pre-event water and different catchment characteristics was found (analysis not shown).

The runoff coefficient was only available in WS04 and examined for temporal changes in relation to event rainfall sums (Figure 10). For events with rainfall sums less than 50 mm, the runoff coefficient was below 0.5 (Figure 10). With increasing event rainfall sum, the runoff coefficient increased to 0.7 (P = 110 mm), while the fraction of pre-event water decreased to 0.1. The overall pattern of the runoff coefficient in relation to event rainfall sums resembled the power law relation defined by Burch *et al.* (1996) (Figure 10).

DISCUSSION

Assessment of pre-event water contribution

In our studied headwaters, we observed large spatial variability in rainfall sum, intensity, and stable isotope composition for the large events, over relatively short distances (100 m). The spatiotemporal variability of $\delta^{18}O$ in event water was larger compared to the spatial variability

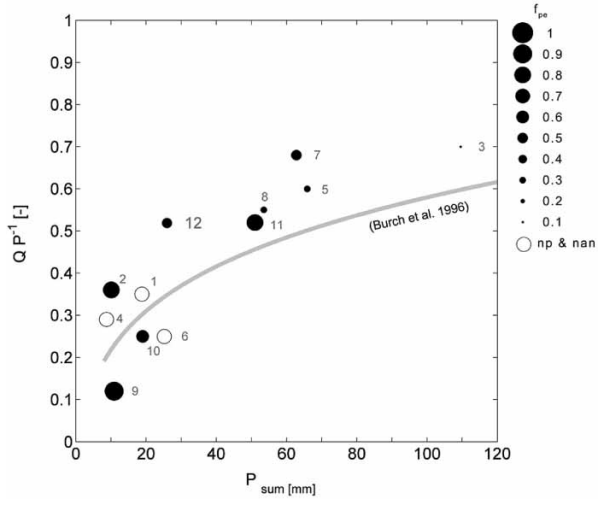

Figure 10 | The runoff coefficient for catchment WS04 as a function of the event rainfall sum (WG-01). The grey line illustrates the Burch *et al.* (1996) derived relation between runoff coefficient and event rainfall sum. Each circle indicates one of the 12 events of this study. The circle size of closed circles indicates the minimum fraction of pre-event water of WS04. Open circles refer to events where IHS was not possible or isotope data were not sampled.

of $\delta^{18}O$ in pre-event water and streamwater samples. These observations support the idea that small forested headwaters are often erroneously assumed to have homogeneous rainfall patterns (Goodrich *et al.* 1995) and isotopic compositions of precipitation (Lyon *et al.* 2008; Holko *et al.* 2012). Lyon *et al.* (2009) found that the spatial and temporal variability of the isotope composition may result in different fractions of pre-event water, depending on the use of $\delta^{18}O$ or $\delta^{2}H$ in the IHS. In this study, however, the differences between fractions of pre-event water computed based on $\delta^{18}O$ and $\delta^{2}H$ were smaller (±10%) compared to the large difference reported by Lyon *et al.* (2009). Furthermore, the differences in fraction of pre-event water using $\delta^{18}O$ or $\delta^{2}H$ were generally smaller than the IHS error propagation estimates. The large uncertainties were the result of, as Genereux (1998) suggested, small differences in $\delta^{18}O$ between event water and pre-event water. Large differences in $\delta^{18}O$ between event and pre-event isotopic composition are generally expected in summer months and therefore summer is considered as the favorable season to perform an IHS (Vitvar & Balderer 1997). This benefit however, was not always so strong for the 13 studied events and an IHS was not always possible. This could have been caused by the altitude of the studied headwaters above 1,100 m. This altitude resulted in a temperature decrease towards 0 °C with snowfall, even during summer, for certain events. The lower temperatures resulted in a more depleted isotopic composition compared to the average seasonal isotopic compositions. With high soil surface temperatures, the snow melted immediately and contributed to runoff generation. Late summer events, such as event 3 or 13, had lower air temperatures and the snow cover persisted, acting as an extra storage of precipitation. As a consequence, the stormflow magnitude in relation to its rainfall sum decreased. During snowmelt no fractionation was observed in stream samples. However, we cannot exclude that fractionated melt water was diluted by pre-event water, or that snow melt contributed to delayed stream flow.

The isotope composition of rainfall was sampled with a higher resolution compared to many other studies (e.g., sampling locations, temporal resolution, and events). Nonetheless, due to the observed spatial variability of stable isotopes in precipitation and stream samples, using the nearest rain gauge for each headwater in the IHS might have

introduced an incomplete accounting of event water in space and time, as described by Buttle (1994). This might have been the case for large events with large spatial gradients of rainfall amounts, intensities, and stable isotopes. Furthermore, forest interception and throughfall can result in changed isotopic signatures (Saxena 1987; Allen *et al.* 2015). Since the rainfall was sampled only in the open field this might have influenced the IHS results. Despite the incomplete sampling of rainfall and uncertainties in the fraction of pre-event water, the general pattern of fast response and recession of the hydrograph, and fraction of pre-event water, were analogous with plot scale tracer experiments by Feyen *et al.* (1999) and Weiler *et al.* (1998, 1999) and two events described by Weiler *et al.* (1999). Our study observed a high variability in fraction of pre-event water between the different events, which is opposite to the perception that humid-forested headwaters have dominant pre-event water during the peak discharge (Buttle 1994). This underlines the idea that when neglecting the spatial and temporal variability of rainfall characteristics and isotopic composition, one might get an incomplete picture of runoff processes.

Rainfall as a dominant factor in runoff processes

The frequent rainfall marked the headwater's wet character and its spatiotemporal dynamic. The fast hydraulic response of the streams and decrease of the fraction of pre-event water indicated the strong connection between rainfall and runoff. A statistical evaluation of controlling mechanisms was not possible because of the irregularly sampled data set (due to technical and logistic constraints). Instead, the minimum fraction of pre-event water was available for most sampled events. Buttle (1994) used the minimum fraction of pre-event water to compare different studies around the world and concluded that pre-event water dominated the peak discharges. Similarly, the minimum fraction of pre-event water was used in our study watersheds to compare processes that occur during the peak discharge. Despite the uncertainty, the minimum fraction of pre-event water, used as a qualitative proxy, indicated the overall pre-event or event water contribution during stormflow and could be related to explanatory variables. Rodhe (1987) found a decreasing relation of fraction of pre-event water with increasing snowmelt (for six headwaters distributed throughout Sweden with 2–6 snowmelt events per headwater). A similar decreasing relation of the fraction of pre-event water with increasing rainfall sums was observed for plot scale experiments (Weiler *et al.* 1999; Kienzler & Naef 2008), in a single urban catchment (Pellerin *et al.* 2008), and in a single pre-alpine headwater (Penna *et al.* 2014). Our study confirmed this relation and proved the validity in neighboring headwaters with different catchment characteristics (WS04–WS19). Renshaw *et al.* (2003) instead described a positive relation of the fraction of pre-event water with increasing precipitation, which might be caused by the smaller event rainfall sums and resulted in dominant pre-event water contribution. Considering all sampled events of WS04–WS19, the minimum fraction of pre-event water largely depended on the rainfall sum and, to a smaller degree, on the rainfall intensity. For individual streams the relation of minimum fraction of pre-event water and rainfall sum was even stronger. In WS07 and WS11, the fewer possible IHS did not allow for a statistical analysis. However, it is likely that in these headwaters the rainfall sum would also be a strongest predictor. The strong relation of rainfall sum and the fraction of pre-event water together with the spatial distribution of rainfall explained to a large degree the differences in pre-event water of WS04-WS19.

Compared to Blume *et al.* (2007), the error made by separating the hydrograph of WS04 into fast flow and baseflow was small due to the clear difference in antecedent baseflow and higher (by orders of magnitudes) stormflow. The runoff coefficient of the different sampled events in WS04 was also similar to the power law defined by Burch *et al.* (1996). Separating the runoff into fast flow and baseflow is extensively criticized (Klaus & McDonnell 2013), since it does not represent the observed dominant pre-event water contribution in forest headwaters (Buttle 1994; McGlynn *et al.* 2002). However, the combination of the runoff coefficient with the minimum pre-event water contribution, provides additional useful information. Instead of separating the hydrograph into fast and slow runoff processes, the runoff coefficient described the volume of discharge produced due to a certain amount of precipitation. In combination with the IHS, it became visible that the volume of discharge contained a certain fraction of event water and both similarly increased with increasing precipitation.

Catchment characteristics as secondary factors in runoff processes

The observed variable fraction of pre-event water in WS04-WS19 was different compared to the more stable observations made in catchments with a similarly high annual precipitation amount (>2,000 mm y^{-1}) such as the Maimai (McGlynn *et al.* 2002) or H. J. Andrews catchment (McGuire & McDonnell 2010). The differences in fraction of pre-event water might be due to the differences in land cover. The Maimai and H. J. Andrews catchment are predominantly forested compared to the mixed land cover (meadows, forests, and large percentage of wetlands 20–50%) of the Zwäckentobel. A higher pre-event water contribution was observed in stormflow of forested catchments compared to wetlands (McCartney *et al.* 1998; Laudon *et al.* 2007) or grasslands (Bonell *et al.* 1990). Plot scale experiments found differences in runoff processes for different soils (Feyen *et al.* 1999) and land covers (Weiler *et al.* 1998). However, no strong relation between the fraction of pre-event water and land cover could be noticed when comparing WS04–WS19 with each other. A small influence of land cover on runoff processes was noticeable for only some events. In WS10 and WS11 (steeper slopes, shallow soils, smaller amount of wetland, and large forested areas), for the larger events, a slightly higher pre-event water contribution and additional weaker relation of pre-event water with rainfall was observed compared with WS04, WS07, and WS19. Instead, a faster response with higher event water contribution was noted in WS19 (constantly grazed short grass, compacted topsoil layer with low infiltration, storage and interception compared with natural grass).

Another factor that might explain the differences in pre-event water between the Maimai and H. J. Andrews catchment and the Zwäckentobel, are the different subsurface characteristics. The vertical cracks of the Maimai and more permeable soil types of the H. J. Andrews facilitate rain water infiltration and fill up the subsurface topography resulting in a subsurface threshold with dominant pre-event water. The Zwäckentobel instead has shallow gleysols with a low matrix permeability, small active storage, and dominant stormflow in the organic soil horizon (20–50 cm), similar to the soils of a nearby hillslope described by Schneider *et al.* (2014). In the Zwäckentobel, a typical riparian zone was lacking but the large areas of wetlands were prominent elements of passive storage (Fischer *et al.* 2015). These elements are activated during the rainfall events and release the stored pre-event water. With increasing rainfall sum, at approximately 50 mm, a change from pre-event dominated to event dominated runoff was found (Figure 10). Hydrometric and isotopic observations of the soil profile were missing. However, we hypothesize that with increasing rainfall the shallow soils saturate and reach, at approximately 50 mm, the maximum storage capacity of the soil (in agreement with soil water retention and moisture information before and during plot scale sprinkling experiments by Feyen *et al.* 1996, 1999). As a result, the distributed wetlands fully connect through preferential flowpaths (creeping soils, animal burrows, or old roots and ephemeral streams), any additional rainfall by-passes the shallow soils and participate in streamflow. This would explain that with increasing precipitation, the amount of runoff produced by the precipitation increases and the fraction of pre-event water decreased. The variable rainfall with additional small storage (organic soil horizon, 20–50 cm) results in a near surface-dependent threshold with subsequently more variable pre-event water contribution, showing similarities to the Babinda model described by Bonell *et al.* (1998). The connectivity of distributed wetlands is better described by the hydrogeomorphic model of Sidle *et al.* (2000), where spatially distributed passive sources progressively become active and connected with the flow network.

Beside the previously described implicit role of catchment characteristics in runoff processes, no relationship between the fraction of pre-event water and catchment characteristics was found in WS04–WS19 or the study of Burch *et al.* (1996) or Taylor & Pearce (1982). A reason could be that in events where observations (stream response and runoff processes) and explanatory variables (precipitation and catchment characteristics) are both spatially variable, it is difficult to determine the dominant influencing factor on runoff processes. Furthermore, it was likely that the frequent precipitation together with the catchment characteristics meant that the headwater was in a continuous wet state; therefore, any potential influence of catchment characteristics on runoff processes was not visible in the data. A similar reduced effect of wet antecedent conditions and flow through the upper soil horizon was

observed by Shanley *et al.* (2002). This may also explain why, despite each event having different antecedent wetness conditions, no clear relation of pre-event water contribution and antecedent proxies was observed. This is opposite to the findings of Shanley *et al.* (2002), Casper *et al.* (2003), Pellerin *et al.* (2007) and James & Roulet (2009). Furthermore, we also did not observe a seasonal change in fraction of pre-event water as had been observed in different pre-alpine headwaters (McGuire & McDonnell 2010; Penna *et al.* 2014).

The IHS gave good qualitative information on the contribution of rainfall and the fraction of pre-event water, nevertheless many questions on the flowpath, the runoff (Lyon *et al.* 2008), and thresholds (Graham *et al.* 2010) are unresolved. Future studies should validate the connectivity, interaction, and different runoff processes of the headwater internal catchment elements (such as wetlands or forest). A multiple tracer approach (using similar tracers used by Fischer *et al.* (2015), $\delta^{18}O$, Ca and DOC) would allow better understanding of the flowpaths and contributing sources during stormflow of headwaters, while a finer temporal sampling resolution would help investigate subtle changes in pre-event water in relation to differences in catchment characteristics.

CONCLUSION

In this study, 13 rainfall–runoff events of different magnitude and intensity were analyzed in five neighboring steep and rainfall dominated headwaters, to assess the pre-event water contribution. The combination of long-term and spatially short-term hydrometeorological measurements, together with event water sampling in different neighboring streams and multiple events, complemented each other and helped to overcome individual limitations.

The pre-event water contribution was found to be temporally variable and depended on rainfall amount and intensity. Small events had high pre-event water contribution. With increasing precipitation, the volume of runoff produced by precipitation increased and a change from pre-event to event water dominated runoff processes occurred. The variable rainfall amount and small active storage (organic soil horizon, 20–50 cm) resulted in a threshold in the upper soil horizon with subsequently more variable pre-event water contribution.

Despite the differences in catchment characteristics between the neighboring streams at headwater scale, no significant difference in minimum fraction of pre-event water contribution was observed. Furthermore, none of the antecedent wetness proxies had any explanatory value on the minimum fraction of pre-event water. This can be explained by the frequent precipitation and by the catchment characteristics keeping the soil in a wet state.

In contrast to the conventional approach (i.e., studying one headwater with few events), our results highlight the necessity to study different neighboring headwaters and a wide range of event magnitudes (many events and many samples), to better understand the dynamic character and controlling factors in runoff processes.

ACKNOWLEDGEMENTS

We thank all the people who helped in the field and the laboratory. Especially we thank Ilaria Clemenzi, Michael Rinderer, Martin Šanda, Russel Smith, Stefan Plötner, Stephan Müller, Karl Steiner, Andrea Kolleger, Ellen Cerwinka, Sandra Pool, Sandra Schärer, Nadja Lavanga, Seraina Kauer, Jana Dusik, Paribesh Pradhan, Andrea Ruecker, Yves Götz, Annagreth Schuler and Werni Ruhstaller, Bruno Kägi, Claudia Schreiner, Michael Hilf, Sandra Röthlisberger, and Ivan Woodhatch. The editor and two anonymous reviewers provided helpful comments, which helped to clarify the text. We also thank the Oberallmeindkorporation Schwyz (OAK), the Department of Environment of the Canton of Schwyz and the municipality Alpthal for the good cooperation.

REFERENCES

Allen, S. T., Keim, R. F. & McDonnell, J. J. 2015 Spatial patterns of throughfall isotopic composition at the event and seasonal timescales. *J. Hydrol.* **522**, 58–66. Doi:10.1016/j.jhydrol.2014.12.029.

Blume, T., Zehe, E. & Bronstert, A. 2007 Rainfall–runoff response, event-based runoff coefficients and hydrograph separation. *Hydrol. Sci. J.* **52**, 843–862. Doi:10.1623/hysj.52.5.843.

Bonell, M., Pearce, A. J. & Stewart, M. K. 1990 The identification of runoff-production mechanisms using environmental isotopes in a tussock grassland catchment, eastern Otago, New Zealand. *Hydrol. Processes* **4**, 15–34. Doi:10.1002/hyp.3360040103.

Bonell, M., Barnes, C. J., Grant, C. R., Howard, A. & Burns, J. 1998 High rainfall, response-dominated catchments: A comparative study of experiments in tropical northeast Queensland with temperate New Zealand. In: *Isotope Tracers in Catchment Hydrology* (C. Kendall & J. J. McDonnell, eds) Elsevier, Amsterdam, The Netherlands, pp. 347–390.

Brown, V. A., McDonnell, J. J., Burns, D. A. & Kendall, C. 1999 The role of event water, a rapid shallow flow component, and catchment size in summer stormflow. *J. Hydrol.* **217** (3–4), 171–190. Doi:10.1016/S0022-1694(98)00247-9.

Burch, H., Forster, F. & Schleppi, P. 1996 Zum Einfluss des Waldes auf die Hydrolgie der Flysch-Einzugsgebiete des Alptals. [The influence of the forest on the hydrology of flysch basins of the Alptals]. *Swiss J. For.* **12**, 925–938.

Burns, D. A. 2002 Stormflow-hydrograph separation based on isotopes: the thrill is gone–what's next? *Hydrol. Processes* **16**, 1515–1517. Doi:10.1002/hyp.5008.

Buttle, J. M. 1994 Isotope hydrograph separations and rapid delivery of pre-event water from drainage basins. *Prog. Phys. Geogr.* **18**, 16–41.

Casper, M. C., Volkmann, H. N., Waldenmeyer, G. & Plate, E. J. 2003 The separation of flow pathways in a sandstone catchment of the northern Black Forest using DOC and a nested approach. *Phys. Chem. Earth Parts A/B/C* **28**, 269–275. Doi:10.1016/S1474-7065(03)00037-8.

Feyen, H., Leuenberger, J., Papritz, A., Gysi, M., Flühler, H. & Schleppi, P. 1996 Runoff processes in catchments with a small scale topography. *Phys. Chem. Earth* **21**, 177–181. Doi:10.1016/S0079-1946(97)85581-4.

Feyen, H., Wunderli, H., Wydler, H. & Papritz, A. 1999 A tracer experiment to study flow paths of water in a forest soil. *J. Hydrol.* **225**, 155–167. Doi:dx.doi.org/10.1016/S0022-1694(99)00159-6.

Fischer, B. M. C., Rinderer, M., Schneider, P., Ewen, T. & Seibert, J. 2015 Contributing sources to baseflow in pre-alpine headwaters using spatial snapshot sampling. *Hydrol. Processes* **29**, 5321–5336. Doi:10.1002/hyp.10529.

Genereux, D. 1998 Quantifying uncertainty in tracer-based hydrograph separations. *Water Resour. Res.* **34**, 915–919. Doi:10.1029/98WR00010.

Geris, J., Tetzlaff, D., McDonnell, J. & Soulsby, C. 2015 The relative role of soil type and tree cover on water storage and transmission in northern headwater catchments. *Hydrol. Processes* **29** (7), 1844–1860. Doi:10.1002/hyp.10289.

Gerrits, A. M. J., Pfister, L. & Savenije, H. H. G. 2010 Spatial and temporal variability of canopy and forest floor interception in a beech forest. *Hydrol. Processes* **24** (21), 3011–3025. Doi:10.1002/hyp.7712.

Goodrich, D. C., Faurès, J.-M., Woolhiser, D. A., Lane, L. J. & Sorooshian, S. 1995 Measurement and analysis of small-scale convective storm rainfall variability. *J. Hydrol.* **173**, 283–308. Doi:10.1016/0022-1694(95)02703-R.

Graham, C. B., Woods, R. A. & McDonnell, J. J. 2010 Hillslope threshold response to rainfall: (1) a field based forensic approach. *J. Hydrol.* **393**, 65–76. Doi:10.1016/j.jhydrol.2009.12.015.

Gurtz, J., Baltensweiler, A. & Lang, H. 1999 Spatially distributed hydrotope-based modelling of evapotranspiration and runoff in mountainous basins. *Hydrol. Processes* **13**, 2751–2768. Doi:10.1002/(SICI)1099-1085(19991215)13:17<2751::AID-HYP897>3.0.CO;2-O.

Hagedorn, F., Bucher, J. B. & Schleppi, P. 2001 Contrasting dynamics of dissolved inorganic and organic nitrogen in soil and surface waters of forested catchments with Gleysols. *Geoderma* **100**, 173–192. Doi:10.1016/S0016-7061(00)00085-9.

Hantke, R. 1967 Geological map of the Canton of Zurich and its neighboring areas. *Q. J. Nat. Hist. Soc. Zurich* **112**.

Hegg, C., McArdell, B. W. & Badoux, A. 2006 One hundred years of mountain hydrology in Switzerland by the WSL. *Hydrol. Processes* **20**, 371–376. Doi:10.1002/hyp.6055.

Holko, L., Dóša, M., Michalko, J. & Kostka, Z. 2012 Isotopes of oxygen-18 and deuterium in precipitation in Slovakia. *J. Hydrol. Hydromech.* **60**, 265–276. Doi:10.2478/v10098-012-0023-2.

Hrachowitz, M., Bohte, R., Mul, M. L., Bogaard, T. A., Savenije, H. H. G. & Uhlenbrook, S. 2011 On the value of combined event runoff and tracer analysis to improve understanding of catchment functioning in a data-scarce semi-arid area. *Hydrol. Earth Syst. Sci.* **15**, 2007–2024. Doi:10.5194/hess-15-2007-2011.

Hsü, K. J. & Briegel, U. 1991 The flysch. In: *Geology of Switzerland*. Birkhäuser, Basel, Switzerland, pp. 65–82. Doi:10.1007/978-3-0348-8663-5_6.

James, A. L. & Roulet, N. T. 2009 Antecedent moisture conditions and catchment morphology as controls on spatial patterns of runoff generation in small forest catchments. *J. Hydrol.* **377**, 351–366. Doi:10.1916/j.jhydrol.2009.08.039.

Jordan, J. P. 1994 Spatial and temporal variability of stormflow generation processes on a Swiss catchment. *J. Hydrol.* **153**, 357–382. Doi:10.1016/0022-1694(94)90199-6.

Keller, H. M. 1970 Factors affecting water quality of small mountain catchments. *J. Hydrol.* **9**, 133–141.

Kennedy, V. C., Zellweger, G. W. & Avanzino, R. J. 1979 Variation of rain chemistry during storms at two sites in northern California. *Water Resour. Res.* **15**, 687–702. Doi:10.1029/WR015i003p00687.

Kienzler, P. M. & Naef, F. 2008 Subsurface storm flow formation at different hillslopes and implications for the 'old water paradox'. *Hydrol. Processes* **116**, 104–116. Doi:10.1002/hyp.6687.

Klaus, J. & McDonnell, J. J. 2013 Hydrograph separation using stable isotopes: review and evaluation. *J. Hydrol.* **505**, 47–64. Doi:10.1016/j.jhydrol.2013.09.006.

Laudon, H., Sjöblom, V., Buffam, I., Seibert, J. & Mörth, M. 2007 The role of catchment scale and landscape characteristics for

runoff generation of boreal streams. *J. Hydrol.* **344**, 198–209. Doi:10.1016/j.jhydrol.2007.07.010.

Lis, G., Wassenaar, L. I. & Hendry, M. J. 2008 High-precision laser spectroscopy D/H and 18O/16O measurements of microliter natural water samples. *Anal. Chem.* **80** (1), 287–293. Doi:10.1021/ac701716q.

Lyon, S. W., Desilets, S. L. E. & Troch, P. A. 2008 Characterizing the response of a catchment to an extreme rainfall event using hydrometric and isotopic data. *Water Resour. Res.* **44**. Doi:10.1029/2007WR006259.

Lyon, S. W., Desilets, S. L. E. & Troch, P. A. 2009 A tale of two isotopes: differences in hydrograph separation for a runoff event when using δD versus δ18O. *Hydrol. Processes* **23** (14), 2095–2101. Doi:10.1002/hyp.7326.

McCartney, M. P., Neal, C. & Neal, M. 1998 Use of deuterium to understand runoff generation in a headwater catchment containing a dambo. *Hydrol. Earth Syst. Sci.* **2**, 65–76. Doi:10.5194/hess-2-65.

McDonnell, J. J., Bonell, M., Stewart, M. K. & Pearce, A. J. 1990 Deuterium variations in storm rainfall: Implications for stream hydrograph separation. *Water Resour. Res.* **26**, 455–458. Doi:10.1029/WR026i003p00455.

McGlynn, B. L., McDonnel, J. J. & Brammer, D. D. 2002 A review of the evolving perceptual model of hillslope flowpaths at the Maimai catchments, New Zealand. *J. Hydrol.* **257**, 1–26. Doi:10.1016/S0022-1694(01)00559-5.

McGlynn, B. L., McDonnell, J. J., Seibert, J. & Kendall, C. 2004 Scale effects on headwater catchment runoff timing, flow sources, and groundwater-streamflow relations. *Water Resour. Res.* **40**, W07504. Doi:10.1029/2003WR002494.

McGuire, K. J. & McDonnell, J. J. 2010 Hydrological connectivity of hillslopes and streams: characteristic time scales and nonlinearities. *Water Resour. Res.* **46** (10), W10543, Doi:10.1029/2010WR009341.

Menzel, L., Lang, H. & Martin, R. 2007 Mean annual actual evaporation 1973–1992. In: *Hydrological Atlas of Switzerland*. Federal Office for the Environment (FOEN), Berne, Switzerland, Table 4.1.

Molnar, P., Densmore, A. L., McArdell, B. W., Turowski, J. M. & Burlando, P. 2010 Analysis of changes in the step-pool morphology and channel profile of a steep mountain stream following a large flood. *Geomorphology* **124**, 85–94. Doi:10.1016/j.geomorph.2010.08.014.

Onda, Y., Tsujimura, M., Fujihara, J. & Ito, J. 2006 Runoff generation mechanisms in high-relief mountainous watersheds with different underlying geology. *J. Hydrol.* **331**, 659–673. Doi:10.1016/j.jhydrol.2006.06.009.

Pearce, A. J. 1990 Streamflow generation processes: an Austral view. *Water Resour. Res.* **26**, 3037–3047. Doi:10.1029/WR026i012p03037.

Pellerin, B. A., Wollheim, W. M., Feng, X. & Vörösmarty, C. J. 2008 The application of electrical conductivity as a tracer for hydrograph separation in urban catchments. *Hydrol. Processes* **22**, 1810–1818. Doi:10.1002/hyp.

Penna, D., Stenni, B., Šanda, M., Wrede, S., Bogaard, T. A., Gobbi, A., Borga, M., Fischer, B. M. C., Bonazza, M. & Chárová, Z. 2010 On the reproducibility and repeatability of laser absorption spectroscopy measurements for δ2H and δ18O isotopic analysis. *Hydrol. Earth Syst. Sci.* **14**, 1551–1566. Doi:10.5194/hess-14-1551-2010.

Penna, D., van Meerveld, H. J., Oliviero, O., Zuecco, G., Assendelft, R. S., Dalla Fontana, G. & Borga, M. 2014 Seasonal changes in runoff generation in a small forested mountain catchment. *Hydrol. Processes* **29**, 2027–2042. Doi:10.1002/hyp.10347.

Renshaw, C. E., Feng, X., Sinclair, K. J. & Dums, R. H. 2003 The use of stream flow routing for direct channel precipitation with isotopically-based hydrograph separations: the role of new water in stormflow generation. *J. Hydrol.* **273**, 205–216. Doi:10.1016/S0022-1694(02)00392-X.

Rinderer, M., Kollegger, A., Fischer, B. M. C., Stähli, M. & Seibert, J. 2012 Sensing with boots and trousers – qualitative field observations of shallow soil moisture patterns. *Hydrol. Processes* **26**, 4112–4120. Doi:10.1002/hyp.9531.

Roa-García, M. C. & Weiler, M. 2010 Integrated response and transit time distributions of watersheds by combining hydrograph separation and long-term transit time modeling. *Hydrol. Earth Syst. Sci.* **14**, 1537–1549. Doi:10.5194/hess-14-1537-2010.

Rodhe, A. 1987 *The Origin of Streamwater Traced by Oxygen-18*. University of Uppsala, Sweden.

Saxena, R. 1987 Oxygen-18 fractionation in nature and estimation of groundwater recharge. University of Uppsala.

Segura, C., James, A. L., Lazzati, D. & Roulet, N. T. 2012 Scaling relationships for event water contributions and transit times in small-forested catchments in Eastern Quebec. *Water Resour. Res.* **48** (7), W07502. Doi:10.1029/2012WR011890,2012.

Shanley, J. B., Kendall, C., Smith, T. E., Wolock, D. M. & McDonnell, J. J. 2002 Controls on old and new water contributions to stream flow at some nested catchments in Vermont, USA. *Hydrol. Processes* **16** (3), 589–609. Doi:10.1002/hyp.312,2002.

Sidle, R. C., Tsuboyama, Y., Noguchi, S., Hosoda, I., Fujieda, M. & Shimizu, T. 2000 Stormflow generation in steep forested headwaters: a linked hydrogeomorphic paradigm. *Hydrol. Processes* **14** (3), 369–385. Doi:10.1002/(SICI)1099-1085(20000228)14:3<369::AID-HYP943>3.0.CO;2-P.

Sklash, M. G. & Farvolden, R. N. 1979 The role of groundwater in storm runoff. *J. Hydrol.* **43**, 45–65. Doi:10.1016/0022-1694(79)90164-1.

Sklash, M. G., Farvolden, R. N. & Fritz, P. 1976 A conceptual model of watershed response to rainfall, developed through the use of oxygen-18 as a natural tracer. *Can. J. Earth Sci.* **13**, 271–283. Doi:10.1139/e76-029.

Stähli, M. & Gustafsson, D. 2006 Long-term investigations of the snow cover in a subalpine semi-forested catchment. *Hydrol. Processes* **20**, 411–428. Doi:10.1002/hyp.6058.

Suecker, J. K., Ryan, J. N., Kendall, C. & Jarrett, R. D. 2000 Determination of hydrologic pathways during snowmelt for alpine/subalpine basins, Rocky Mountain National Park,

Colorado. *Water Resour. Res.* **36** (1), 63–75. Doi:10.1029/1999WR900296.

Taylor, C. H. & Pearce, A. J. 1982 Storm runoff processes and subcatchment characteristics in a New Zealand hill country catchment. *Earth Surf. Processes Landforms* **7**, 439–447. Doi:10.1002/esp.3290070505.

Turowski, J. M., Yager, E. M., Badoux, A., Rickenmann, D. & Molnar, P. 2009 The impact of exceptional events on erosion, bedload transport and channel stability in a step-pool channel. *Earth Surf. Processes Landforms* **34**, 1661–1673. Doi:10.1002/esp.1855.

Vitvar, T. & Balderer, W. 1997 Estimation of mean water residence times and runoff generation by180 measurements in a Pre-Alpine catchment (Rietholzbach, Eastern Switzerland). *Appl. Geochem.* **12**, 787–796. Doi:10.1016/S0883-2927(97)00045-0.

Wassenaar, L. I., Coplen, T. B. & Aggarwal, P. K. 2014 Approaches for achieving long-term accuracy and precision of δ18O and δ2H for waters analyzed using laser absorption spectrometers. *Environ. Sci. Technol.* **48** (2), 1123–1131. Doi:10.1021/es403354n.

Weiler, M., Naef, F. & Leibundgut, C. 1998 Study of runoff generation on hillslopes using tracer experiments and a physically based numerical hillslope model. *IAHS* **248**, 353–362.

Weiler, M., Scherrer, S., Naef, F. & Burlando, P. 1999 Hydrograph separation of runoff components based on measuring hydraulic state variables, tracer experiments, and weighting methods. *IAHS* **258**, 249–255.

First received 8 September 2015; accepted in revised form 22 December 2015. Available online 12 February 2016

8.3 Paper III - Spatial rainfall

Effect of small scale variability in isotopic composition of precipitation on hydrograph separation results

Effect of small scale variability in isotopic composition of rainfall on hydrograph separation results

B.M.C. Fischer[a], H.J. van Meerveld[a], J. Seibert[a,b]

[a]*Department of Geography, University of Zurich, Winterthurerstrasse 190, CH-8057 Zurich, Switzerland*
corresponding author: benjamin.fischer@geo.uzh.ch
[b]*Department of Earth Sciences, Uppsala University, Sweden*

Abstract

Isotope hydrograph separation (IHS) is a valuable tool to study runoff generation processes. To perform an IHS, water samples of baseflow (pre-event water) and stormflow are collected at the stream outlet, while rainfall is collected as either an event total or is sampled sequentially during the event. For small headwaters it is usually assumed that the spatial variability in the isotopic composition of rainfall is small and that, therefore, one sampling location is sufficient. However, few studies have tested this assumption. In this study, we investigated the spatiotemporal variability of the isotopic rainfall composition and its effects on IHS results based on detailed measurements within a small pre-alpine catchment in Switzerland. Rainfall was sampled sequentially at eight locations across the 4.25 km^2 Zwäckentobel catchment and stream water was collected in three subcatchments (0.15, 0.23, and 0.7 km^2) during ten events. The spatial variability in total rainfall, mean and maximum rainfall intensity and the isotopic composition of rainfall was high for some events. The spatial variability in the isotopic composition varied from event to event and there was no clear relation between the isotopic composition of rainfall and total rainfall, rainfall intensity or altitude. For four of the ten studied events the spatial variability in the isotopic composition of rainfall was at least as large as the temporal variability in of the rainfall isotopic composition. The isotope hydrograph separation results varied considerably depending on the data from which rain sampler was used to estimate the isotopic composition of the rainfall, particularly for large events. The differences in the calculated peak pre-event water contributions were as large as 70%. These results demonstrate that the spatial variability in the isotopic composition of rainwater has to be considered for IHS studies even in small catchments, and that using data from only one rain sampler add an additional source of uncertainty.

Keywords: [1] isotope hydrograph separation, precipitation, headwater catchment, spatial variability

1. Introduction

Two-component isotope hydrograph separation (IHS) is a well established method to study runoff generation (Burns, 2002; Buttle, 1994; Klaus and McDonnell, 2013). IHS makes uses of the stable isotopes of oxygen or hydrogen as conservative tracers and allows the determination of the contribution of rainfall (event water) and water that was stored in the catchment prior to the event (pre-event water) to stormflow (Sklash et al., 1976). To be able to perform an IHS, baseflow water samples before the start of the event (pre-event water) and stormflow samples are collected at the catchment outlet. Krupa (2002); Laquer (1990) list different ways to collect rain water samples. Sampling by hand (Hrachowitz et al., 2011; Roa-García and Weiler, 2010), integrated volume samplers (James and Roulet, 2009; Lyon et al., 2008; Pellerin et al., 2008; Smith et al., 1979; Vitvar and Balderer, 1997) and sequential samples for each volume of rain or with a fixed time step (Brown et al., 1999; Jordan, 1994; McDonnell et al., 1990; Penna et al., 2014) are most common in IHS studies. Less frequent are laser spectroscopes which measure the isotopic composition of rainfall in the field with a high temporal resolution and open new possibilities for IHS studies (Berman et al., 2009; Munksgaard et al., 2012; Tweed et al., 2016). IHS relies on a number of assumptions as discussed previously by Buttle (1994) and Klaus and McDonnell (2013). One of the assumptions is that the isotopic signature of event and pre-event water are significantly different and both maintain a constant spatiotemporal isotopic signature, or any variations can be accounted for. Furthermore is the contribution from the vadose zone negligible, or the isotopic signature of the soil water must be similar to that of groundwater while surface storage contributes minimally to the streamflow. The isotopic composition of rainfall can change significantly during an event. McDonnell et al. (1990) highlighted the importance of considering this temporal variation and proposed different weighing techniques to account for the temporal variation in the isotopic composition of rainfall in IHS. Similarly Laudon et al. (2002) proposed a technique to weigh snowmelt to account for the temporal variation in isotopic composition of snowmelt in IHS. Almost all hydrograph separation studies now take the temporal variability in the isotopic composition of event water into account. However, few studies have tested if the assumption of a constant spatial isotopic signature in event water (Buttle, 1994) is valid or how this spatial variability affects IHS results. The common practice in IHS studies for

[1] layout made with the modified Elsevier L$_{atex}$-template

small headwater catchments (< 10km^2) is to use one bulk or sequential rainfall sampler and to assume that the spatial variability in rainfall (Goodrich et al., 1995) and its isotopic composition (McDonnell and Beven, 2014) are negligible. When the spatial variability in the composition of rainfall is considered, this is often done at monthly time scales, using national (Delavau et al., 2015; Katsuyama et al., 2015; Schürch et al., 2003; Seeger and Weiler, 2014; Smith et al., 1979) and global (Araguás-Araguás et al., 2000; Bowen and Good, 2015; Dansgaard, 1964) monitoring networks. For these large scale studies, different relations between the isotopic composition of precipitation and altitude (Holko et al., 2012; Kern et al., 2014; McGuire and McDonnell, 2008), temperature (Dansgaard, 1964; Holko et al., 2012; Schürch et al., 2003) or rainfall amount (Dansgaard, 1964) were observed. Contrary, Holko et al. (2012) and (Schürch et al., 2003) did not observe an amount effect using distributed rain gauges in Slovakia and Switzerland respectively. Detailed studies on small scale spatial variability in the isotopic composition of forest throughfall however showed a substantial spatiotemporal variability in isotopic composition of throughfall for both plot scale (Allen et al., 2015) and catchment scale (James and Roulet, 2009). Only a few studies have looked at the spatial variability in the isotopic composition of rainfall during individual events at the small catchment scale (Holko et al., 2012; McGuire et al., 2005). McGuire et al. (2005) quantified the spatial variability in the isotopic composition of rainfall across the 62 km^2 H.J. Andrews Lookout Creek catchment for 3 events in fall 2002 using 38 samplers and observed significant spatial differences and an elevation effect. Lyon et al. (2009) used two sequential rain sampler locations (two bulk samplers and one incremental sampler) to assess the influence of the spatial and temporal variability in the isotopic composition of rainfall on the calculated pre-event water contribution to streamflow for one event in the 8.8 km^2 Upper Sabino research catchment in Arizona. They observed small differences between the incremental weighted rainfall and the bulk sampled rainfall data, but substantial differences between the different rainfall locations Lyon et al. (2009). These results show that the spatial variability in the isotopic composition of rainfall may significantly affect the hydrograph separation results and that this effect should be studied in more detail. Therefore, we investigated the spatiotemporal variability in the isotopic composition of rainfall across a headwater catchment in Switzerland and determined the effect of the location of the rainfall samplers on the IHS results. We used the dataset of Fischer et al. (2016), who measured and sampled rainfall at eight locations across the 4.3 km^2 Zwäckentobel catchment at 5 mm intervals and sampled streamflow in three 0.15-0.7 km^2 tributary streams for 10 events in order to address the following research questions: (1) What is the spatial variability in the amount of event rainfall and isotopic composition across a small pre-alpine headwater catchment at the event scale? (2) Is the spatial variability in the isotopic composition of rainfall related to total rainfall, rainfall intensity or altitude? (3) Does the choice of the location of the sequential rainfall sampler affect the hydrograph separation results, and if so, does this effect depend on event size.

2. Method

2.1. Study area

The Zwäckentobel is a 4.3 km^2 pre-alpine headwater catchment in Switzerland, located 40 km south of Zurich. The climate is humid with a mean annual temperature of 6°C. It rains approximately every second day; the mean annual precipitation is 2300 mm y^{-1}, of which half falls during the snow-free season (Jun-Oct). The mean annual actual evaporation is approximately 300 mm y^{-1} (Menzel et al., 2007).

Approximately ten perennial streams drain the Zwäckentobel (Figure 1a), of which the Erlenbach catchment (WS04; 0.7 km^2), WS10 (0.23 km^2) and WS19 (0.15 km^2) have been the subject of several previous studies Fischer et al. (2015, 2016); Hegg et al. (2006). These mountain streams respond quickly to rainfall inputs and baseflow levels are usually reached again within a day. The geology of the Zwäckentobel is composed of three different types of Tertiary flysch that consist of calcareous sedimentary layers of schist, marl or sandstone and is covered with shallow creeping gleysols (0.5-2.5 m) (Fischer et al., 2015). The Zwäckentobel had a high percentage of wetlands and different land cover of types which were classified by Fischer et al. (2015) into forest (54 %), partly forested meadows (21 %), meadows (24 %).

2.2. Instrumentation and event sampling

We used the dataset of (Fischer et al., 2016), who collected in headwaters WS04, WS10, and WS19 hydrometric and stable isotope data of 13 rainfall events during the snow free period (Jun-Oct) of 2010 and 2011. Rainfall was measured at 14 locations (Figure 1a), which were located on different transects and across different altitude classes. Eight rain gauges were equipped with sequential rain samplers (adapted after Kennedy et al. (1979) containing 12x100 ml honey jars, each representing 5 mm of rainfall) to collect rainwater for isotope analysis. The sampling design was restricted by logistics because all samples needed to be collected during one day to avoid fractionation; therefore sequential rain sampler were not installed in the upper part of WS04 and WS10 (Figure 1a). Three events from the (Fischer et al., 2016) dataset were excluded from the analyses due to malfunctioning of some of the rain samplers; only the data from events 1 to 6 and 9 to 12 were used for analysis in this study (Table 1). In order to determine which rain gauge was most representative for the Zwäckentobel catchment, we calculated the Mean Relative Difference for event total rainfall using the method of Vachaud et al. (1985):

$$M_{RD_j} = \frac{1}{Z}\sum_{t=1}^{Z}\frac{P_{j,t} - \overline{P_t}}{P_t} \tag{1}$$

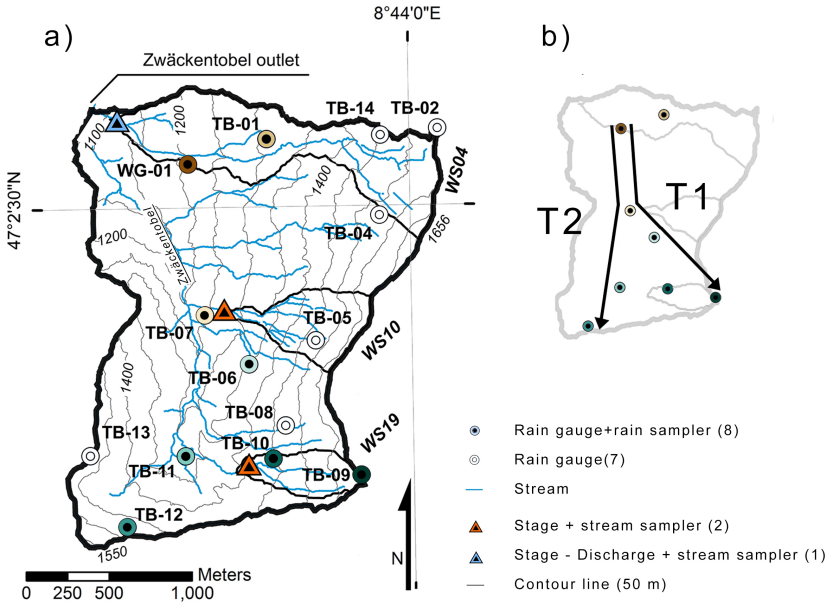

Figure 1: Map of the Zwäckentobel catchment with subcatchments WS04, WS10 and WS19, the location of the rain gauges, the rain samplers (the colors used for the different rain samplers are the same as in Figures 5, 8 and 9) and the stream sampling locations (a), and the two different transects of the rain gauges (T1 and T2) (b)

where M_{RDj} is the Mean Relative Difference for rain gauge j, $P_{(j,t)}$ is the rainfall measured at rain gauge j for event t, ($\bar{P}_t$) is the mean rainfall for all rain gauges for event t, and Z is the number of events (Z=10). The M_{RDj})of the event mean isotopic composition of rainfall was calculated similarly.

Table 1: Hydrometeorological characteristics of the different sampled events: Difference in time between the first and last rain gauge of the rainfall initiation ($P_{startdiff}$), event duration (P_{length}), mean total rainfall for all rain gauges ($P_{tot.}$), mean mean hourly rainfall intensity for rain gauges (I), the mean maximum hourly rainfall intensity of all rain gauges (I_{max}) and maximum specific discharge of WS04 (Q_{peak}). The standard deviations are given in parentheses. For the numer of samples collected per event see Tables 3 and 4.

event nr.	1	2	3	4	5	6	9	10	11	12
year	2010				2011					
day-month	8 Sep	17 Sep	24 Sep	4 Oct	29 Jun	8 Jul	24 Aug	27 Aug	4 Sep	18 Sep
$P_{startdiff}$ [h]	1.8	0.2	0	0	0	1.3	0.1	0.3	0	0.6
P_{length} [h]	10 (.15)	8(.5)	70(1.1)	10(.2)	23(1)	11(.8)	2(.7)	19(.15)	11(.13)	11(.13)
$P_{tot.}$ [mm]	22 (2.6)	11 (1.4)	109 (16)	10 (1)	84 (19)	25 (1.5)	12 (2)	20 (1)	51 (11)	25 (2)
I [mm h^{-1}]	2.2(.3)	1.3 (.2)	1.5 (.2)	0.9 (0.1)	3.6 (.9)	2.5 (.2)	6.0 (1)	1.0 (.1)	1.9 (.4)	1.6 (.2)
I_{max} [mm h^{-1}]	4.5 (.6)	2.3 (.3)	7.6 (1.1)	2.4 (.4)	18 (8.4)	9.0 (.9)	10.0 (3)	7.3 (.7)	7.0 (1.4)	6.0 (1.4)
Q_{peak}[l s^{-1} km^{-1}]	353	106	1010	53	3004	390	86	334	589	504

Discharge and stream water level were measured at the Erlenbach catchment (WS04) and water level was measured at the stream outlet of WS10 and WS19. Before each event, a grab sample was taken from each stream to characterize the pre-event water composition. Automatic samplers (ISCO 6712 with 24x1 L-bottles and Liquid Level Actuator, Teledyne Isco, USA, Figure 1a) were used to collect stream water at the outlets of the three study catchments during the events. The number of water samples for stable isotope analysis differed for each stream and event and ranged from 7 samples for shorter events up to 54 samples for longer events (see supplementary material, Table 2) All water samples were analysed at the stable isotope laboratory of the Department of Geography at the University of Zurich using a Cavity Ring-Down Spectroscope-Picarro L1102-i Liquid Analyser (1^{st} generation analyser, Picarro Inc., 2008), following the procedure of Penna et al. (2010). All stable isotope values are reported as δ-values in per mill (‰) relative to Vienna Standard Mean Ocean Water (VSMOW). The precision for the isotope analyses was < 0.1 ‰ for δ^{18}O, and generally < 0.5 ‰ for δ^{2}H. Due to some technical issues, the precision for δ^{2}H was for some of the samples >1 ‰, in order to be consistent with results of Fischer et al. (2016), only the δ^{18}O data was used for further analysis. None of the collected samples were subjected to significant fractionation (see also Fischer et al. (2016)).

2.3. Isotope hydrograph separation

A two-component isotope hydrograph separation (IHS) was used to quantify the fraction of pre-event water f_{PE} (Eqs.2 and 3) in streamflow for the 10 rainfall-runoff events (Sklash et al., 1976).

$$Q_S = Q_E + Q_{PE} \tag{2}$$

$$f_{PE} = \frac{C_S - C_E}{C_{PE} - C_E} \tag{3}$$

where C describes the stable isotope composition (‰), Q the streamflow (l s^{-1}) and the subscripts S, PE and E represent streamflow, pre-event water (baseflow prior to the event) and event water (rainfall) respectively. The different temporal weighing techniques described by McDonnell et al. (1990) were used to account for the temporal variability in the event water composition: (I) weighted mean value, (II) intensity mean, (III) incremental mean and (IV) incremental intensity mean. The weighted mean (I) and incremental mean (III) were determined using Eq 4:

$$C_E = \frac{\sum_{i=1}^{n} P_i \delta_i}{\sum_{i=1}^{n} P_i} \tag{4}$$

where P is the rainfall amount of sample i to n [mm], δ is the stable isotope composition of the rainfall sample i to n. For the weighted mean (I), the value of C_E based on all samples was used throughout the event, while for the incremental weighted mean (III), the value of C_E depended on the timing of the rainfall samples so that the value of C_E was not influenced by rain water that had not fallen yet. Similarly, for the intensity mean (II) and the incremental intensity mean (IV) we used Eq. 5, where I is the rainfall intensity of sample i to n and δ is the stable isotope composition of the rainfall of sample i to n.

$$C_E = \frac{\sum_{i=1}^{n} I_i \delta_i}{\sum_{i=1}^{n} I_i} \tag{5}$$

The aim of this study was not to highlight the differences in the pre-event water contributions to streamflow due to the choice of the temporal weighing technique as these are already well known (McDonnell et al., 1990) but instead we use the different temporal weighing techniques to compare the differences in the IHS results resulting from the spatial variability in isotope composition with those due to the different temporal weighing techniques. The uncertainty estimates of the pre-event water contributions to streamflow were determined for the incremental intensity mean (IV) based on Genereux (1998) and are given in Fischer et al. (2016).

3. Results

3.1. Spatial variability in event total rainfall and the event weighted mean isotopic composition of rainfall

The spatial variability of event total rainfall, maximum rainfall intensity and the weighted mean δ^{18}O of rainfall varied from event to event (Table 1, Figure 2). Events 3 and 5 had the highest event total rainfall and large spatial differences in event total rainfall and maximum rainfall intensity (Figure 2, c and e). The weighted mean δ^{18}O of rainfall for these events was only available for four rain samplers because rain changed to snow after the maximum discharge was reached. Events 9 and 11 had lower event total rainfall but were also characterized by a relatively large variability in event total rainfall (Figure 2, g and i). The weighted mean δ^{18}O varied between -4.25 and -4.83 ‰ for event 9 (Figure 2g) and between -7.35 and -9.06 ‰ for event 11 (Figure 2i). Events 1, 6, 10 and 12 had smaller spatial differences in event total rainfall (coefficients of variation smaller than 0.1 and a range in event total rainfall smaller than 6 mm) and maximum rainfall intensities, but the spatial variability in the weighted mean δ^{18}O of rainfall was significant (Figure 2, a, f, h and j). The differences between the minimum and maximum weighted mean δ^{18}O was 0.34, 0.88, 0.57, and 3.6 ‰ for events 1, 6, 10 and 12 respectively (Figure 9, a, f, h and j). For the smallest events (events 2 and 4), the difference between the highest and lowest measured event total rainfall was small but the range in the weighted mean δ^{18}O of rainfall was 1.3 ‰ (Figure 2, b and d).

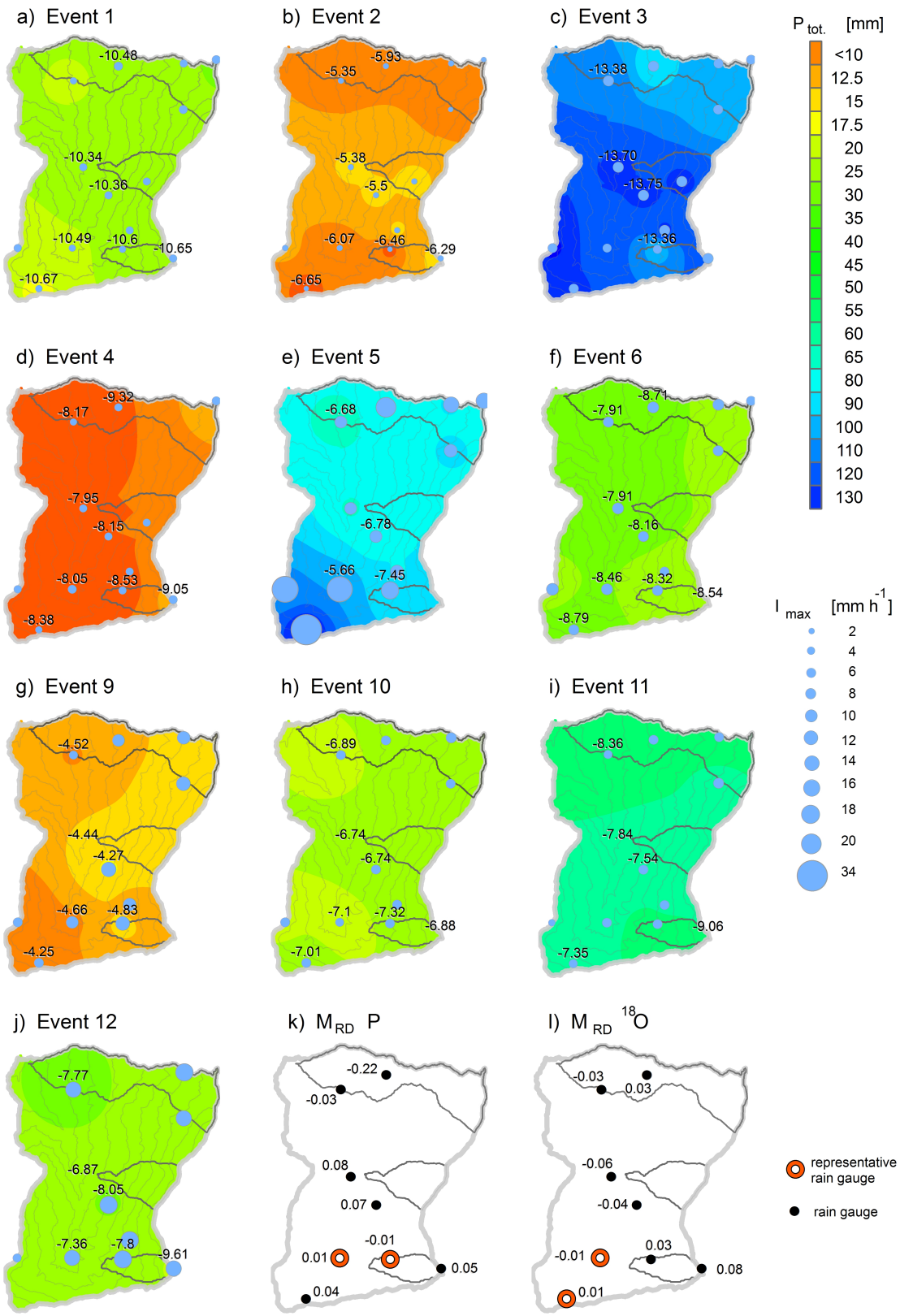

Figure 2: The spatial distribution total rainfall ($P_{tot.}$, interpolated using inverse distance weighing) for different events (a-j). The area of the circle in plots (a-j) represents the event maximum rainfall intensity. The numbers represent the weighted mean $\delta^{18}O$ of rainfall. The mean relative difference of event total rainfall (M_{RD} P) (k) and the mean relative difference of $\delta^{18}O$ (M_{RD} ^{18}O) at those locations where rainfall amounts and isotope composition was measured (l). The rain gauge and samplers with the lowest M_{RD} are highlighted in red in figure (k) and (l) respectively.

Rain gauges TB-10 and TB-11 had a M_{RD} close to zero and were thus the most representative location for event total rainfall (Figure 2k). Rain gauges TB-11 and TB-12 had a M_{RD} close to zero for $\delta^{18}O$ and were thus

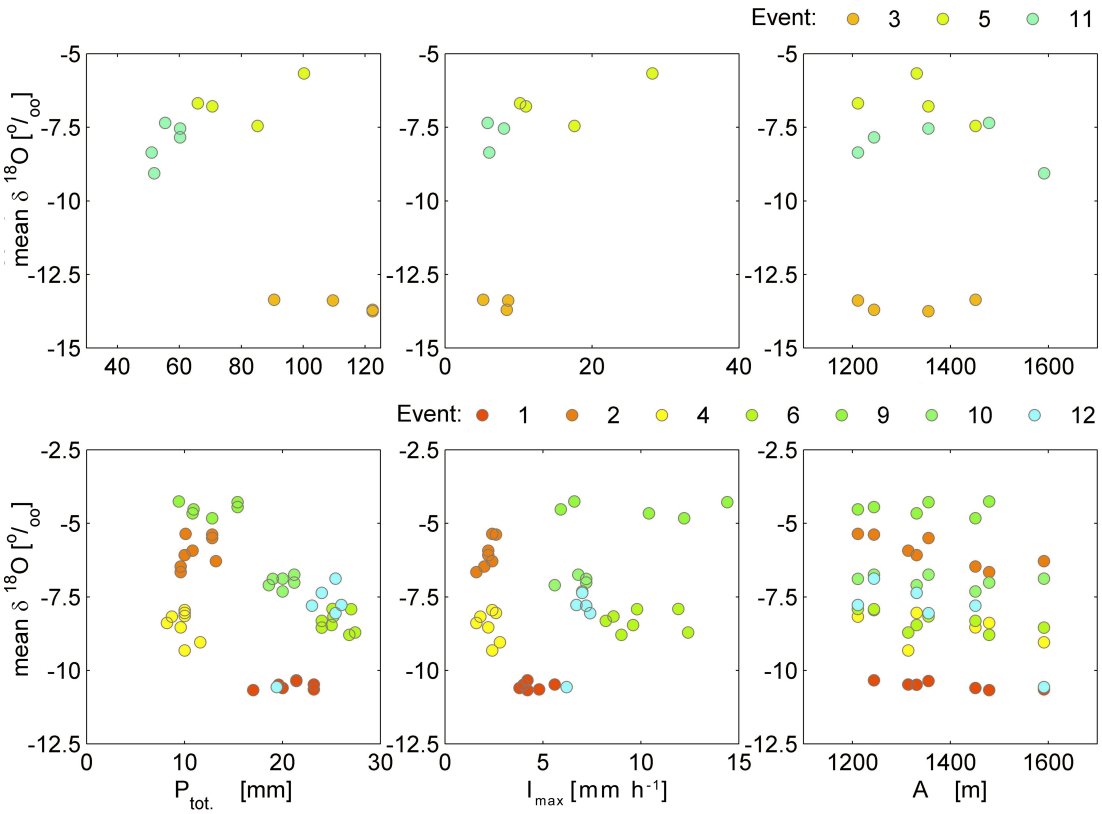

Figure 3: The weighted mean δ^{18}O of rainfall for each sampling location as a function of total rainfall ($P_{tot.}$), maximum rainfall intensity (I_{max}) and altitude (A) for the different rainfall events (represented by the different colors). The top row shows the relations for the large events (>30mm) and the bottom row for small and medium events (<30 mm).

the most representative location for the weighted mean δ^{18}O (Figure 2l). These results suggest that TB-11 was the most representative measurement location for the entire Zwäckentobel catchment. In order to examine if the patterns in event total rainfall or maximum rainfall intensity were related to altitude, we determined the Pearson correlation between total rainfall, maximum rainfall intensity and altitude. For event 5, total rainfall was correlated strongly with rainfall intensity but the correlations between total rainfall or intensity and altitude were weak (Figure 3 and Table 2). There was no correlation between total event rainfall, the maximum rainfall intensity or altitude for any of the other events (Figure 3 and Table 2). There was a weak positive correlation between the weighted mean δ^{18}O of rainfall and total event rainfall for event 2, 10, 11 and 12 and a weak negative correlation for event 5 (Figure 3 and Table 2). The correlation between the weighted mean δ^{18}O of rainfall and the maximum rainfall intensity was strong and positive for event 3 and weakly positive for event 2. There was no strong sign between the weighted mean δ^{18}O and total rainfall or intensity for the other events. There was a strong positive correlation between the weighted mean δ^{18}O of rainfall and altitude for event 3, while this relation was weak for events 1, 2, 5, 6 and 12 (Figure 3 and Table 2). Analyzing the weighted mean δ^{18}O of rainfall of the rain samplers along the two main transects (T1 or T2) or for different altitude classes (below or above 1350 m) resulted in stronger correlations between the weighted mean δ^{18}O of rainfall and event total rainfall, maximum rainfall intensity or altitude but only a few of these correlations were statistically significant (Table 2).

The difference between the maximum weighted mean δ^{18}O and the minimum weighted mean δ^{18}O for the sampling locations (i.e. the spatial range of weighted mean δ^{18}O; S_R) increased slightly with increasing event total rainfall (up to 2.7 ‰) but was very variable for the large events (Figure 4). There was not statistical significant relation between the spatial range of the weighted mean δ^{18}O and the maximum rainfall intensity or event duration (Figure 4).

3.2. Temporal variability in cumulative rainfall and the isotopic composition of rainfall

For events 3, 4, 5 and 11, rainfall started at the same time at all of the rain gauges, while for events 1 and 6 there was more than one hour difference in the time of the initiation of rainfall at the different rain gauges (Table 2). The rainfall became more depleted in δ^{18}O during the events but the exact temporal pattern differed between the events (Figure 5). For events 2, 4 and 9, the δ^{18}O decreased by 1-2 ‰ from onset of rainfall towards the end, for events 1, 6, 10 and 12, δ^{18}O decreased by 2-8 ‰, while for events 3, 5 and 11 it decreased by 4-11 ‰. The decrease in δ^{18}O was more variable for events 3, 5 and 11 than for events 2, 4 and 9, with sudden increases or decreases in δ^{18}O after which it decreased to its minimum. The mean of the difference between the maximum and minimum δ^{18}O for the different rain samplers (i.e., mean temporal range in δ^{18}O; M_{TR}) increased with increasing event total rainfall from 1 up to 10 ‰ (Figure 4). There was no clear relation between the mean temporal range in δ^{18}O and the maximum

Table 2: The pearson correlation coefficient for the relation between the weighted mean δ^{18}O and event total rainfall ($P_{tot.}$), the maximum hourly rainfall intensities (I_{max}) and altitude (A) for the entire data set and individual transects (Figure 1b) or altitude zones. ++, +, 0, - and - - indicate a correlation of 1, [<1-0.5], 0, [<-0.5 - <-1] and -1 respectively. Bold symbols indicate statiscically significant correlations with $p < 0.05$.

event nr.		1	2	3	4	5	6	9	10	11	12
Rainfall											
	$P_{tot.}$-I_{max}	+	+	o	++	++	+	+	+	o	o
	$P_{tot.}$-A	o	o	o	o	+	-	o	o	o	-
	I_{max}-A	o	-	-	o	+	-	o	o	o	o
δ^{18}O											
	All-P	o	+	-	o	o	o	o	+	+	+
	All-I_{max}	o	+	++	o	o	o	o	o	-	o
	All-A	+	+	++	o	+	+	o	o	o	+
T1											
	P	o	o	-	o	- -	+	+	+	+	+
	I_{max}	-	+	++	o	- -	++	+	-	++	o
	A	++	+	++	+	++	++	o	o	o	+
T2											
	P	++	+	- -	+	++	o	o	+	+	-
	I_{max}	o	+	++	+	++	++	-	+	- -	++
	A	++	++	++	o	- -	++	o	+	- -	-
A <1350 m											
	P	+	o	- -	o	- -	o	+	+	++	+
	I_{max}	+	+	++	o	- -	o	- -	++		–
	A	++	++	++	+	++	+	+	+	–	+
A >1350 m											
	P	o	o		o	++	o	-	+	+	+
	I_{max}	-	+		-	++	-	-	+	–	+
	A	+	+		++	++	+	–	o	+	++

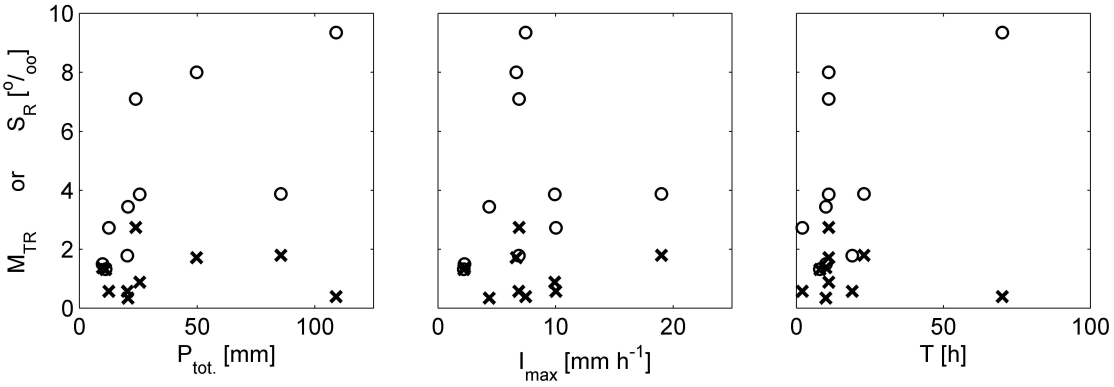

Figure 4: Mean temporal range (M_{TR}, circles) and spatial range (S_R, crosses) of δ^{18}O in rainfall for each event as a function of event mean total rainfall ($P_{tot.}$), mean maximum rainfall intensity (I_{max}) and event duration (T).

rainfall intensity or event duration (Figure 4). The temporal variability in δ^{18}O of rainfall was relatively similar for all eight sampling locations but there were differences between the different rain samplers (Figure 5). The spatial variability of δ^{18}O between the different rain samplers was relatively large during the first 5 mm of rainfall, with a standard deviation of approximately 0.5-1.5 ‰ (Figure 6). The variability of the sampled δ^{18}O between the different rain samplers decreased during events 1, 2, 4, 6, 9 and 10 but for events 3, 5, 11 and 12 it increased throughout the event (Figure 6). Comparing mean temporal range in δ^{18}O (M_{TR}) with the spatial range in the incremental mean δ^{18}O (S_R) for the different events shows that for most events the change in δ^{18}O during the event was larger than the spatial variability in the weighted mean δ^{18}O (Figure 7). However, for small events the spatial variability in δ^{18}O was equal or half of the temporal variability in δ^{18}O (Figure 7). With increasing event total rainfall the temporal range in δ^{18}O became much larger than the spatial variability (Figure 7). The ratio of M_{TR} and S_R did not depend on the maximal rainfall intensity and or the duration of the event (Figure 7).

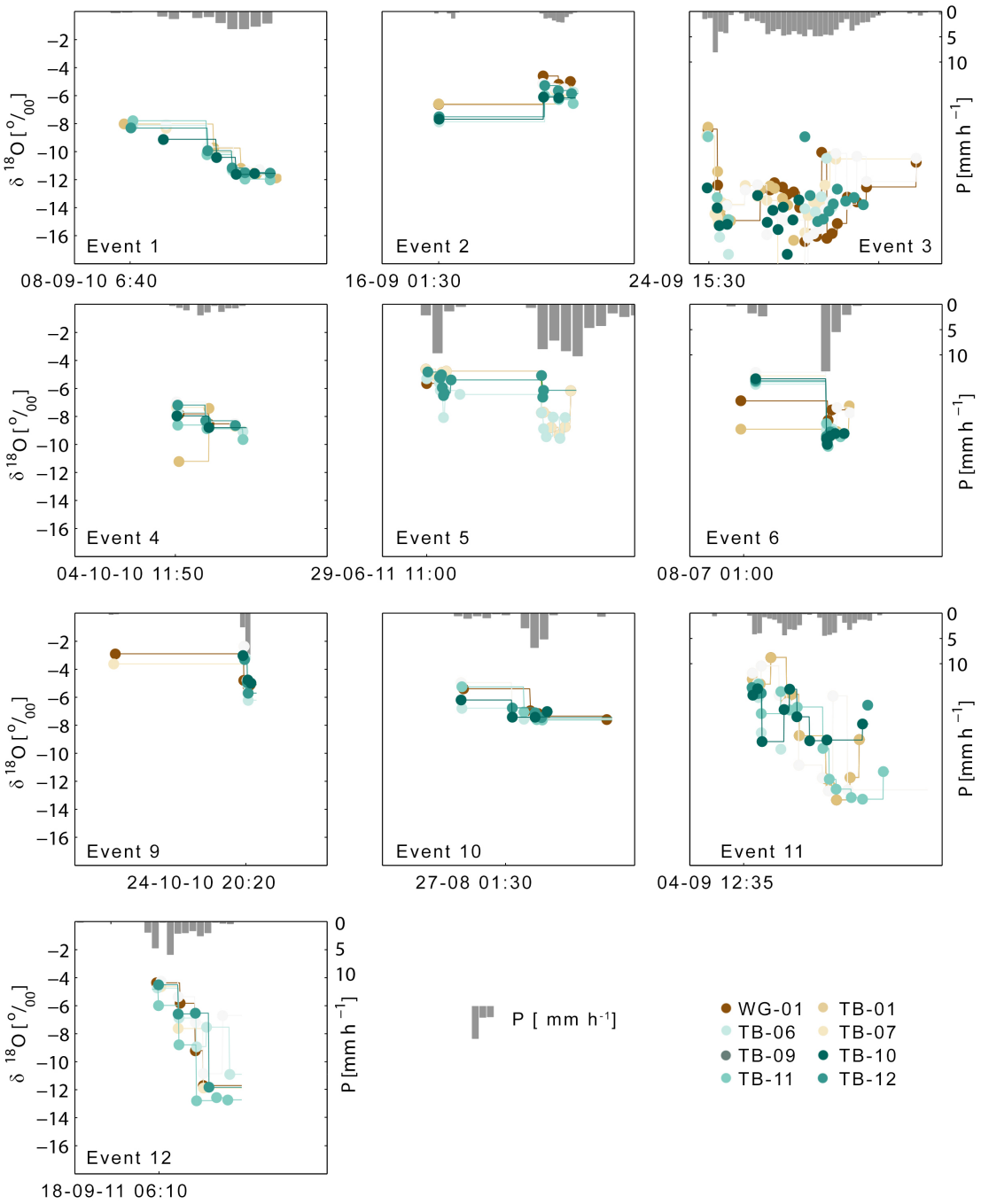

Figure 5: The rainfall (bars) and the δ^{18}O of the rainfall measured at the different rain gauges (circles) for the different events.

3.3. Effect of different temporal weighing techniques on hydrograph separation results

The effect of the different techniques to account for the temporal variability in the isotopic composition of rainfall (techniques I-IV) on the minimum fraction of pre-event water contribution to stormflow was analyzed for WS04, WS10 and WS19 for all events. For events 2, 9 and 10 the differences in the calculated minimum fractions of pre-event water between the four different techniques was small (0.1) but for the other events the differences in the minimum fractions of pre-event water were larger than 0.4, and differed by up to 0.8 for event 11 (Figure 8). For the small and moderate events with a small M_{TR} and a large difference between the event and pre-event water composition the different weighing techniques had a small effect on the minimum fraction of pre-event water in stormflow in WS04, WS10 and WS19 (Figure 10). The differences in the calculated minimum fraction of pre-event water to streamflow increased with increasing M_{TR} and when the differences between the event and pre-event water composition were smaller. For example, the use of the weighted mean and intensity mean (I and II) resulted in a very depleted event water composition for event 3, and therefore a large difference between the event water composition and both pre-event water and stream water, which resulted in large calculated pre-event water contributions (Figure 9). On the other hand, for the incremental mean and the incremental intensity mean techniques (III and IV), the event water composition decreased steadily throughout the event and the difference between the event water composition and both pre-event water and stream water was smaller, which resulted in smaller calculated pre-event water contributions during the event (Figure 9). An opposite effect was seen for medium sized event 11. The weighted mean and intensity mean (I and II) resulted in a more depleted event water composition and a smaller difference between event water and pre-event and stream water during the event, resulting in a much smaller pre-event water contribution than for the incremental mean and incremental intensity mean techniques (III and IV), depletion of δ^{18}O in event water (Figure 9).

3.4. Effect of the location of the rain gauge on hydrograph separation results

The effect of the different rain sampling locations on the IHS results was assessed by determining the pre-event water fractions in streamflow for WS04, WS10 and WS19 using the data from each of the eight rain sampler and the incremental intensity mean (technique IV) to account for the temporal variability in isotopic composition of rainfall at each of the rain gauges. While only a few of the rain gauges are located inside WS04, WS10 or WS19, we determined the pre-event water fractions for each of the rainfall sampling locations because it is common in small catchment studies to use the data from a location near the catchment (Figure 8). The choice of the location of the rain samplers affected whether IHS was possible or not. For event 3 in WS04, the use of the rain sampler in the southern part of the Zwäckentobel prevented the application of IHS. For other events, e.g., event 6 in WS04, IHS was not possible when using the local rainfall sampler but was possible when using neighbouring rain samplers. For some events the minimum fraction of pre-event water was highly dependent on the location of the rainfall sampler but for other events the sampling location had less influence on the IHS results and the range in the calculated minimum fractions of pre-event water was very small (Figure 8). For example, for events 3 and 11 in WS04 the calculated pre-event fractions for the different rainfall samplers differed by up to 0.5 (Figure 9) but for event 2 the differences in the pre-event water fractions were at most 0.1 (Figure 9). Generally, the range in the calculated minimum fraction of pre-event water was small (up to 0.3) for events for which the spatial variability in δ^{18}O in rainfall was small (small S_R) and the difference between event and pre-event water composition was large (Figure 10). The range in the calculated minimum fraction of pre-event was large (up to 0.6) for events with a large spatial variability in the isotopic composition of rainfall and for which the difference between the event and pre-event water composition was small (Figure 10).

In order to assess the relative importance of the spatial variability in the isotopic composition of rainfall on the IHS results, we compared the range in the calculated minimum pre-event water composition due to the location of the rainfall sampler to the range in the calculated minimum pre-event water composition due the different techniques to account for the temporal variability in the isotopic composition of rainfall. For many of the small and moderate events the range in the minimum fraction of pre-event water due to the location of the different rain samplers was larger or equally to the range in the minimum fraction of pre-event water due to the use of different temporal weighing techniques (i.e. the ratio of the range in the minimum pre-event water contribution to streamflow from the different temporal weighing techniques over the range in the minimum fraction of pre-event water contribution for the different rain sampler was less than one; Figure 10). For the large events, the temporal range in δ^{18}O was generally large (large M_{TR}), also compared to the spatial variability in the weighted mean δ^{18}O (S_R). This is reflected in the range of the minimum pre-event water contributions to streamflow. For example for event 5 the range of the minimum fraction of pre-event water for the different spatial sampling locations was one third of the range in the minimum pre-event water contribution to streamflow obtained from the different temporal weighing techniques. This suggests that even for large events for which the temporal variability in the isotopic composition is large, the spatial variability in the isotopic composition of rainfall still has a significant effect on the IHS results.

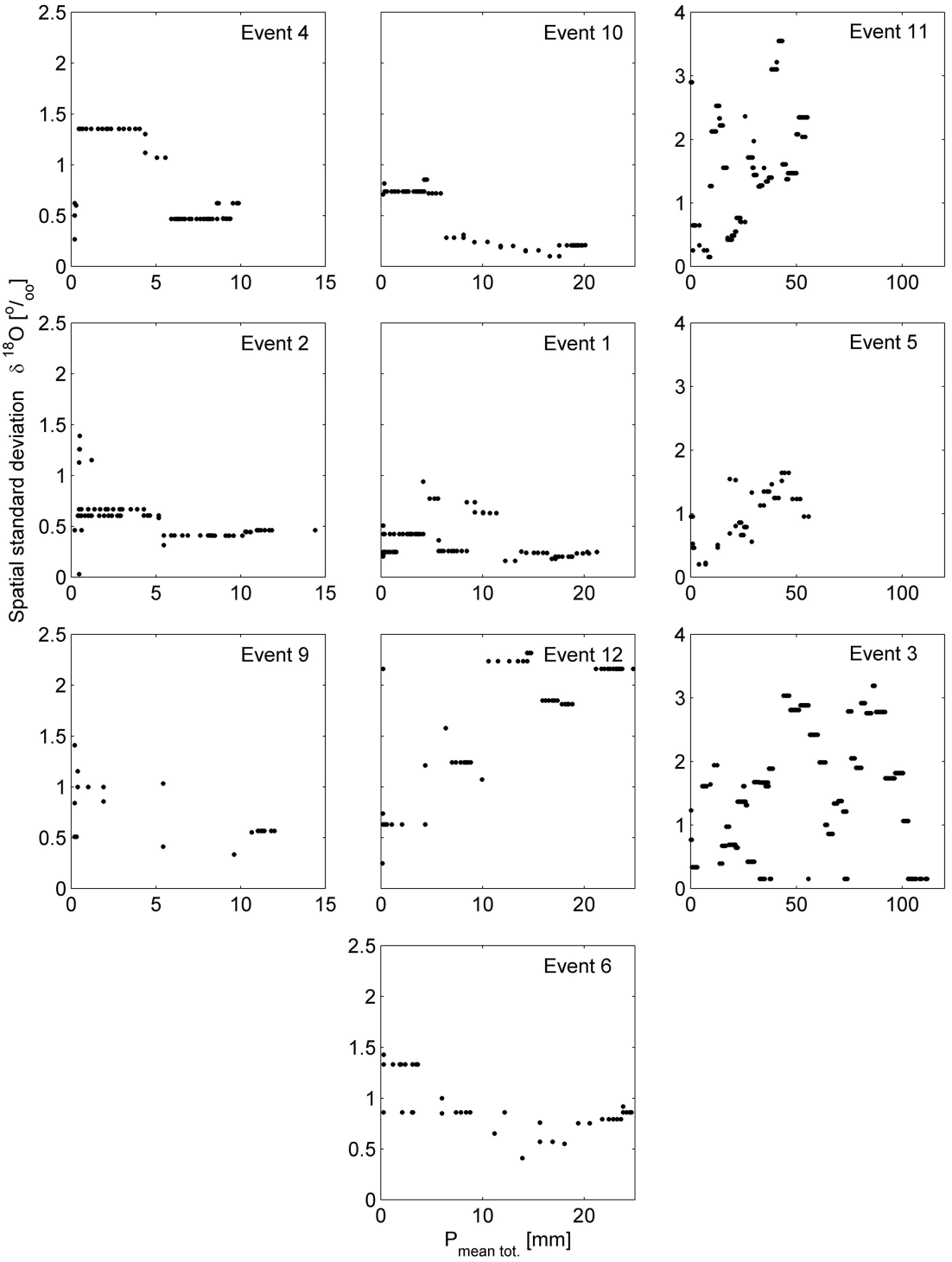

Figure 6: Spatial standard deviation of δ^{18}O in rainfall for the different events as a fuction of the cumulative mean rainfall. $P_{tot.}$ for the small events(left column), the medium sized events (middle column) and the large events (right column). The large events have a different y-range compare to the small and medium events.

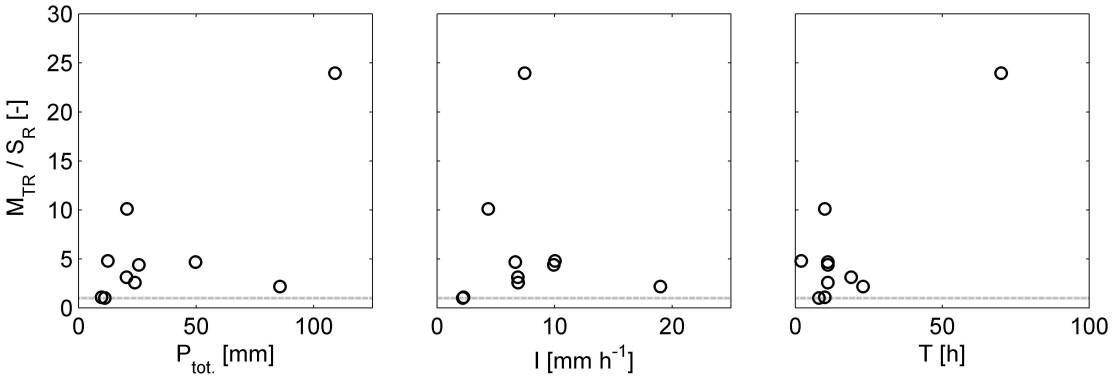

Figure 7: Ratio of the mean temporal range (M_{TR}) and the spatial range (S_R) of $\delta^{18}O$ in rainfall for each event as a function of event mean total rainfall ($P_{tot.}$), mean maximum rainfall intensity (I_{max}) and event duration (T). The gray line represents a ratio where M_{TR} is equal to S_R.

4. Discussion

4.1. Spatiotemporal variability in rainfall and rainfall isotopic composition

We observed differences in the weighted mean $\delta^{18}O$ of rainfall of 0.3 ‰ to more than 2 ‰ over distances of only 250 meter. This spatial variability in the isotope composition of rainfall (i.e., event water) was much larger than the variability in the isotopic composition of baseflow (i.e., pre-event water) sampled throughout the Zwäckentobel (<0.5 ‰; Fischer et al. (2015)). The spatial variability in the isotopic composition of rainfall increased slightly with increasing event total rainfall but was variable for the large events. These differences in the isotopic composition of rainfall are smaller than the large spatial differences of 7 ‰ described by McGuire et al. (2005). This is not surprising considering that the Zwäckentobel catchment is 100 times smaller Lookout creek. The elevation differences in the Zwäckentobel (1084-1656 m a.s.l.) are also smaller than in Lookout Creek (428-1620 m a.s.l.). While the number of rain sampler in the Zwäckentobel study was lower than the 38 bulk samplers used by McGuire et al. (2005) and those used in large scales studies (Schürch et al., 2003; Seeger and Weiler, 2014; Smith et al., 1979), the density of samplers was three times higher in our study compared to the study by McGuire et al. (2005). We therefore argue that the added value of our study lies in the detailed information of small-scale spatial variability in rainfall and the $\delta^{18}O$ of rainfall. The consistent spatial variability in the isotopic composition of rainfall as observed by McGuire et al. (2005) and in larger scale studies, e.g. Smith et al. (1979) was not observed for the Zwäckentobel catchment. These studies attributed to the spatial variability in the isotopic composition of rainfall to the amount effect Dansgaard (1964) or altitude Holko et al. (2012); Kern et al. (2014); McGuire and McDonnell (2008). However, a comparison with these studies is only partly possible because of differences in the temporal resolution of the data (sampled yearly, seasonal, monthly and event time scales) and the size of the catchment and elevation differences. The rainfall pattern and the pattern in weighted mean $\delta^{18}O$ of rainfall were different from one event to the other (Figure 2) and the weighted mean $\delta^{18}O$ of rainfall was not correlated to altitude or rainfall amount, except for event 3 (Figure 3; Table 2). These results suggest the spatial variability has to be characterized for each event separately. The results also suggest that interpolation based on relationships with rainfall amount or altitude that are only based on two gauges (e.g., Lyon et al. (2009); McGuire et al. (2005); Vitvar and Balderer (1997)) should be used carefully. The lack of an amount effect or altitude effect might be caused by variable wind trajectories, which may obscure the relations which were observed by Friedman and Smith (1970). The complex local topography and the location of the neighbouring mountains might have affected local and mesoscale atmospheric circulation and rainfall, as described by (Roe, 2005). The sequential rain samplers gave not only information on the spatial variability of the weighted mean isotopic composition of rainfall but also on the changes in the isotopic composition of rainfall during the event. Rainfall became more depleted throughout the event at all of the rain samplers (Figure 4), as observed by many other rainfall isotope studies (e.g. Berman et al. (2009);

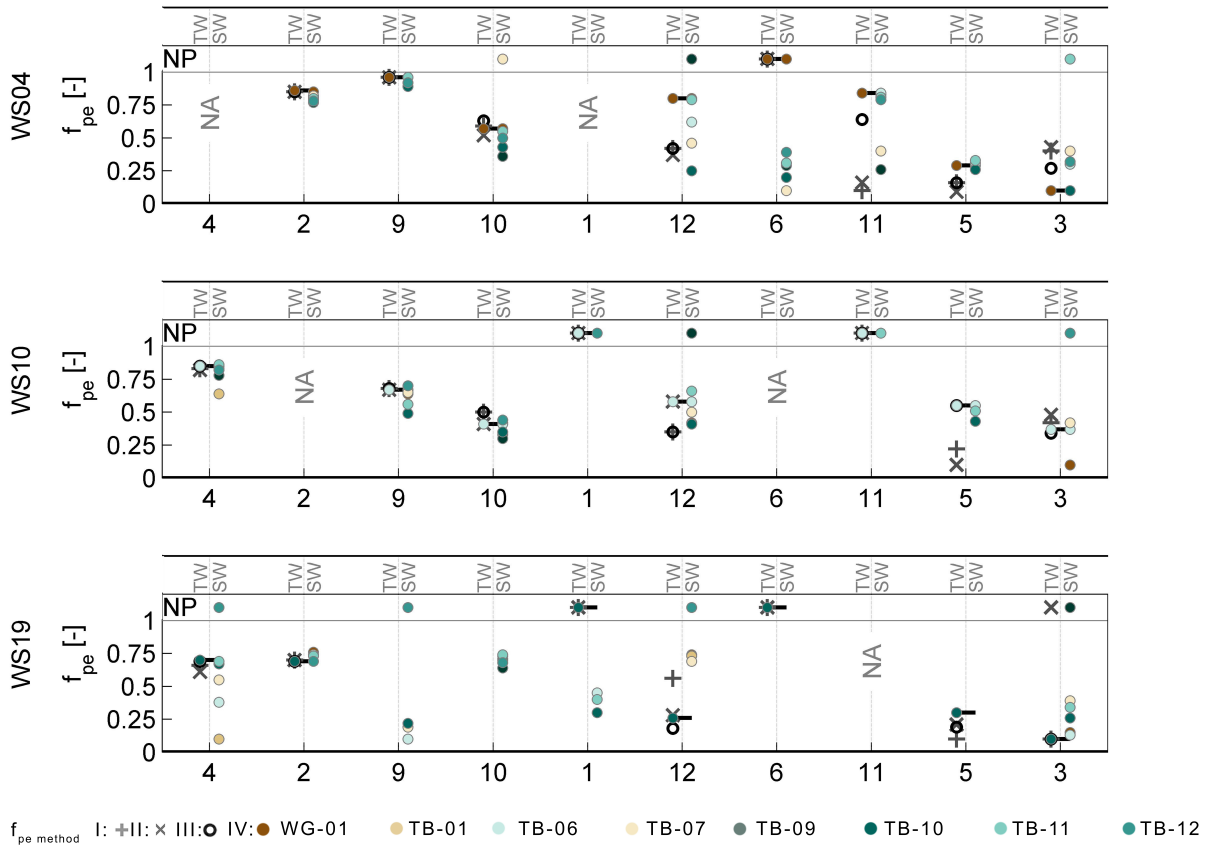

Figure 8: The minimum fraction of pre-event water in WS04 (top row), WS10 (middle row) and WS19 (bottom row) for the different ranked events calculated using the different weighing techniques I-IV, to account for the temporal variation in the isotopic composition of rainfall (T_W) and using the incremental intensity mean for incremental intensity mean for the different rainfall sampling locations (S_W, different colored circles). The horizontal black line indicates the minimum fraction of pre-event water obtained using (technique IV) using the nearest rain sampler (WG-1 for WS04, TB-6 for WS10 and TB-10 for WS19). NP indicates that hydrograph separation was not possible. NA indicates that the event was not sampled. The events are orderd by total precipitation see Table 1.

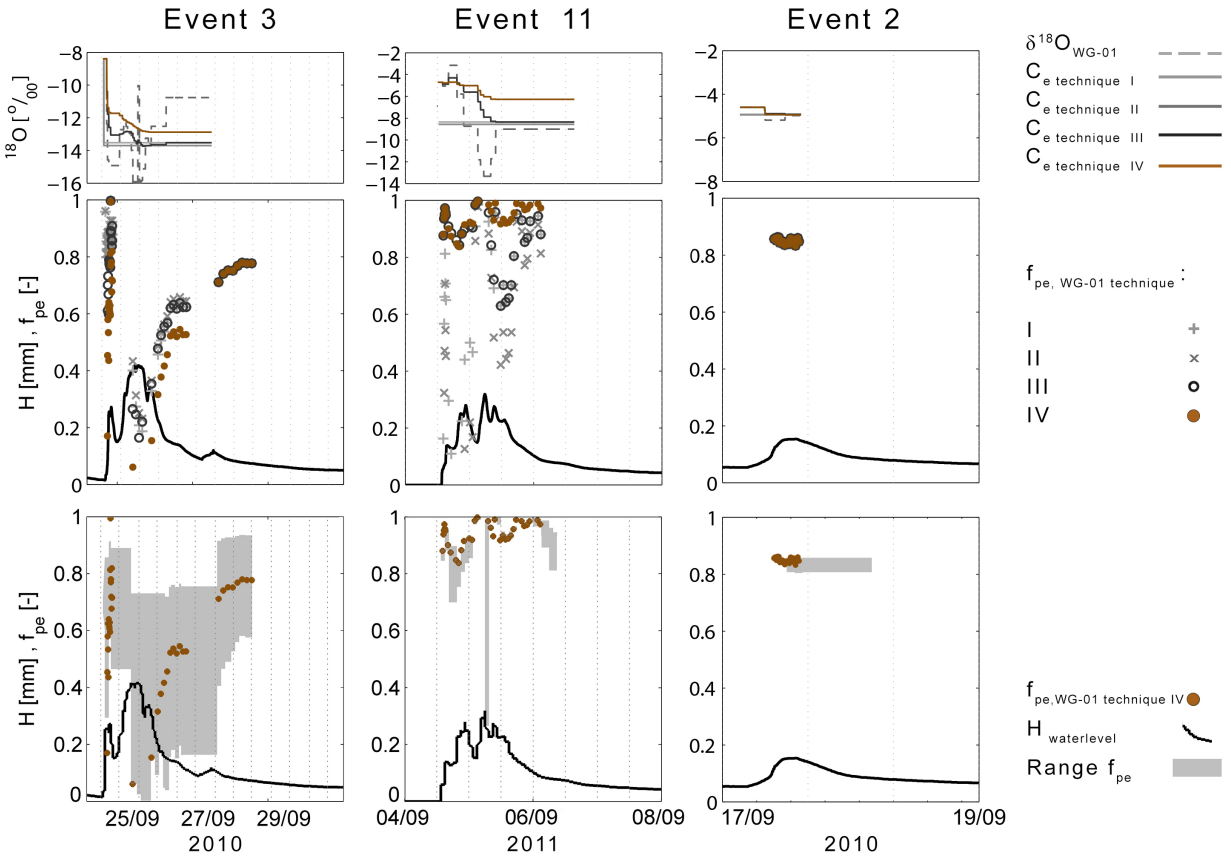

Figure 9: The isotopic composition of rainfall sampled (dashed line, top row of plots), the isotopic composition of rainfall from WG-01 based on the four different weighing techniques (C_e technique I-IV) for event 3 (left column), 11 (middel column) and 2 (right column). The stream water level (black line) and the fraction of pre-event water obtained using the four different weighing techniques C_e I-IV in WS04 (middel row), the range in the pre-event water contribution to streamflow determined using the incremental mean technique (IV, lower row) for the the different rainfall sampling locations (shading).

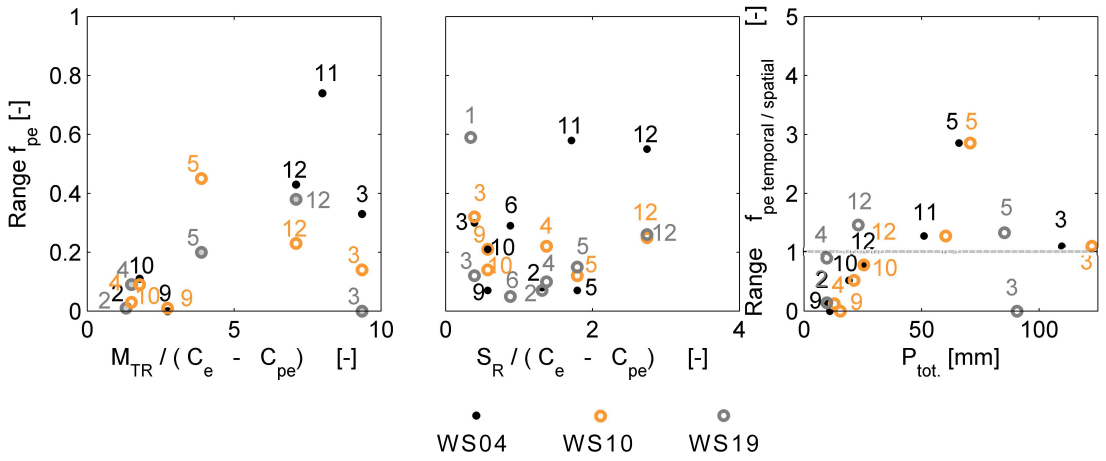

Figure 10: The range in the calculated minimum pre-event water contribution to streamflow for the different weighing techniques to account for the temporal variation in isotopic composition of rainfall as a function of the ratio of the mean temporal range of δ^{18}O (M_{TR}) and the difference between the event (C_e) and pre-event water (C_{pe}) composition (left panel), the range in the calculated minimum pre-event water contribution to streamflow based on the intensity weighted mean for the different rain gauges as a function the ratio of the spatial range of in δ^{18}O (S_R) and the difference between event and pre-event water composition (middel panel) and the ratio between the range in the minimum pre-event water due to the different temporal weighing techniques and the range in the minimum pre-event water due to different rain sampling locations as a function of event total rainfall ($P_{tot.}$, right panel) for WS04, WS10 and WS19 (black circles, open orange and open gray circels respectively). The label next to the symbol represents the event number.

Lyon et al. (2009); McDonnell et al. (1990); Penna et al. (2014)). The temporal variability in the isotopic composition of the rainfall generally increased with total rainfall and event duration but it was not correlated to rainfall intensity.

The spatial variability in the isotopic composition of rainfall was relatively large during the first 5 mm of rainfall and either decreased during the event or increased throughout the event (Figures 4 and 6), suggesting that a large part of the variability was due to the differences in the first rainfall and that the isotopic composition of the rainfall could either become more similar or more different throughout the event. For large events, such as event 3, the differences of $\delta^{18}O$ between the different rain samplers (as represented by the standard deviation) varied throughout the event (i.e. it increased and decreased with increasing total rainfall; Figure 6), largely due to differences in the timing of the different rain bursts. The results from this study show that for many events the temporal variability in the isotopic composition of rainfall was larger than the spatial variability. However for some events, the spatial variability was almost the same or even larger as the temporal variability of the rainfall isotopic composition (Figures 6 and 7). These the results of the spatial and temporal variability suggest that similar to the argument of Goodrich et al. (1995) for rainfall, that one rain gauge can be sufficient to capture the spatiotemporal rainfall characteristics and isotopic composition in small headwater catchments is not valid for the Zwäckentobel catchments, and likely also not for other pre-alpine catchments. Consequently, the promising development laser spectroscopes in the field Berman et al. (2009), may make it easier to better characterize the temporal variability of the isotopic composition of rainfall. However our study demonstrates that the spatial aspect of rainfall and its isotopic composition also must be considered.

4.2. Consequence of the spatiotemporal variability in event water composition on hydrograph separation results

As stated by McDonnell et al. (1990) it is important to account for the temporal variation in the isotopic composition of rainfall. We underline this and could further show that the importance of using sequential sampling increased with an increasing temporal range of isotopic composition of rainfall relative to the difference between the event and pre-event water composition (Figures 10). These differences in fractions of pre-event water due to the different temporal weighing techniques were larger than the uncertainty in the fraction of pre-event water estimated by Fischer et al. (2016). It is common in IHS studies in small catchment to sample rainfall throughout an event to account for the temporal variation in the isotopic composition of the rainfall. However it is less common to sample rainfall at multiple locations to account for the spatial differences in the isotopic composition of rainfall. Lyon et al. (2009) used two different sampling locations in the IHS calculations for one event and showed that the fractions of pre-event water to streamflow were very different for the two samplers. The eight sequential rain samplers in this study for the 10 different events gave a much better insight into the influence of the spatiotemporal variability in the isotopic composition of rainfall on the IHS results. For small events, the resulting range in the calculated minimum fraction of pre-event water was small for all three sub-catchments. This small range in the minimum fraction of pre-event water was partly due to the small spatial variability in the isotopic composition of rainfall for these events (Figure 10). Instead events with a larger spatial variability in the isotopic composition of the rainfall and in events where sequentially sampled rainfall, at different locations, had a different temporal evolution of the stable isotope composition showed a high variability minimum fraction of pre-event water. The effect of the spatial variability was further enhanced and large for events with small differences between event water and pre-event water composition. The spatiotemporal variability of the isotopic composition in rainfall demonstrates the necessity of multiple rain gauges in small headwater catchments to accurately account the isotopic composition of rainfall and reduce the spatiotemporal source of uncertainty in IHS studies.

5. Conclusion

Many IHS studies in small headwater catchments invest into characterizing the temporal variability in the isotopic composition of rainfall at one point but often ignore the spatial variability across the catchment. In this study we observed that the spatial variability in the isotopic composition varied from event to event and there was no relation between the isotopic composition of rainfall and total rainfall, rainfall intensity or altitude. As consequence we show that the IHS assumption, the isotope signature of pre-event or event water is constant in space and time (Buttle, 1994; Klaus and McDonnell, 2013) cannot be assumed to be valid and that because the isotope signature of pre-event or event water is not constant in space and time. Thus one sequential rain sampler is not enough to get robust IHS results for small headwater catchments and that the spatial variability in the isotopic composition of rainfall can significantly influence the IHS results. It is thus necessary to sample rainfall at different locations, also in small headwater catchments, to understand the factors that control runoff generation.

6. Acknowledgments

We thank all the people who helped in the field and the laboratory. Especially we thank Ilaria Clemenzi, Michael Rinderer, Martin Šanda, Russel Smith, Stefan Plötner, Stephan Müller, Karl Steiner, Andrea Kolleger, Ellen Cerwinka, Sandra Pool, Sandra Schärer, Nadja Lavanga, Seraina Kauer, Jana Dusik, Paribesh Pradhan, Danthu Vu & Renato Winkler, Andrea Ruecker, Yves Götz, Annagreth Schuler & Werni Ruhstaller, Bruno Kägi, Claudia Schreiner, Michael Hilf, Sandra Röthlisberger and Ivan Woodhatch. We also thank the Oberallmeindkorporation Schwyz (OAK), the Department of Environment of the Canton of Schwyz and the municipality Alpthal for the good cooperation.

7. References

Allen, S. T., Keim, R. F., McDonnell, J. J., 2015. Spatial patterns of throughfall isotopic composition at the event and seasonal timescales. Journal of Hydrology 522, 58–66.

Araguás-Araguás, L., Froehlich, K., Rozanski, K., 2000. Deuterium and oxygen-18 isotope composition of precipitation and atmospheric moisture. Hydrological Processes 14 (8), 1341–1355.

Berman, E. S. F., Gupta, M., Gabrielli, C., Garland, T., McDonnell, J. J., 2009. High-frequency field-deployable isotope analyzer for hydrological applications. Water Resources Research 45 (10), n/a–n/a.

Bowen, G. J., Good, S. P., 2015. Incorporating water isoscapes in hydrological and water resource investigations. Wiley Interdisciplinary Reviews: Water 2 (2), 107–119.

Brown, V. A., McDonnell, J. J., Burns, D. A., Kendall, C., apr 1999. The role of event water, a rapid shallow flow component, and catchment size in summer stormflow. Journal of Hydrology 217 (3-4), 171–190.

Burns, D. A., 2002. Stormflow-hydrograph separation based on isotopes: the thrill is gone - what's next? Hydrological Processes 16 (7), 1515–1517.

Buttle, J. M., 1994. Isotope hydrograph separations and rapid delivery of pre-event water from drainage basins. Progress in Physical Geography 18 (1), 16–41.

Dansgaard, W., 1964. Stable isotopes in precipitation. Tellus 16 (4), 436–468.

Delavau, C., Chun, K. P., Stadnyk, T., Birks, S. J., Welker, J. M., 2015. North American precipitation isotope (δ18O) zones revealed in time series modeling across Canada and northern United States. Water Resources Research 51 (2), 1284–1299.

Fischer, B. M. C., Rinderer, M., Schneider, P., Ewen, T., Seibert, J., 2015. Contributing sources to baseflow in pre-alpine headwaters using spatial snapshot sampling. Hydrological Processes, n/a–n/a.

Fischer, B. M. C., Stähli, M., Seibert, J., 2016. Pre-event water contributions to runoff events of different magnitude in pre-alpine headwaters. Hydrology Research.

Friedman, I., Smith, G. I., 1970. Deuterium Content of Snow Cores from Sierra Nevada Area. Science 169 (3944), 467–470.

Genereux, D., 1998. Quantifying uncertainty in tracer-based hydrograph separations. Water Resources Research 34 (4), 915–919.

Goodrich, D. C., Faurès, J.-M., Woolhiser, D. A., Lane, L. J., Sorooshian, S., 1995. Measurement and analysis of small-scale convective storm rainfall variability. Journal of Hydrology 173 (1-4), 283–308.

Hegg, C., McArdell, B. W., Badoux, A., 2006. One hundred years of mountain hydrology in Switzerland by the WSL. Hydrological Processes 20 (2), 371–376.

Holko, L., Dóša, M., Michalko, J., Kostka, Z., 2012. Isotopes of oxygen-18 and deuterium in precipitation in Slovakia. ournal of Hydrology and Hydromechanics 60 (4), 265–276.

Hrachowitz, M., Bohte, R., Mul, M. L., Bogaard, T. A., Savenije, H. H. G., Uhlenbrook, S., 2011. On the value of combined event runoff and tracer analysis to improve understanding of catchment functioning in a data-scarce semi-arid area. Hydrology and Earth System Sciences 15 (6), 2007–2024.

James, A. L., Roulet, N. T., 2009. Antecedent moisture conditions and catchment morphology as controls on spatial patterns of runoff generation in small forest catchments. Journal of Hydrology 377 (3-4), 351–366.

Jordan, J., 1994. Spatial and temporal variability of stormflow generation processes on a Swiss catchment. Journal of Hydrology 153 (1-4), 357–382.

Katsuyama, M., Yoshioka, T., Konohira, E., 2015. Spatial distribution of oxygen-18 and deuterium in stream waters across the Japanese archipelago. Hydrology and Earth System Sciences 19 (3), 1577–1588.

Kennedy, V. C., Zellweger, G. W., Avanzino, R. J., 1979. Variation of rain chemistry during storms at two sites in northern California. Water Resources Research 15 (3), 687–702.

Kern, Z., Kohán, B., Leuenberger, M., feb 2014. Precipitation isoscape of high reliefs: interpolation scheme designed and tested for monthly resolved precipitation oxygen isotope records of an Alpine domain. Atmos. Chem. Phys. 14 (4), 1897–1907.

Klaus, J., McDonnell, J. J., nov 2013. Hydrograph separation using stable isotopes: Review and evaluation. Journal of Hydrology 505, 47–64.

Krupa, S. V., dec 2002. Sampling and physico-chemical analysis of precipitation: a review. Environmental Pollution 120 (3), 565–594.

Laquer, F. C., 1990. Sequential precipitation samplers: A literature review. Atmospheric Environment. Part A. General Topics 24 (9), 2289–2297.

Laudon, H., Seibert, J., Köhler, S., Bishop, K., 2002. Hydrological flow paths during snowmelt: Congruence between hydrometric measurements and oxygen 18 in meltwater, soil water, and runoff. Water Resources Research 40 (3), W03102.

Lyon, S. W., Desilets, S. L. E., Troch, P. A., jun 2008. Characterizing the response of a catchment to an extreme rainfall event using hydrometric and isotopic data. Water Resources Research 44 (6).

Lyon, S. W., Desilets, S. L. E., Troch, P. A., 2009. A tale of two isotopes: differences in hydrograph separation for a runoff event when using δD versus δ18O. Hydrological Processes 23 (14), 2095–2101.

McDonnell, J. J., Beven, K., 2014. DebatesâĂŤThe future of hydrological sciences: A (common) path forward? A call to action aimed at understanding velocities, celerities and residence time distributions of the headwater hydrograph. Water Resources Research 50 (6), 5342–5350.

McDonnell, J. J., Bonell, M., Stewart, M. K., Pearce, A. J., 1990. Deuterium Variations in Storm Rainfall: Implications for Stream Hydrograph Separation. Water Resources Re 26 (3), 455–458.

McGuire, K., McDonnell, J., 2008. Stable Isotope Tracers in Watershed Hydrology. In: Stable Isotopes in Ecology and Environmental Science. Blackwell Publishing Ltd, pp. 334–374.

McGuire, K. J., McDonnell, J. J., Weiler, M., Kendall, C., McGlynn, B. L., Welker, J. M., Seibert, J., 2005. The role of topography on catchment-scale water residence time. Water Resources Research 41 (5), 1–14.

Menzel, L., Lang, H., Martin, R., 2007. Mean Annual Actual Evaporation 1973âĂŞ1992. In: Hydrological Atlas of Switzerland, 9th Edition. Federal Office for the Environment FOEN, Bern, Ch. 4.1, p. 4.1.

Munksgaard, N. C., Wurster, C. M., Bass, A., Bird, M. I., 2012. Extreme short-term stable isotope variability revealed by continuous rainwater analysis. Hydrological Processes 26 (23), 3630–3634.

Pellerin, B. A., Wollheim, W. M., Feng, X., Vörösmarty, C. J., 2008. The application of electrical conductivity as a tracer for hydrograph separation in urban catchments. Hydrological Processes.

Penna, D., Stenni, B., Šanda, M., Wrede, S., Bogaard, T. a., Gobbi, A., Borga, M., Fischer, B. M. C., Bonazza, M., Chárová, Z., aug 2010. On the reproducibility and repeatability of laser absorption spectroscopy measurements for δ2H and δ18O isotopic analysis. Hydrology and Earth System Sciences 14 (8), 1551–1566.

Penna, D., van Meerveld, H. J., Oliviero, O., Zuecco, G., Assendelft, R. S., Dalla Fontana, G., Borga, M., 2014. Seasonal changes in runoff generation in a small forested mountain catchment. Hydrological Processes 29 (8), 2027–2042.

Roa-García, M. C., Weiler, M., aug 2010. Integrated response and transit time distributions of watersheds by combining hydrograph separation and long-term transit time modeling. Hydrology and Earth System Sciences 14 (8), 1537–1549.

Roe, G. H., 2005. Orographic precipitation. Annual review of earth and planetary sciences 33, 645–671.

Schürch, M., Kozel, R., Schotterer, U., Tripet, J.-P., 2003. Observation of isotopes in the water cycleâĂŤthe Swiss National Network (NISOT). Environmental Geology 45 (1), 1–11.

Seeger, S., Weiler, M., dec 2014. Reevaluation of transit time distributions, mean transit times and their relation to catchment topography. Hydrol. Earth Syst. Sci. 18 (12), 4751–4771.

Sklash, M. G., Farvolden, R. N., Fritz, P., 1976. A conceptual model of watershed response to rainfall, developed through the use of oxygen-18 as a natural tracer. Canadian Journal of Earth Sciences 13 (2), 271–283.

Smith, G. I., Friedman, I., Klieforth, H., Hardcastle, K., 1979. Areal Distribution of Deuterium in Eastern California Precipitation, 1968âĂŞ1969. Journal of Applied Meteorology 18 (2), 172–188.

Tweed, S., Munksgaard, N., Marc, V., Rockett, N., Bass, A., Forsythe, A. J., Bird, M. I., Leblanc, M., 2016. Continuous monitoring of stream δ18O and δ2H and stormflow hydrograph separation using laser spectrometry in an agricultural catchment. Hydrological Processes 30 (4), 648–660.

Vachaud, G., Passerat De Silans, A., Balabanis, P., Vauclin, M., 1985. Temporal Stability of Spatially Measured Soil Water Probability Density Function. Soil Science Society of America Journal 49.

Vitvar, T., Balderer, W., 1997. Estimation of mean water residence times and runoff generation by180 measurements in a Pre-Alpine catchment (Rietholzbach, Eastern Switzerland). Applied Geochemistry 12 (6), 787–796.

8. Supplements

Table 3: The number of samples (n), the maximum, mean and minimum δ^{18}O [‰] for the different rain sampling locations (rows) and the different events (columns). n RG represents the number of rain sampling locations for which rainfall was collected throughout the entire event.The number of stream water samples (n), the δ^{18}O [‰] of pre-event water (C_{pe}), and the maximum and minimum measured δ^{18}O [‰] of streamwater for the 10 different events in the three headwater catchments.

event nr.	1	2	3	4	5	6	9	10	11	12
n RG	7	8	4	8	4	8	6	6	6	6
WG-01 n		4	25	2	11	4	4	5	11	4
max		-4.6	-8.39	-7.82	-4.61	-6.89	-2.9	-5.39	-3.15	-4.37
mean		-5.35	-13.38	-8.17	-6.68	-7.91	-4.52	-6.89	-8.36	-7.77
min		-6.63	-16.41	-8.53	-9.35	-8.95	-5.27	-7.59	-13.33	-11.7
range		2.03	8.02	0.72	4.74	2.07	2.37	2.2	10.17	7.34
TB-01 n	5	3	12*	2		6				
max	-8.03	-5.52	-8.25	-7.43		-7.26				
mean	-10.48	-5.93	-13.77	-9.32		-8.71				
min	-11.86	-6.59	-20.21	-11.21		-9.42				
range	3.84	1.08	11.95	3.78		2.16				
TB-06 n	4	3	19	3	10	4	5	4	12	3
max	-8.32	-5.12	-8.87	-7.35	-4.61	-5.1	-2.36	-4.96	-3.75	-4.64
mean	-10.36	-5.5	-13.75	-8.15	-6.78	-8.16	-4.27	-6.74	-7.54	-8.05
min	-11.63	-5.73	-20.4	-8.7	-9.35	-9.33	-5.68	-7.52	-12.67	-11.88
range	3.31	0.6	11.53	1.35	4.74	4.23	3.32	2.56	8.92	7.24
TB-07 n	5	3	18	3		6	4	4	11	5
max	-8.05	-5.12	-10.12	-6.97		-4.84	-2.36	-4.96	-3.75	-4.25
mean	-10.34	-5.38	-13.7	-7.95		-7.91	-4.44	-6.74	-7.84	-6.87
min	-11.38	-5.5	-19.5	-8.5		-9.63	-5.68	-7.52	-12.67	-10.86
range	3.33	0.38	9.38	1.52		4.79	3.32	2.56	8.92	6.6
TB-09 n	5	4	9*	3		4		3	4*	5
max	-7.79	-6.02	-8.93	-8.62		-5.53		-5.26	-5.06	-4.83
mean	-10.65	-6.29	-13.51	-9.05		-8.54		-6.88	-9.06	-9.61
min	-12.03	-6.55	-15.3	-9.64		-10.14		-7.62	-13.28	-12.77
range	4.24	0.53	6.37	1.03		4.61		2.36	8.21	7.94
TB-10 n	5	3	5*	3		5	3	4	12	5
max	-8.13	-5.74	-8.88	-7.72	-5.3	-5.7	-3.16	-6.78	-5.35	-4.75
mean	-10.6	-6.46	-13.36	-8.53	-7.45	-8.32	-4.83	-7.32	-7.4	-7.8
min	-11.8	-7.87	-17.33	-9.06	-9.56	-9.66	-6.21	-7.59	-9.72	-10.9
range	3.67	2.13	8.45	1.34	4.26	3.97	3.05	0.81	4.37	6.14
TB-11 n	5	4	13*	3	11	4	3	3	4*	4
max	-8.31	-5.28	-8.94	-7.19	-4.83	-5.46	-3.32	-5.06	-5.31	-4.51
mean	-10.49	-6.07	-13.9	-8.05	-5.66	-8.46	-4.66	-9.06	-5.83	-7.36
min	-11.53	-7.51	-20.25	-8.64	-6.62	-9.87	-5.7	-13.28	-6.56	-11.83
range	3.21	2.23	11.31	1.45	1.79	4.42	2.38	0.7	1.25	7.32
TB-12 n	4	3	13*	2		6	3	4	9	
max	-9.12	-6.11	-10.62	-7.97		-5.32	-3.02	-6.19	-5.38	
mean	-10.67	-6.65	-14.24	-8.38		-8.79	-4.25	-7.01	-7.35	
min	-11.62	-7.69	-17.32	-8.8		-10	-4.98	-7.43	-9.16	
range	2.51	1.58	6.7	0.84		4.68	1.96	1.24	3.78	
M_{TR}	3.44	1.32	9.35	1.5	3.88	3.86	2.73	1.78	8	7.1
S_R	0.34	1.31	0.39	1.37	1.79	0.88	0.57	0.57	1.71	2.74

Table 4: The number of stream water samples (n), the δ^{18}O [‰] of pre-event water (C_{pe}), and the maximum and minimum measured δ^{18}O [‰] of streamwater for the 10 different events in the three headwater catchments.

Event	1	2	3	4	5	6	9	10	11	12
WS04 C_{pe}		-10.5	-10.4		-10.7	-8.45	-8.5	-8.51	-8.96	-9.01
n		23	46		23	15	10	20	26	29
C_{smax}		-9.59	-10.4		-7.03	-8.67	-8.51	-8.08	-8.3	-8.01
Cs min		-10.53	-12.94		-8.81	-9.73	-8.82	-9.23	-9.28	-9.07
WS10 C_{pe}	-10.64		-10.42	-10.7	-9.43		-10.24	-9.79	-8.95	-9.75
n	24		53	24	35		8	10	20	23
C_{smax}	-10.35		-10.42	-10.27	-7.38		-8.4	-8.27	-8.17	-8.65
Cs min	-10.79		-12.42	-10.88	-9.44		-10.24	-8.75	-9.52	-9.76
WS19 C_{pe}	-10.46	-10.19	-10.26	-11.3	-9.1	-8.9				-8.79
n	24	23	54	24	34	13				22
C_{smax}	-9.8	-8.92	-10.26	-10.35	-6.82	-8.55				-7.08
Cs min	-11.04	-10.46	-14.32	-10.89	-8.54	-8.75				-8.8

8.4 Paper IV - Spectroscopy

Technical Note: Evaluation of between-sample memory effects in the analysis of δ^2H and δ^{18}O of water samples measured by laser spectroscopes

Hydrol. Earth Syst. Sci., 16, 3925–3933, 2012
www.hydrol-earth-syst-sci.net/16/3925/2012/
doi:10.5194/hess-16-3925-2012

Hydrology and Earth System Sciences

Technical Note: Evaluation of between-sample memory effects in the analysis of δ^2H and δ^{18}O of water samples measured by laser spectroscopes

D. Penna[1,2], B. Stenni[3], M. Šanda[4], S. Wrede[5,8], T. A. Bogaard[6], M. Michelini[3], B. M. C. Fischer[7], A. Gobbi[1], N. Mantese[1], G. Zuecco[1], M. Borga[1], M. Bonazza[3], M. Sobotková[4], B. Čejková[9], and L. I. Wassenaar[10]

[1]Department of Land, Environment, Agriculture and Forestry, University of Padova, Italy
[2]Faculty of Science and Technology, Free University of Bozen-Bolzano, Italy
[3]Department of Mathematics and Geosciences, University of Trieste, Italy
[4]Faculty of Civil Engineering, Czech Technical University in Prague, Czech Republic
[5]Department of Hydrology, University of Trier, Germany
[6]Faculty of Civil Engineering and Geosciences, Delft University of Technology, The Netherlands
[7]Department of Geography, University of Zürich, Switzerland
[8]Department of Environment and Agro-Biotechnologies, Centre de Recherche Public – Gabriel Lippmann, Luxembourg
[9]Czech Geological Survey, Prague, Czech Republic
[10]Isotope Hydrology Laboratory, International Atomic Energy Agency, Vienna

Correspondence to: D. Penna (daniele.penna@unipd.it)

Received: 19 March 2012 – Published in Hydrol. Earth Syst. Sci. Discuss.: 20 April 2012
Revised: 31 August 2012 – Accepted: 7 October 2012 – Published: 31 October 2012

Abstract. This study evaluated between-sample memory in isotopic measurements of δ^2H and δ^{18}O in water samples by laser spectroscopy. Ten isotopically depleted water samples spanning a broad range of oxygen and hydrogen isotopic compositions were measured by three generations of off-axis integrated cavity output spectroscopy and cavity ring-down spectroscopy instruments. The analysis procedure encompassed small (less than 2 ‰ for δ^2H and 1 ‰ for δ^{18}O) and large (up to 201 ‰ for δ^2H and 25 ‰ for δ^{18}O) differences in isotopic compositions between adjacent sample vials. Samples were injected 18 times each, and the between-sample memory effect was quantifie for each analysis run. Results showed that samples adversely affected by between-sample isotopic differences stabilised after seven–eight injections. The between-sample memory effect ranged from 14 % and 9 % for δ^2H and δ^{18}O measurements, respectively, but declined to negligible carryover (between 0.1 % and 0.3 % for both isotopes) when the firs ten injections of each sample were discarded. The measurement variability (range and standard deviation) was strongly dependent on the isotopic difference between adjacent vials. Standard deviations were up to 7.5 ‰ for δ^2H and 0.54 ‰ for δ^{18}O when all injections were retained in the computation of the reportable δ-value, but a significan increase in measurement precision (standard deviation in the range 0.1 ‰–1.0 ‰ for δ^2H and 0.05 ‰–0.17 ‰ for δ^{18}O) was obtained when the firs eight injections were discarded. In conclusion, this study provided a practical solution to mitigate between-sample memory effects in the isotopic analysis of water samples by laser spectroscopy.

1 Introduction

The use of laser absorption spectroscopy for the determination of water stable isotopes (δ^2H and δ^{18}O, VSMOW-SLAP scale) in water samples is becoming increasingly common worldwide. The availability of lower cost off-axis integrated cavity output spectroscopy (OA-ICOS) instruments and cavity ring-down spectroscopy (CRDS) devices compared to isotope-ratio mass spectrometers (IRMS), allowed researchers to take greater advantage of water isotopes as tracers in hydrological studies. Several studies tested the

performance of OA-ICOS (Lis et al., 2008; Wassenaar et al., 2008; IAEA, 2009b; West et al., 2010; Schultz et al., 2011) and CRDS instruments (Brand et al., 2009; Chesson et al., 2010; Gkinis et al., 2010) for the analysis of water samples, revealing very good comparability with isotope-ratio mass spectrometric techniques. Given the relatively recent advent of laser spectroscopy in hydrological laboratories, some practical aspects and shortcomings in the fiel of water research remain unexplored.

Recently, a comparative study of OA-ICOS spectroscopes tested against a mass spectrometer found poor accuracy of laser spectroscopy results specificall for isotopically depleted water samples (Penna et al., 2010). This poor accuracy was related to between-sample memory effects (MEs) – define as the carryover of the sample being measured by traces of the previous water sample(s) (Olsen et al., 2006). Here we assessed the practical implications of the analysis of water samples characterised by a wide range of isotopic values and different conditions (under which the occurrence of MEs might significantl influenc the fina isotopic measurement) on the performance of different laser spectroscopes. For this experiment we tested three OA-ICOS and CRDS instruments of different generations using a set of ten isotopically depleted water samples.

2 Materials and methods

2.1 Laser spectroscopes and mass spectrometer

The water samples were analysed by six laser spectroscopes (three OA-ICOS: Delft University of Technology, the Netherlands, Czech Technical University in Prague and Czech Geological Survey, Czech Republic; three CRDS instruments: University of Trieste, Italy, University of Zürich, Switzerland, International Atomic Energy Agency, Vienna, Austria) and one mass spectrometer (University of Trieste), used as reference. Due to the rapid evolution of laser spectroscopy technology, we tested early and new generation instruments. The spectroscopes included:

1. OA-ICOS: one Liquid Water Isotope Analyser, model DLT-100 version 908-0008 (firs generation), one version 908-0008-2000 (second generation) and one version 908-0008-3000 (third generation), manufactured by Los Gatos Research Inc. (LGR, Mountain View, California, USA). These instruments are referred to as "LGR-1", "LGR-2" and "LGR-3", respectively. The volume of water for each injection was 750 nl. According to the manufacturer's specification (Los Gatos Research, Inc., 2008), the 1-σ measurement precision was below 0.6 ‰ for δ^2H and 0.1 ‰ for δ^{18}O.

2. CRDS: two Picarro L1102-i liquid analysers (firs generation) and one L2130-i (second generation), manufactured by Picarro (Picarro, Santa Clara, California, USA), named "PIC-1", "PIC-2" (firs generation) and "PIC-3" (second generation). The volume of water for each injection was 2 µl. The manufacturer reported the 1-σ measurement precision below 0.5 ‰ for δ^2H and 0.1 ‰ for δ^{18}O (Picarro, Inc., 2008).

3. IRMS: one Thermo Fischer Delta Plus Advantage mass spectrometer (Thermo Fisher Scientifi Inc., Massachusetts, USA) connected to a GFL 1086 equilibration device. The measurements were carried out with a classical dual-inlet system using a CO_2/H_2 water equilibration technique (Epstein and Mayeda, 1953; Horita et al., 1989). The external 1-σ precision of the instrument was $\pm$0.7 ‰ and $\pm$0.05 ‰ for δ^2H and δ^{18}O measurements, respectively.

For all instruments we used new syringes, adopting the analysis specification as recommended by the manufacturers. Before each analysis run, we performed the standard maintenance, such as changing the injection port septum and checking that the transfer line and the injection block were cleaned.

Further information regarding the theory of operation of the two laser systems is reported elsewhere (OA-ICOS: Sayres et al., 2009; Wang et al., 2009; CRDS: Brand et al., 2009; Gkinis et al., 2010).

2.2 Samples and analysis scheme

The comparative test was performed on ten isotopically depleted samples derived from snow surface samples collected at different locations in Antarctica, provided by the Isotope Geochemistry Laboratory of the University of Trieste. The isotopic composition of the samples ranged from $-$231.7 ‰ to $-$421.1 ‰ for δ^2H and from $-$29.83 ‰ to $-$53.41 ‰ for δ^{18}O. Each sample was analysed ten times by IRMS and the average and standard deviation values were reported (Table 1). Three laboratory measurement standards that bracketed the isotopic composition of the samples were used. These measurement standards were calibrated against IAEA (International Atomic Energy Agency) water standards (Gonfi ntini, 1978) in relation to the VSMOW-SLAP scale and normalised adopting the procedure described in IAEA (2009a). All samples and standards were pipetted into ND8 32 $\times$ 11.6 mm screw neck 1.5 ml vials with PTFE/silicone/PTFE septa with 1 ml of water sample. Vial fillin was done in the same laboratory to ensure sample consistency at all test locations. The samples were measured following the procedure suggested by the Isotope Hydrology Laboratory at IAEA (IAEA, 2009b) and tested by Penna et al. (2010). The scheme consisted of two measurement standards, interpolated by a linear regression, and a control standard not included in the calibration. The regression between measurements and known δ-values for calibration standards was used to convert the measured absolute isotopic ratios to respective δ-values. We adopted a modifie version of this template, sampling each vial 18 times instead of six times in

Table 1. Isotopic compositions of samples and laboratory measurement standards. The reported values represent the average and the standard deviation of ten replicates.

ID	δ^2H (‰)	Std. dev. δ^2H (‰)	δ^{18}O (‰)	Std. dev. δ^{18}O (‰)
1	−231.7	0.5	−29.83	0.02
2	−258.7	0.4	−33.07	0.01
3	−277.5	0.5	−34.96	0.02
4	−303.8	0.4	−38.26	0.03
5	−312.2	0.6	−39.47	0.02
6	−334.7	0.4	−42.24	0.02
7	−338.5	0.5	−43.73	0.02
8	−373.1	0.4	−48.02	0.02
9	−390.4	0.5	−50.20	0.02
10	−421.1	0.5	−53.41	0.02
STD1	−221.8	0.5	−29.06	0.04
STD2	−313.8	0.4	−40.22	0.02
STD3	−422.8	0.4	−53.83	0.02

order to better observe the sequential trend of MEs. The water samples were grouped in two sets of f ve interposed by three triplets of laboratory measurement standards. Each run was started with a dummy sample to prime the transfer line and stabilise the machine and ended with deionised water to clean the syringe (IAEA, 2009b).

We took advantage of the wide isotopic range of the samples and measurement standards in designing the analysis sequence template presented in Table 2, where some adjacent vials were very close in isotopic composition, whereas others differed markedly. This allowed us to test the performance for a broad range of differences in isotopic compositions between adjacent vials (the lowest absolute difference between the heaviest and lightest water was approximately 2 ‰ for δ^2H and 1 ‰ for δ^{18}O, whereas the highest absolute difference between the isotopically heavier and lighter water was approximately 201 ‰ for δ^2H and 25 ‰ for δ^{18}O (Table 2).

ME was computed following Gröning (2011), assuming a constant memory decrease over time. For each pair of adjacent vials, we considered the isotopic difference (d) between the mean of the last three injections of the two samples as their true isotopic difference:

$$d = \left(\overline{i_{18}, i_{17}, i_{16}}\right)_k - \left(\overline{i_{18}, i_{17}, i_{16}}\right)_j \quad (1)$$

where i_{18}, i_{17} and i_{16} represent the isotopic content of the last injections in the sequence, k is a sample and j is the previous sample with respect to k. However, instead of using the value of the last injection as the true value (as in Gröning, 2011), the mean of the last three was computed to avoid possible influence of random flu tuations or the occurrence of "bad injections" (Penna et al., 2010). In the following, the isotopic difference (e) between the average of the last three injections of the second sample and its fi st injection was computed as

$$e = \left(\overline{i_{18}, i_{17}, i_{16}}\right)_k - (i_1)_k \quad (2)$$

where i_1 represents the isotopic content of the firs injection of sample k. The computation of (e) was repeated for all injections of samples k. The ratio f:

$$f = \frac{e}{d} \quad (3)$$

constituted an approximation of ME. The fina value of ME was determined considering an exponential decline with time and multiplying, for each injection of the series, the f-value times a reduction factor (RF) define as follows:

$$\mathrm{RF} = \frac{f}{c} \quad (4)$$

where c was computed as:

$$c = f + f^2 + f^3 \quad (5)$$

to take into account the (most likely small) contribution of previous injections of the firs sample to the total ME (Gröning, 2011).

3 Results and discussion

3.1 Measurement stabilisation and memory effect

The graphs in Fig. 1a, b display the δ^2H and δ^{18}O values of the second triplet of laboratory measurement standards for each instrument, as a function of the number of injections performed during the run (i.e., trend over time during the run). For the firs injections, the curves referring to the second and the third standards (STD2 and STD3) showed a deviation from the δ-values obtained during the central and fina part of the run. On average, at least seven or eight injections were required in order to obtain stable values (i.e., to observe variations between successive injections within the range of the instrumental precision). Conversely, the firs measurement standard (STD1) exhibited more stable behaviour over time. STD2 and STD3 represented waters most affected by high inter-vial isotopic difference, whereas STD1, in the second triplet, was characterised by a relatively small isotopic difference with respect to the composition of the antecedent vial (Table 2). In addition, the same plots were drawn for other samples (not shown), featuring much smaller isotopic difference compared to the previous vial, but almost no variations after the firs two or three injections were observed. Therefore, we related this behaviour to the tendency of each laser spectroscope to buffer the influenc of the isotopic content of the previous sample during the run. This effect was observed for both isotopes, even though the trend for δ^{18}O was generally more variable than for δ^2H. The effect was observable on all spectroscopes, but slightly less evident on CRDS instruments. However, for both laser technologies and particularly for OA-ICOS instruments, the newest generations of instruments showed a marked performance improvement in the stabilisation effect (i.e., smaller difference between the values at the beginning and in the central-fina part

Table 2. Sequence of samples and standards in the analysis run and absolute isotopic differences (IRMS values) between each vial and the previous. DW: deionised water. STD: laboratory measurement standard. Number: sample ID. All values are rounded to improve the readability.

	DW	STD 1	STD 3	STD 2	5	4	3	2	1	STD 1	STD 2	STD 3	6	7	8	9	10	STD 1	STD 3	STD 2
δ^2H difference (‰)	–	166	201	109	2	8	26	19	27	10	201	109	21	4	35	17	31	199	201	109
δ^{18}O difference (‰)	–	21	25	14	1	1	3	2	3	1	25	14	2	1	4	2	3	24	25	14

Figures

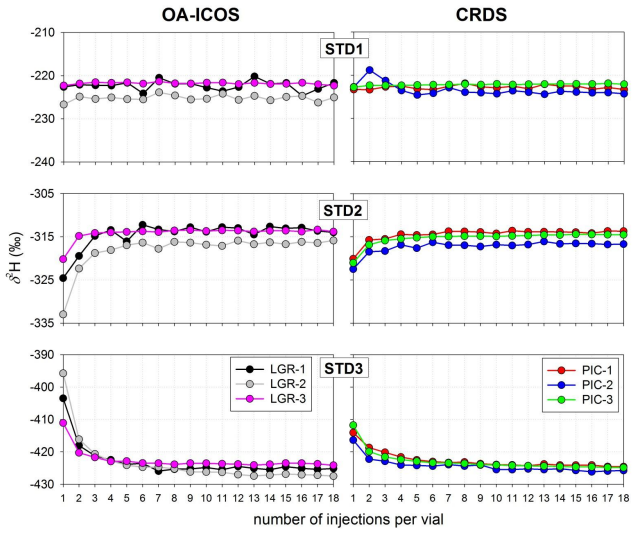

Figure 1a. Sample isotopic stabilization by sequential injection number for three laboratory measurement standards (second triplet in an analysis run) for hydrogen. Left column: OA-ICOS instruments. Right column: CRDS instruments.

Fig. 1a. Measurement stabilisation by sequential injection number for three laboratory measurement standards (second triplet in an analysis run) for hydrogen. Left column: OA-ICOS instruments. Right column: CRDS instruments.

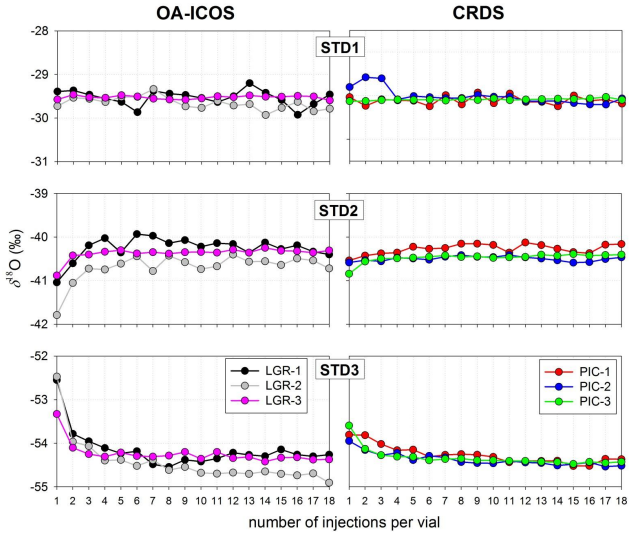

Figure 1b. Measurement stabilization by sequential injection number for three laboratory measurement standards (second triplet in an analysis run) for oxygen. Left column: OA-ICOS instruments. Right column: CRDS instruments.

Fig. 1b. Measurement stabilisation by sequential injection number for three laboratory measurement standards (second triplet in an analysis run) for oxygen. Left column: OA-ICOS instruments. Right column: CRDS instruments.

of the run compared to earlier models) and in the overall low variability (i.e., precision) of the measurements.

Figure 2 shows the ME for the transition between STD1 and STD3 (third triplet in the run), the situation when the highest isotopic difference between adjacent vials occurred. The ME was greater for hydrogen than for oxygen, as observed elsewhere (Gupta et al., 2009). For OA-ICOS instruments the maximum ME ranged approximately from 6 % to 14 % for δ^2H measurements and from 4 % to 9 % for δ^{18}O measurements. For CRDS instruments, the maximum ME ranged approximately from 4 % to 6 % and from 2 % to 4 % for δ^2H and δ^{18}O, respectively. The analysis revealed that the firs eight–ten injections were most affected by MEs for all instruments, whereas the fina six–eight injections exhibited negligible MEs. This was confirme by observing the average and standard deviation of MEs computed separately for the fi st ten and the last eight injections (Table 3a, b). The dataset in this Table was formed by the 18 injections performed during each of the three transitions in an analysis run (considered together) between STD1 and STD3. Analysis of Table 3a, b clearly confirmed for both isotopes and for all spectroscopes, the smaller MEs for the last eight injections out of 18 compared to the firs ten injections. Overall, the average and the standard deviation of MEs ranged between 0.8 % and 3.0 % and between 0.8 % and 3.9 %, respectively, when considering the firs ten injections. However, average values ranged from 0.1 % to 0.3 % for both hydrogen and oxygen isotope species and standard deviation values ranged from 0.1 % to 0.6 % when the last eight injections were considered. This suggests that, even for very high differences in isotopic composition of subsequent samples, discarding the firs ten injections and averaging the remaining ones prevents the fina δ-value from being affected by MEs. Furthermore, Table 3a, b reveals that, on average, ME values were similar for both OA-ICOS and CRDS instruments, the only appreciable difference being the higher percentages of OA-ICOS spectroscopes for the firs two or three injections (Fig. 2).

It is worth noticing that ME values were, on average, slightly lower for the most recent spectroscope models, compared to early ones. Improvement in the reduction of MEs, reflecte also in lower standard deviations of ME, was particularly evident in third generation OA-ICOS instruments (LGR-3), for which discarding six injections would provide an effective solution. Conversely, LGR-2 showed the highest

Table 3a. Average and standard deviations of memory effects (hydrogen) considering the firs ten and the last eight injections out of 18 for three transitions in an analysis run (considered together) between STD1 and STD3.

	First 10 out of 18 injections						Last 8 out of 18 injections					
	LGR-1	LGR-2	LGR-3	PIC-1	PIC-2	PIC-3	LGR-1	LGR-2	LGR-3	PIC-1	PIC-2	PIC-3
Number of samples	30	30	30	30	30	30	24	24	24	24	24	24
Average (%)	1.9	3.0	1.1	1.4	1.3	1.5	0.3	0.2	0.1	0.2	0.2	0.1
Std. deviation (%)	2.9	3.9	1.7	1.3	1.7	1.7	0.3	0.6	0.1	0.1	0.2	0.1

Table 3b. Average and standard deviations of memory effects (oxygen) considering the firs ten and the last eight injections out of 18 for three transitions in an analysis run (considered together) between STD1 and STD3.

	First 10 out of 18 injections						Last 8 out of 18 injections					
	LGR-1	LGR-2	LGR-3	PIC-1	PIC-2	PIC-3	LGR-1	LGR-2	LGR-3	PIC-1	PIC-2	PIC-3
Number of samples	30	30	30	30	30	30	24	24	24	24	24	24
Average (%)	1.4	2.4	0.8	1.0	1.0	1.1	0.3	0.2	0.2	0.1	0.2	0.1
Std. deviation (%)	2.0	2.5	1.1	0.8	1.2	1.0	0.4	0.5	0.1	0.1	0.1	0.1

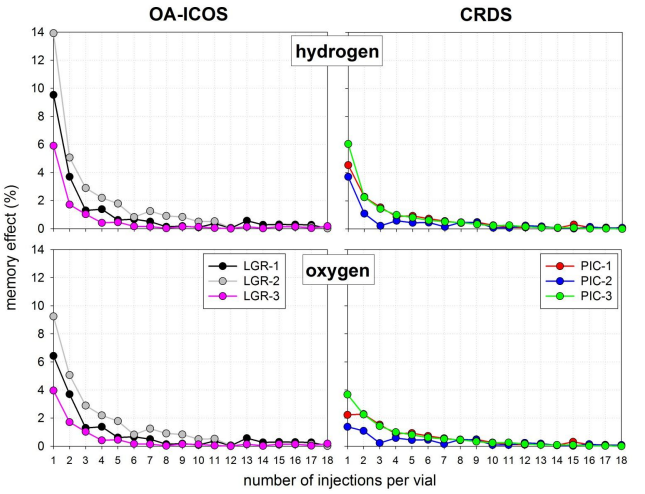

Figure 2. MEs as a function of the number of sequential injections of the same vial for the transition between STD1 and STD3 (third triplet in an analysis run). Upper row: hydrogen. Lower row: oxygen. Left column: OA-ICOS instruments. Right column: CRDS instruments.

Fig. 2. MEs as a function of the number of sequential injections of the same vial for the transition between STD1 and STD3 (third triplet in an analysis run). Upper row: hydrogen. Lower row: oxygen. Left column: OA-ICOS instruments. Right column: CRDS instruments.

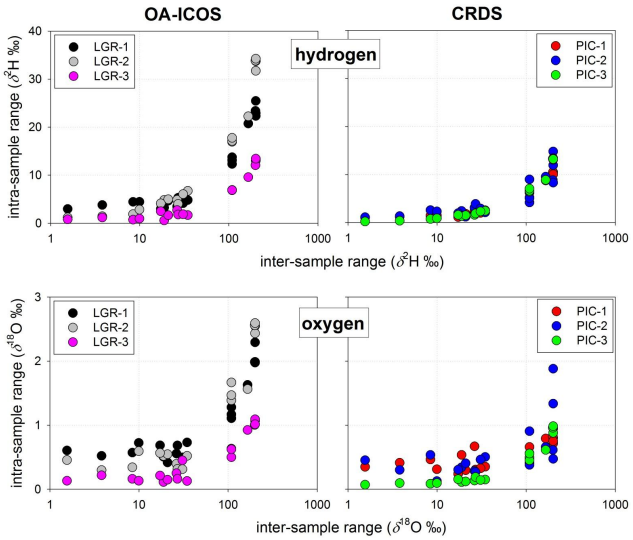

Figure 3. Relation between the isotopic range (maximum-minimum) within each vial (either sample or measurement standard) and the absolute isotopic difference between adjacent vials in the tray. Upper row: hydrogen. Lower row: oxygen. Left column: OA-ICOS instruments. Right column: CRDS instruments.

Fig. 3. Relation between the isotopic range (maximum–minimum of 18 injections) within each vial (either sample or measurement standard) and the absolute isotopic difference between adjacent vials in the tray. Upper row: hydrogen. Lower row: oxygen. Left column: OA-ICOS instruments. Right column: CRDS instruments.

percentage of ME (Fig. 2 and Table 3a, b), even higher than the firs generation machine (LGR-1). This difference did not seem to be related to any specifi variable, since all machines were routinely cleaned and maintained and the sampling conditions were the same for all instruments. An intrinsic variability for one specifi instrument could be assumed, but further analyses are necessary to verify such behaviour.

Theoretically, the difference in MEs between OA-ICOS and CRDS devices (Fig. 2) or the different amount of ME between instruments of various generations (Table 3a, b, especially for LGR machines) might be related to the different analysis times for each injected water sample. In fact, long analysis times (including longer between-sample cavity vacuum pumping) could facilitate the removal of water molecules of the previous sample from the system. Conversely, short analysis times could allow for the persistence of residual water molecules in the vacuum chamber. However, based on our analyses, a dependency on analysis time was not found. In general, LGR-1 (firs generation) took 245 s to inject and measure a sample, LGR-2 (second generation) took 140 s and LGR-3 (third generation) took only 77 s. Nevertheless, the highest values of ME were not observed for the "slowest" firs generation machine, as might have been

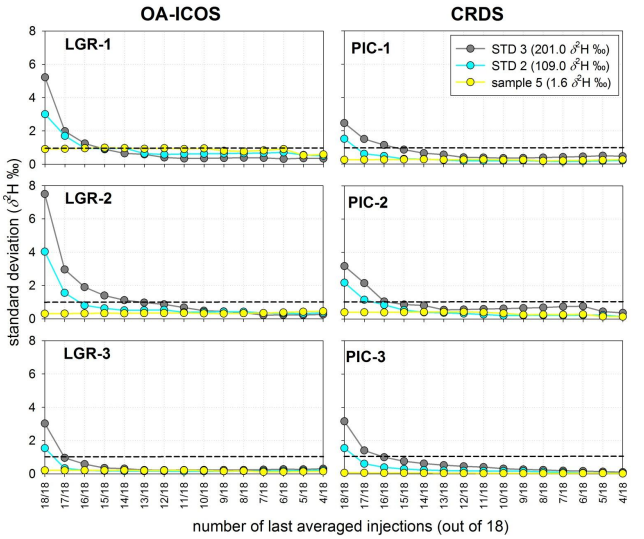

Figure 4a. Standard deviation for δ^2H for two laboratory measurement standards and one sample as a function of number of averaged injections. 18/18 indicates that all 18 injections of the same vial (either standard or sample) were averaged, whereas 17/18, 16/18, 15/18... indicates that only the last 17, 16, 15... injections were averaged (and the remaining discarded). The dotted horizontal line indicates currently acceptable reference precision for δ^2H (1 ‰). The legend depicts the difference between the isotopic composition of the standard/sample displayed and the isotopic composition of the previous vial analysed in the tray.

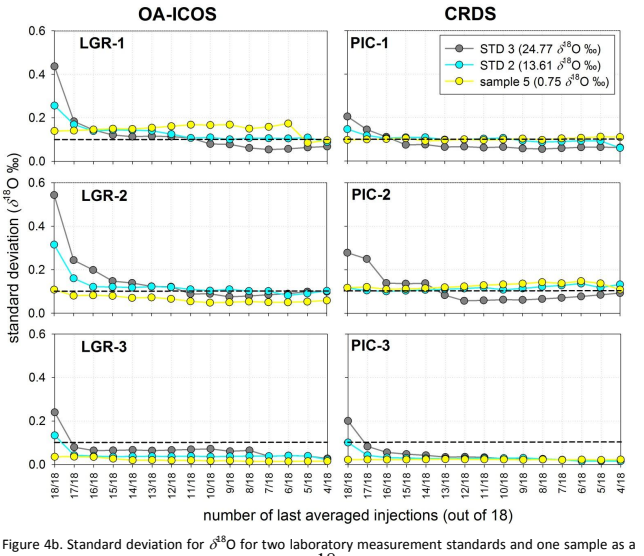

Figure 4b. Standard deviation for δ^{18}O for two laboratory measurement standards and one sample as a function of number of averaged injections. 18/18 indicates that all 18 injections of the same vial (either standard or sample) were averaged, whereas 17/18, 16/18, 15/18... indicates that only the last 17, 16, 15... injections were averaged (and the remaining discarded). The dotted horizontal line indicates an acceptable reference precision for δ^{18}O (0.1 ‰). The legend depicts the difference between the isotopic composition of the standard/sample displayed and the isotopic composition of the previous vial analysed in the tray.

Fig. 4a. Standard deviation for δ^2H for two laboratory measurement standards and one sample as a function of number of averaged injections. 18/18 indicates that all 18 injections of the same vial (either standard or sample) were averaged, whereas 17/18, 16/18, 15/18... indicates that only the last 17, 16, 15... injections were averaged (and the remaining discarded). The dotted horizontal line indicates currently acceptable reference precision for δ^2H (1 ‰). The legend depicts the difference between the isotopic composition of the standard/sample displayed and the isotopic composition of the previous vial analysed in the tray.

Fig. 4b. Standard deviation for δ^{18}O for two laboratory measurement standards and one sample as a function of number of averaged injections. 18/18 indicates that all 18 injections of the same vial (either standard or sample) were averaged, whereas 17/18, 16/18, 15/18... indicates that only the last 17, 16, 15... injections were averaged (and the remaining discarded). The dotted horizontal line indicates an acceptable reference precision for δ^{18}O (0.1 ‰). The legend depicts the difference between the isotopic composition of the standard/sample displayed and the isotopic composition of the previous vial analysed in the tray.

expected, and the "fastest" third generation spectroscope was not the one most affected by MEs (on the contrary, it had the lowest ME). Furthermore, CRDS lasers, that on average showed similar values of ME compared to OA-ICOS instruments, took 540 s (9 min) to perform a measurement, being more than two times, almost four times and more than six times slower than LGR-1, LGR-2 and LGR-3, respectively. Therefore, other influencin factors must explain the differences in ME between the three OA-ICOS generations and for the initial injections between the two technologies. For instance, the length of the transfer line (the longer the line, the higher are supposed the MEs), the heating of the transfer line and of the cavity (higher temperature helps the sample vaporization and likely reduces MEs), the amount of water per unit surface area of the laser cavity, the injection speed (the rate at which the water is injected into the instrument), the pump-out rate, the syringe deterioration, and the variations in vaporiser temperature might all affect the MEs. We do not have the appropriate technical insights and means to fully assess these aspects without involving the manufacturers, which is beyond the scope of this Technical Note.

Furthermore, we analysed and quantifie (data are not reported here) the occurrence of MEs when changing from a very isotopically depleted to a significantl more enriched sample (e.g., from sample 10 to STD1) and vice versa (e.g., from STD1 to STD3). No significan differences in MEs were found.

The four panels of Fig. 3 show, for hydrogen and oxygen and for the six test instruments, the intra-vial range of isotopic δ-values (i.e., maximum minus minimum, when all 18 injections were considered) as a function of the inter-vial range (i.e., the isotopic difference between waters analysed during the run). The strong linear relation (x-axis is logarithmic scale to better display low values of inter-sample difference) observed for all machines revealed that the high measurement variability, obtained when averaging all injections, was related to the isotopic differences between adjacent vials which, in turn, was related to high percentages of ME. The correlation between intra-vial and inter-vial isotopic range declined noticeably when discarding the firs four injections (from 18 to 15) and averaging only the last 14, ten or six injections, as indicated by the decreasing values of the determination coefficien (not reported here). The dependency of the 18 injection-averaged intra-vial variability on the inter-vial isotopic differences was more pronounced for the firs and second generation OA-ICOS instruments compared to firs generation CRDS instruments. However, the performance of the latest generation instruments of both manufacturers (LGR-3 and PIC-3) was almost identical.

3.2 Practical implications on measurement precision

Accepting all injections for a given analysis run, even the ones most affected by MEs, had some practical negative consequence on the measurement precision when evaluating the fina reportable δ-values. Figure 4a, b shows the values of standard deviation for two measurement standards and one sample obtained by averaging a different number of injections (starting from all 18 injections down to four). The standard deviation of the two measurement standards (STD2 and STD3 of the firs triplet), characterised by a high isotopic difference with respect to the previous vial in the tray, were compared with that of sample 5, featuring the lowest isotopic difference with respect to the previous vial in the whole run. For all instruments, the values of standard deviation for the two standards were markedly high (up to 7.5 ‰ for δ^2H and 0.54 ‰ for δ^{18}O) when all 18 injections were accepted and averaged, whereas the standard deviations decreased (i.e., measurement precision increased) with decreasing the number of averaged injections. However, when rejecting the firs six or eight injections the measurements were stable. The highest standard deviations during the firs injections were reached by STD3 (the one with the greatest isotopic difference compared to the previous vial, 201.0 ‰ for δ^2H and 24.77 ‰ for δ^{18}O) followed by STD2 (109.0 ‰ difference for δ^2H and 13.61 ‰ for δ^{18}O). Conversely, sample 5, characterised by a small isotopic difference with respect to the previous vial (1.6 ‰ for δ^2H and 0.75 ‰ for δ^{18}O) generally displayed stable values of standard deviations (in the range 0.1 ‰–1.0 ‰ for δ^2H and 0.05 ‰–0.17 ‰ for δ^{18}O) that indicated the instrumental precision. As mentioned in Sect. 3.1, standard deviations of the firs injections were higher for LGR-1 and LGR-2 compared to PIC-1 and PIC-2, but a very similar precision was achieved by the latest instruments from both manufacturers, revealing the rapid evolution and improvement of laser spectroscopy technology.

4 Conclusions and outlook

In this work, we determined the isotopic composition (δ^2H and δ^{18}O) of ten isotopically depleted water samples, characterised by a wide range of δ-values, using three OA-ICOS and CRDS instruments. We assessed the practical implications on the instrumental performance deriving from the inclusion of injections affected by memory effects (MEs). In summary, we found

1. Measurement stabilisation was reached following seven–eight injections when water samples characterised by a high inter-vial isotopic difference were measured. This behaviour, evident for both isotopes and all instruments, was attributed to the ME that directly influence the measurement variability.

2. Overall, the maximum MEs ranged from 4 % to 14 % for δ^2H and from 2 % to 9 % for δ^{18}O measurements. The firs ten injections out of the 18 were most affected by MEs, with average MEs ranging between 1.1 % and 3.0 % for hydrogen and between 0.8 % and 2.4 % for oxygen. However, when discarding the firs ten injections and considering only the last eight, MEs were negligible for all instruments (average MEs ranged between 0.1 % and 0.3 % for both hydrogen and oxygen). On average, ME values were similar for both OA-ICOS and CRDS instruments, with a significan improvement in the reduction of ME for the most recent generation of spectroscopes (especially OA-ICOS).

3. A strong correlation between the intra-vial range of isotopic values and inter-vial range was found for both technologies when considering all injections, indicating the dependency of the measurement variability on the size of the isotopic difference between adjacent vials. The correlation disappeared when the injections affected by MEs were discarded.

4. Standard deviations for the f nal reportable δ-values were unsatisfactorily high (up to 7.5 ‰ for δ^2H and 0.54 ‰ for δ^{18}O measurements for extreme cases) when all measurement injections were used, including those affected by MEs. However, for samples characterised by only small isotopic differences with respect to the previous vial in the tray or when rejecting the fi st six or eight injections, a marked precision increase was noted, with standard deviations in the range of 0.1 ‰–1.0 ‰ for δ^2H and 0.05 ‰–0.17 ‰ for δ^{18}O.

In this test we assessed the MEs of different laser spectroscopy instruments under standard operating conditions. Specificall , we quantifie the MEs and assessed the impact of MEs on measurement precision. Given the practical perspective of this Technical Note and our experience as users of laser spectroscopes for hydrological and environmental applications, we can outline some operational solutions (a–c in the list below) or post-processing data analysis (d–e) that might be adopted by other users of laser spectroscopy in order to avoid the occurrence of MEs or to reduce their influenc on the fina reportable δ-values. Most of these suggestions consist of practical and basic laboratory procedures and, as such, they do not claim to eliminate the problems derived by the influenc of ME. However, given a simple application, these approaches can be easily followed by users of laser spectroscopy.

a. Samples for laser spectroscopy analysis should be ordered or grouped in order of isotopic compositions, as this can often be estimated ahead of time, with the aim to analyse samples with similar isotopic ratios in the same analysis run. Furthermore, if possible, laboratory measurement standards should closely bracket

the expected range of sample isotopic composition. Additionally, ordering samples according to expected increasing or decreasing isotopic ratios might help to avoid high differences between adjacent unknown sample vials.

b. If samples are truly unknown, group them according to the same water source, sampling location and region of origin. However, keep in mind that, even at the small spatial scale, different water sources (e.g., liquid precipitation, solid precipitation, surface waters, groundwater, soil water etc.) might have significantl different isotopic ratios. Moreover, some physical processes such as seasonal effects and altitudinal effects might result in markedly different isotopic compositions of the same water sources.

c. If a broad range of isotopic composition of unknown samples is suspected, a preliminary run with a wide range of reference standards (very depleted and very enriched) could be carried out. This would allow to analyse samples exhibiting very high differences in isotopic ratios separately. The disadvantage of this approach is additional screening time and analysis cost.

d. It is often advisable to adopt an analysis scheme (e.g. the one suggested in IAEA, 2009b or similar) so that six or more injections are performed and the firs two or more are discarded. However, as demonstrated and reported elsewhere (Gröning, 2011), there are cases when rejecting two or three injections might be insufficien to eliminate ME. Thus, as a quick and preliminary assessment of possible occurrence of ME, check for increasing or decreasing variations (according to the value of the previous sample) in δ-values of subsequent samples that exceed the typical instrumental precision by two or more times. If necessary, run a few samples and apply the procedure presented here in order to decide a proper number of injections to perform and a threshold number of injections to reject.

e. If it is not possible to employ the solutions listed above, post-analysis memory correction calculations, as the ones reported in Gupta et al. (2009) and Gröning (2011), can be applied.

Acknowledgements. This work was partly supported by the Research Project "GEO-RISKS" (STPD08RWBY), University of Padova, Italy and the Project "Giovani Studiosi – Ricerche di carattere innovative e di eccellenza proposte da giovani non strutturati, decreto rettorale no. 800-2011, 23/03/2011", Università di Padova, Department of Land, Environment, Agriculture and Forestry, Italy. The study was also supported by the Czech Ministry of Education Youth and Sports, Czech Republic (CEZ MSM 6840770002), the project "Review of Groundwater Resources in the Czech Republic (OPZP 1559996)" and the National Research Fund of Luxembourg (TR-PHD BFR07-047). We thank two anonymous reviewers and Doug Baer (Los Gatos Research, Inc.) for their useful comments and suggestions that helped to significa tly improve this Technical Note.

Edited by: M. Weiler

References

Brand W. A., Geilmann, H., Crosson, E. R., and Rella, C. W.: Cavity ring-down spectroscopy versus high-temperature conversion isotope ratio mass spectrometry; a case study on δ^2H and δ^{18}O of pure water samples and alcohol/water mixtures, Rapid Commun. Mass Sp., 23, 1879–1884, doi:10.1002/rcm.4083, 2009.

Chesson, L. A., Bowen, G. J., and Ehleringer, J. R.: Analysis of the hydrogen and oxygen stable isotopes ratios of beverage waters without prior water extraction using isotope ratio infrared spectroscopy, Rapid Commun. Mass Sp., 24, 3205–3213, 2010.

Epstein, S. and Mayeda, T. K.: Variations of δ^{18}O of waters from natural sources, Geochim. Cosmochim. Ac., 4, 213–224, 1953.

Gkinis, V., Popp, J. T., Johnsen, S. J., and Blunier, T.: A continuous stream flas evaporator for the calibration of an IR cavity ring-down spectrometer for the isotopic analysis of water, Isot. Environ. Healt. S., 46, 463–475, 2010.

Gonfiantini R.: Standards for stable isotope measurements in natural compounds, Nature, 271, 534–536, 1978.

Gröning, M.: Improved water δ^2H and δ^{18}O calibration and calculation of measurement uncertainty using a simple software tool, Rapid Commun. Mass Sp., 25, 2711–2720, doi:10.1002/rcm.5074, 2011.

Gupta, P., Noone, D., Galewsky, J., Sweeney, C., and Vaughn, B. H.: Demonstration of high-precision continuous measurements of water vapor isotopologues in laboratory and remote fiel deployments using wavelength-scanned cavity ring-down spectroscopy (WS-CRDS) technology, Rapid Commun. Mass Sp., 23, 2534–2542, 2009.

Horita, J., Ueda, A., Mizukami, K., and Takatori, I.: Automatic δD and δ^{18}O analyses of multi-water samples using H_2- and CO_2-water equilibration methods with a common equilibration set-up, Appl. Radiat. Isotopes, 40, 801–805, 1989.

IAEA: Reference Sheet for VSMOW2 and SLAP2 international measurement standards, issued 13 February 2009, International Atomic Energy Agency, Vienna, 5 pp., http://nucleus.iaea.org/rpst/Documents/VSMOW2_SLAP2.pdf, 2009a.

IAEA: Laser Spectroscopy Analysis of Liquid Water Samples for Stable Hydrogen and Oxygen Isotopes, Performance Testing and Procedures for Installing and Operating the LGR DT-100 Liquid Water Isotope Analyzer. International Atomic Energy Agency, Vienna, 2009, ISSN 1018-5518, 2009b.

Lis, G., Wassenaar, L. I., and Hendry, M. J.: High precision laser spectroscopy D/H and ^{18}O/^{16}O measurements of microliter natural water samples, Anal. Chem., 80, 287–293, 2008.

Los Gatos Research, Inc.: Liquid-Water Isotope Analyser, Automated Injection, 2008.

Olsen, J., Seierstad, I., Vinther, B., Johnsen, S., and Heinemeier, J.: Memory effect in deuterium analysis by continuous fl w isotope ratio measurement, Int. J. Mass Spectrom., 254, 44–52, 2006.

Penna, D., Stenni, B., Šanda, M., Wrede, S., Bogaard, T. A., Gobbi, A., Borga, M., Fischer, B. M. C., Bonazza, M., and Chárová, Z.: On the reproducibility and repeatability of laser absorption spectroscopy measurements for δ^2H and δ^{18}O isotopic analysis, Hydrol. Earth Syst. Sci., 14, 1551–1566, doi:10.5194/hess-14-1551-2010, 2010.

Picarro, Inc.: Picarro L1102- i Isotopic Water Liquid Analyzer, 2008.

Sayres, D. S., Moyer, E. J., Hanisco, T. F., St. Clair, J. M., Keutsch, F. N., O'Brien, A., Allen, N. T., Lapson, L., Demusz, J. N., Rivero, M., Martin, T., Greenberg, M., Tuozzolo, C., Engel, G. S., Kroll, J. H., Paul, J. B., and Anderson, J. G.: A new cavity based absorption instrument for detection of water isotopologues in the upper troposphere and lower stratosphere, Rev. Sci. Instrum., 80, 044102, doi:10.1063/1.3117349, 2009.

Schultz, N. M., Griffis T. J., Lee, X., and Baker, J. M.: Identificatio and correction of spectral contamination in ^{2}H/^{1}H and ^{18}O/^{16}O measured in leaf, stem and soil water, Rapid Commun. Mass Sp., 25, 3360–3368, 2011.

Wang, L., Caylor, K. K., and Dragoni, D.: On the calibration of continuous, high-precision δ^{18}O and δ^2H measurements using an off-axis integrated cavity output spectrometer, Rapid Commun. Mass Sp., 23, 530–536, 2009.

Wassenaar, L. I., Hendry, M. J., Chosten, V. L., and Lis, G. P.: High resolution pore water δ^2H and δ^{18}O measurements by $H_2O_{(liquid)}$-$H_2O_{(vapor)}$ equilibration laser spectroscopy, Environ. Sci. Technol., 42, 9262–9267, 2008.

West, A. G., Goldsmith, G. R., Brooks, P. D., and Dawson, T. E.: Discrepancies between isotope ratio infrared spectroscopy and isotope ratio mass spectrometry for the stable isotope analysis of plant and soil waters, Rapid Commun. Mass Sp., 24, 1948–1954, 2010.

Acknowledgments

Writing the acknowledgments seems like autumn, nostalgically looking back to the warm summer feeling and reflecting to the path which led to these papers. How it all started? Maybe growing up next to a small river during the kinder-garden years which was the best playground and unconsciously formed the base for my curiosity for water...
... the wake up came in 2006 in the Makanya catchment driving through the headwaters, evermore wondering where all the water was coming from and going to... ... ending up in the Alptal which is beside some boundary and initial conditions not that different. I still remember the job interview in Zurich and I am really grateful to you Jan, that you chose me and gave me the opportunity to take this roller-coaster ride with you as my Doktorvater. Starting and see growing H_2K as it is today, and giving me the freedom to further grow. Manfred, many thanks for your supervision, providing us a warm bed in the Swiss hydrology and of course the Alptal. Huub, bedankt voor de bagage die je me mee hebt gegeven en ons klein Makanya paper (mijn eerste echt paper). Marloes bedankt voor de mooie tijd in Makanya, het laten zien wat echt catchment hydrology is en de hulp en bijdrage van ons paper.
This thesis just could not have been possible without the support and help of many people [1] who helped in the field during the nice and sunny snapshot campaigns and ghastly wet days when hunting for stormflow samples and final doing all the lab work to get the raw data. Therefore many thanks to your tremendous efforts: Holly, Ellen, Daniel, Inge, Seraina+Marcel, Käthi, Andri, Isabelle, Silvan, Oskar, Danthu, Renato and the AUA Laboratory at EAWAG for chemical analyses. All the team of the Swiss Federal Institute for Forest, Snow and Landscape Research (WSL)-Gebirgshydrologie und Massenbewegungen. Tobias, thanks for the first steps and introduction in field sampling in Ossingen. Kari für Deine hilfe beim Wasser und Daten sampeln im Erlenbach, Martin (installing the rain gauges + samplers and ping pong e-mails ;) ,Michal, Hana, Lukáš, Russel (+Laura and Erin) for the good time in Zürich help in the field and the how2 of the elephant, Stefan U., Elgard, Stefan P., Stephan M., Sandra P.(thanks for all the filtering of all those ... water samples), Sandra S, Nadja, Jana (really grateful for all the running through the catchment and help in organizing) and Andrea (in the field, lab and great you continued!). The lab crew: thanks for the help in the lab and supporting me with baby sitting or trouble shooting: Bruno, Claudia , Michael, Sandra, and of course the man with the golden hands Ivan aka Woody. Not to forget my great master students: Andrea, Damien, David, Yves and Alexandra. It was a big motivation, pleasure to see you growing, working together and contributing to my thesis. You can be proud of what you achieved!
I am great full that the Oberallmeindkorporation Schwyz (OAK) let me play within the Zwäckentobel and the Department of Environment of the Canton of Schwyz and the municipality Alpthal for the good cooperation. Criticism is always hard but a good lecture to get both feet on the ground therefore thanks for the effort and feedback to the different editors (Bettina Schaefli, Markus Weiler, Doerthe Tetzlaff and Nevil Quinn) and reviewers, unfortunately anonymous, but grateful for all the effort reading the first version of the papers and provided helpful comments, which improved the manuscripts.
Barbara and Sandro, es hat mich gefreut mit Euch über die isotopen zu ratschen und 1000 dank für die extra Messungen. The ZVV, Mobility Carsharing (all those save km to the Alptal), SBB for the impressive transportantion system (please don't change!), the LATEX community, designer of the Stockholm University PhD Thesis template and colorbrewer.org. P.J. p.v. maar bedankt voor alles! Daniele, Giulia and all the LGR-Picarro paper team thanks for the collaborations and to the next ones. Annagreth & Werni und Martin, vielen dank für Euren sichern Haven im Zwäcken-tobel. Ob im Schnee, Regen oder schönen Wetter es war immer fein bei Euch vorbei zu schauen, zwischendurch zu geniesen und mal zu ratschen. Gerardo, grazie per le più gustose verdure di Zurigo. Liebe Petra und RoLiHa, vielen dank für die schönen Abende bei Euch zuhause und Petra das wir den Isotopensamler in Dein Blumenbeet stellen durften! The Uni-GIUZ - team (Ruth, Yvonne, Sabina, Ivana, Yvonne, Andrea, Martin, Magrit, Lukas, Cornelia and Paolo), IT (Roya, Andi, Thomas and Joerg) and the Biblio-zora team (especially Gary for the extra papers). Patricia und Ljubica for all your support. $_2$B and $_3$G + K78 for sharing and giving support during the years. All the different constellations of H_2K and above all the support from Nans+Georgie, Philipp+(Sarah+Sara), Ilja and Maria+(Edu, Giulio and Linus). Tracy for your help and

[1] If your name is not listed please forgive my grey cells, they're getting older ;). Your contribution was still highly valued and I am in deep shame.

motivation during all the writing +(Joachim, Lena and Dario). Michi vielen Dank für alles und hab noch unser erstes treffen in Züri und die vielen schönen gemeinsamen km in Alptal und zähen Stunden währender der diss und unseren gemeinsamen paper.
By moving upstream, the gravitational center moved down south and being submerged into new cultures, habits and rain the contact with my friends and family was not as much as I hoped. Nevertheless citing an old dutch saying: what's inside a well sealed barrel does not sour (or something like that) all of you have still a warm place in my heart: Pfefferlers, Bruinsmas, Jan en Vroon. Fee+ LL en Simon jammer dat je/jullie niet bij kon zijn want eigenlijk was het gewoon hetzelfde wat we altijd al samen deden: Dammetjes bouwen in de Orchy river of lekker banjeren / biken in de regen. Off course all the hippo-clan + extensions, Jan, Marjolijn, Nils and Mette, Pieter, Jules, Steven, Tamara, Merle, Alvaro, Simone, Paribesh, Shailee and Sophie. Maarten, Femke en Minas als bijna buren in het veld en in Zürich bedankt voor de mooie tijd!! Bernardo, Eli e Chris grazie per tutti i bei momenti in Zurigo!!!

Caty, Alberto, Fede e Franci grazie per tutto! Xavi, Martin en natuurlijk de oudjes bedankt voor al jullie support! THE most important, how can I thank you Ila! Keeping me in balance, giving me energy, patience, love and helping during the harsh and beautiful moments in the lab, field, at home and to finish this roller coaster ride together!!!

Benjamin Fischer
Zürich, March 2016

... to level spectroscopes.